Pablo de Olavide University
Department of Physiology, Anatomy and Cellular Biology

THE ROLE OF THE CEREBRAL CORTEX DURING CLASSICAL EYEBLINK CONDITIONING IN THE RABBIT

Claudia Ammann

Doctoral Thesis directed by:
Agnès Gruart i Massó and Javier Márquez Ruiz
Seville, Spain 2017.

Pablo de Olavide University
Department of Physiology, Anatomy and Cellular Biology

Claudia Ammann

THE ROLE OF THE CEREBRAL CORTEX DURING CLASSICAL EYEBLINK CONDITIONING IN THE RABBIT

Doctoral Thesis directed by

Agnès Gruart i Massó and Javier Márquez Ruiz

Seville, Spain 2017.

Ms. Agnès Gruart i Massó, Full Professor of the Physiology, Anatomy and Cellular Biology Department/Experimental Science Faculty at the Pablo de Olavide University, and Mr. Javier Márquez Ruiz, Associate Professor of the Physiology, Anatomy and Cellular Biology Department/Experimental Science Faculty at the Pablo de Olavide University, **DECLARE** that:

The present scientific work entitled "The role of the cerebral cortex during classical eyeblink conditioning in the rabbit" has been realized by Ms. Claudia Ammann under their direction and supervision, and it meets the requirements and scientific rigor to be presented and defended as Doctoral Thesis.

Seville, May 3, 2017

Fdo: Agnès Gruart i Massó

Fdo: Javier Márquez Ruiz

To my beloved grandpa.
I still remember your last words.
'Get this Thesis done!'
I wish you could witness this moment.

Acknowledgements

It is nearly impossible to name everyone that has been a part of this process at some point. This is why I want to thank everyone who has contributed in any way to the completion of this Doctoral Thesis.

I would especially like to thank my advisors Agnès Gruart and Javier Márquez Ruiz for their constant guidance, support, and constructive reviews and criticism. Javier who has been patient and understanding since the first day I started working with him. I admire your infinite ambition.

Enormous thanks to Pablo Celnik for including me in his highly competent group at Johns Hopkins University in Baltimore for almost two years. Beyond the precious knowledge and friendships I gained during this period, this opportunity has been invaluably helpful for the next step in my academic career.

I also would like to thank Javier Medina and Ryan Roemmich for their constructive reviews and for approving the scientific quality of this work as worthy of obtaining the International Mention.

Thanks to my family - I can't even express in words how much I appreciate you. My parents Brita and Axel who gave me the opportunity to fulfill my dreams, supported me from the first day on, and accepted (with sadness, though) the geographic distance. Special thanks also to my grandma, Annelies, for her unconditional compassion and care and for providing a unique look to the cover of this book with her painting. Thanks to my grandpa Dieter - your steady will to learn set an example of excellence for me as a role model. You left us too soon…

Finally, I would like to thank all my lab mates and friends. I will never forget our lab jokes (specially the Friday ones), our lunch conversations, and the uncountable moments of laughs and tears. I undoubtedly could not have done this without you!

Resumen

El aprendizaje es un proceso por el que se adquieren o modifican determinados comportamientos que permiten al individuo adaptarse a los cambios que tienen lugar en el entorno. El sistema motor del párpado y de la membrana nictitante han sido ampliamente utilizados como modelo experimental para el estudio de las bases neuronales que subyacen al aprendizaje asociativo, mayoritariamente mediante el uso de distintos paradigmas de condicionamiento clásico del reflejo palpebral. En las últimas décadas, el cerebelo y el hipocampo han sido propuestos como las estructuras cerebrales responsables de procesar los códigos neuronales necesarios para generar una respuesta condicionada en este tipo de aprendizaje, no obstante, existen estudios que apuntan a la participación de otras regiones neuronales. De este modo, los cambios observados en la actividad neuronal en diversas estructuras corticales durante el aprendizaje sugieren la participación de las vías sensoriales y motoras en la generación de la respuesta aprendida. El trabajo realizado en la presente Tesis Doctoral aborda el papel de la corteza cerebral durante el condicionamiento clásico del reflejo palpebral en el conejo. En primer lugar, se caracterizó la proyección monosináptica desde la corteza motora al núcleo facial mediante la inyección de un trazador anterógrado en la región cortical correspondiente al músculo *orbicularis oculi*. Mediante este proceso, se identificó por vez primera en conejos la existencia de proyecciones neuronales directas desde la corteza motora hacia el núcleo facial. Posteriormente, y con el fin de caracterizar el papel de la corteza cerebral durante el condicionamiento clásico, se registró extracelularmente la actividad de las neuronas situadas en la región palpebral correspondiente al músculo *orbicularis oculi* en la corteza motora durante el proceso de aprendizaje. El registro de las neuronas activadas antidrómicamente desde el núcleo rojo y el núcleo facial durante el condicionamiento del reflejo palpebral mostró un incremento de la tasa de disparo de dichas neuronas que se anticipó ($\geq$ 50 ms) a la respuesta condicionada. Con el fin de verificar la importancia de la corteza motora durante el proceso de adquisición del aprendizaje asociativo motor, se examinó si la modulación de la excitabilidad de las neuronas motoras inducida por medio de la estimulación eléctrica transcraneal, sería capaz de modificar el proceso de aprendizaje. De la misma manera, se estudió la contribución de la corteza sensorial en la adquisición del condicionamiento, mediante el uso de un flash de luz débil como estímulo condicionado, aplicando corrientes eléctricas transcraneales sobre la corteza visual primaria durante el aprendizaje. La modulación de la excitabilidad neuronal de las

cortezas motora y visual tuvo un impacto significativo sobre el aprendizaje consistente en un cambio en el porcentaje de respuestas aprendidas dependiente de la polaridad de la corriente aplicada. Cuando se administró corriente anodal sobre la corteza motora se observó un aumento en el número de respuestas aprendidas, mientras que la corriente catodal aplicada sobre la corteza visual lo disminuyó. Con respecto a la calidad de la respuesta aprendida, se observó para la corteza motora que con la estimulación anodal las respuestas fueron de mayor magnitud, mientras que la estimulación catodal retrasó levemente el inicio de las respuestas condicionadas y redujo magnitud de las mismas. Por último, se midieron las variaciones térmicas del tejido cerebral mediante un termistor implantado de forma epidural situado bajo el electrodo de estimulación transcraneal para descartar que los efectos observados en el aprendizaje motor durante la estimulación eléctrica estuviesen influenciados por un aumento de temperatura del tejido estimulado. Los resultados obtenidos no mostraron cambios significativos en la temperatura cerebral ni durante, ni después de la estimulación transcraneal. En su conjunto, la presente Tesis Doctoral revela que la participación de la corteza motora durante el condicionamiento clásico es fundamental para la correcta adquisición de las respuestas motoras aprendidas. Además, apoya la hipótesis de un papel relevante de la corteza sensorial en este tipo de aprendizaje asociativo motor. Por último, los datos mostrados en esta tesis constituyen la primera evidencia experimental sobre la ausencia de cambios térmicos asociados a la estimulación eléctrica transcraneal.

Abstract

Learning is defined as the acquisition or modification of specific behaviors that allow the individual to adapt to changes occurring in the surrounding environment. The primary focus of many investigations has been the characterization of neural bases underlying learning. Thus, the motor system of the eyelid and the nictitating membrane has been extensively used as an experimental model to study the mechanisms and neural structures determining associative learning, mainly by the use of different paradigms of classical eyeblink conditioning. Over several decades, the cerebellum and the hippocampus have been proposed as the brain structures responsible for processing the neural codes underlying the generation of learned eyeblink responses. However, some researchers raised the hypothesis of the participation of other brain regions. Specifically, reported changes in neuronal activity in various cortical structures during learning suggest the involvement of sensory and motor pathways in the generation of conditioned responses. The main approach of the experimental work presented in this Doctoral Thesis was to investigate the role of the cerebral cortex during the classical conditioning of eyeblink responses. First, projections from the motor cortex to the facial nucleus were characterized by injecting an anterograde tracer in the cortical region corresponding to the *orbicularis oculi* muscle. Hence, monosynaptic neural projections from the rabbit's motor cortex were identified in the facial nucleus. On the other hand, extracellular unitary activity in the palpebral region of the motor cortex corresponding to the *orbicularis oculi* was recorded during eyeblink conditioning. As a result, motor cortex neurons activated antidromically from the red nucleus as well as the facial nucleus showed an increase of their firing rates well in advance ($\geq$ 50 ms) with regard to the conditioned response onset. With the aim to verify the importance of the motor cortex during the acquisition process of associative learning it was examined whether modulating excitability of motor cortex neurons by means of transcranial current stimulation would be able to modify the learning process. Similarly, the contribution of the sensory cortex during the acquisition of eyeblink conditioning – using light stimulation as conditioned stimulus – was studied by applying transcranial electrical currents to the primary visual cortex during learning. The induced modulation of neuronal excitability in the motor and visual cortex resulted in a significant impact on learning consisting of a polarity-dependent change in the percentage of learned responses. Specifically, an increase in the number of learned responses was observed when stimulation with anodal polarity was applied to the motor cortex, whereas

cathodal polarity decreased the number of conditioned responses when applied to the visual cortex. Regarding the quality of responses as observed for the motor cortex, anodal stimulation promoted increased magnitude, whereas cathodal stimulation reduced magnitude and slightly delayed the beginning of learned responses. Finally, thermal changes of the brain tissue were measured by means of an epidurally implanted thermistor placed under the transcranial current stimulation location to rule out that tissue heating of the stimulated site interfered with the observed effects on motor learning. No significant changes in brain temperature were induced either during or after the application of transcranial stimulation. In brief, this Doctoral Thesis reveals that the participation of the motor cortex during classical eyeblink conditioning is essential for the correct acquisition of learned responses. In addition, the results support the hypothesis of the involvement of the sensory cortex in this type of associative motor learning. Finally, the data presented in this thesis shows for the first time experimental evidence supporting the absence of thermal changes in the brain tissue due to the transcranial current stimulation.

ABBREVIATIONS:

BDA, biotinylated dextran amine; **BDNF**, brain-derived neurotrophic factor; **CS**, conditioned stimulus; **CR**, conditioned response; **DBS**, deep brain stimulation; **EEG**, electroencephalographic recording; **EMG**, electromyographic recordings; **fMRI**, functional magnetic resonance imaging; **FN**, facial nucleus; **IP**, interpositus nucleus; **LFP**, local field potential; **LTD**, long-term depression; **LTP**, long-term potentiation; **MC**, motor cortex; **NMDA**, N-methyl-D-aspartate; **NTC**, negative temperature coefficient; **PB**, phosphate buffer; **PSTH**, peristimulus time histogram; **RN**, red nucleus; **S1**, primary somatosensory cortex; **SMS**, static magnetic stimulation; **tACS**, transcranial alternating stimulation; **tDCS**, transcranial direct current stimulation; **TLT**, transcranial infrared laser therapy; **TMS,** transcranial magnetic stimulation, **tRNS**, transcranial random noise stimulation; **UR**, unconditioned response; **US**, unconditioned stimulus; **V1**, primary visual cortex; **VEP**, visual evoked potential

INDEX

1. INTRODUCTION

1.1. Associative learning

'*Learning refers to a change in behavior that results from acquiring knowledge about the world, and memory is the process by which that knowledge is encoded, stored, and later retrieved'* (Schacter and Wagner, 2013).

Learning and memory are two closely related brain processes that lead to adaptive changes in behavior. The stabilization of the neural changes that take place after the learning allows for the consolidation of the memories and their long-term maintenance. The more the environment changes, the more 'plastic' the behavior should be. In turn, this plasticity is a reflection of the organism's nervous system, i.e., the more plastic the nervous system, the more learning and memory capacity the organism has (Morgado Bernal, 2005). Ramón y Cajal (1852 - 1934) was the first to propose the hypothesis of plastic changes in number and strength of neural connections that represent the physical basis of learning (Sotelo, 2003). Nowadays, learning and memory is one of the most intensively studied subjects in the field of neuroscience, and modern neuroscientists investigate the processes of learning and memory by using extremely diverse strategies. It is important to emphasize that the study of the physiological bases of learning and memory is relevant because it allows, in the long term, the design of diverse therapies and treatments, especially for those situations in which mnesic (pertaining to memory) capacities are impaired, as in patients with certain neurodegenerative diseases.

Memory converges in two different types: *explicit* (or declarative) memory and *implicit* (or non-declarative) memory. *Explicit* memory consists in the conscious form of recovering earlier experiences and remembering information about people, places, and things. On the other hand, *implicit* memory is expressed by unconsciously acquired knowledge manifested in an automatic manner. In turn, implicit memory can be distinguished in two types: *non-associative* and *associative*. Without going in further detail, non-associative learning (single or repeated presentation of a single type of stimulus) comprehends two forms of learning: sensitization and habituation. The present work focuses specifically on associative learning, which is defined as the acquisition of the association between two stimuli or between a stimulus and a behavior. In contrast to sensitization and habituation, associative learning is dependent on the timing of the stimuli. Two principal forms of associative learning have been abundantly

applied and investigated in the past, and are still today frequently used learning paradigms in many laboratories: *classical conditioning*, or learning the relationship between two stimuli, and *operant conditioning*, or learning the relationship between the organism's action and the outcome of that action (Schacter and Wagner, 2013).

Classical conditioning was first described by Ivan P. Pavlov (1849 – 1936), a Russian born physiologist and psychologist. It was during his studies on salivation and its associated pancreatic and gastric secretions when he first observed the phenomenon of the 'conditional reflex', or *conditioned response* (CR). His famous experiment showed how the presentation of an *unconditioned stimulus* (US), in this case meat powder, produced salivation in a dog. The evoked salivation is a reflex (innate) response, i.e., the animal required no previous learning to present that behavior. This type of response is called *unconditioned response* (UR). Furthermore, when a tuning fork sounded repeatedly right before presenting the meat powder, the dog started associating the sound with the presentation of the meat powder. Eventually, the dog began to salivate with the sound of the tuning fork. This meant that the sound was now the *conditioned stimulus* (CS) paired with the meat powder as the US, expressing a CR (Pavlov, 1927; **Figure 1.1**). The UR and the CR are generally similar, but often not identical, in type or magnitude (Trigo et al., 1999a; Gruart et al., 2000a). To achieve the learned association, it is important that the CS always precedes the US, keeping a critical interval of time between them. Accordingly, this type of associative learning is called Pavlovian conditioning and is one of the oldest and most systematically studied phenomena in psychology (Rescorla, 1988).

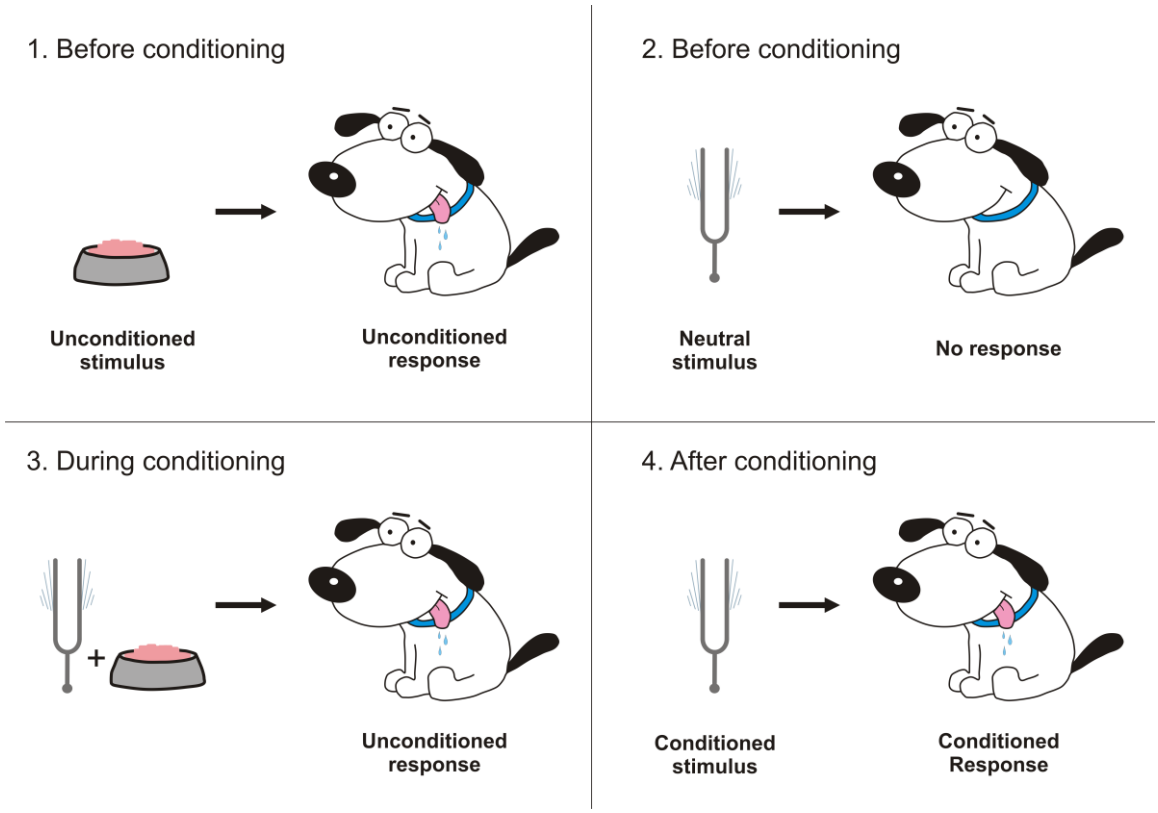

Figure 1.1 Pavlovian or classical conditioning paradigm: The presentation of an unconditioned stimulus (US) produces an unconditioned response (UR, in this case, salivation). Repeated combination of US with a neutral stimulus (in this case, tuning fork sound) produces association of the neutral stimulus, now conditioned stimulus (CS), with the US, expressing a conditioned response (CR) in the experimental subject.

1.2. Classical eyeblink conditioning

Classical conditioning of eyelid responses is a form of associative motor learning which is gradually acquired. This learning paradigm was first established for scientific use in humans in the 1920s (Cason, 1922). However, reported shortcomings from human studies (explicit awareness, voluntary responses, etc.) and the need to deepen the understanding of this type of learning through the use of invasive laboratory techniques were motivation enough to develop nictitating membrane and eyeblink paradigms in the awake animal, specifically in the rabbit (Freeman and Steinmetz, 2011). Thus, since the 1960s the classical eyeblink conditioning has been extensively used by multiple researchers as a satisfactory experimental animal model for the investigation of neuronal mechanisms and pathways underlying the acquisition of new motor capabilities (Gormezano et al., 1962, 1983; Woody et al., 1970; Berthier and Moore,

1986; Gruart et al., 2000a; Medina et al., 2002; Márquez-Ruiz et al., 2012, 2016; Pacheco-Calderón et al., 2012; Carretero-Guillén et al., 2015). The main advantages of using the rabbit as a model are their high tolerance for movement restriction, the absence of alpha responses, i.e., no eyelid reflex response to the tone or flash used as CS (Grant and Adams, 1944; Gruart et al., 2000a), and easy acquisition of eyelid movement measures compared to other smaller animals like rodents. Nevertheless, classical eyeblink conditioning has been successfully performed in other animal models examining characteristics and neuroanatomical bases of associative learning, as it has been shown for rats (Schmajuk and Christiansen, 1990; Stanton et al., 1992), mice (Aiba et al., 1994; Chen et al., 1996; Heiney et al., 2014), and cats (Norman et al., 1974; Gruart et al., 1994) among other animal species.

The classical conditioning of eyelid responses consists of the presentation of a neutral CS (generally a tone) preceding the US (generally an air puff presented to the cornea that causes the eye to blink) by 0.1–1.0 seconds. The *delay* paradigm represents the standard organization of stimuli presentation in eyeblink conditioning. Here, the CS co-terminates with the US and the optimal conditioning in rabbits occurs when the interval between CS onset and US onset is in the range of 250 to 500 ms (Gormezano, 1966). For the *trace* paradigm the animal (or human) has to generate a memory trace of the CS (tone, light flash, electrical stimulus, etc.) in order to associate it with the later presented US (generally air puff to the cornea). Thus, there is a time gap (0.1–0.5 s) between the end of the CS and the beginning of the US (Delgado-García and Gruart, 2006). Eye movements and CRs are usually measured and determined with Hall-effect devices (Koekkoek et al., 2002), the search-coil technique (Gruart et al., 1994), or by means of the electromyographic (EMG) activity (Márquez-Ruiz et al., 2012) of the *orbicularis oculi* muscle ipsilateral to the US presentation (**Figure 1.2**).

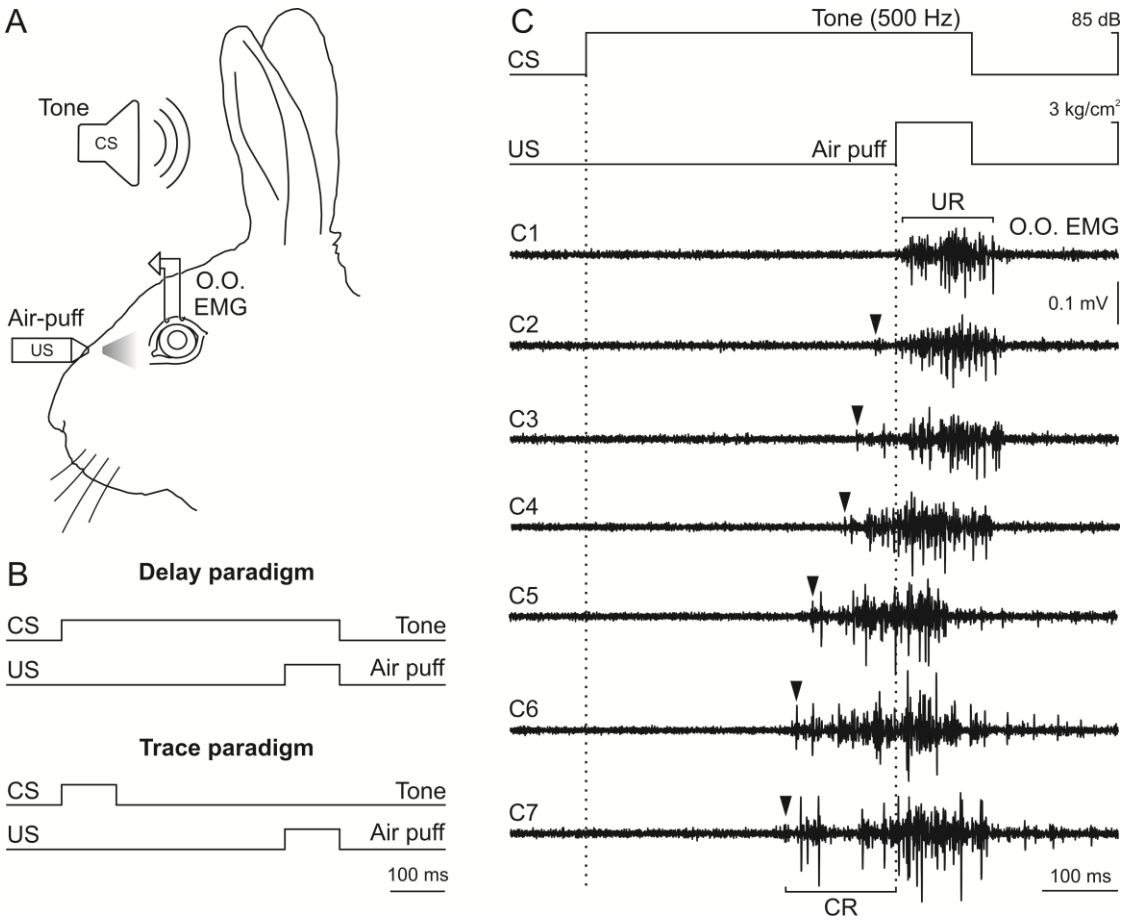

Figure 1.2 Eyeblink conditioning paradigms and electrophysiological recording of CRs. ***A,*** Experimental design of classical eyeblink conditioning performed in rabbits representing the location of recording electrodes for *orbicularis oculi* electromyographic activity (O.O. EMG). ***B,*** Two classically used conditioning paradigms based on a different temporal relationship between conditioned stimuli (CS) and unconditioned stimuli (US). In the delay paradigm (top) CS co-terminates with the US whereas the trace paradigm presents a constant time interval between both stimuli (bottom). ***C,*** The figure shows the eyeblink conditioning progress with the use of a delay paradigm. The conditioning paradigm (CS and US presentations) and *orbicularis oculi* muscle activity recordings (O.O. EMG) from the same animal are represented for seven consecutive conditioning sessions (C1 – C7). Across sessions the initial unconditioned response (UR), consisting of a reflex response right after receiving the US, converts to an eyelid response that precedes the US, termed conditioned response (CR, arrows). Modified from Cheron et al., 2015.

1.3. Neuronal projections to the *orbicularis oculi* muscle

An eye blink is a fast narrowing of the palpebral fissure, implicating the motion of a series of muscles: the *orbicularis oculi* and, in those species with a nictitating membrane, the retractor bulbi and most of the extraocular eye muscles. An eye blink can be triggered by stimuli of different sensory modalities, involving the somatosensory, visual, acoustic, or vestibular system (Delgado-García et al., 2002). The eyelid motor system presents a series of singularities worth mentioning. First of all, the facial musculature is formed of special, visceral-modified muscle fibers that present different neural control than the skeletal motor system (Morecraft et al., 2004). Furthermore, the eyelid motor system is load-free and has an almost negligible mass, expressed as a low inertial damping (Delgado-García and Gruart, 2006). Interestingly, earlier studies have concluded that the *orbicularis oculi* motoneurons receive no information with respect to the position of the upper lid before the initiation of reflex blinks, i.e., no propioceptive feedback signals from the involved muscles (Trigo et al., 1999b). Consequently, no propioceptive coordinating mechanisms involving the red nucleus (RN) and cerebellum are implicated (Courville, 1966; Lindquist and Martensson, 1970; Mizuno and Nakamura, 1971). *Orbicularis oculi* motoneurons are located in the facial motor nuclei occupying preferentially the dorsolateral subdivision of the nucleus (Radpour, 1977; Holstege and Collewijn, 1982; Komiyama et al., 1984; Porter et al., 1989; Morcuende et al., 2002). With the use of the attenuated rabies virus as a retrograde transsynaptic marker injected in the *orbicularis oculi* muscle, Morcuende and colleagues (2002) were able to establish a fairly complete picture of the neural circuits underlying eye blinks in the rat. Their results illustrated the pathways by which sensory inputs of trigeminal, auditory, vestibular, and visual origins are capable of generating eyelid responses. On the other hand, they underlined the participation of reticular, rubral, cerebellar, and cortical neurons to eyelid control. Together, this study provided an extensive representation of the premotor networks controlling eyelid responses with a special highlight on the three major motor systems, (1) motor cortex (MC), (2) RN and pararubral area, and (3) reticular formation, and their contribution to eye blinks in cooperation with the cerebellar structures. **Figure 1.3** illustrates a schematic presentation of the major neural structures labeled via injections of retrograde tracers placed in the *orbicularis oculi* muscle as has been done by Morcuende and colleagues (2002) as well as by Gonzalez-Joekes and Schreurs (2012).

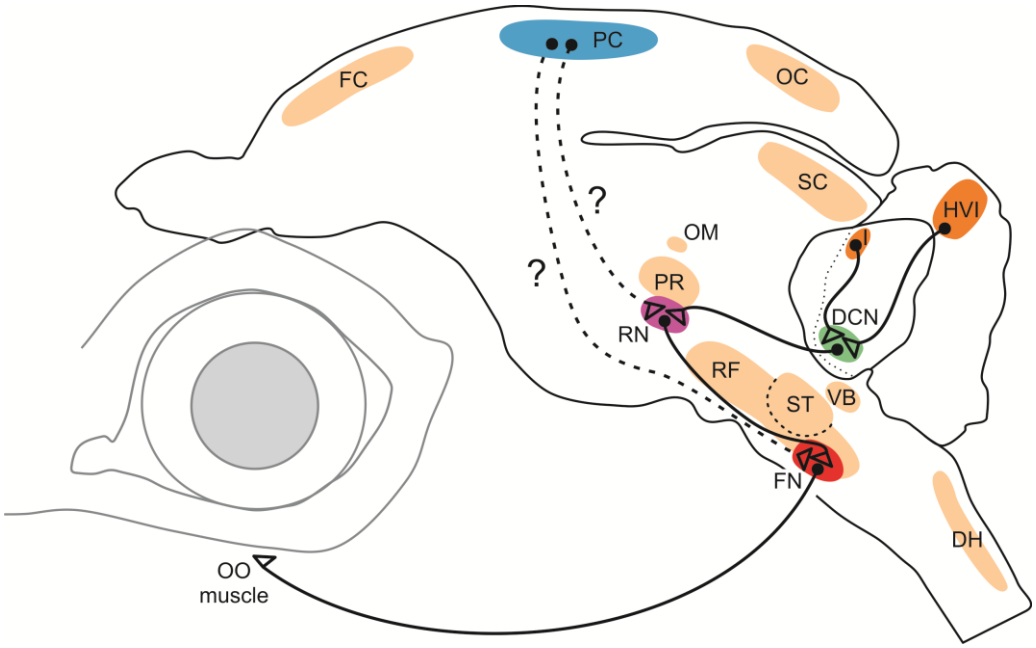

Figure 1.3 Schematic presentation of neuronal projections and main neural structures active during spontaneous eyeblinks in the rabbit. DCN, deep cerebellar nuclei; DH, dorsal horn; FC, frontal cortex; FN, facial nucleus; HVI and I, cerebellar cortex lobules; OC, occipital cortex; OM, oculomotor nucleus; OO, orbicularis oculi; PC, parietal cortex; PR, pararubral nucleus; RF; reticular formation; RN, red nucleus; SC, superior colliculus; ST, spinal trigeminal nucleus; VB, vestibular nucleus. Continuous projections = in previous studies experimentally proven. Dotted projections = hypothetical. Colored structures represent main regions, which have been labeled after injections of a retrograde tracer in the orbicularis oculi muscle in Morcuende et al. 2002, and Gonzalez-Joekes and Schreurs, 2012.

1.4. Neuronal structures underlying classical eyeblink conditioning

After more than 50 years of eyeblink conditioning studies, the research about the critical neural site/s of learning-related plasticity during this associative learning, i.e. the site/s where the acquisition and retention of new eyelid CRs is taking place, is currently still a subject of intense debate and controversy (Welsh and Harvey, 1989; Kelly et al., 1990; Aou et al., 1992; Gruart et al., 2000b; Christian and Thompson, 2003; Lee and Kim, 2004; Jiménez-Díaz et al., 2006; Freeman and Steinmetz, 2011; Pacheco-Calderón et al., 2012; Siegel et al., 2015). In 1942, Brodgen and Gantt provided the first evidence that the cerebellum is a key structure for associative motor learning (Thompson et al., 2000). In addition, on the basis of mathematical modeling,

David Marr (1969) and James Albus (1971) independently suggested that the cerebellum might be involved in learning motor skills. In the 80s, Thompson and colleagues were pioneers in demonstrating, based on aspiration lesions in the rabbit, the crucial role of the cerebellum in delay eyeblink conditioning (McCormick et al., 1981, 1982). Several lesion and inactivation studies proposed specifically the anterior interpositus nucleus (IP) as the neural site necessary for acquisition and retention of CRs (Lavond et al., 1985; Chapman et al., 1990; Clark et al., 1992; Steinmetz et al., 1992a-b; Christian and Thompson, 2005). Additionally, findings from electrophysiological studies suggested that the anterior IP is in fact driving the generation of CRs (Nicholson and Freeman, 2002; Green and Arenos, 2007; Halverson et al., 2010). However, a series of studies started a debate, still ongoing at the present time, about the definite role of the cerebellum and its nuclei during eyeblink conditioning. In this context, numerous findings have suggested that the cerebellum, and specifically the IP, may be involved more in the performance of ongoing CRs or on their proper timing (Welsh and Harvey, 1989, 1991; Kelly et al., 1990; Bloedel et al., 1991; Garcia and Mauk, 1998; Gruart et al., 2000c; Delgado-García and Gruart, 2002; Seidler et al., 2002; Sánchez-Campusano et al., 2011), rather than in the acquisition process itself. Moreover, electrophysiological recordings of different cerebellar nuclei regions revealed that the IP firing starts with (rather than precedes) the onset of reflex responses and CRs in cats, concluding that the IP cannot be the site for generation and storage of CRs (Gruart and Delgado-García, 1994; Gruart et al., 2000c; Delgado-García and Gruart, 2002, 2005). It must be taken into consideration that Delgado-García and colleagues used the search-coil technique to measure precise movement and position of the eyelid, while previous studies with opposite findings measured the passive movement of the nictitating membrane.

Regarding the more cognitively complex trace conditioning, where the CR occurs in absence of any sensory stimulus, findings suggests that acquisition of learning becomes hippocampus dependent (Moyer et al., 1990; Kronforst-Collins and Disterhoft, 1998; Weiss et al., 1999; Takatsuki et al., 2003; Tseng et al., 2004; Gruart et al., 2006). However, new data indicate that additional neural structures – such as the cerebellum, prefrontal cortex, and amygdala – perform essential roles in the trace paradigm (Woodruff-Pak et al., 1985; Kotani et al., 2003; Siegel and Mauk, 2013; Siegel et al., 2015) and that hippocampal cell types fire indistinctly during the CS-US interval for

both trace and delay conditioning paradigms (Berger et al., 1983; Múnera et al., 2001). Thus, similar input and output pathways are proposed for trace and delay conditioning, especially the same dependence on cerebellum and the related brainstem areas. However, the molecular substrates underlying both paradigms are thought to be different (Yang et al., 2015). The fact that sensory receptors are activated by changes in the presented stimulus, and not through its sustained presence, motivated several authors to acknowledge the delay paradigm as a particular case of trace conditioning (Manto et al., 2012).

A still unanswered question is which site or sites drive the acquisition of this type of associative motor learning. The two popular sites involved in the eyeblink conditioning (the cerebellum and hippocampus) have been shown to carry part of the neural codes necessary to generate the CR, but several studies support the idea that the acquisition is taking place at a different site (Delgado-García and Gruart, 2006). Thus, in recent years many other cerebral cortical and subcortical structures have been reported to be involved in different aspects of acquisition, storage, retrieval, and extinction processes. For instance, the prefrontal (Siegel and Mauk, 2013; Caro-Martín et al., 2015), cingulate (Weible et al., 2003), and the somatosensory (Leal-Campanario et al., 2006; Ward et al., 2012) cortices, neuronal premotor networks (Morcuende et al., 2002), and subcortical structures such as the striatum (Blázquez et al., 2002), the amygdalar complex (Boele et al., 2010; Sakamoto and Endo, 2010), some thalamic nuclei (Sears et al., 1996; Bahro et al., 1999; Campolattaro et al., 2007), and the RN (Haley et al., 1988; Sakamoto and Endo, 2010; Pacheco-Calderón et al., 2012) have been shown to participate in the generation of conditioned eyeblinks. Recent proposals suggest the joint involvement of cerebellar (cortex, nuclei), cortical (hippocampal, prefrontal), and subcortical (amygdala, striatum) structures in different aspects (cognitive, motor, associative strength, etc.) of classical eyeblink conditioning (Siegel et al., 2015; Yang et al., 2015).

1.4.1. The motor cortex (MC) and classical eyeblink conditioning

Surprisingly, the previously proposed list of neural sites involved in classical eyeblink conditioning does not include the MC. The MC has a well-defined and repeated

representation of facial muscles (Huang et al., 1988; Morecraft et al., 2001; Müri, 2016), and traditionally has been assumed to be one of the main neural sites involved in the acquisition and proper performance of new motor abilities (Evarts et al., 1983; Monfils and Teskey, 2004; Doyon and Benali, 2005; Brecht et al., 2013; Gloor et al., 2015; Hayashi-Takagi et al., 2015; Kaufman et al., 2015). In fact, MC dynamic activities have been described to be interacting with cerebellar and striatal contributions to different types of motor sequence learning (Houk et al., 1996; Hikosaka et al., 2002; Penhune and Steele, 2012; Santos et al., 2015). In addition, anatomical results revealed the existence of a monosynaptic pathway from the vibrissa MC to facial motor neurons in the rat proposing an important role of this direct pathway in the generation of complex whisker movements during tactile exploration (Grinevich et al., 2005).

However, few studies have addressed the involvement of MC in the generation of learned eyelid movements. Woody and his group were among the first to suggest a role for the MC in associative learning by recording increased unit activity mediated through neurons whose microstimulation evoked eye blinks. The enhanced firing activity preceded the CRs by a delay appropriate for conduction between MC and *orbicularis oculi* muscles (Woody et al., 1970; Woody and Yarowsky, 1972). In addition, they showed impaired acquisition of CRs with bilateral lesions of cortical motor areas (Woody et al., 1974). However, the reported electrophysiological measures were questioned by others concluding that the behavioral response measured by Woody and colleagues was not representative for a typical long-latency CR, but was probably a short-latency response caused by sensitization of the unconditioned reflex blink to the CS (Christian and Thompson, 2003). Some years later, Aou and colleagues (1992) reported similar increased spike activity within the MC after eyeblink conditioning in conscious cats, supporting the hypothesis that cortical excitability increases facilitated the responsiveness to the CS and that the generation of CRs may depend on neural circuitry and mechanisms of the MC. Birt and colleagues (2003) studied the neuronal responses to a CS and an US in the MC of awake cats in more detail. They found that both stimuli induced an increase in unitary activity; however, less activity was observed for the CS compared to the US. More recently, the hypothesis about the role of the MC during eyeblink conditioning was strengthened by the reported decrease in CR acquisition, as well as an initial defacilitation of CR-related neuronal activity of RN neurons, evoked through a reversible inactivation of MC (Pacheco-Calderón et al.,

2012). Additionally, the observed reduction of CRs elicited by the loss of N-methyl-D-aspartate (NMDA) receptor function (hypothesized to play a crucial role in the processes of learning and memory formation) provided evidence that the memory of acquired CRs is localized in MC (Hasan et al., 2013). Nevertheless, a more comprehensive examination regarding the involvement of MC during classical eyeblink conditioning and its projections to other motor areas is still needed.

1.4.2. The sensory cortex and classical eyeblink conditioning

The cortical sensory activity during classical eyeblink conditioning is generally mentioned as input of sensory information with reference to the CS pathway. The most commonly used CS modalities are a tone activating the auditory cortex (McCormick et al., 1981) or patterned/flashing lights stimulating the visual cortex (Morrell and Naitoh, 1962), and electrical or vibratory stimuli, triggering the somatosensory cortex (Das et al., 2001; Márquez-Ruiz et al., 2012, 2016). Sensory pathways are supposedly of subcortical origin but the sensory cortex may modulate these subcortical pathways (Halverson and Freeman, 2006, 2010a; Halverson et al., 2009). However, cortical CS inputs have not been investigated in great detail with respect to the eyeblink conditioning process. The current findings indicate that most likely there is no common circuit structure for the different CS modalities (Freeman and Steinmetz, 2011).

Regarding the auditory cortex, early studies have shown that lesions of the cerebral cortex that comprised the auditory cortex did not hinder acquisition or retention of delay conditioning. However, animals failed to generate short-latency CRs (Oakley and Russell, 1972, 1977). Steinmetz and his group (1987) examined the subcortical auditory CS pathway and proposed the cochlear nucleus projection to the lateral pontine nuclei as one possible pathway implicated in eyeblink conditioning. In recent years, additional auditory structures implicated in the CS pathway have been discovered, such as the inferior colliculus and the auditory thalamus, and more specifically the medial auditory thalamic nuclei (Campolattaro et al., 2007; Freeman et al., 2007; Halverson et al., 2010; Halverson and Freeman, 2010b). Regarding the auditory cortex, single unit recordings in rabbits (Kraus and Disterhoft, 1982) and neuroimaging techniques during delay

conditioning in the human (Molchan et al., 1994) revealed that this cortical area experiences learning-related modifications during eyeblink conditioning.

The somatosensory CS pathway has been less studied and little is known about the implicated neural structures. A few studies proposed that vibratory or weak electrical stimuli conditioning depends on the middle cerebellar peduncle (Solomon et al., 1986; Lewis et al., 1987; Hesslow et al., 1999). Interestingly, more recent investigations paid attention to the involvement of the primary somatosensory cortex (S1) during eyeblink conditioning. Thus, results based on c-Fos immunoreactivity reported significant c-Fos production in somatosensory cortex in conditioned animals, proposing that cortical areas among other brain structures process associative learning (Jiménez-Díaz et al., 2006). Furthermore, using vibrissa stimulation as an effective CS showed that trace eyeblink conditioning induced a learning-dependent row-specific expansion of cortical barrels (grid-like array of neurons and glial cells in S1 representing the vibrissa area) in rabbits, whereas cortical barrel lesions impaired eyeblink conditioning, proposing S1 as a site for long-term memory storage (Gálvez et al., 2006, 2007). Moreover, direct electrical stimulation of S1 through intracortical microstimulation (Leal-Campanario et al., 2006) or transcranial stimulation (Márquez-Ruiz et al., 2016) could successfully substitute for vibrissa stimulation during classical conditioning in behaving rabbits. These results together with the finding that direct neuromodulation of S1 modified the acquisition of associative learning in rabbits (Márquez-Ruiz et al., 2012), provide little information about the underlying somatosensory CS pathway, but propose the involvement of the sensory cortex during the acquisition of conditioned eyeblink responses.

With regard to the visual cortex, similar to the auditory CS pathway, decortications or lesions of the visual cortex did not block the acquisition or retention of visual eyeblink conditioning (Hilgard and Marquis, 1935; Oakley and Russell, 1977; Mauk and Thompson, 1987; Hesslow, 1994). Succeeding investigations in rabbits proposed a visual CS pathway consisting of the lateral geniculate nucleus, superior colliculus, visual cortex and pretectal nuclei. However, only the combined lesion of all these areas could completely abolish acquisition of a visual eyeblink conditioning (Koutalidis et al., 1988). Recent studies considered a possible pathway consisting of inputs from the ventral lateral geniculate nucleus and nucleus of the optic tract to the medial basilar

pons and its projection to the cerebellar cortex and anterior IP (Halverson and Freeman, 2010a). Remarkably little attention has been paid to the role of the primary visual cortex (V1) during the acquisition process of classical eyeblink conditioning using light stimulation as CS. Just recently, visual cortex lesions were shown to impair long-delay and trace conditioning of eyeblink responses (Steinmetz et al., 2013), and first evidence for a learning-related activation of V1 during trace eyeblink conditioning resulted from a functional magnetic resonance imaging (fMRI) study performed in rabbits (Miller et al., 2008). However, direct measures of V1 activity and reversible V1 modulation during eyeblink conditioning are required to provide more information about the role of V1 throughout the associative learning process.

1.5. Neuronal activity during motor learning

Animals and human beings have a remarkable capacity for learning novel motor skills through their interaction with the environment. However, new motor skills cannot be acquired by a fixed neural control system. Thus, sensorimotor control systems must constantly adapt over a lifetime. How might this occur? An attractive idea, proposed by the psychologist Donald Hebb (1904 – 1985), is that: '*When an axon of cell A is near enough to excite a cell B and repeatedly or persistently takes part in firing it, some growth process or metabolic change takes place in one or both cells so that A's efficiency as one of the cells firing B, is increased*.' (Hebb, 1949). In other words, neuronal connections are strengthened when pre- and post-synaptic elements at a synapse are active together, i.e., when the activity of one neuron repeatedly causes, or contributes to, the firing of another neuron, the synapse between them is intensified. This called *Hebb's rule* is supposedly describing how memories are formed in the brain based on the described mechanism usually termed *long-term synaptic plasticity*. These long-lasting changes have been repeatedly approached by experimentally induced *long-term potentiation* (LTP) or *long-term depression* (LTD) in synaptic strength. Thus, Bliss and colleagues discovered that a few seconds of high-frequency electrical stimulation could enhance synaptic transmission in the rabbit hippocampus for days or even weeks (Bliss and Gardner-Medwin, 1973; Bliss and Lømo, 1973). It is commonly accepted that LTP involves usually the activation of NMDA receptors (Collingridge et al., 1983; Harris et al., 1984). However, recent studies indicated the involvement of

several additional receptors (Gruart et al., 2015). Moreover, one molecule, the brain-derived neurotrophic factor (BDNF), has aroused particular interest in studies of plasticity and is intimately involved in LTP-like plasticity processes (Akaneya et al., 1997; Lu, 2003).

If synaptic connections could only be enhanced and never attenuated, synaptic transmission would rapidly saturate – the strength of the synaptic connection might reach a point beyond which further enhancement is not possible. This led to the suggestion that neurons must have mechanisms to down-regulate synaptic function to counteract LTP. In fact such an inhibitory mechanism, termed LTD, was first discovered in the cerebellum and induced by conjunctive low-frequency stimulation of parallel fibers and climbing fibers in the cerebellar cortex (Ito and Kano, 1982; Ito et al., 1982). Moreover, LTD occurring at the synapses of parallel fibers and Purkinje cells has been proposed as a primary cellular mechanism for motor learning (Mauk et al., 1998; Ito, 2000; Hirano, 2014), including classical eyeblink conditioning (Medina et al., 2000; Koekkoek et al., 2003). Surprisingly, many forms of LTD also require activation of NMDA receptors (Desmond et al., 1991; Calabresi et al., 1992; Mulkey and Malenka, 1992).

Since the discovery of long-term synaptic plasticity, numerous studies have confirmed repeatedly that these specific neuronal changes underlie different forms of learning, such as learning of a new motor skill (Rioult-Pedotti et al., 1998, 2000) or classical CRs (Aiba et al., 1994; Shibuki et al., 1996; Gálvez et al., 2006; Gruart et al., 2006). In addition, it has been shown that all phases of classical eyeblink conditioning are dependent on *de novo* protein synthesis (Inda et al., 2005) and that structural plasticity occurs in the neocortex during eyeblink conditioning, demonstrating learning-dependent spine proliferations in the sensory cortex during training (Chau et al., 2014)

1.6. External modulation of neuronal activity during learning

For many years already the human has been remarkably fascinated by the idea of modulating learning, especially to improve or recover learning by modifying the neuronal activity. In recent decades, numerous researchers have been enthusiastic about

the method of inducing electric fields in the brain to alter learning by using different forms of non-invasive brain stimulation techniques. Since Barker mentioned in 1985 the presentation of electromagnetic pulses – produced by means of a magnetic field generator or 'coil' – to the cerebral cortex resulting in the induction of a focused electric field in the brain tissue, the technique termed transcranial magnetic stimulation (TMS) has experienced a rapid increase of applications to study cognition, motor function, as well as neurologic and psychiatric disorders (Hallett, 2000; Wassermann and Lisanby, 2001; Gershon et al., 2003; Rossi and Rossini, 2004). TMS is capable of generating electric fields with sufficient magnitude and density to depolarize neurons, but also presents neuromodulatory capacities when pulses are applied repetitively (repetitive TMS – rTMS) at subthreshold intensities (Rossi et al., 2009). Besides TMS, another technique based on the application of weak current through the scalp showed to induce changes in neuronal excitability mainly of the underneath lying neurons (Nitsche et al., 2008; Brunoni et al., 2012), though the electric field is more broadly distributed in the brain compared to TMS (Salvador et al., 2015). One specific form of electric current stimulation based on applying continuous weak currents through the scalp (Nitsche and Paulus, 2000) and termed transcranial direct current stimulation (tDCS) has been intensively studied in the last years. Despite the different modes of action, prolonged application of both rTMS and tDCS can induce after-effects on the excitability of neurons lasting minutes or even hours (Nitsche and Paulus, 2000; Iyer et al., 2003; Peinemann et al., 2004; Di Lazzaro et al., 2012; Márquez-Ruiz et al., 2012; Kuo et al., 2013; Koo et al., 2016). In the same manner, tDCS has been successfully used to modulate non-invasively learning processes (Reis et al., 2008; Bolognini et al., 2009; Reis and Fritsch, 2011; Ammann et al., 2016). Recently, more complex paradigms of transcranial current stimulation have been developed that rely on modulating current intensity rather than utilizing a constant current (Antal and Herrmann, 2016). The most widely used of these forms are transcranial alternating current stimulation (tACS) (Marshall and Binder, 2013; Márquez-Ruiz et al., 2016) and random noise stimulation (tRNS) (Terney et al., 2008; Paulus, 2011). tACS seems to interact with ongoing cortical oscillations enhancing, or reducing, the activity at specific electrocortical frequencies and their potentially related functions (Antal et al., 2008a; Fröhlich and McCormick, 2010; Kanai et al., 2010; Feurra et al., 2011; Schmidt et al., 2014). In turn, tRNS is a special form of tACS based on using alternating currents in a frequency spectrum generally between 0.1 Hz and 640 Hz. Recent studies

have demonstrated the modulatory effects of tRNS on cortical excitability and motor learning, similarly to rTMS and tDCS (Terney et al., 2008; Prichard et al., 2014).

The present study made use of tDCS to modulate cortical excitability with the purpose of investigating the role of the cerebral cortex during classical eyeblink conditioning. The following sections will focus on introducing the general aspects of this method, the underlying mechanisms, and its implication in learning.

1.7. Transcranial direct current stimulation (tDCS)

The historical origins of using electrical stimulation on tissue and for therapy follow the history of the discovery of electricity itself. Thus, in 43 – 48 AC Scribonius Largus used electro-sensitive animals such as the torpedo fish to deliver a strong direct electric current over the scalp of a patient with the purpose reducing headache pain (Priori, 2003). However, it was during the mid-18th century when the concept of electricity inspired more and more experimenters. The milestone experiments performed by Luigi Galvani (1737 – 1798) and Alessandro Volta (1745 – 1827), contributing to the discovery of bioelectricity and the generation of electricity through a voltaic pile (Galvani, 1791; Mauro, 1969; Boller et al., 1989), initiated the application of electricity in form of galvanic or direct currents as a treatment for various clinical conditions, particularly for mental disorders. Galvani's nephew Giovianni Aldini (1762 – 1834) was one of the first in applying a voltaic cell for transcranial brain stimulation (**Figure 1.4**) and reported successful treatment of patients suffering 'melancholic insanity' (Priori, 2003).

Many other researchers over the past two centuries made extensive use of the transcranial application of direct currents for the treatment of various disorders, obtaining variable results. However, just recently the technique of using low-intensity currents experienced resurgence in the field of basic and clinical research and for therapeutic applications, showing the ability to modulate cortical functions of the brain (Priori et al., 1998; Nitsche and Paulus, 2000). tDCS uses a low-intensity (usually 1 – 2 mA) constant current, applied directly to the head via two or more big size electrodes, which partially penetrates the skull and enters the brain (Miranda et al., 2006, 2013).

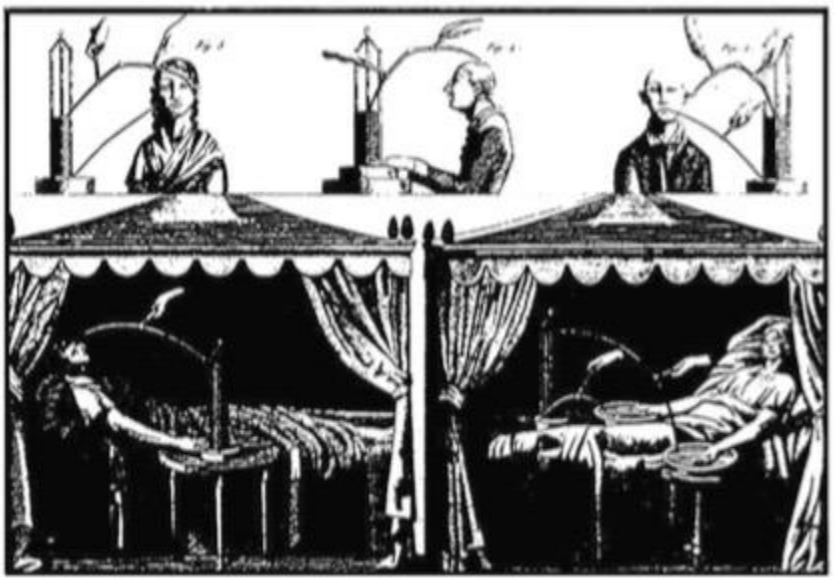

Figure 1.4 First experimental treatment of mental disorders with galvanic currents applied on the scalp by Giovanni Aldini in 1804. Patients undergoing brain polarization with different electrode positions on the scalp connected to a voltaic cell (top). Polarization of two recently deceased patients connected directly (left) or by saline solution (right) to a voltaic cell. Taken from Priori, 2003.

The size of the electrode, together with the applied intensity, determines the current density administered to the skull, which is an important parameter directly related to the strength of the electric field (Nitsche et al., 2008). tDCS can be applied with two different polarities, i.e., anodal or cathodal currents. Commonly assumed and as already demonstrated by neuronal recordings of early animal studies applying DC currents (Creutzfeldt et al., 1962; Bindman et al., 1964), anodal tDCS leads to an increase of neuronal excitability of the cerebral cortex underlying the active electrode, whereas cathodal tDCS, where the current direction is reversed, induces an excitability decrease (Nitsche and Paulus, 2000; Liebetanz et al., 2002; Nitsche et al., 2003a; Márquez-Ruiz et al., 2012). This initial promising finding, the easy and mainly well-tolerated application and the ability to induce long-lasting after-effects (Nitsche and Paulus, 2000, 2001; Batsikadze et al., 2013; Kuo et al., 2013) have resulted in an explosion of investigations in motor (Boggio et al., 2006a; Galea and Celnik, 2009; Reis et al., 2009; Hummel et al., 2010; Galea et al., 2011; Jayaram et al., 2012; Hardwick and Celnik, 2014; Cantarero et al., 2015), cognitive (Fregni et al., 2005; Marshall et al., 2005; Andrews et al., 2011) and perceptual domains using tDCS (Antal et al., 2004a; Ragert et al., 2008; Barbieri et al., 2016).

1.7.1. Basic mechanisms underlying tDCS

Although there is increasing interest for using tDCS as a non-invasive neuromodulation technique, little is known about the molecular and/or cellular mechanisms underlying its effects (Márquez-Ruiz et al., 2012). It must be taken into consideration that the net effect of tDCS depends on the stimulated brain region (Dieckhöfer et al., 2006), the number of tDCS sessions (Monte-Silva et al., 2013), the applied current intensity (Batsikadze et al., 2013) and the brain state (Silvanto and Pascual-Leone, 2008; Krause and Cohen Kadosh, 2014), among other parameters. tDCS is commonly defined as a 'subthreshold' or 'neuromodulatory' stimulation technique, since tDCS does not produce sufficient depolarization of the underlying neurons which would elicit action potentials (Nitsche et al., 2005). To understand the physiological mechanisms underlying these effects, it is important to dissociate: a) the immediate tDCS effects observed in cells exposed to simultaneous exogenous electrical fields and b) effects mediated by protein modifications requiring longer stimulation periods, lasting for several minutes after tDCS application.

From a physical point of view, immediate effects are elicited when an external electric field causes displacement of intracellular ions, thus altering the internal charge distribution and modifying neuronal membrane potential (Ruffini et al., 2013; Márquez-Ruiz et al., 2014), characterized by regions of depolarization and hyperpolarization across the neuron (**Figure 1.5**).

Thus, both polarities, anodal and cathodal, induce depolarization and hyperpolarization at the same time depending on the neuron's segment (Rahman et al., 2013, 2014; Kronberg et al., 2017). Animal studies have shown both neuronal morphology (Radman et al., 2009) and axonal orientation (Kabakov et al., 2012) are critical aspects to consider when explaining tDCS-induced responses, since the maximal effects occur when electric fields are applied parallel to the somato-dendritic axis (Bikson et al., 2004). Beyond these somatic changes produced in presence of the exogenous field, animal studies have also demonstrated the importance of presynaptic effects during current application (Kabakov et al., 2012; Márquez-Ruiz et al., 2012; Bikson and Rahman, 2013).

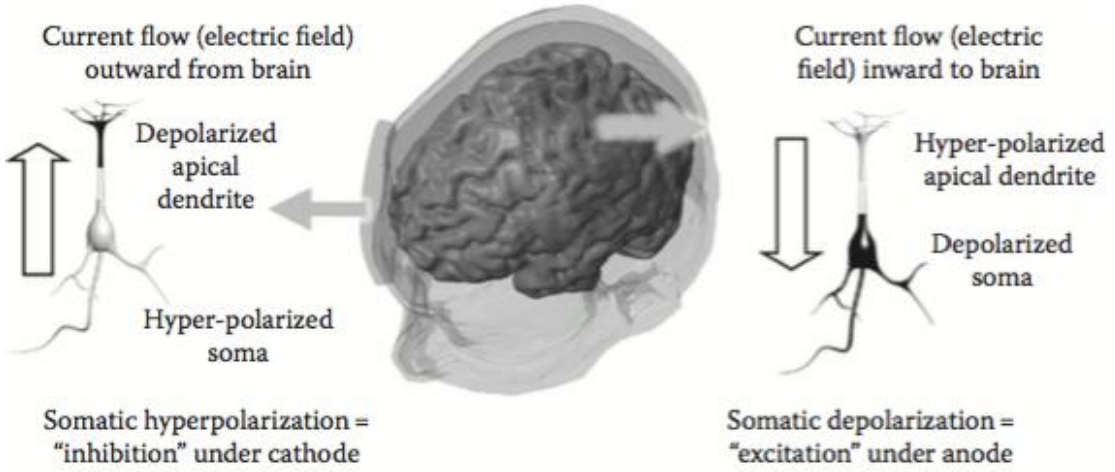

Figure 1.5 Simplified immediate tDCS effects on neuronal excitability. An inward current flow under the anode induces a somatic depolarization and a generic increase in excitability and function. Note that at the same time apical dendrites are hyperpolarized. On the other side, an outward current under the cathode produces a somatic hyperpolarization and a generic decrease in excitability and function. Note that in this case apical dendrites are depolarized. This figure shows that tDCS polarity cannot be exclusively associated to one direction (increase or decrease) of neuronal excitability. Taken from Bikson et al., 2012.

Early evidence for long-term effects in response to polarizing DC currents came from Bindman and colleagues (1964). Thus, they recorded long-term changes in neuronal excitability of the cerebral cortex in rats up to several hours after applying the currents, suggesting DC effects on plasticity comparable to LTP (**Figure 1.6**).

These findings have been confirmed recently by Rohan and colleagues (2015) demonstrating that *in vivo* tDCS enhanced posterior plasticity induction (LTP), eliciting long-lasting plastic changes in the hippocampus. Interestingly enough, Kronberg and colleagues (2017) applied direct currents in apical and basal dendritic compartments at Schaffer collateral synapses in CA1 of rat hippocampal slices concurrently with plasticity induction protocols (LTP/LTD). The authors showed that both anodal and cathodal currents acted as modulators of synaptic plasticity resulting in plasticity biased towards potentiation (i.e., LTP was enhanced and LTD was reduced, depending on the dendritic location).

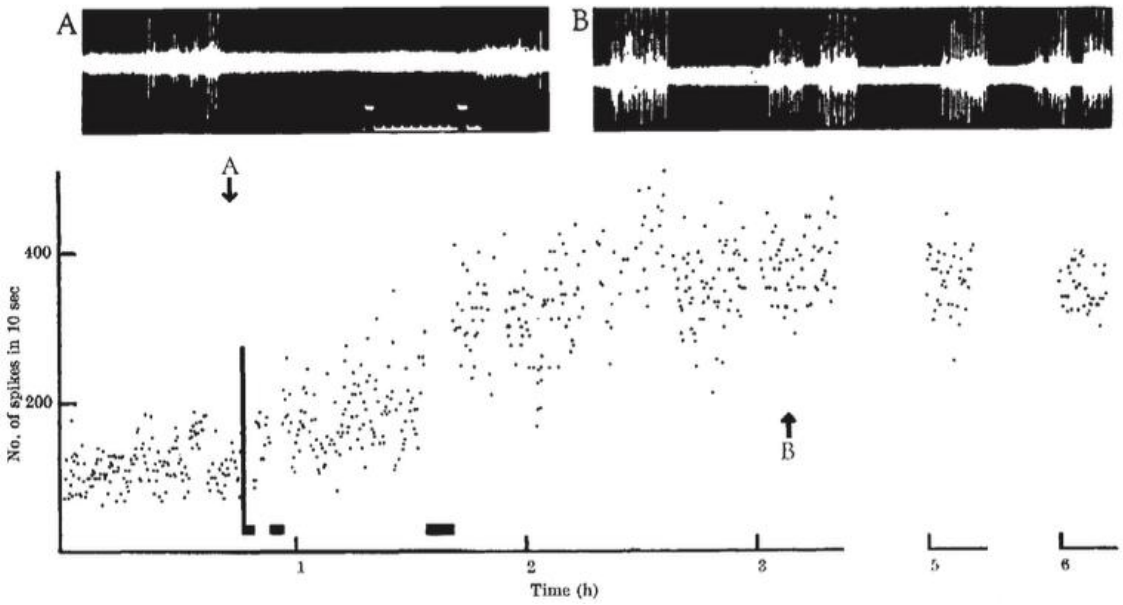

Figure 1.6 Long-term effects on neuronal excitability induced through polarizing anodal currents. Extracellular unitary recordings show neuronal activity (number of spikes in 10 sec) before and after passage of surface current in the exposed sensory cortex of an anaesthetized rat. The upper panel illustrates recording traces of a neuron immediately before (A) and 1h 20 min after (B) the end of polarization. Taken from Bindman, 1964.

Long-term effects as measured indirectly in human studies (recording motor evoked potentials, MEPs, elicited by transcranial magnetic pulses over MC) are mediated by NMDA and γ-aminobutyric acid type A ($GABA_A$) receptors (Stagg and Nitsche, 2011). Animal studies have confirmed the involvement of NMDA receptors and BDNF (Fritsch et al., 2010; Rohan et al., 2015; Podda et al., 2016) for the long-term effects observed after anodal tDCS, and adenosine A1 receptors (Márquez-Ruiz et al., 2012) after cathodal tDCS. Finally, the involvement of glial cells, and astrocytic Ca^{2+} surges in particular, has been recently related to anodal tDCS effects through astrocytic Ca^{2+}/IP_3 signaling (Monai et al., 2016). Thus, tDCS effects might not exclusively act through the induction of LTP/LTD-like processes, but rather through the modulation of the homeostatic cellular background regulating the intensity and direction of synaptic plasticity (Cirillo et al., 2017). Together, all these findings give strong rationale for the use of tDCS for learning protocols to modulate behavior, since LTP/LTD-like processes and DC-stimulation effects may share some common molecular substrates.

1.8. tDCS and learning

As previously mentioned, numerous researchers based their investigations on the neuromodulatory effect of tDCS addressing the question whether such intervention could be behaviorally relevant, i.e., capable of modulating learning and memory. Since neuronal plastic modifications of synaptic connections are thought to underlie learning and memory formation (see section 1.5), it seems plausible that learning acquisition and memory consolidation could be modified by tDCS. Thus, improvement of memory and learning processes in healthy people (Reis et al., 2008), in patients recovering deteriorated learning abilities after brain lesions (Wessel et al., 2015), and in patients with neurological diseases (Broeder et al., 2015) are being investigated extensively in both basic and clinical research studies. To make mention of a few examples, tDCS of the prefrontal cortex resulted in improved cognitive functions such as working memory in healthy and neurologically-affected subjects (Fregni et al., 2005; Boggio et al., 2006b; Ohn et al., 2008; Jo et al., 2009; Andrews et al., 2011; Orlov et al., 2016). On the other hand, tDCS applied over speech-related cortical areas enhanced language learning in healthy and nonfluent aphasic subjects (Flöel et al., 2008; Fiori et al., 2011; Meinzer et al., 2014). In fact, there is a long list of tDCS investigations showing interesting results from learning studies but probably one of the most extensively studied forms of learning in combination with the application of electrical currents is motor learning (Ammann et al., 2016; Buch et al., 2017).

Motor learning encompasses various forms of learning including, but not exclusive to, error-based, reinforcement, use-dependent plasticity and cognitive strategies (Krakauer and Mazzoni, 2011), each likely involving different neuronal substrates. It becomes more complicated given that these forms of learning likely all contribute to the learning process when acquiring a new skill (Kitago and Krakauer, 2013). To mention a few interesting findings, simultaneously applied anodal tDCS over MC during motor skill learning facilitated skill acquisition over several consecutive days of training in healthy subjects (Reis et al., 2009; Schambra et al., 2011; Saucedo Marquez et al., 2013). Specifically, tDCS promoted between-session improvement (Reis et al., 2009) and long-term retention processes (Saucedo Marquez et al., 2013). Regarding motor adaptation learning, a recent study applied tDCS to distinct brain regions while participants learned a visuomotor rotation task. Specifically, they found cerebellar

anodal tDCS resulted in faster reduction of errors caused by a consistent visuomotor rotation (Galea et al., 2011; Block and Celnik, 2013), whereas anodal tDCS over MC showed a marked increase in retention of the newly learned rotation (Galea et al., 2011). By using tDCS, this study was able to show an important dissociation in acquisition and retention processes related to motor adaptation and further highlighted the distinct roles of the cerebellum and MC in this type of learning.

Regarding associative motor learning like classical eyeblink conditioning, for the moment only very few human studies have investigated the neuromodulatory properties of tDCS to examine its impact on this type of learning. For instance, Zuchowski and colleagues (2014) reported modified acquisition and timing of CRs by cerebellar tDCS in a polarity-dependent manner. However, a recent study was not able to confirm these findings by applying tDCS on the cerebellum (Beyer et al., 2017). Moreover, Kotilainen and colleagues (2015) obtained faster acquisition of CRs in a semantic discrimination eyeblink conditioning with anodal tDCS over prefrontal cortex, but further investigations are required for an accurate interpretation of these results. The indications of a possible involvement of MC in the acquisition of CRs (see section 1.4.1) motivate further testing of tDCS over MC during associative motor learning.

1.8.1. Animal models for studying tDCS effects on learning

Although more investigations are needed to provide a better understanding of the effects induced by tDCS, its impact on motor learning and use for exploring neural substrates underlying motor learning have been demonstrated successfully. In other words, the potential of this technique for basic studies and future clinical treatments seems promising. However, in order to understand the neuronal mechanisms underlying the interaction between weak current application and learning processes, new animal models combining tDCS with behavioral tests are needed.

It must be taken into consideration that there are challenging differences in the methodology between human and animal model applications of tDCS and that future approaches should try to unify tDCS protocols for a better translation of results. Key differences between human and animal protocols are the size and relative position of

stimulating electrodes, the location of the electrodes in relation to the cerebral tissues (transcutaneously, transcranially, or epidurally), and the state (anesthetized or awake, constrained or freely moving) of the animal during the tDCS intervention (Márquez-Ruiz et al., 2014). Additional approaches that have provided fundamental insights of the underlying mechanisms of tDCS effects and how the membrane potential of neurons is modified are slice preparations (*in vitro*) (Bikson et al., 2004; Radman et al., 2009; Rahman et al., 2013).

The methodological challenge in animal models for tDCS protocols is probably the main reason for the reduced number of publications examining tDCS effects in the learning animal. Regarding classical eyeblink conditioning, Márquez-Ruiz and colleagues (2012) demonstrated potentiated or depressed acquisition of CRs produced by anodal or cathodal tDCS over S1 of rabbits when stimulation of the whisker pad was used as CS (**Figure 1.7**).

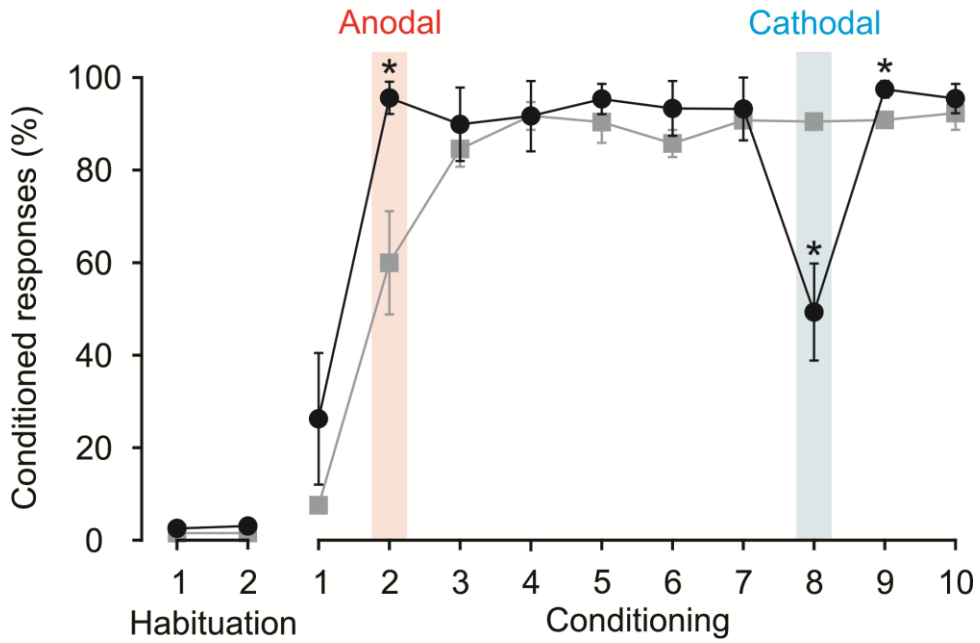

Figure 1.7 Effects of tDCS applied over somatosensory cortex on classical eyeblink conditioning in rabbits. The evolution of learned eyeblink responses (percentage of CRs) for an experimental tDCS group and a control group are represented. The experimental group received anodal tDCS during the second conditioning session (C2) and cathodal tDCS during C8. Learning acquisition was significantly enhanced through anodal and impaired through cathodal tDCS. Modified from Márquez-Ruiz et al., 2012.

These findings aroused new insights into the mechanisms underlying associative learning, highlighting the potential of tDCS for modulating new behavior acquisition and for studying the role of the sensory cortex during eyeblink conditioning. Moreover, the results from Márquez-Ruiz and colleagues provide an ideal starting point for studying other cortical regions, such as the MC, and their function during this type of motor learning.

1.9. tDCS and sensory perception

The nature of sensory perception and its complex neuronal processing in the brain and particularly the neuromodulation of sensory experience are currently highly investigated concepts. Thus, the application of tDCS in humans proved to be capable of modulating sensory perception thresholds (Antal et al., 2003; Rogalewski et al., 2004; Ragert et al., 2008), as well as pain perception (Boggio et al., 2008; Lefaucheur et al., 2008; Antal et al., 2008b). Moreover, in regard to pain threshold modulation, a rat study showed that a combination of DC:AC current applied through the skin overlying the anterior pole of the frontal lobe induced significant anti-nociceptive effects in the animals measured by tail-flick and hot-plate tests (Nekhendzy et al., 2004). The modulation of somatic perception presents another interesting topic which has been addressed by the previously mentioned study from Márquez-Ruiz and colleagues (2012). The authors reported amplitude modulation of local field potentials (LFPs) recorded in S1 induced by concurrent tDCS over the same brain region, as well as polarity-dependent modulation of CRs acquisition when whisker stimulation was used as CS. They proposed that tDCS is capable of modulating the intensity of whisker perception. The same group demonstrated that natural whisker perception could be substituted by synthetic tactile perception induced through tACS applied over S1 in behaving rabbits (Márquez-Ruiz et al., 2016). Since earlier studies not only demonstrated changes in the S1 excitability after the application of direct currents, but also of visual cortices (Creutzfeldt et al., 1962; Cambiaghi et al., 2011), another interesting unanswered question to investigate is whether tDCS applied over V1 in the awake animal is capable of modulating visual sensory perception when a light stimulation is used as CS in a classical conditioning protocol.

1.10. Safety aspects and limitations of tDCS

Undoubtedly, the number of positive findings described in the preceding paragraphs highlights the potential use of tDCS for modulation of new behavior acquisition and retention, identification of processes underlying learning, and characterization of the role of different brain regions. Furthermore, tDCS may have significant clinical applications, such as neurological rehabilitation and therapeutic treatment. However, it is important to acknowledge that many limitations and experimental challenges of this technique must be overcome in future investigations. The low focality inherent to this technique (Miranda, 2013), the need for developing new translational-designed animal models (Jackson et al., 2016), the considerable variability across findings and experimental protocols (Bennabi et al., 2014; Horvath et al., 2014), and subsequently, the challenge of reproducing and predicting effects (Wiethoff et al., 2014; Dyke et al., 2016; Nuzum et al., 2016; Ammann et al., 2017), are only some of the known limitations of tDCS.

On the other hand, one of the many advantages, tDCS is considered a well-tolerated technique (Brunoni et al., 2012; Bikson et al., 2016), but caution is always required with an investigational tool. Moreover, given that most montages produce current flow through more than one brain region, animal models provide an essential tool to increase safety confidence and identify hazards before applying tDCS at higher intensities or with long durations, especially in vulnerable populations (e.g., children). With this in mind, a pioneering study was performed by Liebetanz and colleagues (2009) to address possible harmful effects of higher intensities and longer durations of cathodal tDCS applied over the rat skull. Their findings show that current densities higher than 14.3 mA/cm^2 for durations greater than 10 minutes provoked first DC-induced lesions in the cortex. Current densities generally used in clinical studies are in the range from 0.03 to 0.08 mA/cm^2 (Nitsche et al., 2008) – more than two orders of magnitude lower than the value reported from Liebetanz and colleagues. The authors concluded that tissue heating might be the most relevant reason for the observed deleterious effects induced by cathodal tDCS. This, in turn, raises the question whether lower current densities of tDCS are also capable of warming up the underlying brain tissue, even without producing visible lesions. For the moment, the only studies addressing possible temperature effects of tDCS on brain tissue are based on the results of computational

models (Bikson et al., 2009; Datta et al., 2009). Thus, direct physiological measures of the brain temperature during tDCS application are urgently needed, especially to confirm that the repeatedly observed effects of tDCS on behavior are not completely or in part a result of tissue warming of the brain region underneath the tDCS electrodes.

2. OBJECTIVES

Classical conditioning of eyeblink responses has been extensively studied for more than 50 years in human (Cason, 1922) and particularly in animal (Gormezano et al., 1962) investigations. Given that this type of learning involves the generation of motor responses, prior research has been especially focused on characterizing the role of movement-related brain areas, such as the cerebellum and the cerebellar nuclei during this associative learning (Freeman and Steinmetz, 2011). Surprisingly, little attention has been awarded to the role of the MC, despite the knowledge that this brain region is a critical neural site involved in the acquisition and performance of new motor abilities (Doyon and Benali, 2005; Shmuelof and Krakauer, 2011). Regarding classical eyeblink conditioning, there is some evidence from earlier studies pointing towards an implication of the MC in the acquisition process of this learning (Woody et al., 1991; Aou et al., 1992; Birt et al., 2003). However, a comprehensive characterization of the firing activity of MC neurons during classical conditioning has not been accomplished yet. A similar situation can be found with respect to other cortical cortex areas and their barely-explored role during the learning of CRs.

For these reasons the **general aim** of this study was to examine and characterize cortical activity and its contribution to the acquisition of classical conditioned eyeblink responses. For this purpose, the following **specific objectives** were addressed experimentally:

1. Characterize the firing activity of identified neurons in the MC during the acquisition of classical eyeblink conditioning and investigate MC projections to specific nuclei involved in motor responses of the *orbicularis oculi* muscle.

2. Underline the importance of the MC during eyeblink conditioning by taking advantage of tDCS techniques to modulate the MC excitability during the associative learning process.

3. Explore the contribution of the sensory cortex in classical conditioning of eyeblink responses through describing the impact of tDCS on V1 during learning and by comparing with the effects obtained from previously performed MC modulation.

4. Continuously measure epidural brain temperature below the tDCS site during and after prolonged exposure to transcranial direct currents to rule out that tissue heating induced by tDCS interfered with the observed effects on learning.

3. MATERIAL AND METHODS

3.1. Animals

All experiments were carried out on adult rabbits (New Zealand White albino, from Isoquimen, Spain) weighing 2.3 - 2.7 kg upon arrival. Before and after surgery, animals were maintained in the same room but placed in independent cages. Animals were kept on a 12 h light/dark cycle and with a continuous control of humidity (55 ± 5 %) and temperature (21 ± 1 ºC). Food and water were available *ad libitum.* All experiments were performed in accordance with Spanish (BOE 34/11370-421, 2013) and European Union (2010/63/EU) guidelines for the use of laboratory animals in chronic experiments. In addition, these experiments were submitted to and approved by the local Ethics Committee of Pablo de Olavide University (Seville, Spain).

3.2. Experimental preparation

3.2.1. Experimental groups

The present Doctoral Thesis studied the role of the cerebral cortex during classical conditioning of eyelid responses in the awake rabbit. A total of four experiments were carried out. The first experiment (**Experiment 1, n = 10**) served to characterize MC neuronal activity using extracellular single-unit recordings with glass micropipettes during classical eyeblink conditioning and to identify different groups of MC neurons antidromically activated from the contralateral facial nucleus (FN) or the ipsilateral RN related to associative learning. Moreover, injections with a neuronal tracer were carried out to explore possible monosynaptic projections from MC to FN. In a second series of experiments, modulation of MC excitability was examined using non-invasive tDCS which was performed by passing electrical currents through a silver chloride (Ag/AgCl) disc electrode placed over the MC skull during learning (**Experiment 2, n = 6**). Moreover, to explore the contribution of the sensory cortex to the mentioned learning process and to compare with MC modulation results, electrodes for visual evoked potential (VEP) recording and tDCS application were placed over V1 (**Experiment 3, n = 3**). Finally, to rule out that tissue heating induced by the transcranial stimulation underlies the observed tDCS effects epidural thermal variations of the transcranially

stimulated site were measured by implanting a Negative Temperature Coefficient (NTC) thermistor below the tDCS electrodes (**Experiment 4, n = 3**).

3.2.2. Preoperative and anesthesia

The animals fasted for 12 hours prior to surgery. The day of surgery they received a protective injection of atropine sulfate (0.5 mg/kg) to prevent unwanted vagal responses. After that, animals were anesthetized via intramuscular injection with a mixture of ketamine (50 mg/mL, Imalgene, Merial Laboratorios, Spain) and xilazine (20 mg/mL, Rompun, Bayer, Germany) at an initial dosage of 0.85 mL/kg. Once anesthetized, the upper part of the head, part of the nape and the lower edges of the ears were shaved and disinfected with an antiseptic solution (Betadine®, Mundipharma GmbH, Germany). A local anesthesia (EMLA® Cream, AstraZeneca, Germany) was applied on the ear's edges and a flexible cannula (Abbocath®) was introduced in the vein, in general, of the right ear to establish a controlled intravenous flow (10 mg/kg per h) of anesthesia for surgery. A temperature probe was inserted rectally and coupled with a temperature control system (TR-200, Fine Science Tools INC., Germany) for retro-alimentation of a heating pad placed under the animal. In this way, body temperature was kept constant at physiological values during the surgery. Afterward, the head of the animal was fixed to the stereotaxic apparatus (Model 1240, David Kopf Instruments, CA, USA) by means of zygoma clamps, adjustable tooth bar and a nose clamp. Surgical material and area were sterilized before use.

An anteroposterior (AP) incision in the skin along the midline of the head, from the front leading edge to the lambdoid suture, was performed. The skull was exposed by retracting the muscles. Subsequently, the periosteum of the exposed surface of the skull was removed and washed with Ringer solution at 38 °C. The animal's head was correctly positioned to mark the position of *Bregma* and *Lambda* as stereotaxic cero. With the help of an alignment tool for rabbits (Model 1244, David Kopf Instruments, CA, USA), a depth difference of 1.5 mm ($\Delta P_{(\beta-\lambda)}$ = 1.5 mm) between *Bregma* y *Lambda* was established. The stereotaxic-cero marks served as reference points for the correct placement of stimulating and recording electrodes, taking advantage of the stereotaxic coordinates of the Rabbit Atlas (Girgis and Shih-Chang, 1981).

3.2.3. Implantation of stimulation electrodes

Experiment 1: To identify antidromically the MC neurons, bipolar stimulating electrodes were implanted in the ipsilateral RN and in the contralateral FN in one group of animals (n = 7; **Figure 3.1**). These electrodes were manufactured with varnished silver wires (0.2 mm, California Fine Wire Company, CA, USA). Two 65 mm-long segments of wires were stretched and glued together with cyanoacrylate (Loctite®, Henkel AG & Co. KGaA, Germany) cutting a bevel at one end to allow penetration of the electrode into the tissue. The glued and cut silver cables were connected to a stainless steel needle for better attachment of the electrode to a micromanipulator.

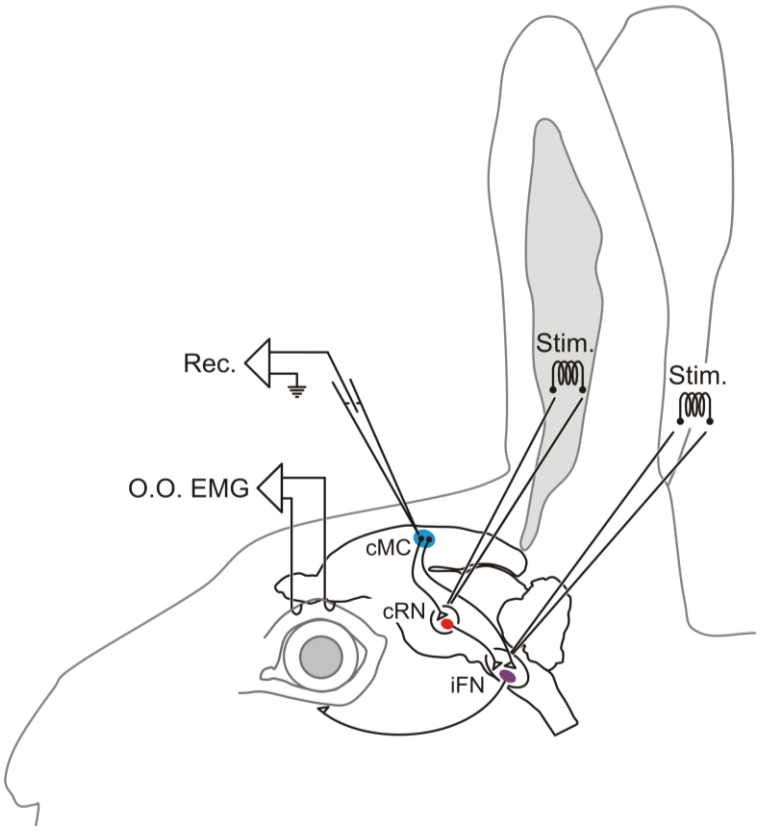

Figure 3.1 Stimulation and recording sites for Experiment 1. Schematic presentation of stimulating electrodes in contralateral red nucleus (cRN) and ipsilateral facial nucleus (iFN) with respect to the trained eye (left) during classical conditioning, and recording site at contralateral motor cortex (cMC) by the use of glass micropipettes. Animals were chronically implanted with EMG recording bipolar hook electrodes in the left *orbicularis oculi* muscle (EMG O.O.).

Prior to electrode implantation, a hole was drilled in the skull with a dental drill (NSK Volvere max, Nakanishi Inc., Japan) according to the stereotaxic coordinates obtained from the atlas (Girgis and Shih-Chang, 1981). The coordinates were 8.5 mm AP to *Bregma* and 1.5 mm lateral (L) for RN and 3.6 mm AP to *Lamdba* and -2.0 mm L for FN. With respect to FN location the electrode was introduced with an angle of 20º AP

and 5º L to avoid the intersection of the dural venous sinuses. The dura mater was removed using a sterile needle and the electrodes were carefully introduced. The approximate depth was obtained from the atlas, whilst the precise depth of the electrode ($Depth_{RN}$ = 13.0 mm; $Depth_{FN}$ = 15.0-17.0 mm) was achieved by observing the maximum response of eyelid movement induced by bipolar electrical stimulation using square pulses of 50 µs duration and intensities of 1.2 ± 0.3 mA (mean ± standard error of the mean - SEM, n = 7) applied to the corresponding electrode. Finally, the electrodes were fixed to the skull using dental cement (Duralay, Dental Mfg.Co., IL, USA).

3.2.4. Implantation of tDCS electrodes

Experiment 2 – 4: In rabbits, as opposed to humans, the skin overlying the cranium is highly movable with respect to the underlying bones. For this reason, tDCS was applied through electrodes placed directly over the skull. Different types of stimulating electrodes were used for tDCS stimulation. For **Experiment 2** and **4** tDCS was carried out using a prefabricated silver chloride disk electrode (Ag/AgCl, 0.5 cm^2, ø 8 mm, 1 mm thickness, A-M Systems, Germany), whilst for **Experiment 3** a precisely focused active stimulating electrode (Márquez et al., 2012, 2016; Ruffini et al., 2014) was manufactured consisting of four silver-ball electrodes. A 380 µm silver wire (A-M Systems, Germany) was cut into pieces of different lengths and one end of each piece was burned with a lighter until a ball (ø 1 mm) was formed. Finally, the electrodes showed lengths between 4 and 7 cm. In order to insulate the wire, the electrode was introduced into a flexible tubing (Silicone Tubing, A-M Systems, Germany) with an inside diameter of 500 µm, exposing both ends. For correct placement of each silver-ball electrode, a small mark was made on the skull (according to the stereotaxic coordinates) using the dental drill. Once the marks were obtained, the four silver-ball electrodes were placed symmetrically 2 mm distanced from the corresponding coordinate point (AP = 10.0 mm, L = -7.0 mm for V1; Polyanskii et al., 2010). Subsequently, the electrodes were fixed carefully with cyanoacrylate and dental cement to the skull in order to ensure that no liquids seeped under the electrodes.

In case of the silver chloride disk electrode, the electrode was placed on the skull only throughout the experimental sessions. For this, during surgery, a plastic tube (ø 8 cm, 8

mm length) was fixed vertically with cyanoacrylate to the skull according to the stereotaxic coordinates. For **Experiment 2** (n = 6) and **4** (n = 3) the tube was placed on MC (AP = -2.0 mm, L = 2.0 mm; Pacheco-Calderón et al., 2012), filled with gauze and plugged with a plastic piece to avoid the skull becoming dirty throughout the days without experiments. During experiments the silver disk electrode was inserted with electro-gel in the plastic tube for tDCS application.

3.2.5. Implantation of electrodes for recording the electroencephalographic (EEG) activity

Experiment 3: For EEG recording of VEPs four silver-ball electrodes (1 mm ø, A-M Systems, Germany) were placed epicranially above V1 (AP = 10.0 mm, L = -7.0 mm. The complete procedure for fabrication and placement of the silver-ball electrodes is explained in the previous section 3.2.4.

3.2.6. Implantation of electrodes for electrical activity recording of the orbicularis oculi

Experiment 1 – 3: For classical conditioning of eyelid responses the animals were equipped with implanted recording bipolar hook electrodes in the left *orbicularis oculi* muscle for evaluation of the CRs. These electrodes were made of 7-strands Teflon-coated stainless-steel wire (A-M Systems, Germany) with an external diameter of 50 µm (bared), 6 cm long and bared ~ 1 mm at the tip. Before implantation in the *orbicularis oculi* muscle, one end of the wire strands was fanned and folded as a hook in order to maximize muscle attachment. The prepared wire was inserted into the muscle with the aid of a syringe needle (21 G) which served as a guide during the procedure.

3.2.7. Access to recording sites

Experiment 1: Animals were prepared for chronic extracellular recording of unitary activity in the MC area during classical eyeblink conditioning (**Figure 3.1**). For this, under septic conditions, a window (6 mm x 4 mm) was drilled through the parietal bone centered on the right MC region (AP = -2.0 mm, L = 2.0 mm) corresponding to the

eyelid area (Pacheco-Calderón et al., 2012). The window was carefully cleaned with Ringer solution at 38 ºC and traces of dust and bone fragments were removed. A sterile stainless-steel needle (21G) with a curved tip was fixed with dental cement in the central area of one window border (the closest to the midline of the skull) serving as stereotaxic reference point throughout the recording sessions. A recording chamber around the window was constructed with dental cement which covered the excavated bone edges. The dura mater was maintained intact and, between the experimental sessions, the surface was protected with an inert silicone cover (Silastic®, BioPlexus Corporation, CA, USA) and sterile gauze on which a small amount of antibiotic (Gentamycin 0.3%) was applied. Finally, the hole was sealed by a layer of bone wax (Ethicon®, Johnson & Johnson Intl., NJ, USA).

3.2.8. Placement of reference electrodes

Experiment 1 – 3: A silver electrode in contact with the dura mater was attached to the left parietal bone as electrical reference point for extracellular unitary-activity recordings (**Experiment 1**) and, in case it was necessary, for EMG recordings (**Experiment 1-3**). The electrode was prepared with silver wire (0.65 mm) forming a loop at one end to facilitate posterior grasping by the amplifier equipment. The opposite end of the electrode was braided and filed to avoid damaging the dura mater. A hole was drilled in the left parietal bone with the coordinates AP = 10.0 mm and L = -6.0 mm (except for animals of Experiment 3 where the hole was made on the right side to avoid interference with the silver-ball electrodes for tDCS). The reference electrode was carefully introduced in the hole and fixed to the skull with dental cement.

3.2.9. Implantation of epidural NTC thermistor for brain temperature measurement

Experiment 4: In the last group of animals (n = 3), the brain temperature was measured to examine epidural thermal variations of the transcranially-stimulated site during and after prolonged tDCS. With this in mind, a NTC thermistor (10 Ω of resistance, ø 2.41×6.5mm, Series B57863S, EPCOS, Germany) was implanted in the epidural space of MC. For implantation a hole (ø 2 mm) was drilled in the frontal bone 10 mm apart from the transcranial stimulation site and, thereby, the NTC was

horizontally introduced along the inferior side of the skull without damaging the dura mater. Previously, the distance from the drilled hole to the corresponding MC coordinates (AP = -2.0 mm, L = 2.0 mm) was measured and marked with an indelible marker on the NTC wires to determine the depth the NTC had to be introduced in the hole to end up directly above the MC. Finally, the hole was carefully closed with dense dental cement to protect the intracranial space.

3.2.10. Implantation of the head-holding system and connectors

Experiment 1 – 4: The stimulating and recording electrodes (**Experiment 1 – 3**), as well as the NTC thermistor (**Experiment 4**) were soldered to a 9-pin socket placed on the frontal part of the animal's head. In all animals (except in the animals used for immunohistology) a head-holding system was implanted, consisting of three bolts (20 mm long, ø 2 mm) cemented to the skull perpendicularly to the stereotaxic plane (**Figure 3.2,** number 1). One bolt was placed above the frontal bone to the right of the cranial midline and the other two were placed above the parietal bone on each side of the midline. To obtain solidity for the whole head-holding system, five stainless-steel screws with blunt end (5 mm long, ø 2 mm) were fixed to the skull and interconnected with themselves, with the skull and with the three bolts using dental cement. A single dental cement turret attached to the skull was constructed holding the restraining system of the head, the multiple electrodes, the recording chamber (Experiment 1) and the 9-pin socket soldered with the electrode terminals. Finally, the edges of the skin around the turret were closed by stitches in the front and rear end of the incision and an antiseptic and healing ointment (Blastoestimulina®, Almirall Prodesfarma S.A., Spain) was applied on the wounds.

3.2.11. Injection of neuronal tracers

Experiment 1: One group of animals (n = 3) was used for injection of the anterograde neuroanatomical tracer biotinylated dextran amines (BDA) with the purpose of marking possible MC-efferent axonal projections in the FN, specifically in the *orbicularis oculi* region. First, a hole (ø 2 mm) was drilled in the skull according to the MC coordinates (AP = -2.0 mm, L = 2.0 mm). Subsequently, a 10 µl microsyringe (Hamilton®, NV, USA) was filled with 9 µl BDA tracer and situated on the micromanipulator arm

according to the MC coordinates. The dura mater was carefully removed using a bended needle. The microsyringe was lowered until touching the surface of the cortex and from this point it was introduced 3 mm in the brain via the micromanipulator. At different points of depth (3, 2, and 1 mm from the brain surface) an amount of 3 µl of BDA tracer was injected with a rate of 0.3 µl/min during 10 min in each mentioned point. A period of 10 min was established between each injection before ascending to the next point of depth so that the injection of a total of 9 µl BDA was completed after 60 min. The microsyringe was carefully removed and the hole was covered with dental cement. Finally, the edges of the skin in the front and rear end of the incision were closed with stitches and a healing and antiseptic ointment was applied on the wounds.

3.2.12. Postoperative

Once the surgery was finished, the intravenous cannulation of the ear vein was removed and the injection site was covered with sterile gauze attached with tape. To prevent infections, 1 ml (1.000.000 U.I.) of Penicillin G Procaine (Penilevel®, Laboratorios ERN S.A., Spain) was applied via intramuscular injection. After surgery, the animals stayed in their cages for recovery and observation for at least one week.

3.3. Experimental procedures

3.3.1. Immobilization of the experimental subject

Experimental sessions began two weeks after surgery. Each animal was placed in a Perspex restraining box (**Figure 3.2**, number 2) designed for limiting animal's movements (Gruart et al., 2000a). The recording room was kept softly illuminated. The first two sessions consisted of adapting the animal to both the restrainer and the experimental conditions; no stimulus was presented (max. 30 min each session). In a third session, the animal was presented to similar conditions but with the head fixed by means of the implanted bolts of the head-holding system to an attached arm of the recording table. The sessions previous to the experimental sessions served to reduce the stress level of the animals and to familiarize them with the experimental conditions.

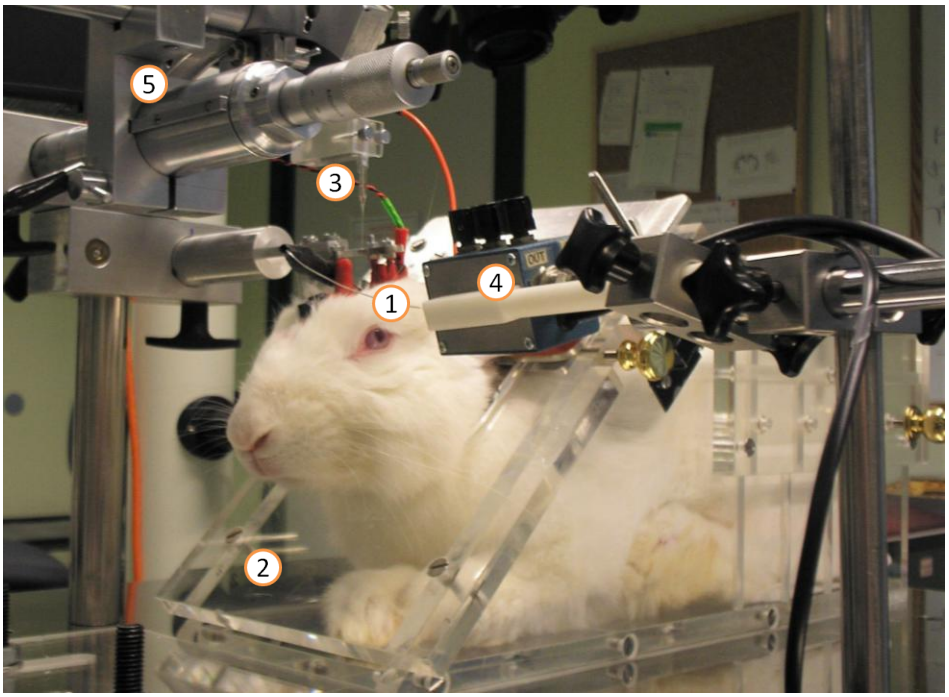

Figure 3.2 Experimental set up for extracellular unitary recording in the awake animal. 1, Head-holding system consisting of three bolts attached to the skull by dental cement; 2, Perspex restraining box designed for limiting animal's movements; 3, Glass micropipette filled with NaCl attached to holder; 4, NEX-1 preamplifier connected to micropipette and ground; 5, Micromanipulator.

3.3.2. Identification of the palpebral MC neurons

Experiment 1: To ensure the appropriate recording site for firing activity, bipolar stimulation was performed in the region of the supposed coordinates for palpebral MC (AP = -2.0 mm, L = 2.0 mm). The aim was to activate multisynaptic pathways resulting in the activation of motoneurons related to the *orbicularis oculi* and to record the muscle activation via the implanted electrodes in the eyelid. The electrodes for MC stimulating were similar to the implanted electrodes used for stimulation of RN and FN, manufactured with varnished silver wires (0.2 mm, California Fine Wire Company, CA, USA). For the experiment the animal was placed in the restraining box and positioned on the recording table. The head was fixed to the arm of the table, and bone wax, gauze and silicone cover sealing the recording window were removed with the aid of a surgical microscope (M 400-E, Leica, ©Leica Microsystems, Switzerland). Then, the cerebral surface was carefully cleaned with super fine tweezers (#5) without damaging the dura mater. The electrode was fixed to a specific holder which, in turn, was attached

to the micromanipulator (Model Camberra, Narishige, Japan). On the other end, it was connected to an isolation unit (ISU 165, Cibertec, Spain) to adjust scale, intensity and polarity of stimulation. The electrode was moved to the coordinates corresponding to the palpebral MC. The surrounding dura mater was locally removed before introducing the electrode at the point of interest. Then, the electrode was gradually lowered with the micromanipulator. First, the applied electrical stimulation consisted of trains of 10 bipolar square pulses with a pulse duration of 50 μs and frequency of 200 Hz generated by a stimulator device (CS-20, Cibertec, Spain). Once contralateral *orbicularis oculi* activation was observed, stimulation was changed to 50 μs bipolar square pulses with a frequency of 0.5 Hz. Various EMG activations were recorded and the exact coordinates were annotated for posterior extracellular unitary-activity recording experiments.

3.3.3. Recording of extracellular unitary activity and identification of MC neurons

Experiment 1: Extracellular unitary activity of MC neurons was recorded using manufactured glass micropipettes (Corning, MA, USA; **Figure 3.2,** number 3) with an external and internal diameter of 3 and 2.5 mm, respectively. The pipettes were produced with a glass microelectrode puller (Model PE-2, Narishige, Japan) adjusting the parameters to produce pipette tips with an adequate length (~ 20 mm). Subsequently, the sealed pipette tips were broken carefully under an optical microscope to obtain tips with a diameter between 4 and 5 μm (3 – 5 MΩ of resistance). At the beginning of each experimental session the fabricated glass pipettes were filled with 2 M NaCl. The animal was placed in the restraining box and positioned on the recording table. The head was fixed to the arm of the table and the recording window was cleaned as previously explained in section 3.3.2. The micropipette was partially covered with aluminum foil to reduce electromagnetic noise and fixed to a specific holder which, in turn, was attached to the micromanipulator (Model Camberra, Narishige, Japan). The conducting solution of the glass micropipette was connected by a silver wire to a NEX-1 preamplifier (x100) (Biomedical Engineering, NY, USA; **Figure 3.2,** number 4) and from there to a differential amplifier (x20) (AM 502, Tektronix, OR, USA). The previously implanted ground together with the aluminum folder covering the micropipette was connected to the preamplifier. Recording was filtered using a bandwidth between 1 Hz and 10 kHz. In order to display the signal, it was transmitted to an audiomonitor (AUMON 14, Cibertec, Spain), to the acquisition system (1401-plus,

CED, UK), to a digital phosphor oscilloscope (TDS 3014C, Tektronix, OR, USA) and an analog-digital scope (HM-407, HAMEG Instruments GmbH, Germany). The next step was to place the micropipette precisely above the tip of the implanted reference needle using the micromanipulator. If the tip of the pipette broke during the procedure, it was replaced by a new one. Once the micropipette was adjusted to the coordinates of the reference needle, the calculations of approximation to the palpebral MC were performed. The insertion angle of the pipette varied between 0 and 5 degrees in the lateral axis. Before introducing the pipette at the point of interest, the surrounding dura mater was locally removed. Then, the micropipette was gradually lowered with the micromanipulator (**Figure 3.2**, number 5). The extracellular unitary activity recording was carried out along depths between few micrometers from the cerebral surface and maximum 9 mm.

Antidromic or orthodromic (i.e., synaptic) field potentials were evoked by electrical stimulation of RN or FN and served to identify the MC neurons of interest. The applied electrical stimulation consisted of 50 μs bipolar square pulses with a frequency of 0.5 or 0.1 Hz generated by digital stimulator devices (CS-220, CS-20, Cibertec, Spain). Each stimulator was connected to an isolation unit (ISU 165, Cibertec, Spain) for scale, intensity, and polarity adjustment of stimulation. The applied intensity of RN and FN stimulation was, generally, 200% of the individual threshold necessary to induce first potential fields, ensuring the generation of action potentials. Criteria to determine whether the recorded and the activated neuron were the same, and to discriminate somatic vs. axonic recordings, were systematically followed. First, the stimulus intensity was reduced to confirm the immediate (and no gradual) disappearance of the activation (all or nothing concept of a unitary activation) to rule out that the observed activation represented a population field of neurons. Second, it was checked whether the latency of the activation was constant over several given stimuli, being a typical property of antidromic activations. Finally, a collision test was carried out which consisted of providing an electrical stimulus of different time intervals (0.5 – 1.5 ms) immediately after a spontaneously occurring action potential of the neuron of interest. A window discriminator (PDV 225, Cibertec, Spain) was adjusted to detect these spontaneous firings and to generate an electrical stimulus in RN or FN via the Cibertec stimulators. In case of an antidromically-activated neuron, the spontaneously occurring orthodromic spike collides with and abolishes the electrically activated spike (Lipski,

1981), which resulted from the stimulation of RN or FN in this experiment. It is important to point out that the method of antidromic identification is biased towards the detection of neurons with fast-conducting axons, whereas sub-populations with very slow-conducting, nonmyelinated axons (especially present in the neocortex) are often missed and not identified (Swadlow, 1998; Firmin et al., 2014).

For proper identification of the recording sites, at the end of all recording sessions small electrolytic lesions were carried out in selected places. Lesions were performed with the help of tungsten electrodes (1MΩ of resistance) using a direct current at 0.5 – 1 mA for 10 to 20 s. Once a recording session was finished, the recording micropipette was raised and removed. The recording chamber was sterilized and closed again with the inert silicone cover, gauze and bone wax.

3.3.4. EEG recording of visual evoked potentials (VEPs)

Experiment 3: The characterization of VEPs in the visual cortex produced through light stimulation was carried out by using the same silver-ball electrodes as for tDCS application. To select the most representative VEP recording of each animal, thirty VEPs were recorded from each of the 4 epicranially-implanted silver-ball electrodes, using a NEX-1 preamplifier (x10) (Biomedical Engineering) and a Tektronix AM 502 differential amplifier. The averaged (n = 30) VEPs recorded from each electrode served to select the most appropriate silver-ball electrode which was used along the subsequent experimental sessions. The light flashes were generated by a Photic Stimulator (GRASS PS33 PLUS, Grass Instruments, MA, USA) placed 12 cm from the right eye of the animal. For VEP recording, light stimulation was presented in trains of 20 flashes at 1 Hz and the Photic Stimulator was set at intensity 1.

3.3.5. Recording of the electromyographic activity of the orbicularis oculi

Experiment 1 – 3: For eyeblink conditioning sessions, EMG activity from the *orbicularis oculi* muscle was recorded with implanted recording bipolar hook electrodes connected to a preamplifier and an AC/DC differential amplifier (x1000) with a bandwidth of 10 Hz to 10 kHz (Model 3000, A-M Systems, Germany).

3.3.6. Measurement of the brain temperature

Experiment 4: For brain temperature measurement an epidural NTC thermistor (10 Ω resistance, ø 2.41×6.5mm, Series B57863S, EPCOS, Germany; **Figure 3.3*A***) implanted above the MC was used as thermally sensitive resistor. The resistance of the thermistor decreased exponentially with increasing temperature. With this in mind, the NTC translator was connected to a conditioning circuit which adjusted the exponential variations in a linear fashion. With the purpose of determining the brain temperature via the voltage (V) variations of the NTC, a simple theoretical equation was applied (1):

(1) $$y\,(V) = \frac{1}{4} * x\,(^{o}C) - 7.5$$

Where *y* is the voltage in volts and *x* the temperature in degrees Celsius.

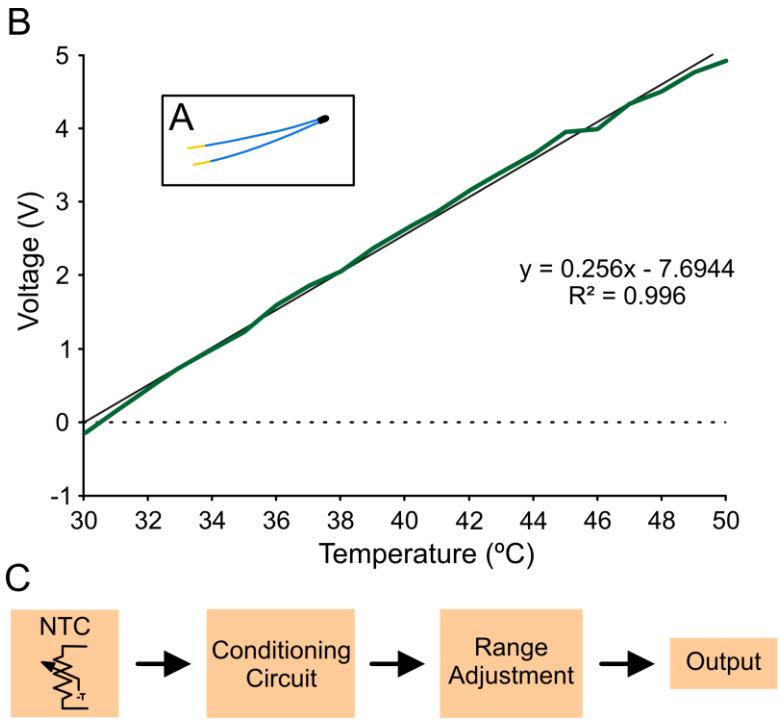

Figure 3.3 Measurement of brain temperature with a Negative Temperature Coefficient (NTC) thermistor ***A,*** NTC. ***B,*** Experimentally obtained linear output equation of the NTC thermistor. ***C,*** NTC circuit: NTC translator connects to conditioning circuit which adjusts the exponential variations to a linear increase. Finally, the range adjustments for voltage (from 0 to 5 V) and for temperature (from 30º to 50º C) are executed.

Finally, the range adjustments for voltage (from 0 to 5 V) and for temperature (from 30 to 50 ºC) were executed (**Figure 3.3*C***). Prior to the brain temperature measurement with simultaneous tDCS, the NTC was experimentally tested outside the animal brain. For this purpose, the voltage variations were measured at different water temperatures ranging from 30 to 50 ºC. The recorded values represented in **Figure 3.3*B*** show a high approximation to the theoretical equation (1).

3.3.7. tDCS

tDCS was delivered by a battery-driven linear stimulus isolator (A395 Linear Stimulus Isolator, WPI, FL, USA) and the current characteristics like duration and down- and up-ramping were established by a high-performance data acquisition interface and software (1401-plus, Spike2 version 7, CED, UK). Two different types of active electrodes were used. For **Experiment 2** and **4** tDCS application was carried out with a prefabricated silver chloride (Ag/AgCl) disc electrode, whilst a precisely focused active stimulating electrode consisting of four silver-ball electrodes was applied for **Experiment 3**. During experimental sessions, the silver chloride disk electrode was inserted to the epicranial plastic tube previously implanted on the skull. To establish conductivity between the disc electrode and the tissue, a generous amount of electro-gel (ELECTRO-GEL™, Electro-Cap International, Inc., OH, USA) was introduced to the plastic tube. In both cases a saline-soaked sponge electrode (surface area = 35 cm^2) attached to the contralateral ear (except Experiment 3 where it was the ipsilateral ear) served as counter electrode (**Figure 3.4**).

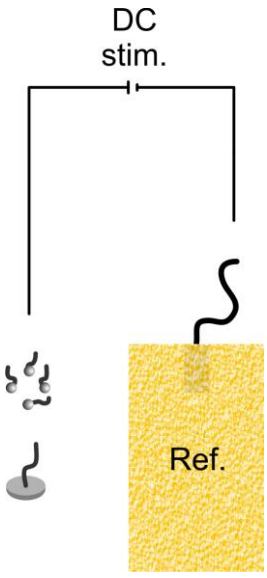

Figure 3.4 Electrode configurations for tDCS (DC stim.). According to the experiment two different types of epicranial active electrodes were used. For Experiment 2 and 4 a prefabricated silver chloride disk electrode was used, whilst for Experiment 3 stimulation was applied by means of four silver-ball electrodes. In both cases a saline-soaked sponge electrode attached to the ear served as reference electrode (Ref.).

Experiment 2-4: For tDCS application, weak direct currents with anodal or cathodal polarity (when the anode or cathode was placed above the region of interest, respectively) were employed between active and reference electrodes. Depending on the experiment, the applied stimulation durations consisted of repeated periods of approximately 10 min (in total ~ 30 min) for classical conditioning experiments (**Experiment 2** and **3**) or a single period of 20 min for studying tDCS after-effects on VEPs in **Experiment 3**, whilst for **Experiment 4** a tDCS duration of 60 or 120 min served to investigate whether tDCS induces tissue heating. For the tDCS experiments with the silver-disc electrode (0.5 cm^2), the current density was 2 mA/cm^2 for 1 mA of intensity, whilst for the four silver-ball electrodes (4 x 0.016 cm^2) it was 15.63 mA/cm^2, i.e., 3.91 mA/cm^2 for each ball to reach 1 mA. According to the current distribution in a spherical rabbit head model (Miranda et al., 2006; Márquez-Ruiz et al., 2012), the maximum current density in the stimulated brain tissue for the silver-ball electrodes was 0.37 mA/cm^2 when 1 mA was applied. Consistent with the experimental requirements, tDCS intensities applied in the different experiments presented in this Doctoral Thesis ranged from 14.6 μA to 2 mA. The exact information of applied tDCS duration, intensity and density currents will be specified for each experiment in the Results section.

3.3.8. Classical eyeblink conditioning

Classical conditioning of eyelid responses was achieved using either delay or trace conditioning paradigms. Depending on the experiment performed, one of two different CS (tone or flashes) and an air puff directed to the left cornea as US were applied. The air puffs were delivered from a pressure ejection system (Biomedical Engineering) and applied through the opening of a plastic pipette (ø 3 mm) attached to a holder fixed to the recording table. The first two conditioning sessions consisted of the sole random presentation of the corresponding stimulus selected as CS (habituation sessions, H1 – H2). Generally, each animal was trained for ten successive days (conditioning sessions, C1 – C10) presenting CS and US. In addition, in the case of **Experiment 3** up to four extra sessions (C11-C14) were performed, whilst for **Experiment 1** the conditioning sessions with simultaneous neuronal recording were executed during extended periods (up to 40 sessions). Conditioning sessions generally consisted of 66 trials, i.e., 6 series of 11 trials each (when tDCS was applied during conditioning, series 1, 3, and 6

received no tDCS [OFF], whereas series 2, 4, and 6 received active tDCS [ON]). Successive trials were separated at random by intervals of 50 – 70 s. Of the 66 trials, six were test trials in which the CS was presented alone. A conditioning session lasted for about 80 min (**Figure 3.5*B***). Except for sessions where the recording of one single cell (Experiment 1) could be maintained longer than the mentioned duration, the conditioning session was extended (up to 180 min).

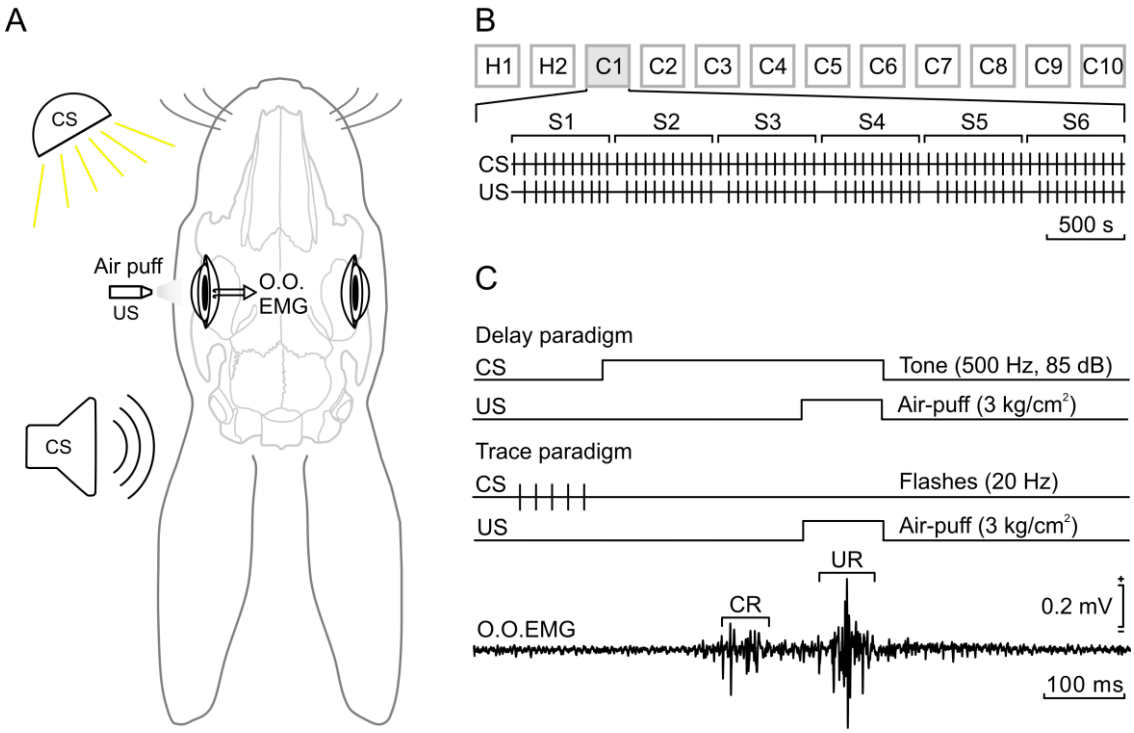

Figure 3.5 Classical eyeblink conditioning protocol ***A,*** Experimental design with indication of different conditioned stimuli (CS – tone or flash), unconditioned stimulus (US – air puff) and location of EMG recording electrodes (O.O. EMG). ***B,*** Each conditioning protocol consisted of 2 habituation and 10 conditioning sessions (for Experiment 1 and 3 extra conditioning sessions were carried out). Conditioning sessions consisted of 66 trials (6 series of 11 trials each) separated at random by intervals of 50-70 s. Of the 66 trials, 6 were test trials in which the CS was presented alone. ***C,*** Delay and trace paradigm protocols. From top to bottom, delay paradigm with tone as CS and air puff as US, trace paradigm according to experiment with CS (flashes) and air puff as US, and a representative EMG recording (O.O. EMG) from the *orbicularis oculi* muscle with indication of conditioned response (CR) and unconditioned or reflex response (UR).

3.3.8.1. Trace and delay paradigms

Experiment 1 and 2: For the delay paradigm of eyeblink conditioning a 350 ms binaurally tone was presented to the animal as CS. After 250 ms, the tone was followed by a puff of air with 100 ms of duration and a pressure of 3 kg/cm^2 directed at the left cornea as US. Thus, the tone co-terminated with the air puff (**Figure 3.5*A,C***, delay paradigm). A function generator (AFG 3022B, Tektronix, OR, USA), triggered by a digital output (1401-plus, CED, UK), was used to produce the pulse with the specific tone characteristics (Sine wave, 500 Hz, 175 cycles, 1V). An amplifier (PA Amplifier FS-2035, FONESTAR SISTEMAS, S.A., Spain) converted the pulse in a tone (85 dB) through a speaker.

Experiment 3: For the trace paradigm of eyeblink conditioning, a CS (flashes of light) of 100 ms duration was followed 250 ms from its end by a 100 ms, 3 kg/cm^2 puff of air directed at the left cornea as US. The binocular light flashes (100 ms, 20 Hz) were generated by a Photic Stimulator (GRASS PS33 PLUS, Grass Instruments, MA, USA) placed 60 cm from the animal's head (**Figure 3.5*A,C***, trace paradigm).

3.3.9. Histology

3.3.9.1. Perfusion and tissue processing

At the end of each experiment, the animals were anesthetized with sodium pentobarbital (50 mg/kg, ip) and perfused through the left ventricle with 9‰ saline followed by 4% paraformaldehyde in phosphate buffer (PB, 0.2 M, pH 7.4). The proper location of the EMG recording electrodes was then checked. Subsequently, the brain was removed and preserved 24 h in 4% paraformaldehyde solution. Previous to the processing of the tissue, brains were cryoprotected with 30% sucrose in 0.2 M PB. To carry out the cutting of the fixed tissue, the brains had to descend completely to the bottom of the sucrose container. Brains destined for microscopic observation were cut into coronal sections (50 μm) with the aid of a freezing sledge microtome (SM2000R, Leica Biosystems Nussloch GmbH, Germany). The obtained slices were stored in 0.2 M PB in successive series until used. Selected sections including the recording and stimulated sites were mounted on gelatinized glass slides and stained using the Nissl

technique with 0.1% toluidine blue, in order to determine the proper location of stimulating and recording sites and to exclude tDCS-related tissue damage.

3.3.9.2. Immunohistochemistry

Experiment 1: Brains were immediately cryoprotected for fluorescence immunohistochemistry after perfusion with 30% sucrose in PB. To carry out the cutting of the fixed tissue, the brains had to descend completely to the bottom of the sucrose container. Then, coronal sections (50 μm) were obtained with a sliding freezing microtome (SM2000R, Leica Biosystems Nussloch GmbH, Germany) and stored at –20 °C in a solution of glycerol (30%) and ethylene glycol (30%) in PB until used. Tissue was processed "free-floating" for immunohistochemistry and all of the sections studied passed through all procedures simultaneously to minimize any difference from immunohistochemical staining itself. In order to analyze the projections from MC to FN a double label was performed using primary antibody against the enzyme choline acetyltransferase (ChAT, Millipore Iberica S.A.U, Spain), which synthesizes acetylcholine and avidin against biotinylated dextran amine (BDA-10,000 MW; Molecular Probes, USA) injected as described above. Next, the sections were incubated for 1 h with 10% normal donkey serum (NDS) (AbDSerotec, MorphoSys, UK) in phosphate buffered saline (PBS) with 0.2 % Triton-X-100 (Sigma-Aldrich, MO, USA) and then they were incubated overnight at room temperature with goat polyclonal IgG anti-ChAT (1:100) with PBS containing 0.2 % Triton-X-100 and 3 % NDS. The second day, sections were washed and incubated for 1 h with anti-goat IgG secondary antibody generated in donkey and conjugated with Alexa 555 (1:200, MilliporeIberica S.A.U, Spain) in PBS containing 0.2 % Triton-X-100 and 3 % NDS and, subsequently, sections were incubated with avidin conjugated with Alexa 488 (1:200, MilliporeIberica S.A.U, Spain). Finally, sections were mounted on slides and coverslipped using Prolong Gold antifade reagent fluorescent mounting medium (Millipore Iberica S.A.U, Spain). The sections were observed under a confocal microscope (TCS SPE, Leica, Biosystems Nussloch GmbH, Germany). Z-series of optical sections (1 μm apart) were obtained using sequential scanning mode. These stacks were processed with Image J software (http://rsb.info.nih.gov/ij/).

3.4. Data collection and analysis

3.4.1. Data acquisition

Extracellular unitary-activity, VEP recordings, tDCS converted signals, unrectified EMG activity of the *orbicularis oculi* muscle, 1-V rectangular pulses corresponding to CS, US, and air-puff stimulations presented during the different experiments were stored digitally on a computer through an analog/digital converter (1401-plus, CED, UK) for quantitative off-line analysis. Collected data were sampled at 25 kHz for unitary-activity recording in MC, at 20 kHz VEP recordings or at 10 kHz for EMG recordings, with an amplitude resolution of 12 bits. A computer program (Spike2 version 7 from CED, UK) was used to display single, overlapping, averaged, and raster representations of unitary activity, EEG and temperature recordings, and EMG activity of the *orbicularis oculi* muscle.

3.4.2.Extracellular unitary activity analysis

Experiment 1: In most cases, it was easy to identify the recorded MC neurons by isolating the neuron of interest from other neurons during experimental recording sessions. In cases where it was not possible to isolate and record a single cell, Spike Sorting (with Spike2) was performed for classifying the different recorded neurons. Finally, an event channel for each identified neuron was created in which each event corresponded to a spike. The program enabled the representation of peristimulus time histograms (PSTHs) and/or the firing rate of recorded neurons. When necessary, PSTHs were converted to firing rate following this equation (2) (Rieke et al., 1997):

(2) $$Firing\ rate\ \left(\frac{spikes}{s}\right) = \left(\frac{No.\ of\ spikes\ per\ bin}{No.\ of\ repetitions}\right)\ x\ \left(\frac{1000}{bin\ size\ (in\ ms)}\right)$$

With the aid of cursors, the latency, the PSTHs, and the instantaneous firing rate of unitary recordings could be quantified.

3.4.3. VEP analysis before and after tDCS

Experiment 3: To describe and represent the changes in V1 excitability after anodal or cathodal tDCS application, the VEPs induced by the light stimulation were averaged for control and post-stimulation situation. Each average consisted of representative VEPs ($n \leq 300$) of 30 min recording (20 flashes every 2 min) discarding the VEPs with artifacts. To determine whether tDCS induced modulatory effects on VEPs properties, the amplitude and onset latency of the components P1 and N1 of the averaged VEPs (every 300 s) were measured with the aid of cursors (Spike2) and statistically analyzed.

3.4.4. Analysis of conditioned responses

Experiment 2 – 3: In order to characterize the eyelid responses, the EMG recording of the *orbicularis oculi* muscle was rectified and integrated, to obtain the integrated area (IA). Subsequently, the CR onset was defined as the point where the IA of the CR (IA_{CR}) overtook the integrated activity during the 200 ms before CS onset (control situation, $IA_{control}$; **Figure 3.6**).

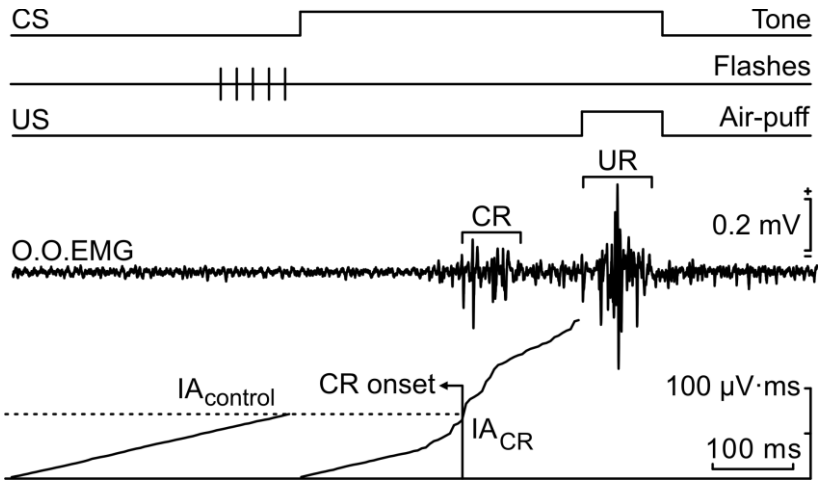

Figure 3.6 Analysis of conditioned responses. From top to bottom, CS (tone, flashes) and US (air puff) presentations, representative EMG recording from *orbicularis oculi* (O.O. EMG) with indication of conditioned response (CR) and unconditioned response (UR), and integrated area (IA) of the EMG recording before CS onset ($IA_{control}$) and of the CR (IA_{CR}) after CR onset. The CR onset was defined as the point where the integrated activity of the CR (IA_{CR}) overtook the integrated activity during the 200 ms before CS onset ($IA_{control}$). CR and UR are indicated. Calibration as indicated.

The strength of the response was quantified calculating the relative area value for each response as the ratio between IA_{CR} and $IA_{control}$. When this ratio value was 1.1 (for Experiment 2) or 1.2 (for Experiment 3) the response was considered a CR. The threshold ratio value was set at 1.1 for Experiment 2 due to the recorded EMG noise level of one animal. The CR latency was calculated as the time difference between the CS initiation and the CR onset. According to the experiment and the aim of the quantification, the analysis was performed with all data (CRs and non-CRs) or only with the CRs.

3.4.5. Statistical analysis

The computed results were processed for statistical analyses using the SPSS-software (IBM SPSS Statistics for Windows, Version 20.0, IBM Corp., NY, USA) and SigmaPlot 11.0 (Systat Software, CA, USA) package. The statistical significance was set at $P < 0.05$. Unless otherwise indicated, data are always represented as the mean ± SEM.

Experiment 2: Statistical significance of CRs-values between experimental and control group throughout each conditioning session was inferred by one-way analysis of variance (ANOVA). In the same way, to determine the significant differences of relative area and onset latency values between specific days, *t*-tests for between-group analysis and one-way repeated measures ANOVA ($ANOVA_{RM}$) with factor SESSION for within-group analysis were executed. When a statistical significance was found, *post hoc* pairwise comparisons using Bonferroni correction for multiple comparisons was performed.

Experiment 3: Acquired data of VEP amplitude and latency from before and after tDCS application were statistically analyzed with Friedman of repeated measures analysis ($Friedman_{RM}$) since data did not permit normality assumption. For adjustment of multiple comparisons a Student-Newman-Keuls *post hoc* method was executed. For the statistical analysis of evolution of CRs percentage, relative area and latency of eyelid responses, $ANOVA_{RM}$ with the factor SESSION and Bonferroni as *post hoc* procedure for correction of multiple comparisons were applied.

Experiment 4: The course of the brain temperature values (raw and normalized) before, during and after tDCS (both anodal and cathodal) was statistically analyzed by $ANOVA_{RM}$ with the factor TIME. Greenhouse-Geisser was applied to correct for non-sphericity. *Post hoc* comparisons using Bonferroni method were performed for correction of multiple comparisons.

4. RESULTS

Experiment 1

4.1. Characterization of the MC activity during classical eyeblink conditioning

The neuronal activity of the MC was recorded to identify and characterize palpebral MC neurons during the conditioning of eyelid responses in the rabbit. Moreover, the MC projections to RN and FN were studied. An immunohistological study was carried out to demonstrate the existence of direct neuronal connections from MC to FN. Recorded neurons were identified by their antidromic activations as a result of electrical-pulse stimulation of the ipsilateral RN and contralateral FN and with the help of the collision test. Once identified, the firing activity of these neurons was observed during the performance of the classical eyeblink conditioning in order to analyze whether a relationship between firing rate and motor learning performance could be established. A schematic representation shows the experimental design for this experiment (**Figure 4.1*A***).

4.1.1. Identification of the palpebral MC region

The MC eyelid recording area was successfully approached following a previous electrophysiological study (Pacheco-Calderón et al., 2012) and by bipolar pulse stimulation of the cerebral cortex in accordance with available stereotaxic coordinates (Girgis and Shih-Chang, 1981). Depending on intensity, the electrical pulses given in the area corresponding to the palpebral motor neurons activated the contralateral *orbicularis oculi* muscle as already reported in a recent study (Pacheco-Calderón et al., 2012). The **Figure 4.2** shows a representative EMG activation of the *orbicularis oculi* after stimulating the contralateral palpebral MC (Stim. MC). The stimulation evoked an activation of the eyelid with a latency of 10.1 ± 0.3 ms (n = 20; range: 9.2 – 11.7 ms). Taken into account the anatomical distance, the small variability in latency of muscle activation from MC is suggestive of a disynaptic projection.

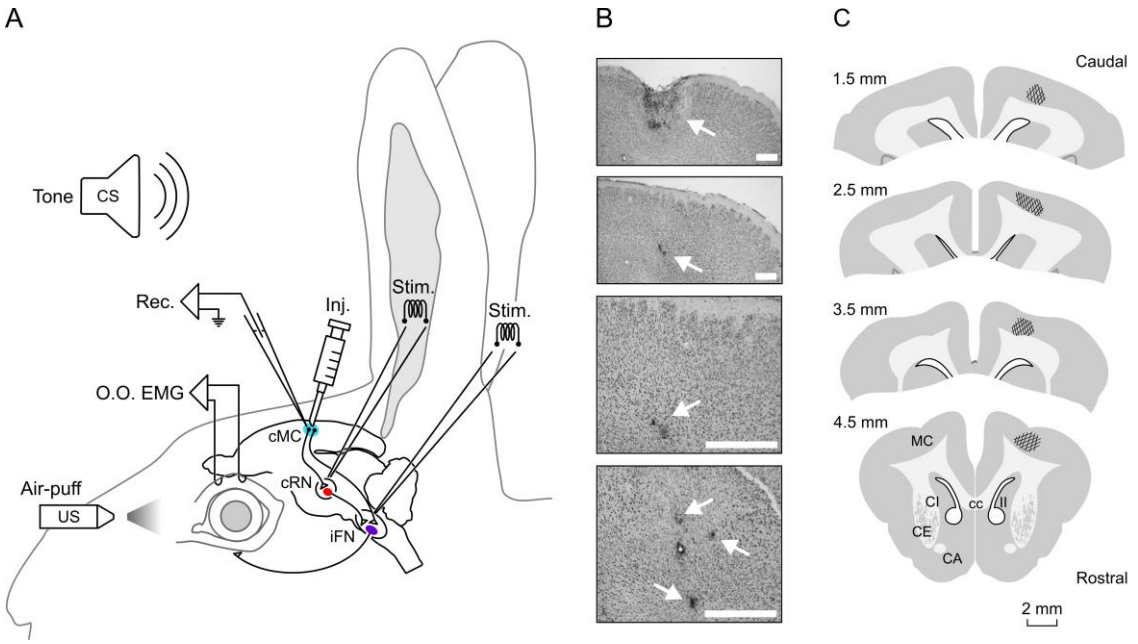

Figure 4.1 Experimental design. ***A***, Classical conditioning of eyelid responses was achieved with the help of a delay-conditioning paradigm. Animals were chronically implanted with EMG recording bipolar hook electrodes in the left *orbicularis oculi* muscle (EMG O.O.) in order to evaluate the evoked CR. The US consisted of an air puff presented to the ipsilateral cornea and the CS consisted of a binaurally tone. MC neurons contralateral (cMC) to the left eye were recorded with a glass micropipette (Rec.) inserted into MC areas. Stimulating microelectrodes (Stim.) were implanted in the contralateral red nucleus (cRN) and ipsilateral facial nucleus (iFN) with respect to the trained eye. For subsequent histological studies microinjections (Inj.) with BDA tracer were carried out in MC. ***B***, Photomicrographs of MC coronal sections illustrating recording window (top picture and arrow) and electrolytic marks (three bottom pictures and arrows) made with stimulating electrodes implanted in selected recording sites are represented. CA, anterior commissure; cc, corpus callosum; CE, external capsule; CI, internal capsule; II, lateral ventricle. Calibration bars: 1 mm. ***C***, Diagrams illustrating the recording sites following the atlas of Girgis and Shih-Chang (1981).

Small electrolytic-lesion marks made at the end of the recording sessions indicated that MC neurons related to the reflex, spontaneous and conditioned eyelid responses occupied a dorsal position in the rostral part of the rabbit cortical motor area (**Figure 4.1*B*-*C***). With the help of these electrolytic marks and collected information regarding stereotaxic coordinates, a reconstruction of the location of recorded MC neurons (n = 257) included in this study was made. **Figure 4.1*C*** illustrates that these neurons formed a cell column (AP = 1.5-4.5 mm; L: 2-4 mm) over the dorsal MC (Girgis and Shih-Chang, 1981), i.e., the facial area of the MC is not located laterally like in cats or primates (Nieoullon and Rispal-Padel, 1976; Nudo et al., 2001; Hashimoto et al., 2013).

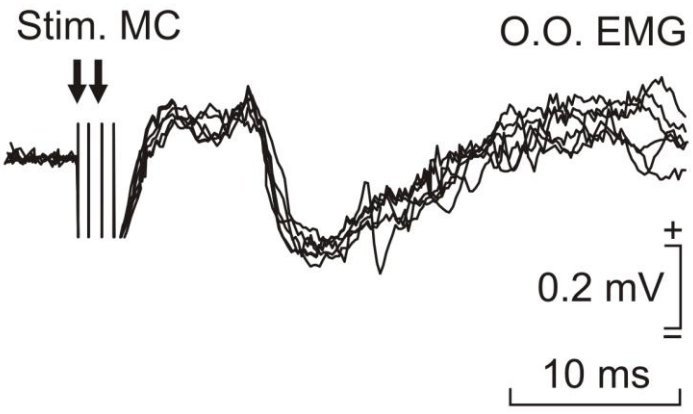

Figure 4.2 Direct *orbicularis oculi* activation by bipolar pulse stimulation of the MC. Representative EMG activity (O.O. EMG) of the *orbicularis oculi* muscle after stimulating the contralateral palpebral MC (Stim. MC) with double (2-ms interval) pulses. Calibration as indicated.

4.1.2. Immunohistological identification of direct neuronal connections to the facial nucleus

To further confirm that the identified MC region was involved in eyelid responses, the anterograde BDA tracer was injected in the MC recording area of three animals (**Figure 4.3*A-B***) and axon terminals located within the FN were checked. For identification purposes FN motoneurons were labeled with ChAT (**Figure 4.3*C-D, G***). Confocal photomicrographs of BDA labeling showed the presence of relatively few anterogradely labeled axons near or closely apposed to ChAT-expressing FN motoneurons (**Figure 4.3*E-F, H-I***). Apart from the longer distance, the low density of MC axon terminals present in the dorsolateral FN could explain the low number of antidromic MC neurons activated from this nucleus (n = 25) as compared with those activated from the RN (n = 189), corresponding to a much larger and denser projection (Davies et al., 1994; Horn et al., 2002).

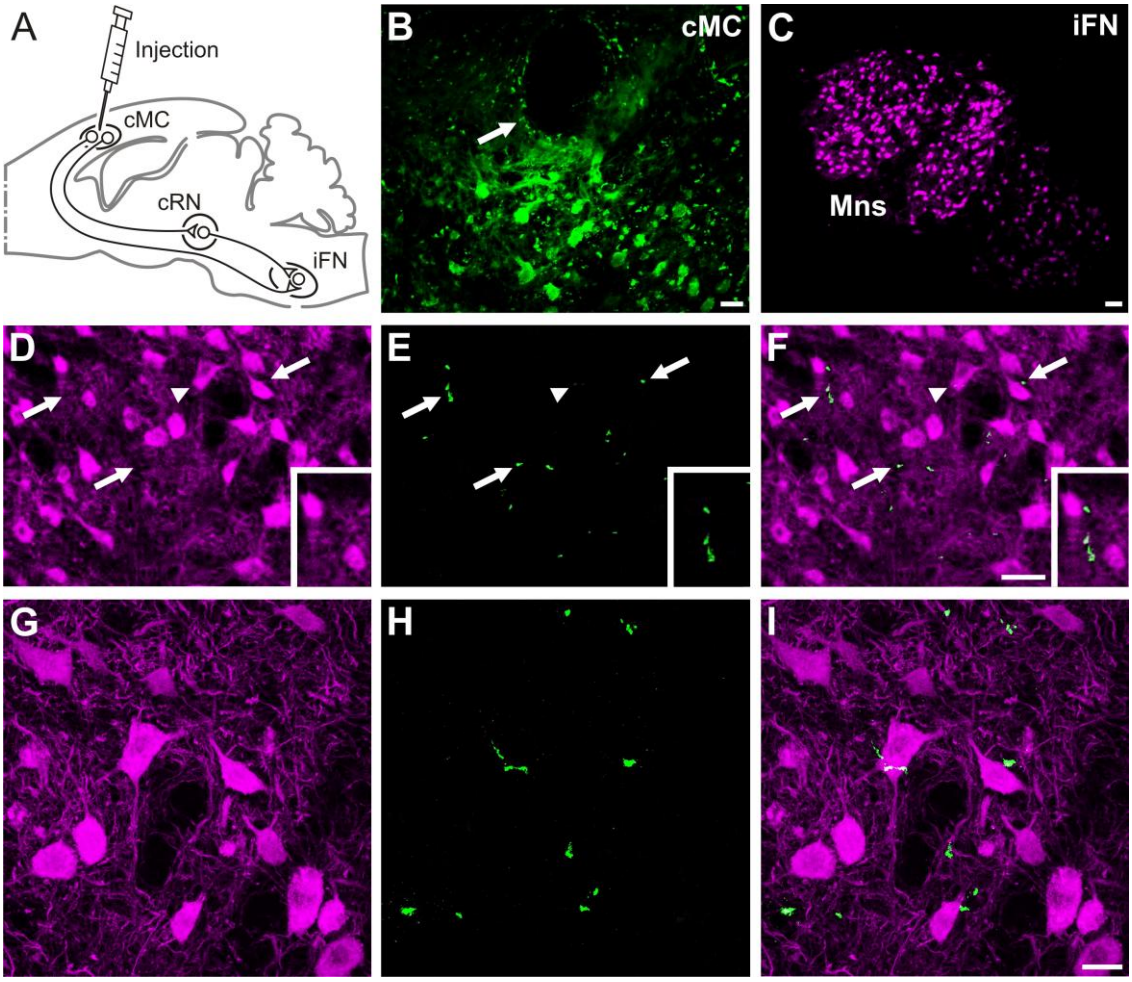

Figure 4.3 Confocal photomicrographs of BDA labeling and ChAT-expressing cells. ***A***, Diagram of BDA tracer injection in the MC contralateral to the left eye (cMC). ***B***, BDA-labeled cells located in the MC near the injection site (arrow). Scale bar: 30 µm. The photomicrograph is a 2D projection of 24 consecutive focal planes located 1 µm apart. ***C***, FN motoneurons expressing ChAT. Scale bar 100 µm. ***D-F***, ChAT-expressing FN motoneurons (magenta) and fibers labeled with BDA (green). Arrows indicate axons anterogradely labeled with BDA. Scale bar: (displayed in ***F***) ***D-F***, 50 µm. Insets in ***D-F*** are enlarged (30%) views of labeled FN motoneurons and MC projecting axons. Photomicrographs are 2D projections of 29 consecutive focal planes located 1 µm apart. ***G-I***, Same ChAT-expressing cells indicated in ***D-F*** with arrowheads. Note the axons anterogradely labeled with BDA near or closely apposed to ChAT-expressing FN motoneurons. Scale bar (displayed in ***I***) ***G-I***, 25 µm. Photomicrographs are 2D projections of 22 consecutive focal planes located 0.5 µm apart.

4.1.3. Electrophysiological identification of the recorded MC neurons

The electrophysiological recordings in MC during classical conditioning of eyelid responses in well-trained animals (after 8th day of conditioning) revealed a number of neurons with a firing activity related to the performance of the motor learning. The different identified neuronal groups are exposed in the following sections.

4.1.3.1. Identified MC neurons projecting to the facial nucleus

The electrical stimulation of the FN activated, in total, 25 neurons recorded in the contralateral palpebral MC (**Figure 4.4.1*A***). With the aid of the collision test and by means of the typical non-variable activation latency – in case of fast conducting axons (Swadlow, 1998) – the neurons were identified as antidromically-activated neurons (**Figure 4.4.1*B***). The antidromic stimulation of these neurons evoked a mean activation latency of 5.03 ± 0.18 ms (mean ± SEM, n = 25) at the palpebral motor area, with an activation range between 2.02 and 6.63 ms.

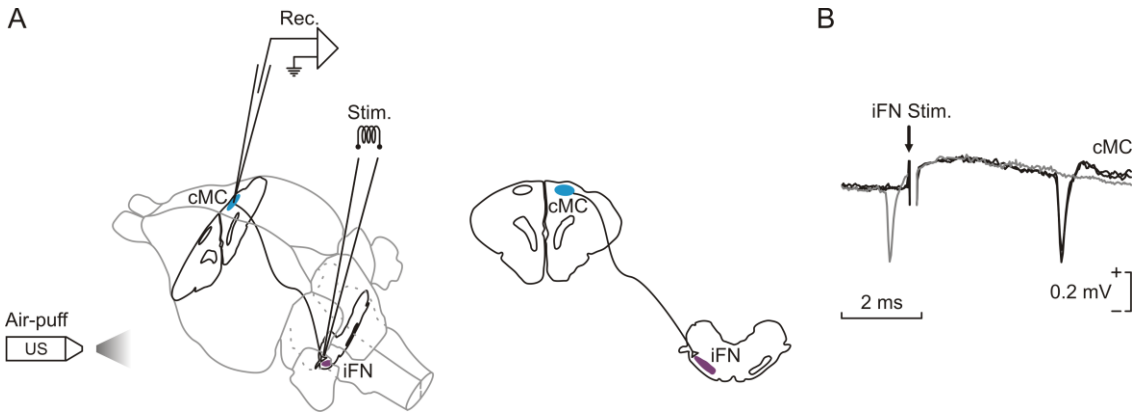

Figure 4.4.1 *A*, Schematic representations of direct neuronal projections from the micropipette recording site in contralateral MC (cMC, Rec.) to the stimulated site (Stim.) in ipsilateral facial nucleus (iFN) with respect to the left eye. ***B***, Representative examples of antidromic activations (black lines) in the cMC elicited through iFN stimulation and a collision test (grey line) of cMC neurons. Calibration as indicated.

Once identified, the firing activity of these neurons was studied during the classical conditioning of eyelid responses. Neurons with an observed firing activity increase preceding the performed CRs were classified in a group. The results show that 6 of the 25 neurons with direct projections to the FN presented an anticipated firing rate increase in regard to the CRs. Specifically, the enhanced firing activity initiated 74.43 ± 6.37 ms after tone onset and occurred 112.86 ± 19.50 ms prior to the beginning of the CRs (187.29 ± 13.14 ms after tone initiation). The **Figure 4.4.2** shows one representative antidromically-activated neuron projecting to FN during the CS-US presentation.

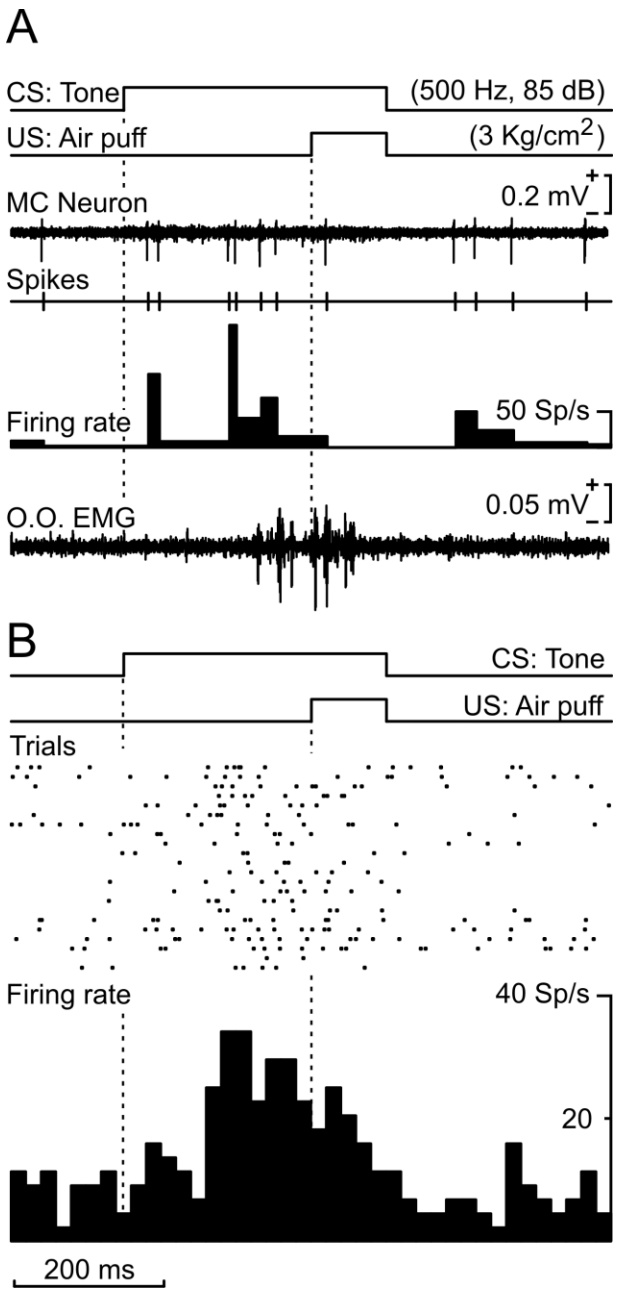

Figure 4.4.2 Firing activity of MC neurons electrically activated from FN during classical eyeblink conditioning. ***A,*** A representative example of the firing activity of a MC neuron antidromically activated by FN stimulation and recorded in a well-trained animal. From top to bottom are represented the conditioning paradigm (CS and US presentations), the raw activity of the MC neuron, the event channel (Spikes), firing rate of the selected neuron, and the raw EMG activity of the *orbicularis oculi* muscle (O.O. EMG) during a single CS-US presentation ***B,*** Conditioning paradigm, raster plot of all spikes collected from the same MC neuron during 22 successive trials, and the averaged firing rate (spikes/s). Calibration as indicated.

This shows a representative trial demonstrating the raw firing activity and firing rate for the neuron and the corresponding EMG activity of the *orbicularis oculi* for a single CS-US presentation (**Figure 4.4.2*A***), and a raster plot of all spikes (n = 22) and the averaged firing rate (spikes/s) for the same neuron (**Figure 4.4.2*B***).

Finally, a PSTH highlights the averaged firing rate increase of the 6 identified neurons with a relationship to the conditioning protocol during the CS-US interval, presenting the firing activity as spikes per seconds (**Figure 4.4.3**).

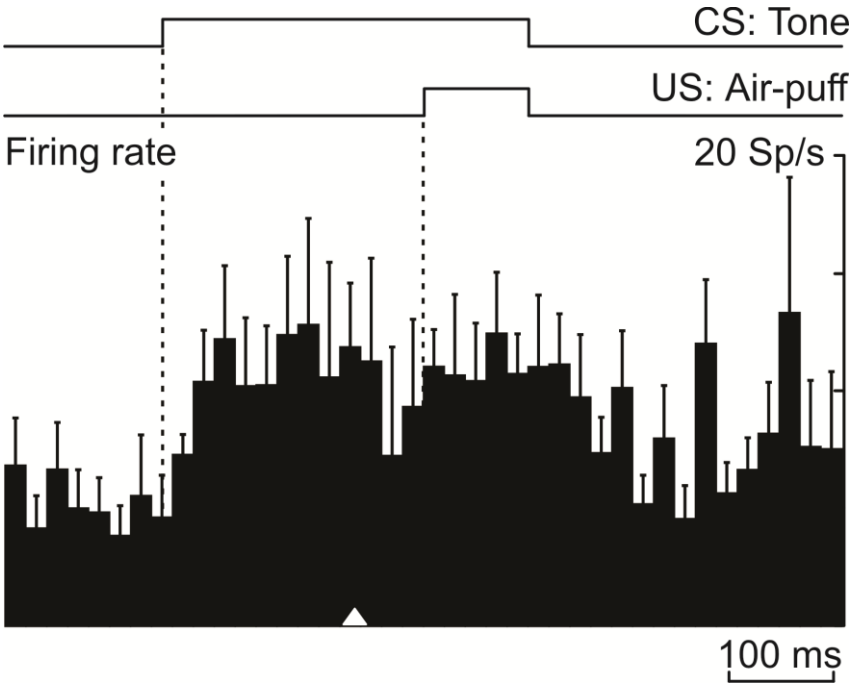

Figure 4.4.3 Averaged firing rates of MC neurons antidromically activated from FN (n = 6). The averaged firing rates are represented as mean values ± SEM. From top to bottom are illustrated the conditioning paradigm and the peristimulus time histogram (PSTH) representing the averaged firing rate in spikes per second (Sp/s). Note that a first peak firing rate of MC neurons appears prior to the CR initiation and a second peak during the US presentation. The white triangle at the bottom indicates the mean CR onset latency recorded from the *orbicularis oculi* muscle. Calibration as indicated.

4.1.3.2. Identified MC neurons projecting to the red nucleus

The electrical pulse stimulation of the RN (**Figure 4.5.1*A***) evoked 189 antidromic activations in the ipsilateral palpebral motor area corresponding to the left eyelid. The activations were identified with the help of the collision test (**Figure 4.5.1*B***) and by means of their typical non-variable activation latency – in case of fast conducting axons (Swadlow, 1998). The mean activation latency after electrical stimulation was 3.36 ± 0.09 ms (mean ± SEM, n = 189), presenting a range between 1.47 and 7.73 ms. The firing activity of the identified neurons were studied during the classical conditioning of eyelid responses with the objective to investigate whether a relationship between the firing rate and the CS-US interval could be established.

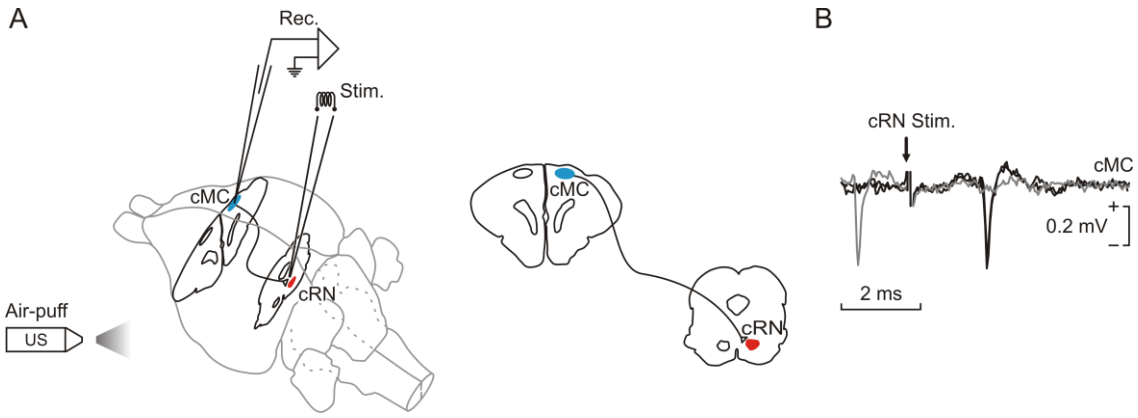

Figure 4.5.1 ***A***, Schematic representations of direct neuronal projections from the micropipette recording site in contralateral MC (cMC, Rec.) to the stimulated site (Stim.) in contralateral red nucleus (cRN) with respect to the left eye. ***B***, Representative examples of antidromic activations (black lines) in the cMC elicited through cRN stimulation and a collision test (grey line) of cMC neurons. Calibration as indicated.

It is important to point out that although a total of 189 neurons were antidromically activated from the RN, only 20 of them (i.e., 10.5%) presented a firing rate related to CRs. Specifically, the increase of firing activity began 100.79 ± 10.26 ms after tone initiation and preceded the CR by 59.70 ± 9.50 ms. The CRs initiated 160.49 ± 8.94 ms after the CS onset. The **Figure 4.5.2** shows a representative example of one MC neuron antidromically activated from the RN with a firing rate increase preceding the CR onset; presenting (***A***) raw firing activity and firing rate of the neuron and EMG activity of the *orbicularis oculi* during one CS-US presentation trial, (***B***) firing rate (spikes/s)

and firing raster plot across all trials (n = 20) of the same neuron during the CS-US presentation. Finally, a PSTH highlights the averaged firing rate of the 20 neurons with a firing activation anticipated to the CR onset during the CS-US interval (**Figure 4.5.3**).

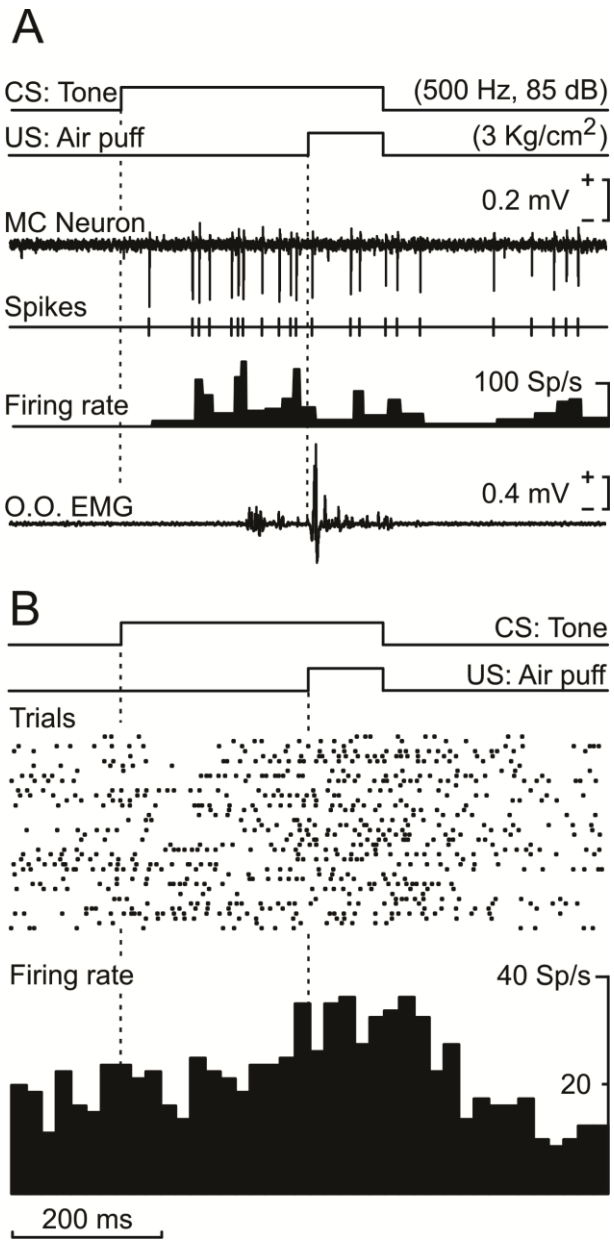

Figure 4.5.2 Firing activity of MC neurons electrically activated from RN during classical eyeblink conditioning. ***A,*** A representative example of the firing activity of a MC neuron antidromically activated by RN stimulation and recorded in a well-trained animal. From top to bottom are represented the conditioning paradigm (CS and US presentations), the raw firing activity of the MC neuron, the event channel (Spikes), firing rate of the selected neuron, and the raw EMG activity of the *orbicularis oculi* muscle (O.O. EMG) during a single CS-US presentation ***B,*** Conditioning paradigm, raster plot of all spikes collected from the same MC neuron during 40 successive trials, and the averaged firing rate (spikes/s). Calibration as indicated.

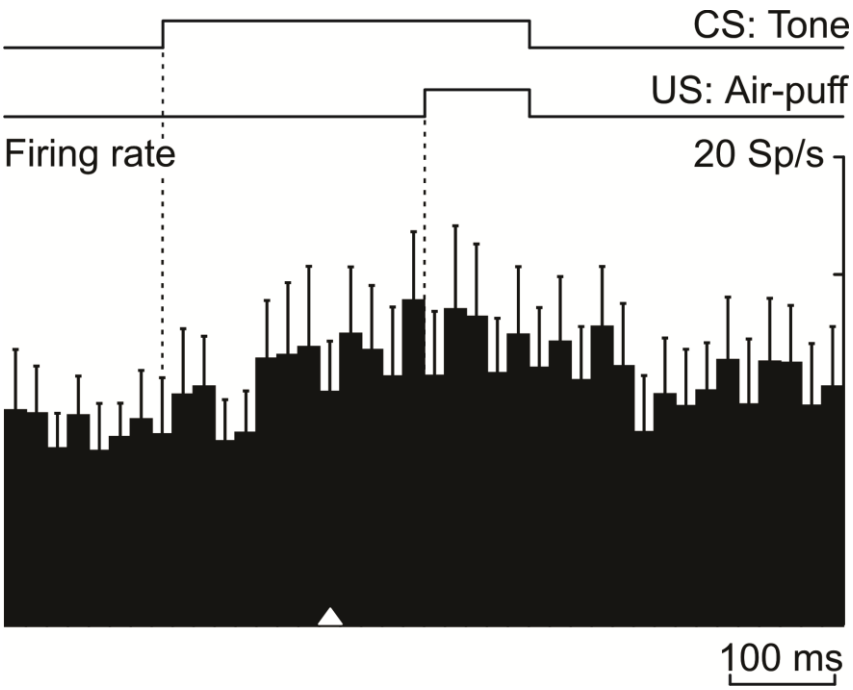

Figure 4.5.3 Averaged firing rates of MC neurons antidromically activated from RN (n = 20). The averaged firing rates are represented as mean values ± SEM. From top to bottom are illustrated the conditioning paradigm and the peristimulus time histogram (PSTH) representing the averaged firing rate in spikes per seconds (Sp/s). Note that the neuronal firing rate presents a slight and continuous increase prior to the CR initiation. The white triangle at the bottom indicates the mean CR onset latency recorded from the *orbicularis oculi* muscle. Calibration as indicated.

4.1.3.3. Classification of non-activated MC neurons

Many of the recorded neurons in MC could not be antidromically activated neither from RN nor from FN. Regardless, these neurons were recorded during the classical conditioning of eyelid responses to determine whether they were involved in the performance of CRs. As a result, 43 neurons showed a clear firing rate increase preceding the CR onset. The firing activity increase with a mean onset latency of 78.70 ± 6.48 ms (mean ± SEM, n = 43) after tone initiation showed an anticipation of 84.67 ± 7.01 ms in regard to the beginning of the CRs. The mean onset latency of the CRs was 163.37 ± 5.53 ms. After identifying the anticipatory nature of these non-activated neurons, the classification into different neuronal types according to their mode of firing during the CS-US presentation was carried out. Subsequently, three types of non-activated neurons were established.

The neurons type A (**Figure 4.6.1*A, B*** and **4.6.2*A***) presented an irregular spontaneous firing rate, with mean values ranging from 3 to 15 spikes/s. The averaged firing rates of 11 type A neurons recorded from well-trained animals (i.e., from the 8th conditioning session) are represented in **Figure 4.6.2*A***. Type A neurons fired a burst of action potentials with a mean onset latency of 73.49 ± 7.59 ms after tone initiation, preceding the EMG activation of the *orbicularis oculi* muscle by 111.75 ± 10.22 ms during the CS-US interval, i.e., during the generation of the CR. The mean onset latency of the CRs was 185.24 ± 12.18 ms. Characteristically, the peak firing of type A neurons took place during the CS-US interval, reaching low mean peak firing rates (20 – 30 spikes/s) at ≈ 200 ms from the CS presentation (**Figure 4.6.1*B*** and **4.6.2*A***). Their firing rates decreased steadily during the UR presentation until reaching (irregular) tonic firing 0.2 – 0.3 s afterwards.

Type B neurons (**Figure 4.6.1*C, D*** and **4.6.2*B***) presented a more stable and higher (10 – 20 spikes/s) spontaneous firing rate than type A neurons. As shown in **Figure 4.6.1*C-D*** and **4.6.2*B***, this type of neuron presented two successive bursts of action potentials. An initial firing rate peak (≈ 20 spikes/s) observed 63.50 ± 9.39 ms after tone initiation, preceding 104.92 ± 12.47 ms the generation of the CR which initiated at 168.42 ± 8.88 ms after the tone onset. After the descending of the first firing peak a second burst (≈ 25 spikes/s) immediately following the US presentation was observed, presenting a mean onset latency of 235.97 ± 14.75 ms after initiation of the tone. The averaged firing rates of 15 type B neurons recorded from well-trained animals (i.e., from the 8th conditioning session) are represented in **Figure 4.6.2*B***.

Finally, type C neurons (**Figure 4.6.1*E, F*** and **4.6.2*C***) presented a spontaneous firing rate (≈ 10 spikes/s) similar to that presented by type B neurons. MC neurons included in this group presented a slow increase in their firing rates during the CS-US interval, starting 88.05 ± 12.37 ms after the CS initiation and reaching their peak firing (347.87 ± 14.68 ms after the CS start; 20 – 40 spikes/s) by the time of the US presentation.

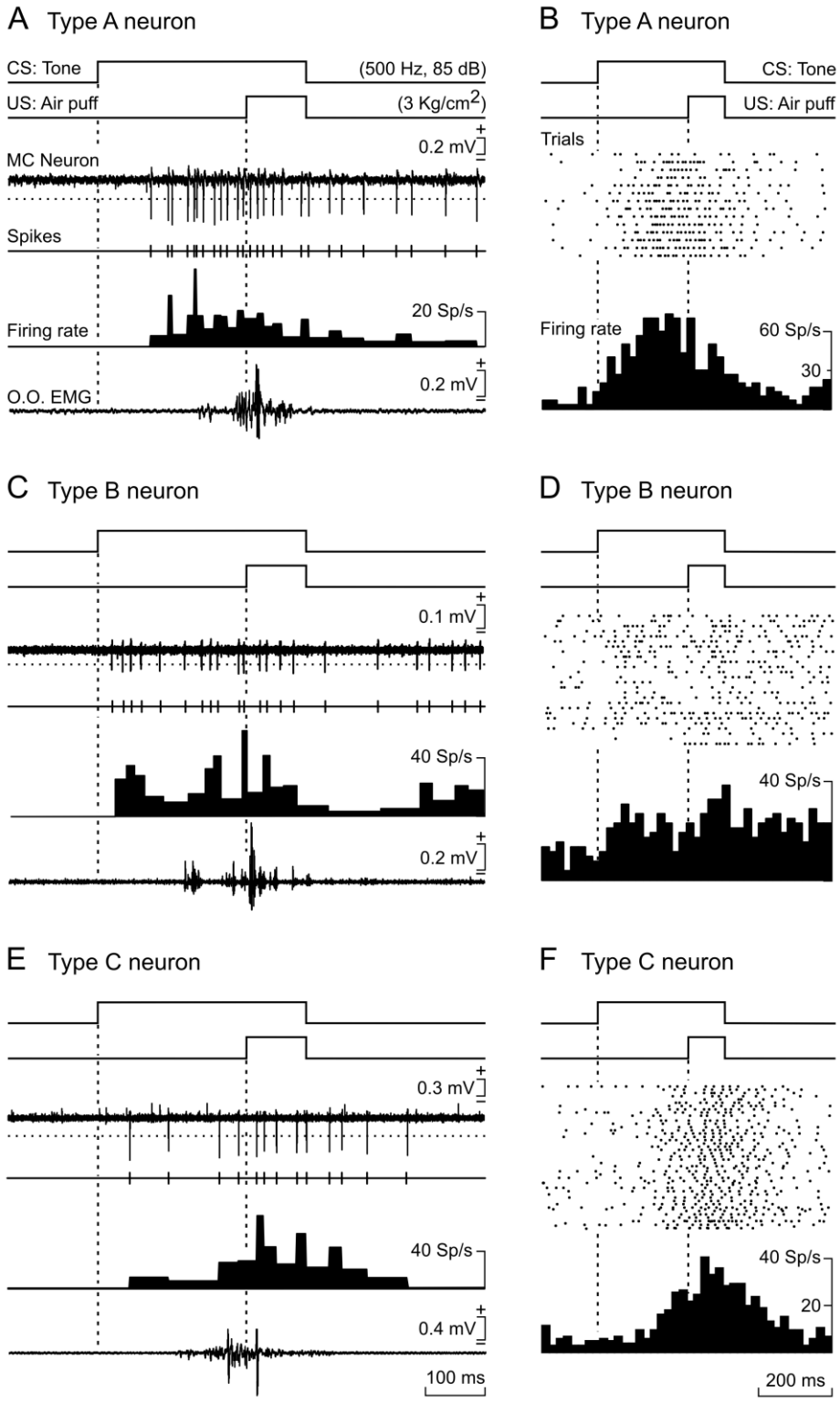

Figure 4.6.1 Different types of MC neurons activated during classical eyeblink conditioning using a delay paradigm. ***A-B***, Firing properties of type A neurons. ***A***, From top to bottom are illustrated the conditioning paradigm, the raw activity of a representative type A neuron, the event channel and firing rate of the selected neuron, and the raw EMG activity of the *orbicularis oculi* (O.O. EMG) muscle during a single CS-US presentation. *(Figure legend continued on page 71)→*

←*(continued Figure legend from page 70)* ***B***, Conditioning paradigm, raster plot of all spikes collected from the same MC neuron during 15 successive trials, and the averaged firing rate. Type A MC neurons were characterized by an increased firing rate prior to the CR and a noticeable decrease of their firing rate during US presentation. ***C-D***, Same as in ***A-B*** for a representative type B MC neuron recorded for 26 trials. Type B neurons were characterized by an initial firing peak preceding the CR and by a second increase of firing rate during US presentation. ***E-F***, Same as in ***A-B*** for a representative type C MC neuron recorded for 53 trials. Type C neurons were characterized by a continuous increase in their firing rate preceding the CR and by reaching the maximum peak during US presentation. Time calibration in E is also for A and C. Time calibration in F is also for B and D.

As shown, the averaged population of type C neurons preceded the beginning of the CR by 92.72 ± 23.51 ms. The mean onset latency of the CRs was 180.77 ± 24.81 ms after the CS onset. The averaged firing rates of 17 type B neurons recorded from well-trained animals (i.e., from 8th conditioning session) are represented in **Figure 4.6.2*C***.

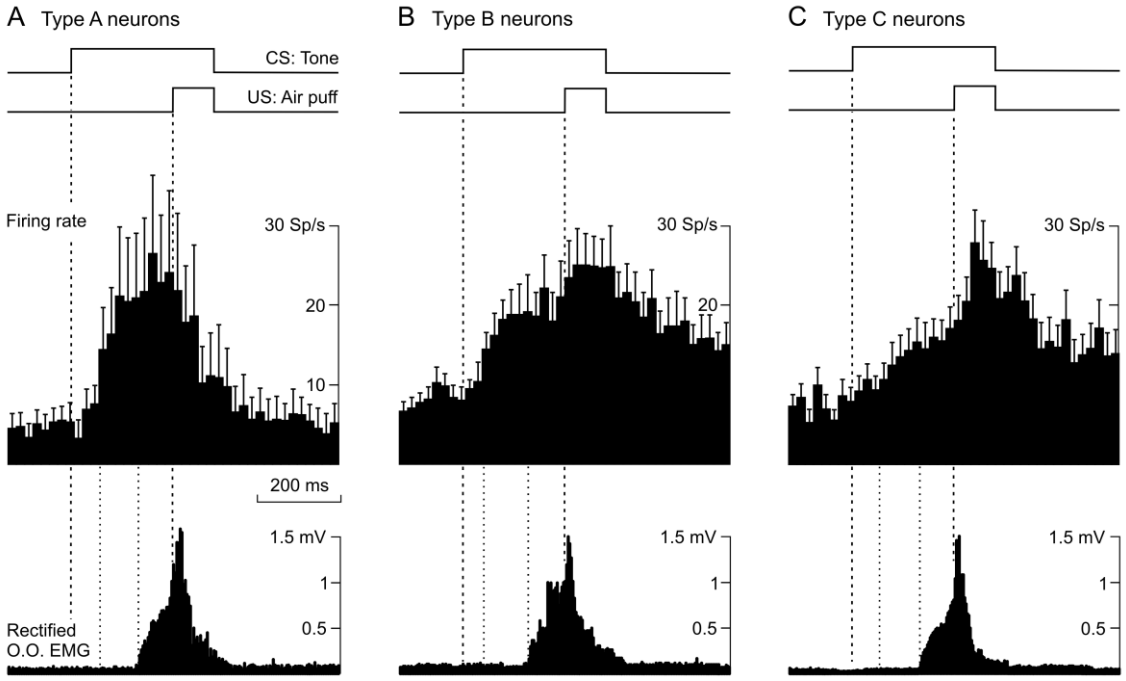

Figure 4.6.2 Averaged firing rates of representative type A, B, and C MC neurons recorded from well-conditioned animals. All recordings were performed after the 8th conditioning session. Averaged firing rates are represented as mean values ± SEM. ***A***, From top to bottom are illustrated the conditioning paradigm, the averaged firing rate of type A neurons (n = 11), and the average of the rectified EMG responses of the *orbicularis oculi* (O.O. EMG) muscle. Note that their peak firing rate appeared before US presentation and that they did not respond during the unconditioned response. ***B***, Same as in ***A*** but for type B neurons. Averaged firing rates and rectified EMG responses collected from n = 15 type B neurons. These MC neurons were characterized by the presence of an initial peak in their firing rate prior to the CR and then by a second increase of their firing rate during the US. *(Figure legend continued on page 72)*→

←*(continued Figure legend from page 71)* ***C***, Same as in ***A*** for type C neurons (n = 17). These MC neurons presented a continuous increase in their firing rate beginning well before (> 90 ms) the start of CRs and reaching the maximum during US presentation – i.e., during the generation of the unconditioned eyelid response.

In summary, these results provide evidence of direct neuronal projections from the palpebral motor area to RN and FN in the rabbit. A minor proportion of the activated neurons present firing activities related to the performance of eyelid CRs. Additionally, three types of non-activated MC neurons are activated during the CS-US interval well in advance of the initiation of the EMG activity of the *orbicularis oculi* muscle, i.e., of the CR. The exact projecting sites of these non-activated neurons are not directly identified in this present work. Regardless, these neurons might project to FN or RN, but activation by electrical stimulation of the corresponding axons was not viable probably due to very slowly conducting axons as later explained in the Discussion section.

Experiment 2

4.2. Modulation of MC excitability during the acquisition of eyeblink conditioning

To underline the importance of MC activity during the acquisition process of associative motor learning, the second series of experiments examined whether modulation of the excitability of MC neurons via tDCS application could alter the learning process of classical conditioning of eyelid responses. Here a group of animals (n = 6) was prepared for a delay paradigm of classical eyeblink conditioning during simultaneous tDCS (active or sham) on MC.

4.2.1. Modulation of learning acquisition during classical eyeblink conditioning induced by MC-tDCS

The conditioning protocol consisted of a 350 ms tone as CS and a 250 ms puff of air (3 kg/cm^2) initiated 100 ms after the onset of the tone and directed to the left cornea as US.

Thus, the tone and the air puff co-terminated. The presence of CRs was determined by recording the EMG activity of the ipsilateral *orbicularis oculi* muscle (**Figure 4.7*A* and *C***).

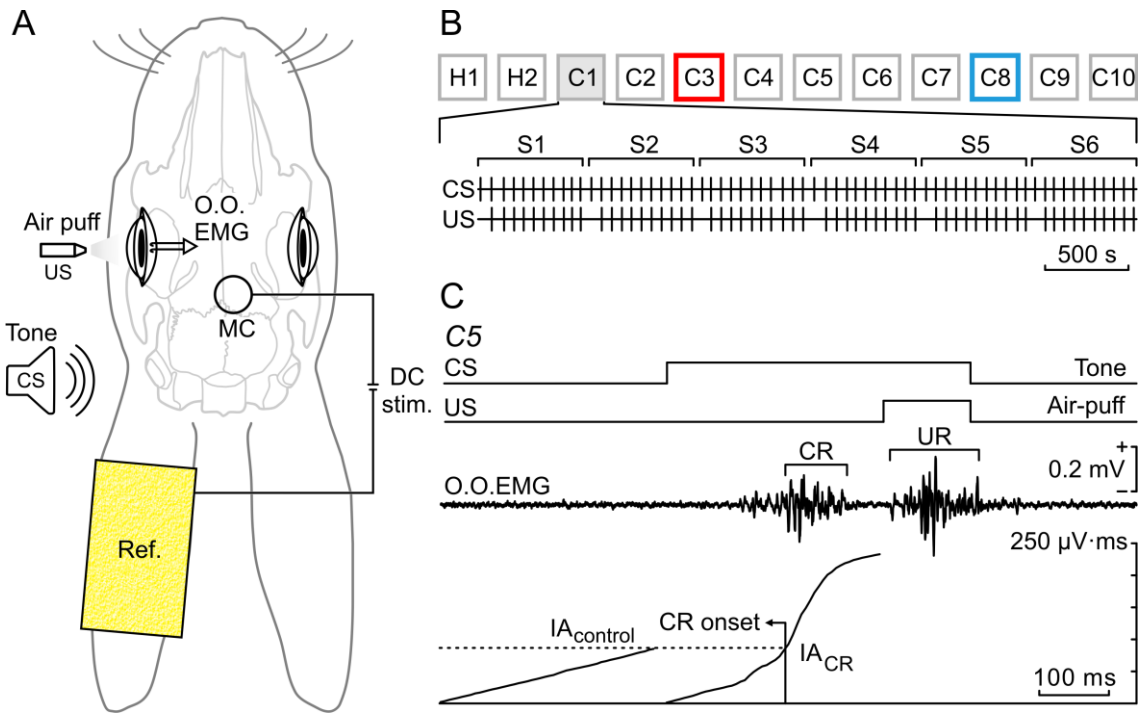

Figure 4.7 Experimental design for classical eyeblink conditioning and simultaneous tDCS application on motor cortex (MC). ***A,*** Indication of electrode location over the MC for tDCS contralateral to the left eye. Both anodal and cathodal tDCS currents were applied through a silver chloride disk electrode (area in contact with the skull: 0.5 cm^2) inserted in a plastic tube (ø 8 mm) implanted over MC whilst a large (35 cm^2) saline-soaked sponge electrode placed on the contralateral ear served as a counterelectrode (Ref.). Classical conditioning of eyelid responses was achieved using a delay-conditioning paradigm. Animals were chronically implanted with EMG recording bipolar hook electrodes in the left *orbicularis oculi* muscle (O.O. EMG) in order to evaluate the evoked CR. A binaurally tone (350 ms, 500 Hz, 85 dB) was used as CS, followed 250 ms from its beginning by an air puff (100 ms, 3 kg/cm^2) as US presented to the left cornea. ***B,*** A total of 2 habituation and 10 conditioning sessions were carried out. Simultaneous anodal tDCS was applied on conditioning day 3 (C3, red box) and cathodal tDCS was applied on conditioning day 8 (C8, blue box). Conditioning sessions consisted of 66 trials (6 series of 11 trials each) separated at random by intervals of 50-70 s. Of the 66 trials, 6 were test trials in which the CS was presented alone. ***C,*** From top to bottom are illustrated CS and US presentations, and a representative EMG recording (O.O. EMG) collected from session C5. As criteria, the presence of EMG activity, during the CS interval and prior to US beginning, lasting >10 ms and initiated after CS onset was considered as a CR. In addition, the integrated EMG activity (IA) recorded during the CS interval (IA_{CR}) had to be greater than the integrated EMG activity recorded immediately before CS presentation ($IA_{control}$). The CR onset was defined by the point where IA_{CR} overtook $IA_{control}$. CR and UR are indicated. Calibration as indicated.

This experimental design allowed the recording of classical eyeblink responses and the simultaneous application of tDCS to the contralateral palpebral area of the MC (**Figure 4.7*A***). The first two conditioning sessions consisted of the sole CS presentation. Each animal was trained on the CS and US for ten successive days. Conditioning sessions always consisted of 66 trials (**Figure 4.7*B***). In order to characterize the eyelid responses, the EMG recording of the *orbicularis oculi* was rectified and integrated to obtain the integrated area (IA). Subsequently, the CR onset was defined as the point where the integrated activity of the CR (IA_{CR}) overtook the integrated activity during the 200 ms before CS onset ($IA_{control}$) (**Figure 4.7*C***). When this ratio between IA_{CR} and $IA_{control}$ was ≥ 1.1 the response was considered a CR.

To characterize the impact of tDCS on MC excitability during classical conditioning, anodal and cathodal tDCS were presented to the experimental group (n = 3) during session C3 and C8, respectively. Based on a previous study showing a very low learning rate on C2 when a tone was used as CS (Pacheco-Calderón et al., 2012), day C3 was chosen as the anodal session in order to achieve the strongest impact of anodal tDCS on learning, with the explanation that tDCS applied too early might not induce a visible increase of CRs. tDCS applied during a conditioning session consisted of anodal/cathodal current (anodal = 1 mA; cathodal = -1mA; 2 mA/cm^2 of current density; ~30 min) during series 2, 4 and 6 (tDCS-ON) within the same conditioning session. To rule out any sensory detection of tDCS (Nitsche and Paulus, 2000; Nitsche et al., 2007), sham stimulation in the sham group (n = 3) implicated the same electrode placement and conditioning protocol, except for tDCS duration, consisting in this case of a 30 s application. In **Figure 4.8.1** the evolution of the learning curves throughout the conditioning sessions is represented for the two animal groups.

Sham-group animals reached asymptotic values of CR percentage (>80% of CRs per session) for their learning curves by the 5^{th} conditioning session. The presence of concurrent anodal tDCS during C3 was associated with a statistically significant increase in the percentage of CRs, reaching 81.32 ± 8.39 % (mean ± SEM, n = 3), whilst the CR percentage for the sham group was 23.19 ± 19.11 % on day C3 (P = 0.049, one-way ANOVA). The application of cathodal tDCS on C8 did not induce any significant change (P = 0.749, one-way ANOVA) on CR percentage (93.68 ± 3.30 %) compared with the sham values (95.29 ± 3.32 %).

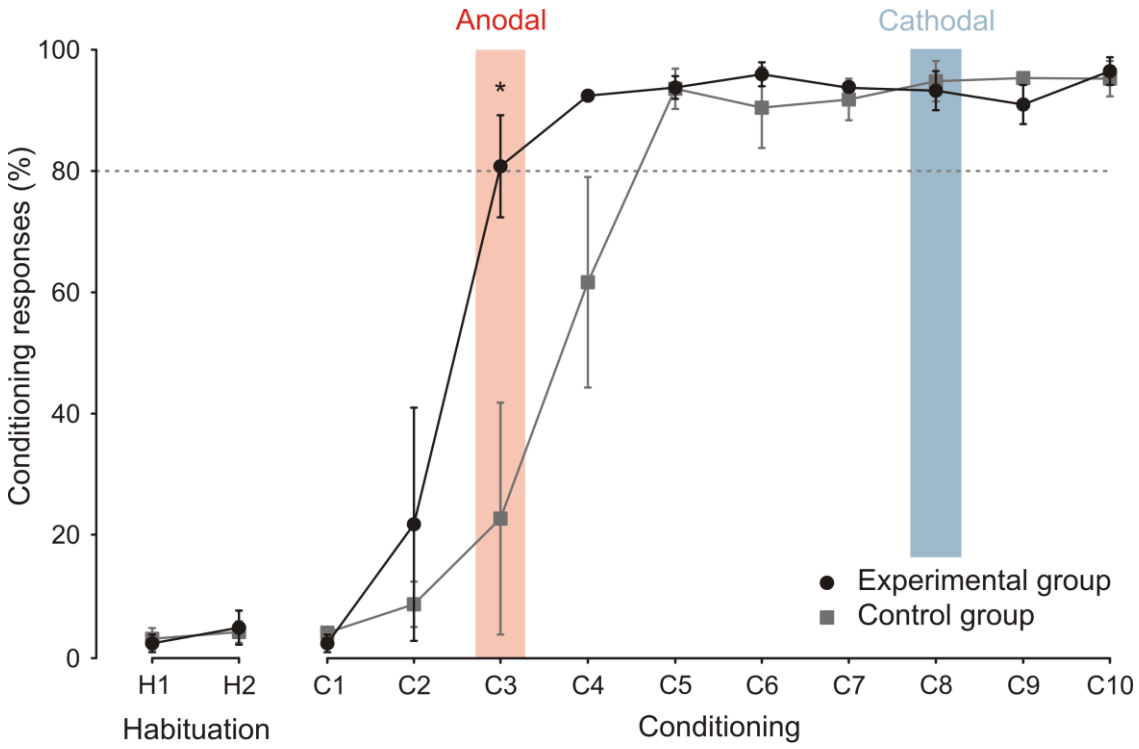

Figure 4.8.1 Effects of simultaneous tDCS over MC on classical eyeblink conditioning using a delay paradigm. Evolution of CR percentage across the conditioning sessions for a control group of animals (grey squares and line) and the experimental group (black circles and line). The animals received anodal tDCS during session C3 and cathodal tDCS during session C8 with a duration of ~30 min (experimental group) or 30 s for sham stimulation (control group). Dotted horizontal line represents threshold of asymptotic CR percentages. n = 6. *, P<0.05, one-way ANOVA. Error bars represent SEM.

The **Figure 4.8.2** shows representative *orbicularis oculi* EMG recordings from one animal of the experimental group representing a control trial (series 1; black traces) before tDCS stimulation started and one trial during anodal tDCS (red trace) from session C3, as well as a control trial and one cathodal trial (blue trace) obtained from the session C8. Note that during cathodal tDCS the CR is still present, but the response seemed to be delayed and of less strength for this animal.

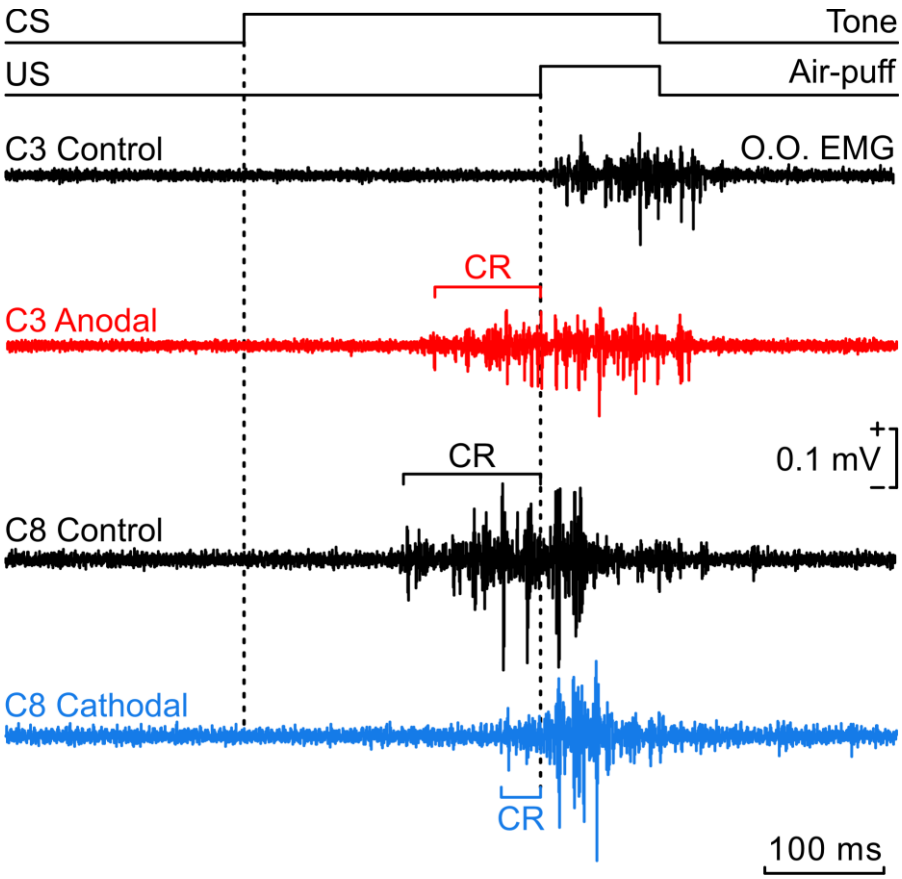

Figure 4.8.2 The conditioning paradigm (CS and US presentations) and representative *orbicularis oculi* electromyographic (O.O. EMG) recordings collected from the same animal during the session C3 from a control series (traces in black) and during the course of anodal tDCS (trace in red), and the same for cathodal session C8 representing a control series and a trial with the presence of cathodal stimulation (trace in blue). Conditioned responses (CR) are indicated. Note that CR for cathodal session C8 presents longer latency and smaller area. Calibration as indicated.

4.2.2. Modulation of palpebral conditioned responses by MC-tDCS

Although no significant differences were found for CR percentage during the cathodal session compared to the sham group, CRs during the presence of cathodal tDCS seemed to be of longer latencies and reduced strength as mentioned in the previous section (**Figure 4.8.2**). For this reason, besides the given CR percentage curve, the quality of CRs was analyzed once between-group (for anodal and cathodal) and once within-group (only for cathodal) by quantifying CR strength and CR onset latency. The relative area value for response strength was calculated as the ratio between IA_{CR} and

$IA_{control}$ for the experimental and sham group. For an appropriate comparison between experimental and control animals relative area values were normalized by dividing each individual average (of sessions C3 and C8) by the average of the highest individual relative area (strongest response) observed across the learning curve. Similarly, the CR onset latency values (time difference between the CS initiation and the CR onset) from sessions C3 and C8 were normalized to the individual average with the lowest latency (fastest response) observed across the learning curve. **Figure 4.9*A*** illustrates the comparison for relative area and latency values between experimental and sham group for sessions C3 and C8 where 100% represents the maximum (strongest or fastest) response average. CRs during anodal tDCS (74.30 ± 11.84%; mean ± SEM) were significantly stronger than the sham (36.09 ± 4.88%) group (P = 0.041; *t*-test; n = 3). With respect to the CR latency, responses were faster (87.60 ± 3.38%) during the anodal stimulation compared to sham (79.54 ± 2.16%) on C3. However, the difference was not statistically significant (P = 0.304; *t*-test; n = 3). Given that no significant differences in strength or latency were shown for the application of cathodal tDCS compared to the sham group, a within-group comparison (only experimental group) was performed to test whether CRs were qualitatively different compared with the days before (C7) and after (C9) the cathodal session (C8). Since the low sample size (n = 3) most likely results in a low statistical power (Button et al., 2013), this time the analysis was performed with the raw data calculating the averages of relative area and latency from each series (series 2, 3, 4, 5, and 6) for all three sessions (C7, C8, C9). On session C8 series 1 was used as a control trial (without tDCS), therefore not included in the analysis, excluding also series 1 from C7 and C9 to keep the number of averages equal for each session (a total of 15 values per session for three animals).

One-way $ANOVA_{RM}$ was performed with the factor SESSION and the results show a significant overall effect for both relative area (P = 0.035) and latency (P = 0.027). The Bonferroni correction was used for multiple comparisons. Significantly (C7 vs. C8; P = 0.049) weaker (1.86 ± 0.10) responses were detected for the cathodal session compared with the day before (2.17 ± 0.09). Although non-significant (C8 vs. C9; P = 0.277), CRs from session C8 also seemed to be less strong than the day after (2.07 ± 0.11, C9; **Figure 4.9*B*** left). On the other hand, the **Figure 4.9*B*** (right) shows slower CRs, i.e., higher latencies (191.70 ± 3.15 ms) for the cathodal session (C8). Even if a significant overall effect was detected for CR latency, the *post hoc* test could not detect statistical

significance (C7vsC8|P = 0.069; C8vsC9|P = 0.277) comparing C8 with the day before (182.63 ± 2.71 ms, C7) and after (185.50 ± 2.75 ms, C9). Altogether, the successful modulation of CR acquisition and performance via tDCS applied on MC emphasizes the importance of this cortical area during classical eyeblink conditioning.

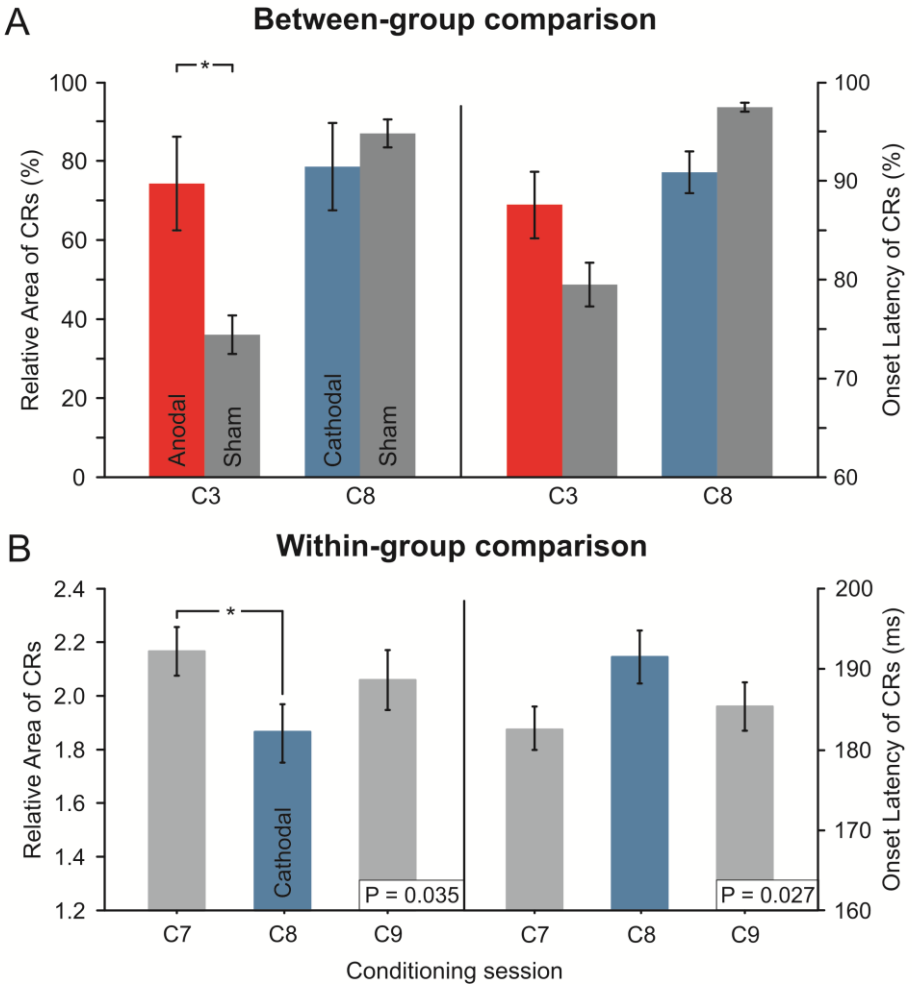

Figure 4.9 Modulation of relative area (strength) and latency of CRs by application of tDCS. The relative area value was calculated as the ratio between IA_{CR} and $IA_{control}$. The CR onset latency was calculated as the time difference between CS initiation and CR onset. ***A***, Between-group comparison (experimental and sham group) with normalized values of relative area and onset latency (100% = maximum response) of CRs for session C3 and C8. Note that CRs from session C3 present stronger and seemingly faster (however the latter without statistical significance) responses in the experimental group compared to the sham group. *, P<0.05, n = 3 per group, *t*-test. ***B***, Within-group comparison (only experimental group) of raw relative area and latency of CRs collected from the sessions C7 (before cathodal session) and C9 (after cathodal session) and from the session with simultaneous cathodal tDCS (C8). Analysis resulted in an overall SESSION effect for relative area (P = 0.035) and latency (P = 0.027). Note that CRs from C8 resulted to be weaker and slower. However, Bonferroni correction could not detect significant differences between sessions for CR latency. *, P<0.05,**, P<0.01 one-way $ANOVA_{RM}$, Bonferroni as *post hoc* test. Error bars represent SEM.

Experiment 3

4.3. Modulation of sensory cortex excitability during the acquisition of eyeblink conditioning

The previous experiments demonstrated the involvement of the MC during the acquisition process of eyeblink conditioning through concurrent extracellular unitary recordings and transcranial modulation of MC's excitability. In addition, prior research has shown that cortical sensory perception processes can be modulated (via tDCS) during eyeblink conditioning and alter learning acquisition. Thus, the authors demonstrated that the sensory cortex (S1) is implicated in the CS pathway when whisker stimulation was used as CS (Márquez-Ruiz et al., 2012). Following this concept of modulating sensory perception during learning, the next step of the present Doctoral Thesis was to study the involvement of a different sensory input (V1) during eyeblink conditioning. The aim was to test whether modulating the cortical excitability of V1 by the use of tDCS would have a similar impact on classical eyeblink conditioning when light stimulation was used as CS. VEP measurements were used as physiological markers of cortical excitability. To study this, animals (n = 3) were prepared for chronic recording of VEPs and classical eyeblink conditioning with simultaneous tDCS on V1.

4.3.1. Long-lasting neuromodulatory effects on induced VEPs by the application of primary visual cortex (V1) tDCS

To describe cortical excitability variations of V1 induced by tDCS, VEPs elicited by contralateral flash stimulation were recorded before and after the transcranial stimulation (**Figure 4.10*A***). The VEPs consisted of a first positive component (P1) with a peak latency of 21.11 ± 1.89 ms and a late negative component (N1) with a peak at 48.85 ± 1.91 ms (mean ± SEM, n = 3; **Figure 4.10*C***). To rule out the possibility that observed VEPs were provoked by an artifact different to the light flash, the operating flash was covered and, consequently, as shown in **Figure 4.10*B*** no VEP was induced in V1.

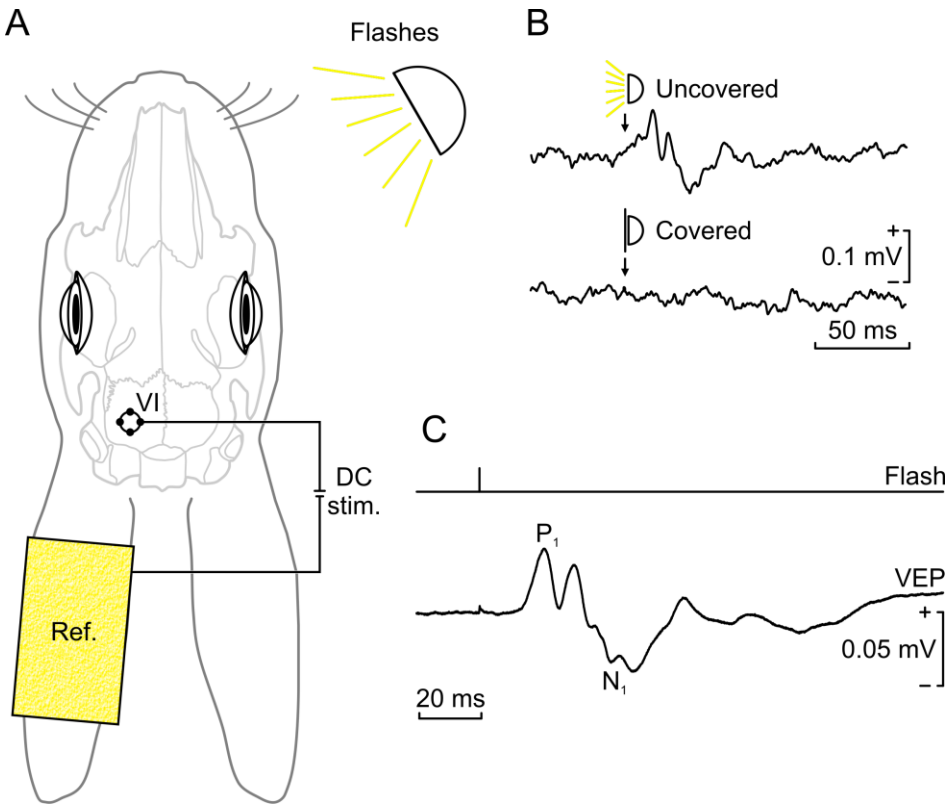

Figure 4.10 Experimental design for visual evoked potential (VEP) recordings after application of tDCS. ***A***, Experimental scheme with indication of electrode location over primary visual cortex (V1) for VEP recordings and tDCS (DC stim.). Both anodal and cathodal tDCS currents were applied between the 4 silver-ball electrodes (black circles) implanted over the V1 and a large (35 cm^2) sponge electrode (Ref.) placed on the ipsilateral ear. VEPs were evoked by light flashes at a distance of 14 cm from the right eye and recorded with the silver electrodes on V1. ***B,*** Representative EEG recording of V1 with the uncovered (above) and covered (below) flash. ***C,*** Average of VEPs (n = 40) collected from a representative animal and indication of P1 and N1 component. Calibration as indicated.

With this in mind, VEPs induced via trains of flashes (20 flashes, 1 Hz) were continuously recorded 30 min before (control) and 60 min after (after-effect) tDCS presentation (**Figure 4.11.1*A***). VEPs were assessed using the same epicranial electrodes as for direct current stimulation (not simultaneously). TDCS was applied for 20 min at an intensity of 2 mA for anodal and at –2 mA for cathodal stimulation.

In contrast to Experiment 2, this time the currents were delivered between four silver-ball electrodes placed on the left V1 and the saline-soaked sponge attached to the ipsilateral ear as a reference electrode. The current density was 31.26 mA/cm^2, i.e., 7.82 mA/cm^2 for each silver ball to reach the ± 2 mA.

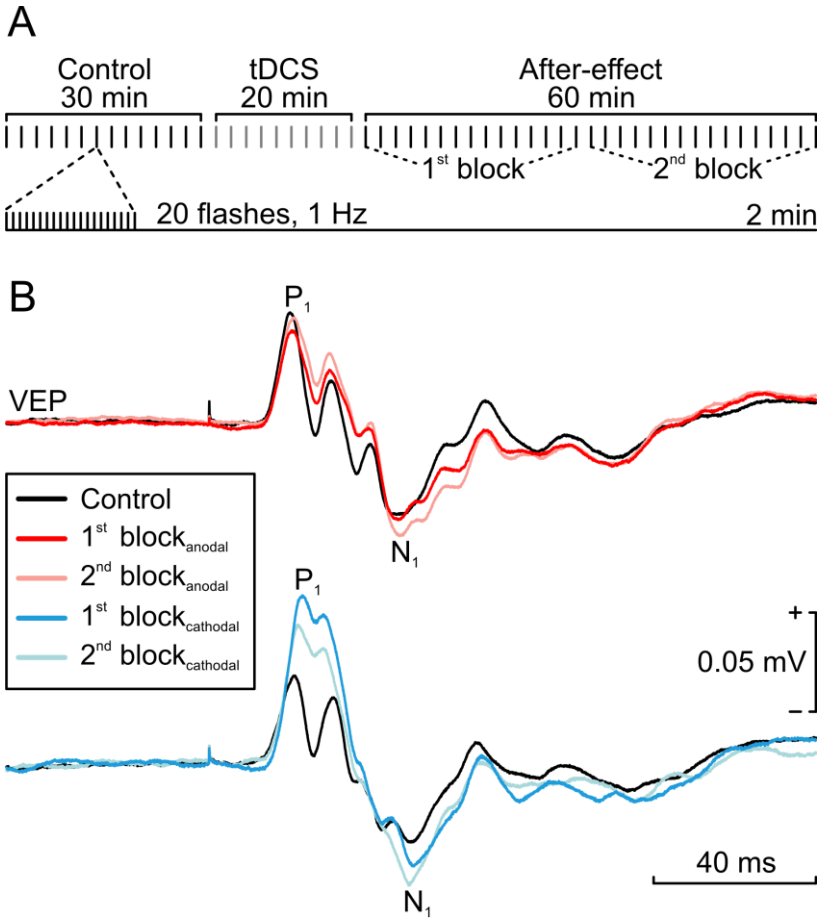

Figure 4.11.1 Modulation of VEPs induced by tDCS. ***A,*** Stimulation protocol for VEP recording of V1. Twenty light flashes at 1 Hz every 2 minutes were applied. VEPs were continuously recorded 30 min before (Control) and 60 min after (After-effect) tDCS presentation. Anodal and cathodal tDCS was administered during 20 min over V1 on separated sessions. ***B,*** Representative averages of VEPs recordings before tDCS (n = 295, black traces) and after 20 min tDCS presentation on V1. Anodal after-effects during the first 30 min (1^{st} $block_{anodal}$) presented by darker red traces (n = 276) and during the second half hour (2^{nd} $block_{anodal}$) of post-tDCS by light red traces (n = 289). Cathodal after-effects during the first 30 min (1^{st} $block_{cathodal}$) represented by darker blue traces (n = 290) and during the second half hour (2^{nd} $block_{cathodal}$) of post-tDCS by light blue traces (n = 277). Calibration as indicated.

The results showed that anodal tDCS had little-to-no after-effect on the shape of VEPs, whilst cathodal tDCS induced a noticeable increase of the P1 component amplitude and a slight delay of P1 and N1 peak latency (**Figure 4.11.1*B***). As shown in **Figure 4.11.2** the effects as represented by the mean amplitude and latency changes of P1 and N1 VEP-components before and after tDCS application, underline the significant

modulation of V1 excitability induced by cathodal tDCS. Peak amplitude values were normalized to the average value of the control situation. The analysis revealed no statistically significant changes (P = 0.425, $Friedman_{RM}$, Student-Newman-Keuls procedure as *post hoc* test) between P1 amplitude after anodal tDCS and P1 amplitude of the corresponding control situation, whilst P1 amplitudes presented statistically significant changes ($P \leq 0.001$, $Friedman_{RM}$, Student-Newman-Keuls procedure as *post hoc* test) after cathodal tDCS compared to the control situation. These changes could be observed in each point during the entire 60 min after-effect recording, showing maximum amplitude increase of 234.58 ± 33.19% (mean ± SEM, n = 3) in the first 5 min after tDCS application (**Figure 4.11.2*A***).

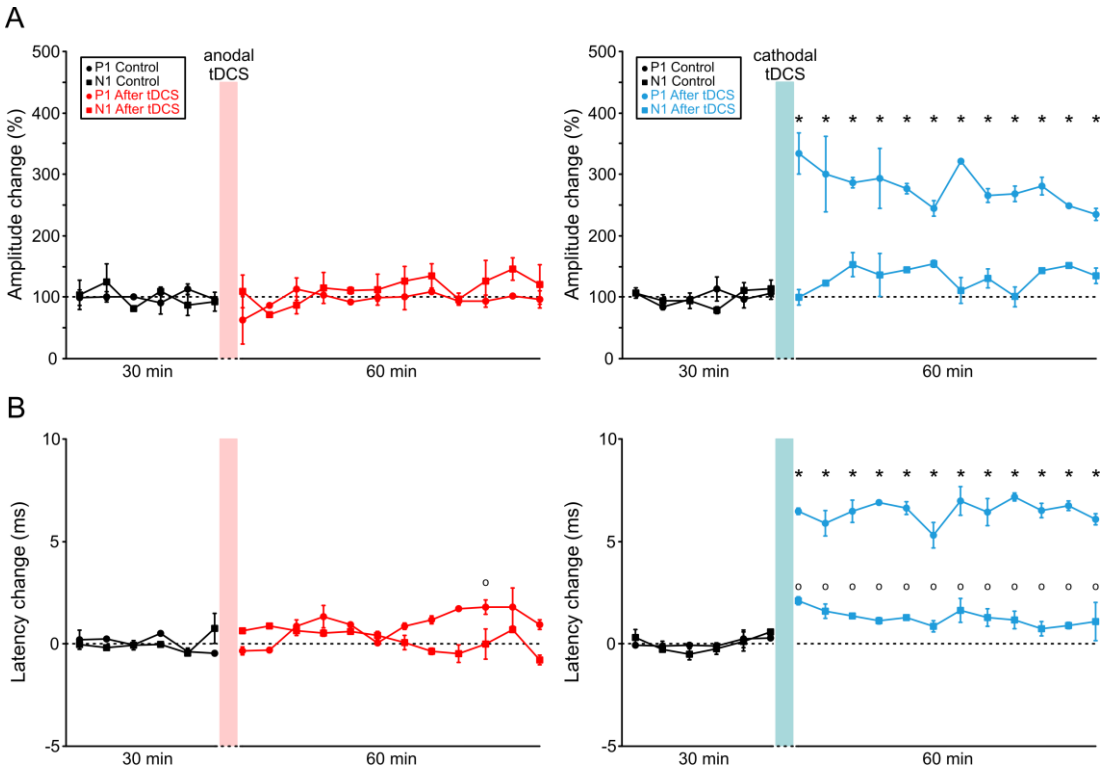

Figure 4.11.2 Peak amplitude and peak latency changes quantified for P1 and N1 components after 20 min anodal and cathodal tDCS presentation (red and blue columns, respectively). ***A,*** Mean averages (n = 3 animals) represented every 5 minutes for amplitude change (%) in P1 (circles) and N1 (squares) 30 minutes before (black lines) and 60 minutes after anodal (red lines) or cathodal (blue lines) tDCS. ***B,*** Same as in ***A*** for latency change (ms). ***A-B***, For statistical analysis each post-stimulation value was compared with the control value immediately previous to the tDCS presentation * = P1, ^{0} = N1, P<0.05 ($Friedman_{RM}$ for non-parametric test, *post hoc* Student-Newman-Keuls test). Error bars represent SEM (some error bars are too small to be shown).

The VEP peak latency values were normalized to the baseline value consisting of the average of all control values. A similar procedure was performed for the peak amplitude values. With respect to the peak latency of the two VEP components, no statistical significance was found after the application of anodal tDCS, with the exception in one point for P1 latency 50 min after anodal stimulation ($P \leq 0.05$, $Friedman_{RM}$, Student-Newman-Keuls procedure as *post hoc* test). Cathodal tDCS induced after-effects with significant differences ($P \leq 0.05$, $Friedman_{RM}$, Student-Newman-Keuls procedure as *post hoc* test) in both P1 and N1 latency values up to 60 min after stimulation compared to the control situation (**Figure 4.11.2*B***). The maximum peak latency change of the P1 component occurred in the second half an hour of post-tDCS recording and was based on a delay (7.15 ± 0.19 ms) of the P1 peak compared to the control values of P1 peak latency. Regarding the N1 component the greatest latency change was observed in the first 5 min after cathodal tDCS with the N1 peak occurring 2.08 ± 0.14 ms later compared to the N1 peak of the control VEPs.

4.3.2. Modulation of learning acquisition during classical eyeblink conditioning induced by V1-tDCS

In order to characterize the extent to which changes in V1 excitability induced by tDCS were able to modify associative learning in rabbits, a trace paradigm of classical eyeblink conditioning was performed with the simultaneous application of tDCS. For that, a binocular train of flashes (100 ms, 50 Hz) was used as CS, followed 250 ms later by an air puff (100 ms, 3 kg/cm^2) directed to the left cornea as US (**Figure 4.12*C***).

This experimental design allowed recording of CRs and the concurrent presentation of tDCS to the ipsilateral V1 (**Figure 4.12*A***). The first two conditioning sessions consisted of the sole CS presentation (H1 and H2). Each animal was trained for ten successive days (C1 – C10) with the paired presentation of CS and US. Conditioning sessions always consisted of 66 trials (6 series of 11 trials each). Anodal and cathodal tDCS were presented during conditioning day 2 (C2) and day 8 (C8), respectively (**Figure 4.12*B***), similar to a prior study using the same animal model (Márquez-Ruiz et al., 2012). tDCS applied during conditioning consisted of anodal or cathodal current (anodal = 2 mA; cathodal = -2 mA; density current: 7.82 mA/cm^2 for each silver ball; ~30 min) presented in series 2, 4, and 6 (tDCS-ON) within the same conditioning

session. The EMG recording of the *orbicularis oculi* was used to characterize and define CRs. The EMG activity was rectified and integrated, to obtain the integrated area (IA). Subsequently, the CR onset was defined as the point where the integrated activity of the CR (IA_{CR}) overtook the integrated activity during the 200 ms before CS onset ($IA_{control}$) (**Figure 4.12*C***). When this ratio between IA_{CR} and $IA_{control}$ was ≥ 1.2, the response was considered a CR.

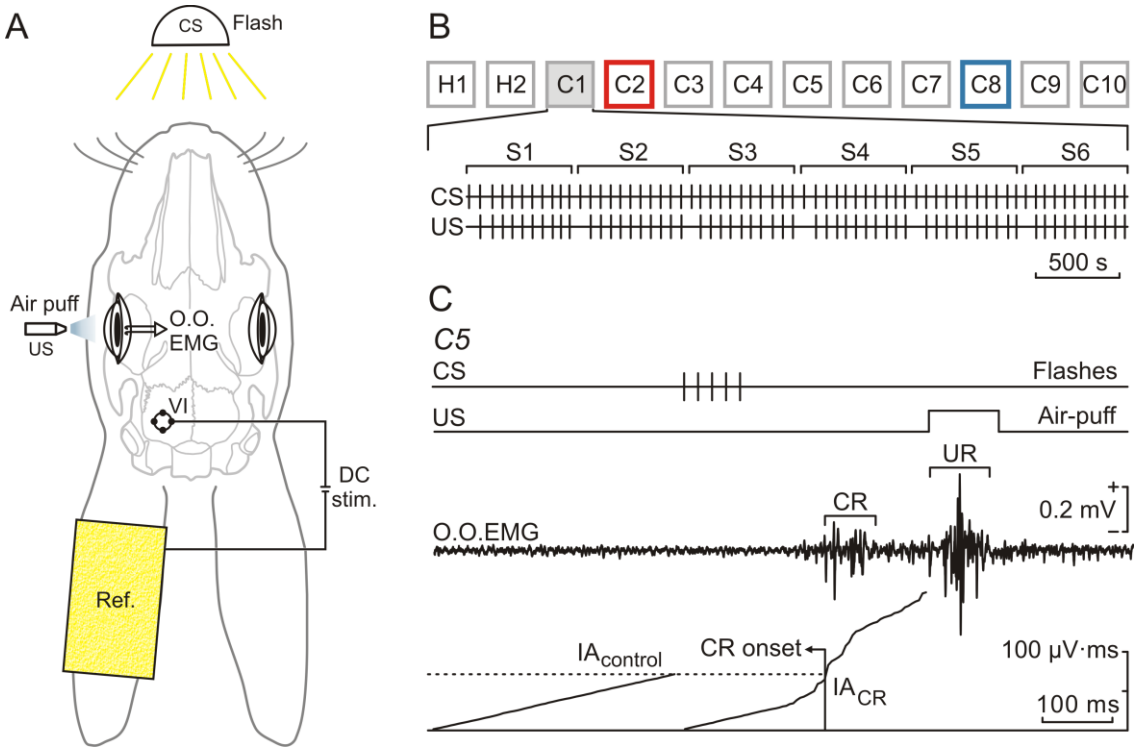

Figure 4.12 Experimental design for classical eyeblink conditioning and simultaneous tDCS on V1. ***A,*** Indication of electrode location over V1 for tDCS (black circles). Both anodal and cathodal tDCS currents were applied between the 4 silver-ball electrodes (surface area in contact with the skull: 4 x 0.016 cm^2) implanted over V1 and a large (35 cm^2) sponge electrode (Ref.) placed on the ipsilateral ear. Classical conditioning of eyelid responses was achieved with the help of a trace-conditioning paradigm. Animals were presented with a binocular train of light flashes (20 Hz, 100 ms) as CS, followed 250 ms later by an air puff (100 ms, 3 kg/cm^2) presented to the left cornea as US. Animals were implanted with recording bipolar hook electrodes in the left *orbicularis oculi* muscle (O.O. EMG) in order to evaluate the evoked CR. ***B,*** A total of 2 habituation and 10 conditioning sessions were carried out. Simultaneous anodal tDCS was applied on conditioning day 2 (C2, red box) and cathodal tDCS was applied on conditioning day 8 (C8, blue box). Conditioning sessions consisted of 66 trials (6 series of 11 trials each) separated at random by intervals of 50-70 s. Of the 66 trials, 6 were test trials in which the CS was presented alone. ***C***, From top to bottom are illustrated CS and US presentations, and a representative EMG recording (O.O. EMG) collected from the same animal during session C5. *(Figure legend continued on page 85)→*

←*(continued Figure legend from page 84)* As criteria, the presence, during the CS-US interval, of EMG activity lasting >10 ms and initiated after CS onset was considered as a CR. In addition, the integrated EMG activity (IA) recorded during the CS-US interval (IA_{CR}) had to be greater than the integrated EMG activity recorded immediately before CS presentation ($IA_{control}$). The CR onset was defined by the point where IA_{CR} overtook $IA_{control}$. CR and UR are indicated. Calibration as indicated.

After characterizing CRs, the evolution of the learning curve (n = 3) was calculated for all conditioning sessions (**Figure 4.13**). One-way $ANOVA_{RM}$ with factor SESSION was performed and the results showed that the presence of concurrent anodal tDCS during C2 did not induce statistically significant changes (P = 0.660, $ANOVA_{RM}$, Bonferroni as *post hoc* analysis) in the percentage of CRs compared to the habituation sessions, reaching 32.71 ± 23.16% (mean ± SEM) of CRs during the anodal session. On day C3 (57.49 ± 27.16%) a significant increase (P = 0.015) was reached in CR percentage compared to the habituation sessions, with the highest percentage of CRs on C6 (76.69 ± 9.50%, P < 0.001).

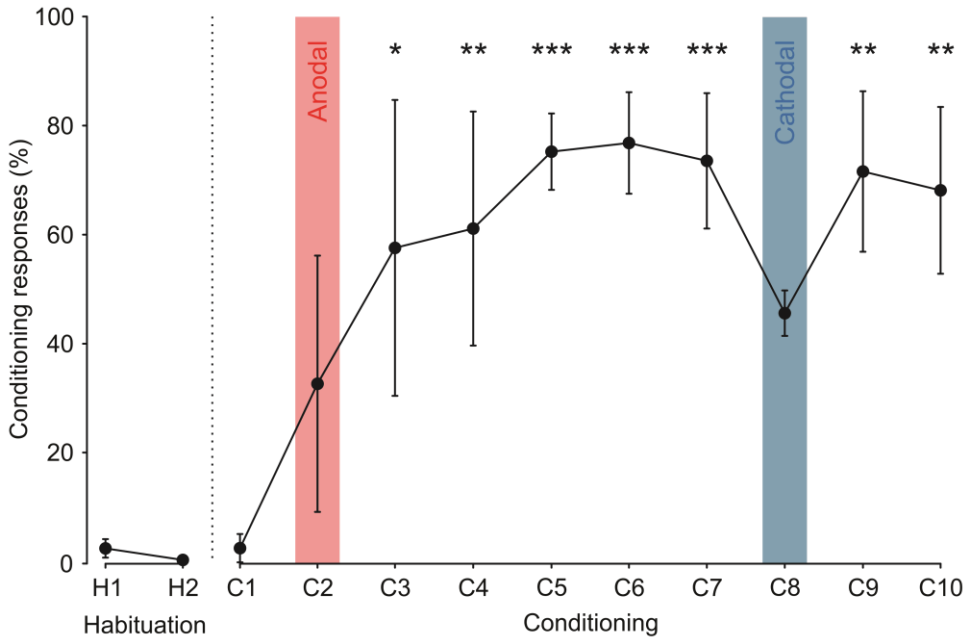

Figure 4.13 Evolution of CR percentage and tDCS effects over V1 on acquisition of classical eyeblink conditioning using a trace paradigm. Animals received anodal tDCS during session C2 and cathodal tDCS during session C8. n = 3. *, P<0.05; **, P<0.01; ***, P<0.001, one-way $ANOVA_{RM}$ comparing conditioning days (C1 – C10) with H2, Bonferroni correction as *post hoc* analysis. Error bars represent SEM.

The application of cathodal tDCS on C8 was associated with a decrease in the amount of CRs (45.63 ± 4.31%) sufficient to produce a lack of statistical significance (P = 0.089) when comparing the CR percentage of day C8 with the values of the habituation sessions. Note that response variability was also reduced on C8.

The lack of controls considerably reduces reliability of the results. Thus, extra conditioning sessions with two animals were performed to strengthen the previously stated findings. The main question was whether cathodal effects could be reproduced and specifically whether anodal tDCS would induce significant effects on learning in strongly trained animals, or whether motor learning becomes more resistant to the modulation of cortical excitability due to a longer training exposure resulting in a general lack of tDCS effects. Two animals were trained for several extra conditioning sessions. The additional training days consisted of conditioning sessions without tDCS (C11, C13) and two sessions with concurrent anodal (C12) and cathodal (C14) tDCS. The measures obtained from C11 were used as control values to compare with the active tDCS sessions (C12, C14). Anodal and cathodal sessions were 48 hours apart to avoid interference of stimulation effects. Besides CR percentage, the CR quality expressed by strength (relative area) and onset latency was analyzed and quantified. The relative area was defined as the ratio between IA_{CR} and $IA_{control}$ for each response and the onset latency as the time difference between CS initiation and the CR onset (**Figure 4.12*C***). **Figure 4.14*A*** shows representative EMG recordings from a strongly trained animal illustrating CRs from control (trace in black, C11), anodal tDCS (trace in red, C12) and cathodal tDCS (trace in blue, C14) sessions. CRs presented similar latencies whilst the relative area seemed to vary across conditions (control, anodal, cathodal).

To confirm these observations, the quantitative analysis of all CRs was performed by calculating the mean relative area and latency of the series 2, 3, 4, 5, and 6 of each session. On session C8, series 1 was used as a control trial (without tDCS) and not included in the analysis. Series 1 from C7 and C9 were also excluded to keep the number of averages equal for each session (a total of 10 values per session for two animals). For an appropriate comparison between experimental and control sessions, relative area values were normalized via dividing the average of each series (of sessions

C11, C12, and C13) by the average of the highest observed relative area (strongest response) observed across the control series.

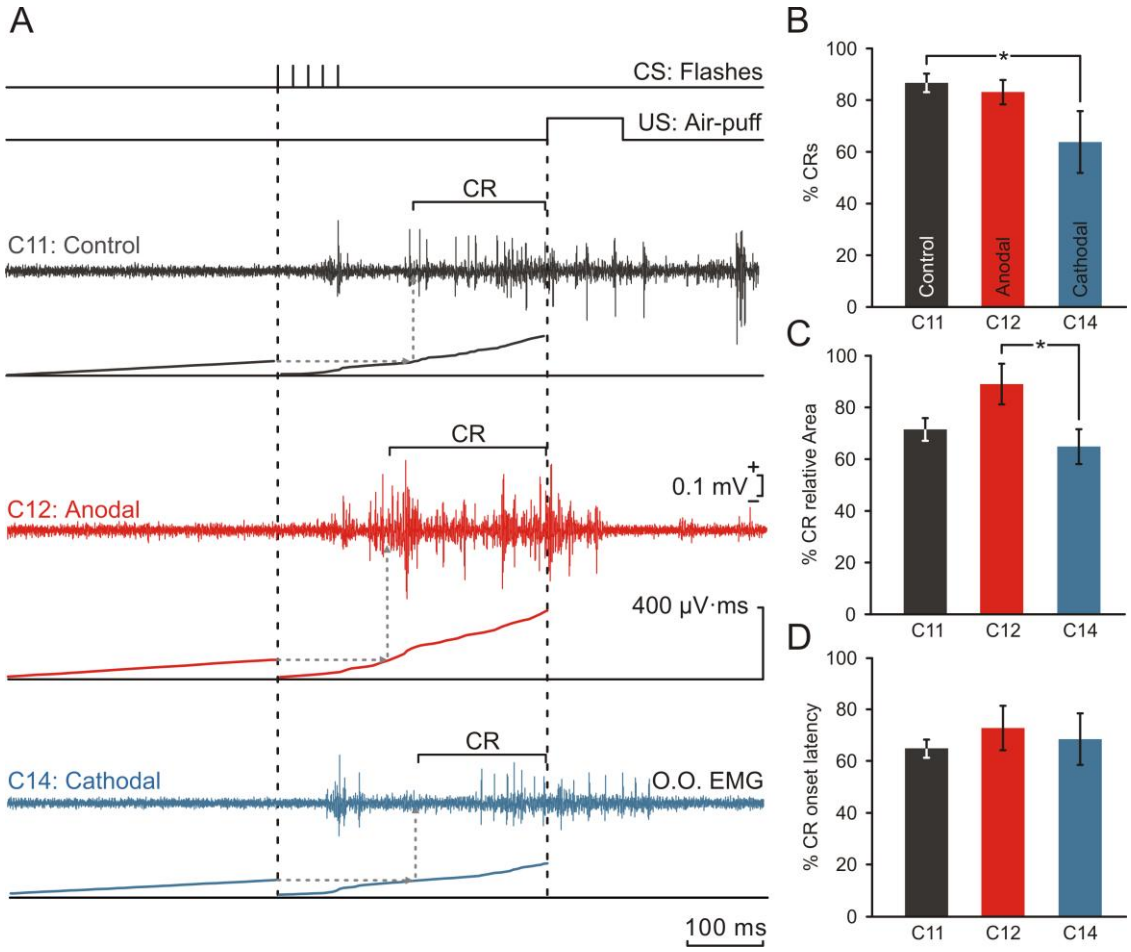

Figure 4.14 tDCS effects on performance and timing of CRs in strongly-trained animals. ***A***, Representative *orbicularis oculi* (O.O. EMG) recordings collected from a strongly-trained animal presenting responses from a control session (traces in black), anodal tDCS session (trace in red), and cathodal tDCS session (trace in blue). The presence, during the CS-US interval, of EMG activity lasting >10 ms and initiated after CS onset was considered as a CR. The integrated EMG activity (IA) recorded during the CS-US interval (IA_{CR}) had to be greater than the integrated EMG activity recorded immediately before CS presentation ($IA_{control}$). The CR onset was defined by the point where IA_{CR} overtook $IA_{control}$. ***B-D***, Modulation of CR percentage (***B***), CR strength (***C***) and CR onset latency (***D***) induced by tDCS in strongly-trained animals. Normalized values (100% = maximum response) from the recordings collected from three (control, anodal, cathodal) extra conditioning sessions*, $P<0.05$, one-way $ANOVA_{RM}$. Error bars represent SEM.

Similarly, the CR onset latency values (time difference between the CS initiation and the CR onset) from session C11, C12, and C13 were normalized by dividing the average of each series by the lowest latency (fastest response) observed across the control series. One-way $ANOVA_{RM}$ was performed with the factor SESSION and the results represented in **Figure 4.14*B*** demonstrated once more that cathodal tDCS reduced the number of CRs ($P = 0.044$; $ANOVA_{RM}$, $n = 10$; Bonferroni correction as *post hoc* test), whilst no significant differences were found between the control and anodal session ($P = 1.000$). With regard to the response strength (relative area), the statistical analysis revealed a significant main effect ($P = 0.038$, $ANOVA_{RM}$, $n = 10$). CRs during the anodal tDCS session showed significant stronger responses compared to the cathodal session (**Figure 4.14*C***) as revealed by *post hoc* comparisons using Bonferroni (anodal vs. cathodal: $P = 0.042$; control vs. anodal: $P = 0.195$; control vs. cathodal: $P = 1.000$). Responses during the anodal session appeared slightly earlier compared to the control session. However, the statistical analysis did not reveal significant differences ($P = 0.668$). Similarly, CRs during cathodal tDCS showed no change in onset latency after flash presentation compared to the control session (**Figure 4.14*D***).

Given these points, the presentation of cathodal currents on V1 significantly impaired CR performance by reducing the number of CRs. Moreover, anodal V1-tDCS seemed to have no impact on CR quantity during classical eyeblink conditioning, as has been observed for anodal MC-tDCS. In turn, CR strength was significantly enhanced with anodal tDCS over V1 compared to the CRs from the cathodal session, showing some similarities with the anodal tDCS effects over MC (Experiment 2). However, the lack of a control group receiving sham tDCS on V1 complicates the interpretation of the results.

Experiment 4

4.4. Testing thermal epidural effects during tDCS over the cerebral cortex

Finally, the last series of experiments served to rule out that tissue heating induced by the transcranial stimulation interfered with the observed tDCS effects of the previous experiments. The aim was to examine the epidural thermal variations of the transcranially stimulated site during and after prolonged tDCS in the alert rabbit.

For brain temperature measurement, a NTC thermistor was epidurally implanted on the MC and tDCS was simultaneously applied through a silver chloride (Ag/AgCl) disc electrode over the MC skull (**Figure 4.15**).

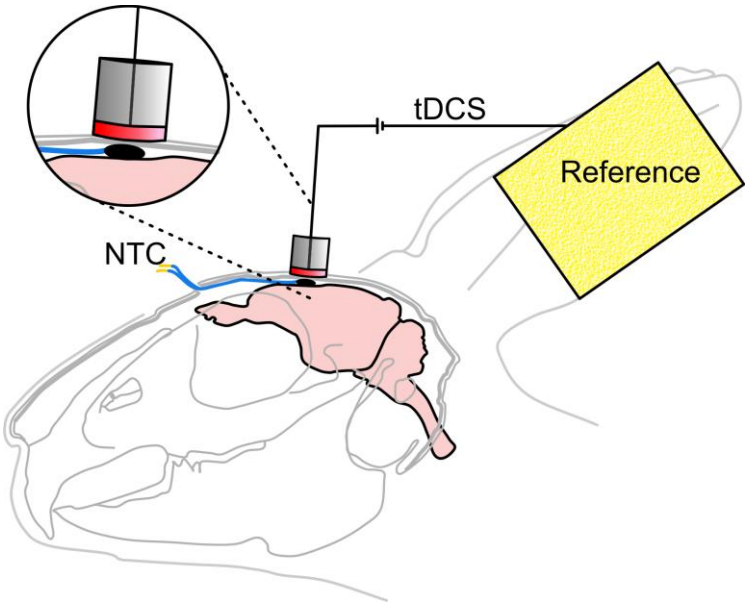

Figure 4.15 Experimental design for brain temperature measurement with concurrent tDCS application indicating the electrode location over MC. tDCS currents were applied through a silver chloride disk electrode (0.5 cm^2) inserted in a plastic tube (ø 8 mm) implanted over MC whilst a large (35 cm^2) saline-soaked sponge electrode placed on the contralateral ear served as a counterelectrode (Reference). An epidural NTC (Negative Temperature Coefficient) was placed on MC (under the epicranial stimulating electrode) for continuous brain temperature measurement.

Before starting the experimental series, the correct operation of the NTC thermistor was tested by introducing a small amount of electro-gel (previously heated up until 45 ºC) in the plastic tube over the skull envisioned for the tDCS application. Immediately, a short-latency increase of the epidural brain temperature was observed, reaching the maximum change (Δ 0.45 ºC) after 60 s (**Figure 4.16**). During experimental sessions, the brain temperature was continuously recorded before, during and after anodal and cathodal tDCS. The stimulation was applied with different current densities during 60 or 120 min (depending on the magnitude of current density).

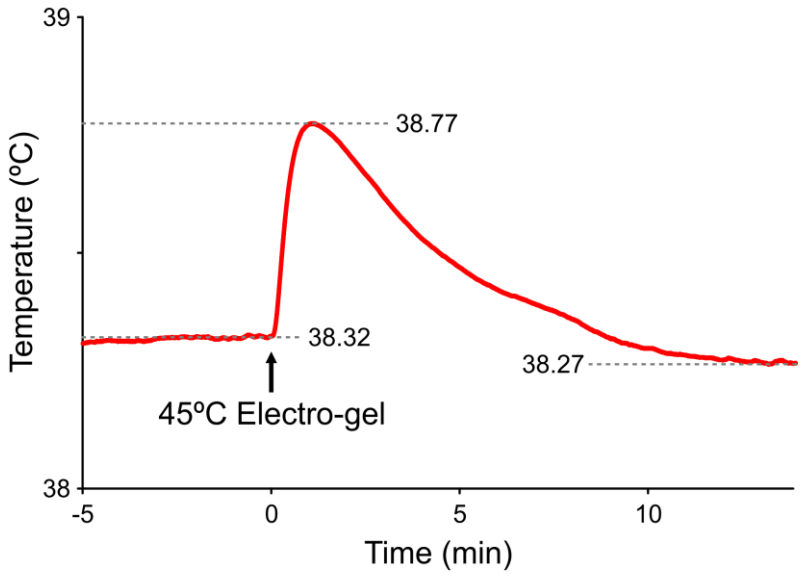

Figure 4.16 Testing for correct operation of the NTC thermistor. Electro-gel was heated up to 45° C and inserted in the plastic tube over the skull. Immediately after, epidural brain temperature rapidly (60 s) increased (Δ 0.45°C) and ten minutes later normal brain temperature was reached again.

In order to reproduce tDCS conditions used in humans, in a first series of recordings the current density was set at ±0.029 mA/cm^2 (usually applied in humans), stimulating with an tDCS intensity of ±14.6 µA in accordance with the disc electrode surface (0.5 cm^2). **Figure 4.17*A*** illustrates that this current density did not induce noticeable temperature variations in a representative animal.

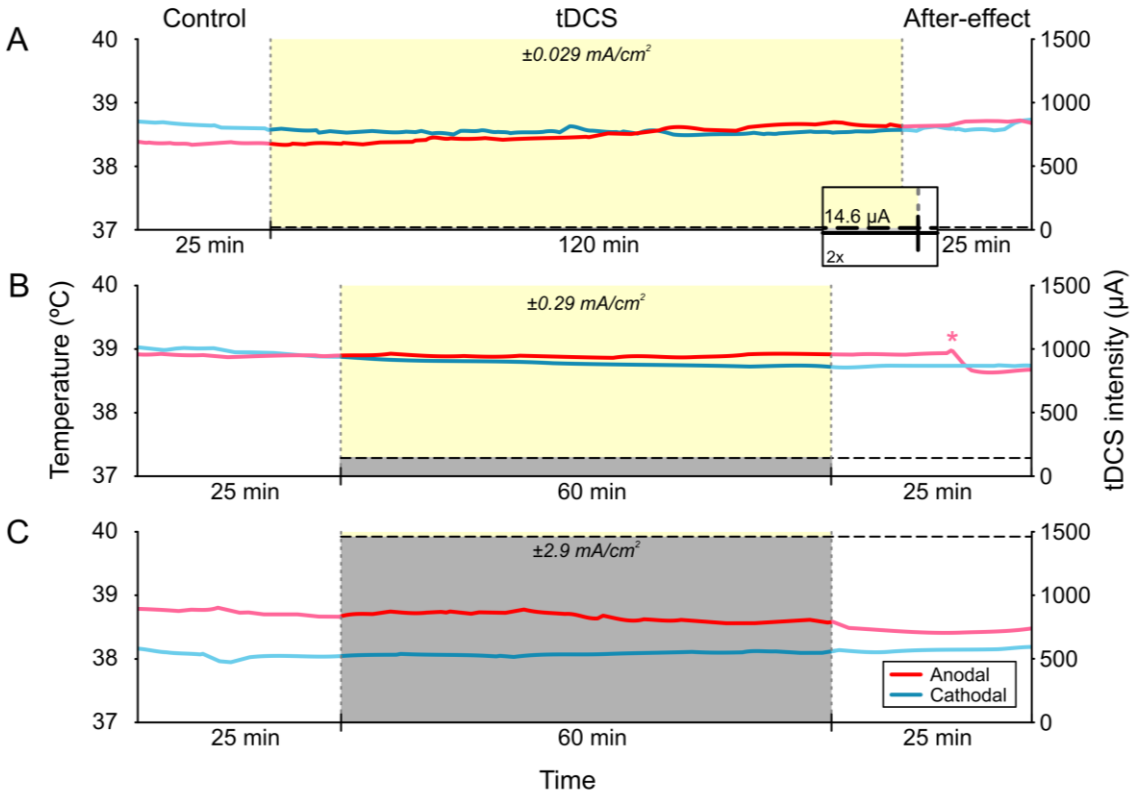

Figure 4.17 Thermal effects of tDCS over the cerebral cortex for a representative animal. ***A-C,*** Continuous measurement of epidural brain temperature before (25 min), during (120 or 60 min) and after (25 min) anodal (red lines) and cathodal (blue lines) tDCS presentation. Anodal and cathodal currents were presented on separate days. Brain temperature (°C) recordings for tDCS current densities that are usually applied in humans (±0.029 mA/cm^2, ±14.6 µA) (***A***), one order of magnitude higher (±0.29 mA/cm^2, ±146.0 µA) (***B***), and, until two orders of magnitude higher (±2.9 mA/cm^2, ±1460.0 µA) than generally used in humans (***C***). Magnitude of tDCS intensity marked with grey background. Insertion in ***A*** serves to highlight the very low tDCS intensity. *Temperature change due to movement of the animal in the restriction box.

A second and third experimental series were performed to investigate whether higher tDCS current densities were able to induce relevant thermal changes. Thus, current density was increased one order of magnitude above (±0.29 mA/cm^2) the one applied in humans, i.e., tDCS intensity was set at ±146 µA for 60 min (**Figure 4.17*B***). In the third series, current density was augmented up to two orders of magnitude higher (±2.9 mA/cm^2) than normally used in humans. To reach the mentioned current density, the tDCS intensity was increased until ±1460 µA and applied over 60 min (**Figure 4.17*C***). Evidently, none of the used current densities induced a major variation of brain temperature neither during nor after the application of tDCS for this representative animal.

The data for three animals was quantified and illustrated in **Figure 4.18**. The temperature measures were averaged every 5 min for each session for both anodal and cathodal conditions. The results show that the application of the lowest current density of tDCS (0.029 mA/cm^2) over 120 min did not reveal statistically significant (Anodal/P = 0.370, Cathodal/P = 0.289, n = 3, ANOVA$_{RM}$) variations of the brain temperature along the entire session, showing a maximum temperature variation of 0.40 ± 0.28 ºC for the anodal session (mean ± SEM) and 0.38 ± 0.25 ºC for the cathodal session (**Figure 4.18*A***).

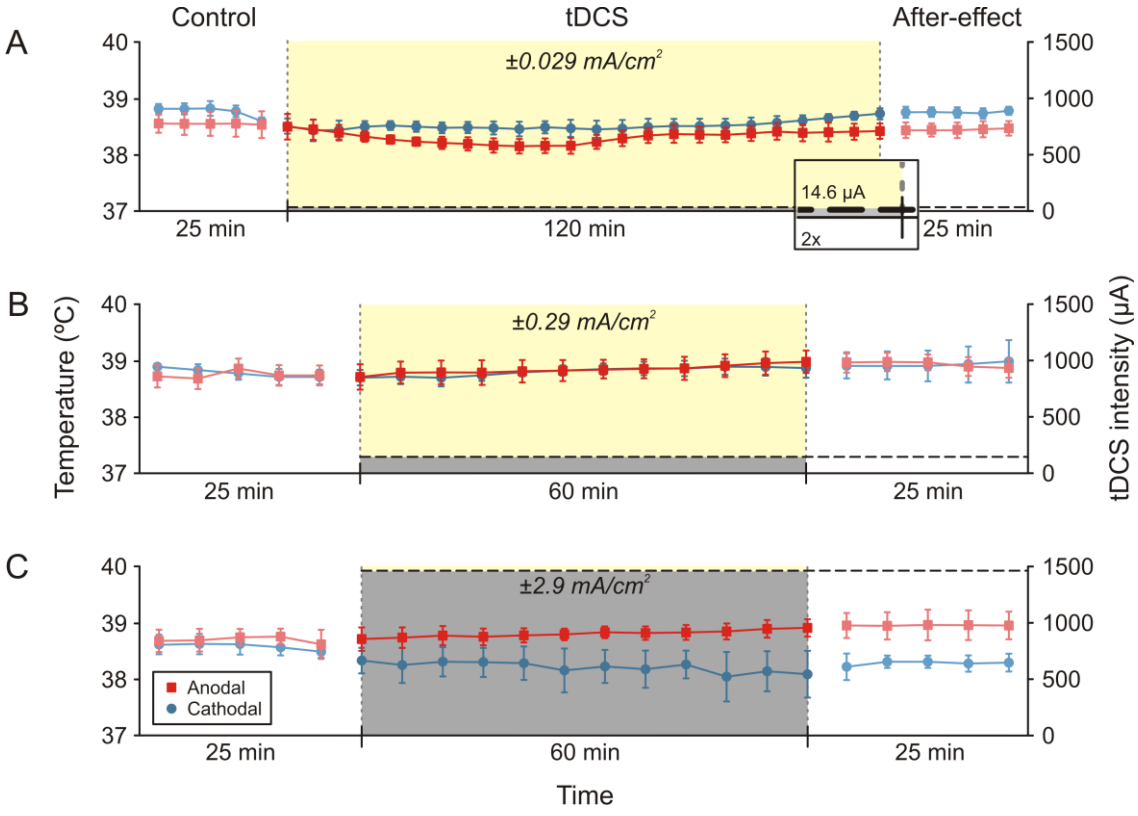

Figure 4.18 Averaged raw thermal effects of tDCS over the cerebral cortex. ***A-C,*** Averages (n = 3) calculated for every 5 min of epidural temperature (°C) measurement before (25 min), during (120 or 60 min) and after (25 min) tDCS. Anodal and cathodal currents were applied on separate days. Current densities similar to those used in humans (±0.029 mA/cm^2, ±14.6 µA) (***A***), one order of magnitude higher (±0.29 mA/cm^2, ±146.0 µA) (***B***), and until two orders of magnitude higher (±2.9 mA/cm^2, ±1460.0 µA) (***C***) than generally applied in humans were used. Magnitude of tDCS intensity marked with grey background. Insertion in ***A*** serves to highlight the very low tDCS intensity. Error bars represent SEM. One-way ANOVA$_{RM}$ applied for each condition revealed a non-significant main effect for all conditions (n = 3).

Similarly, the averaged temperature values for tDCS current density of one order of magnitude higher than usually used in humans (±0.29 mA/cm^2) presented no statistical significance for 60 min anodal (0.29 mA/cm^2, P = 0.255, n = 3, ANOVA$_{RM}$) or cathodal application (0.29 mA/cm^2, P = 0.563, ANOVA$_{RM}$). The maximum observed change of brain temperature across the anodal session was 0.26 ± 0.13 ºC, whereas the cathodal session presented a maximum variation of 0.28 ± 0.31 ºC (**Figure 4.18*B***). Finally, the current density of two orders of magnitude higher (±2.9 mA/cm^2) than generally applied in humans also resulted in non-significant (Anodal/P = 0.536, Cathodal/P = 0.440, n = 3, ANOVA$_{RM}$) thermal changes during and after tDCS application. In this case, the maximum changes of temperature were 0.34 ± 0.39 ºC and 0.58 ± 0.55 ºC for anodal and cathodal presentation, respectively (**Figure 4.18*C***). During the 60 min of cathodal tDCS (-2.9 mA/cm^2) a decreasing trend of brain temperature can be observed. The higher inter-subject variance and the individual data show that this observed trend is driven by a single animal. Nevertheless, this steady and slow decrease besides other minor and slow appearing temperature variations observed across the three experimental series are unlikely to be caused by the application of tDCS but rather by natural physiological temperature fluctuations (Kawamura et al., 1966).

To minimize baseline variations between animals, data of each animal was normalized to the average value of its baseline (before tDCS) temperature and represented in **Figure 4.19**. As can be observed, the resulting normalized curves did not differ noticeably from the curves presenting raw temperature values. Accordingly, statistical analysis did reveal non-significant thermal variations for all three current densities (±0.029 mA/cm^2, ±0.29 mA/cm^2, ±2.9 mA/cm^2) of anodal and cathodal tDCS (**Table 1**).

In summary, these results confirm that modulation of learning observed in Experiment 2 (tDCS applied through a disc electrode) was not influenced by thermal changes in the brain tissue generated under the tDCS electrodes. For Experiment 3 (4 silver-ball electrodes) possible thermal variations induced by tDCS cannot completely be discarded since applied current densities were higher (up to 7.82 mA/cm^2 per ball when 2 mA tDCS was used).

Polarity	Current density (mA/cm^2)	P – values *Raw data* (°C)	P – values *Normalized data* (%)
Anodal	0.029	0.370	0.370
	0.29	0.255	0.255
	2.9	0.536	0.535
Cathodal	0.029	0.289	0.288
	0.29	0.563	0.562
	2.9	0.440	0.441

Table 1. Statistical results of brain temperature measured continuously before, during and after tDCS applied with three different current densities. $ANOVA_{RM}$ showed non-significant ($P > 0.05$) temperature variations across each experimental session.

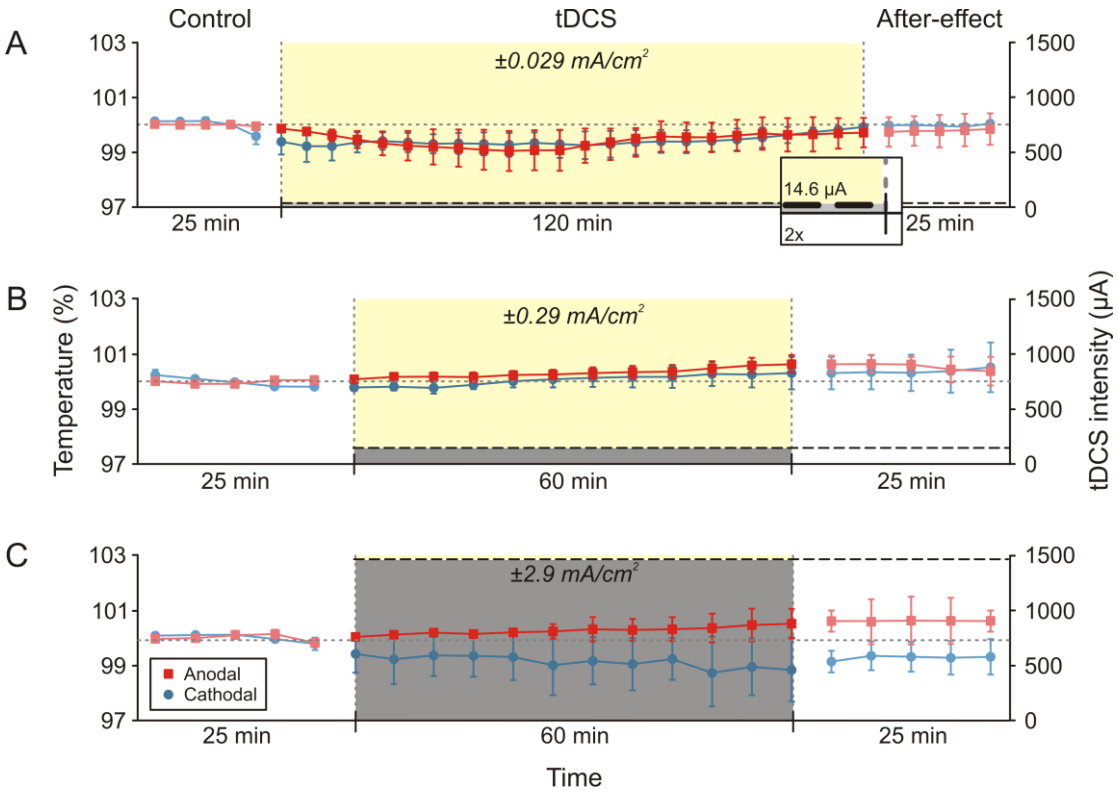

Figure 4.19 Averaged and normalized thermal effects of tDCS over the cerebral cortex. ***A-C,*** Temperature measures of each animal were normalized to the average value of its baseline (before tDCS) temperature. Averages (n = 3) calculated for every 5 min of epidural temperature measurement before (25 min), during (120 or 60 min) and after (25 min) tDCS. Anodal and cathodal currents were applied on separate days. *(Figure legend continued on page 95)→*

←***(****continued Figure legend from page 94****)*** Current densities similar to those used in humans (±0.029 mA/cm^2, ±14.6 µA) (***A***), one order of magnitude higher (±0.29 mA/cm^2, ±146.0 µA) (***B***), and until two orders of magnitude higher (±2.9 mA/cm^2, ±1460.0 µA) (***C***) were used. Magnitude of tDCS intensity marked with grey background. Insertion in ***A*** serves to highlight the very low tDCS intensity. Error bars represent SEM. One-way ANOVA$_{RM}$ applied for each condition revealed a non-significant main effect for all conditions (n = 3).

5. DISCUSSION

5.1. New insights into cerebral cortex's function during associative learning

The experimental work of the present Doctoral Thesis provides novel findings about associative motor learning and enriches the understanding of neural structures implicated in the acquisition process of classical conditioned eyeblink responses. Despite the commonly assumed roles of the cerebellum and hippocampus in the generation of learned eyeblink responses (Christian and Thompson, 2003; Thompson and Steinmetz, 2009), the present study strongly proposes a major role of the MC in the acquisition of classical conditioned eyelid responses in the rabbit. Earlier studies pointed towards a possible participation of this cortical structure in the associative learning process (Woody et al., 1970, 1974; Megirian, 1973; Aou et al., 1992; Birt et al., 2003). However, carefully-performed electrophysiological recordings of MC activity and antidromic identification of MC neurons were still missing to support this hypothesis. In the present work, MC neurons present a clear increase in their firing rate well in advance (≥ 50 ms) with respect to the CR onset and could be characterized and partially identified as monosynaptic projections to FN or RN. In addition, the acquisition of eyeblink conditioning was modulated by shifting the neuronal excitability of the MC and sensory cortex (V1 – present results; S1 – Márquez-Ruiz et al., 2012), clearly confirming the implication of the cerebral cortex in associative motor learning. Therefore, the final outcomes of the present Doctoral Thesis provide exciting and novel insights into the complex 'machinery' of this seemingly simple learning of eyeblink responses and suggest a distributed network of various neural structures implicated in the acquisition of classical eyeblink conditioning – as has been already suggested by previous studies (Siegel et al., 2015; Yang et al., 2015) – rather than an exclusive involvement of one or few regions.

5.2. Role of the MC during classical eyeblink conditioning

5.2.1. Activity of different MC neurons during eyeblink conditioning

After years of discussion and debate about the implicated neural regions in the acquisition of classical eyeblink conditioning, the present results clearly show for the

first time that the MC neurons are involved in the generation of eyelid CRs. Recorded neurons were classified as MC neurons projecting to FN or RN, and as MC neurons with an unidentified projection site (non-activated neurons, Types A-C). Importantly, the firing of several recorded MC neurons from the different types started during the CS-US interval well in advance (>50 ms) of the beginning of CRs. The classification of non-activated MC neurons was based on the firing pattern from each neuron. Thus, type A neurons increased their discharge rates across conditioning sessions during the CS-US interval and reached peak firing during that interval, while type B cells presented a second peak during the US presentations. Since this firing pattern seemed to be more similar to the firing pattern observed from the MC neurons projecting to FN, type A and B neurons might well project to FN. It is possible that these neurons form part of sub-populations with very slowly-conducting, nonmyelinated axons in the MC as has been observed for the wrist and hand area of the primate motor cortex (Humphrey et al., 1978). These types of neurons are often omitted by antidromic activations, since this method is biased towards the detection of neurons with fast-conducting axons (Swadlow, 1998; Firmin et al., 2014). Type C cells increased their firing rate across the CS-US interval, reaching peak values at the time of US presentation. A similar activation pattern was observed for most MC neurons projecting to RN. Thus, it is possible that type C neurons project to RN through slowly-conducting axons based on the same explanation as for type A and B neurons. Together, the identification of MC neurons presenting firing activities initiated well in advance to the CRs onset weakens the hypothesis of the exclusive role of the cerebellum (Christian and Thompson, 2003; Thompson and Steinmetz, 2009) in the generation of CRs during the classical eyeblink conditioning.

5.2.2. MC control of the orbicularis oculi muscle

The intrinsic organization of the FN showing different groups of motoneurons innervating facial muscles is well preserved across mammals (Morecraft et al., 2001; Sherwood, 2005). In particular, *orbicularis oculi* motoneurons occupy the dorsolateral subdivision of the nucleus in primates (Porter et al., 1989; Morecraft et al., 2001), cats (Radpour, 1977; Shaw and Baker, 1985; Holstege et al., 1986), rabbits (Holstege and Collewijn, 1982), mice (Komiyama et al., 1984), and rats (Martin and Lodge, 1977). At

the same time, facial muscles have distributed and repeated representations in different MC areas (Morecraft et al., 2001; Müri, 2016). Although it has been suggested that direct descending projections from the MC in the FN are present only in catarrhine primates, in relation to their enhanced facial expressions (Sherwood, 2005), the present results indicate, by the use of neuronal tracers and unitary activity recordings, the presence of a relatively modest monosynaptic projection of MC neurons into the *orbicularis oculi* subdivision of the FN in the rabbit. In this regard, Grinevich and colleagues (2005) have described a more definite monosynaptic pathway from the vibrissa MC to facial motoneurons in rats. Although MC projections to *orbicularis oculi* motoneurons in rabbits did not appear as dense as those described for vibrissa motoneurons in the rat, the effects of MC stimulations on the EMG activity of the *orbicularis oculi* muscle (Figure 4.2) indicate the presence of functional post-synaptic influences of the MC projecting neurons on *orbicularis oculi* motoneurons. Fanardjian and Manvelyan (1987) have reported similar findings in acute electrophysiological experiments carried out in anesthetized cats demonstrating that stimulation of MC resulted in evoked polysynaptic excitatory and inhibitory potentials in facial motoneurons. As reported here, MC neurons projecting to FN and non-activated MC neurons (Types A, B, and C), and in a less clear manner neurons projecting to RN, started firing well in advance of the initiation of CRs (anticipated firing to CR between approx. 130 and 50 ms). In contrast, identified *orbicularis oculi* motoneurons start their firing ≈ 2 ms before the initiation of EMG activity of the innervated muscle (Trigo et al., 1999a). These differences are suggestive of a slowly building depolarization of facial motoneurons preceding their firing during the generation of eyelid CRs. A comparison between the short latencies in the activation of facial motoneurons during corneal reflex responses (Baker et al., 1980; Shaw and Baker, 1985; Trigo et al., 1999a) and the long latencies for MC activation of *orbicularis oculi* motoneurons (present results) proposes, respectively, the contribution of somatic projections of second-order trigeminal neurons and distal dendritic projections of MC neurons on these motoneurons. This suggestion is supported by acute electrophysiological experiments carried out in anesthetized cats (Fanardjian et al., 1983; Fanardjian and Manvelyan, 1987). As described by the authors and confirmed by prior studies (Tanaka et al., 1971; Iwata et al., 1972), the spinal trigeminal nucleus is one of the principal relay centers passing information to the neurons of the FN that participate in short-latency reflex responses. On the other hand a gradual or slowly building polarization appears to be

activated through distal dendritic projections, which might be the pathway for relatively long-latency responses (Fanardjian et al., 1983) of MC neurons projecting on the facial motoneurons. In addition, the different depolarization profiles and the strength of activation of facial motoneurons during the corneal reflex and during CRs (Trigo et al., 1999a) explain at least in part the different profiles and kinematics of reflex vs. conditioned eyelid responses (Trigo et al., 1999a; Gruart et al., 2000c). In brief, the present results show first evidence in the rabbit of direct, albeit sparse, descending MC projections in the FN, specifically in the subdivision representative for the *orbicularis oculi* motoneurons.

Besides the mentioned MC projections, MC commands also reach the FN across cortical projections to the RN. Indeed, prior research showed that the RN receives substantial inputs from the MC (Miller and Gibson, 2009; Gruber and Gould, 2010) and the firing of RN neurons projecting to the contralateral FN is significantly disfacilitated by MC inactivation (Pacheco-Calderón et al., 2012). The antidromically identified MC neurons described here, and possibly type C neurons recorded in MC, seem to project to the RN.

5.2.3. Motor areas and classical eyeblink conditioning

Different studies have confirmed the presence of activity-dependent mechanisms in the dendrites of MC pyramidal neurons and cortical reorganizations in relation to the acquisition of new motor abilities (Doyon et al., 2003; Doyon and Benali, 2005). For example, an increase in dendritic length of layer V pyramidal neurons (Gloor et al., 2015) as well as a substantial synaptic remodeling of dendritic spines (Brecht et al., 2013; Ma et al., 2016) have been described as a result of the acquisition of a motor learning task. In addition, it also has been reported that both synaptic remodeling and the acquired learning can be removed with the help of optogenetic tools (Hayashi-Takagi et al., 2015). These cortical plasticity processes taking place in distal dendrites are dependent on proper NMDA-specific glutamate receptor functions (Hasan et al., 2013) and seem to be regulated by somatostatin-expressing inhibitory neurons (Chen et al., 2015). Earlier studies proposed an essential role of MC for the execution of CRs after examining functional and reversible ablation of the cortex induced by cortical

spreading depression achieved through KCL injections (Megirian, 1973). Finally, two seminal studies convincingly demonstrated the presence of depolarizing excitatory post-synaptic potentials (EPSPs – increases the likelihood of postsynaptic action potential occurring) in the pericruciate cortex of awake cats in response to CS and US presentations (Birt et al., 2003) and that the activation of recorded cortical units by CS presentations preceded the onset of the evoked classical CRs (Aou et al., 1992). In summary, the findings collected by several research groups further support the present results, confirming the hypothesis that the MC is involved in the acquisition of classically conditioned eyelid responses.

Certainly, a distributed network of motor areas is probably implicated in the learning process of classical eyeblink conditioning. As described earlier, MC commands also reach the FN across cortical projections to the RN. In fact, a smaller portion of the antidromically activated MC neurons projecting to the RN (20 of 189 neurons), together with the type C MC neurons described here which possibly project to the RN, seem to carry motor command signals preferentially related to the performance of CRs, along with other eyelid motor behaviors. A characteristic that is also present in RN neurons projecting to the FN (Pacheco-Calderón et al., 2012). Thus, the results of the present study show that both the monosynaptic MC-FN as well as the MC-RN-FN pathways seem to be implicated in the generation of CRs.

On the other hand, it is well known that the MC also sends descending projections to the cerebellum via pontine nuclei (Brodal, 1987; Kosinski et al., 1988), a fact already taken into consideration in previous studies on classical eyeblink conditioning (Ivkovich and Thompson, 1997). It should be noted here that this important projection reaches the cerebellum providing an efference copy of cortical motor commands (Holst and Mittelstaedt, 1950; Sperry, 1950). Feedback projections from cerebellar nuclei to different cortical areas are then capable of modulating those motor commands for better performance of the aimed motor responses, especially having a greater impact on timing of the CRs than to their generation and/or initiation (Sánchez-Campusano et al., 2007; Yang et al., 2015).

As shown in prior research (Pacheco-Calderón et al., 2012), the reversible inactivation of the MC evoked a significant reduction in the integrated EMG amplitude of both

conditioned and unconditioned responses, more noticeable in the former. These results and the fact that the present study directly demonstrated the involvement of the MC in the acquisition of classical eyeblink conditioning in the rabbit are in contrast with those of classic studies indicating that even large MC lesions do not seem to affect the acquisition or performance of CRs in rabbits and cats (Oakley and Russell, 1977; Mauk and Thompson, 1987; Ivkovich and Thompson, 1997), suggesting that MC is not necessary for classical conditioning of eyeblink responses. Nevertheless, Kelly and colleagues (1990) described the presence of noticeably modified CRs in the decerebrate-decerebellate rabbit. Similarly, in different forms of Pavlovian conditioning, functional decortications prevented acquisition of CRs capable of disrupting the baseline activity (Bures and Buresova, 1963; Russell et al., 1969). The interpretation of lesion studies should be treated with caution since behavior is usually tested > 1 week after the intervention, i.e., other brain areas might experience reactive and compensatory changes that could have an effect on post-operative behavior (Freeman and Steinmetz, 2011). Such compensatory function – in this case, after acute inactivation of the IP – has been recently observed and demonstrated for the RN and the surrounding pararubral area, as these areas are able to substitute for the respective motor roles of cerebral cortical and cerebellar structures in the eyeblink conditioning (Pacheco-Calderón et al., 2012). This is because they receive afferents from different sensory modalities (Padel et al., 1988) and present rich intrinsic circuits (Haley et al., 1988; Horn et al., 2002).

In summary, in accordance with the above contentions, it can be proposed that the MC is an important cerebral structure in the generation and performance of eyelid CRs. Furthermore, previous investigations suggest the presence of additional neural centers, besides the MC and the cerebellum, with a limited capacity to generate CRs.

5.3 Modulation of associative learning by changing motor cortex's excitability

The second series of experiments of the present Doctoral Thesis aimed to confirm and underline the role of the MC and its impact on the motor learning process during the acquisition of classical eyeblink conditioning. The results clearly proved that MC

neurons fire a burst of action potentials preceding the EMG activation of the *orbicularis oculi* muscle during the CS-US interval – i.e., during the generation of CR. To study whether modulating the excitability of the MC neurons could modify the learning process and/or the quality of learned responses, weak direct currents on MC were applied during the acquisition of classical eyeblink conditioning.

5.3.1. Enhancement of acquisition of classical eyeblink conditioning induced by anodal MC-tDCS

The application of direct current stimulation has been shown to be a reliable technique of modulating cortical excitability in human (Nitsche and Paulus, 2000, 2001; López-Alonso et al., 2015; Ammann et al., 2017), and in animal studies both *in vivo* (Bindman et al., 1964; Cambiaghi et al., 2010; Márquez-Ruiz et al., 2012) and *in vitro* (Radman et al., 2009; Rahman et al., 2013). Accordingly, the present results clearly demonstrated that the modulation of MC excitability via the concurrent application of tDCS induced a significant impact on the associative learning process. Specifically, the rate of learned responses was increased during the CR acquisition (day C3) when anodal tDCS was applied on the palpebral MC area (Figure 4.8.1). Thus, these results support the previously stated hypothesis proposing a critical role of the MC during the acquisition of eyeblink conditioning. On the other hand, it is also shown for the first time that tDCS-induced modulation of the animal's MC excitability elicited improved motor performance during the acquisition of a learning task.

Currently, only a few studies based on animal models have examined the role of the cerebral cortex during learning by applying modulatory weak direct currents over the scalp. One reason for this lack of literature might be the technical challenge of applying tDCS *in vivo,* especially in the behaving animal during the task performance. Dockery and colleagues (2011) applied anodal and cathodal tDCS over the frontal cortex in order to measure its effects on performance in spatial working memory and skill learning based on avoidance in rats. The authors found no measurable short-term effects of anodal or cathodal tDCS on performance when applied before working memory training. Nevertheless, long-term benefits from cathodal stimulation appeared on day 21 (without stimulation). This observation was established by improved

retention of the task in comparison with the control group. The findings support that diminishing the excitability of the frontal cortex via acute stimulation paired with working memory training and skill learning of a novel task induces long-term benefits. Furthermore, Márquez-Ruiz and colleagues (2012) studied the susceptibility of the eyeblink conditioning to S1 modulation using the same animal model as in the present study, with the difference that electrical stimulation of the whisker pad was used as CS instead of a tone or flash. Consistent with the polarity-specific effects, the acquisition of the learning was potentiated or weakened (based on the rate of learned eyeblink responses) by the concurrent application of anodal or cathodal tDCS, respectively. The authors demonstrated the implication of S1 during eyeblink conditioning proposing that cortical sensory perception processes required for associative learning were modulated by tDCS leading to an improved (via anodal tDCS) or impaired (via cathodal tDCS) perception of the sensorial stimulus at the whisker pad. A recent study also demonstrated that modulation of S1 excitability via bilateral anodal tDCS improved accuracy of reaching movements, and selectively changed quality of movement components in rats performing a skilled forelimb reaching task for 20 consecutive days while concurrently receiving tDCS (Faraji et al., 2013). In conformity with the mentioned studies, the present results reveal that, besides the cortical modulation of sensory inputs, MC excitability also plays an important role during the acquisition of a motor learning task, specifically the learning of conditioned eyelid responses. Interestingly, while S1 was susceptible to cathodal tDCS resulting in learning impairment (Márquez-Ruiz et al., 2012), quantity of learned eyeblink responses was not reduced when cathodal currents were applied over MC. However, as discussed in the next section (5.3.2), eyeblink response quality measured by response magnitude and onset latency was altered by cathodal tDCS.

The implicated cortical mechanisms and structures in learning, specifically motor learning, have been explored more extensively in humans using tDCS. However, the direct comparison of tDCS effects between animal and human studies ends frequently with discordant conclusions, due to the lack of similarity between the experimental designs used in animals and clinical practice protocols. Nevertheless, the use of animal models is crucial to extend our knowledge of basic processes underlying behavioral and electrophysiological effects observed in human studies (Márquez-Ruiz et al., 2014),

and great efforts have been made in the last years to develop human-research-oriented animal models of tDCS to improve translational aspects (Jackson et al., 2016).

With this in mind and similar to the present results, Nitsche and colleagues (2003b) showed for the first time in the human that the excitability increase of the primary MC induced by anodal tDCS applied during training enhances performance in the acquisition and early consolidation phase (i.e. stabilization of the motor memory rapidly after its initial acquisition) of an implicit motor sequence learning task illustrated by reduced reaction times – a common way to quantify this type of motor learning. MC activity was seemingly not altered by cathodal stimulation. A series of tDCS investigations showed similar results and confirmed the implication of MC during motor sequences learning (Savic and Meier, 2016). Thus, based on an extended list of human studies that focused research on understanding the role of different cortical areas during motor learning, the use of tDCS seems to be a potential technique for this purpose (Ammann et al., 2016).

With regard to associative learning paradigms, the involvement of the cerebellum during classical eyeblink conditioning (mainly delay paradigm) has been repeatedly demonstrated in human and animal studies (Gerwig et al., 2007; Freeman and Steinmetz, 2011; Yang et al., 2015). Nevertheless, the fact that S1 modulation showed a significant impact on the amount of learned responses (Márquez-Ruiz et al., 2012) together with the evidence of MC neurons' implication in the acquisition process of CRs (as demonstrated by the present work) suggested the logical step of testing the modulatory properties of tDCS over MC during the acquisition of this associative learning, instead of testing the stimulation over the cerebellum. However, the idea of testing cerebellar tDCS and, if possible, with simultaneous recording of cerebellar neurons to better understand the role of this structure during the acquisition of eyeblink conditioning, represents an interesting aim for future animal studies. In this context, first approaches have been performed by Zuchowski and colleagues (2014) in humans showing a significantly enhanced acquisition of CRs with anodal tDCS over the cerebellum ipsilateral to the US, and a markedly reduced acquisition rate of learned responses with cathodal tDCS compared to the sham condition, confirming the already reported polarity-specific modulation of cerebellar tDCS (Jayaram et al., 2012). In contrast to these findings (Zuchowski et al., 2014) but in accordance with the MC-

tDCS results from the present study, Kaski and colleagues (2012) showed that acquisition and timing of CRs was not modified by cathodal stimulation, in this case with the electrode placed over the inion in humans. Moreover, a recently performed study could only detect modulation of CR acquisition at a trend level induced by anodal and cathodal cerebellar tDCS compared to sham when a cephalic reference electrode was used. No changes on CR acquisition were observed with an extracephalic reference, and for both tDCS montages no significant effects either on CR timing or extinction and savings were found (Beyer et al., 2017).

In brief, findings acquired by using tDCS over different brain regions in humans and animals during learning support the hypothesis of a distributed neuronal network implicated in the acquisition of classical CRs, including MC as a vital part of this learning circuit.

5.3.2. Null effect with cathodal MC-tDCS on the number of learned responses during acquisition of eyeblink conditioning

The application of cathodal tDCS during the performance of associative learning did not show a significant impact on the number of performed CRs when the animal was already well-trained. This result was rather unexpected, since previous findings showed that S1 modulation via applying cathodal tDCS significantly reduced the percentage of CRs in a similar experimental design (Márquez-Ruiz et al., 2012). The decrease of S1 excitability induced by cathodal tDCS was potent enough to modulate the sensory input and consequently alter the acquisition process, but when applied on MC, this cathodal-induced shift of neuronal excitability seemed to be ineffective once the animal was well-trained to the paradigm. This finding could be suggestive for a well-consolidated motor memory (Goedert and Willingham, 2002; Muellbacher et al., 2002; Robertson et al., 2004) generated in the MC being less susceptible to changes (i.e., interference) of cortical excitability in advanced conditioning days (in this case, C8).

Márquez-Ruiz and colleagues (2012) recorded sensory LFPs concurrently with the application of S1-tDCS during the conditioning. For this, the electrodes for tDCS (four silver balls) were placed around a small hole in the parietal bone where the

implantation of a tungsten microelectrode was used for the recording of LFPs. In the present study, the tDCS electrode (silver disc) was placed on the parietal bone without the need of a hole since no intracortical recordings were performed. However, Márquez-Ruiz and his group covered the hole with dental cement to avoid shunting through the skull cavity (Jackson et al., 2016), and consequently the ultimate current flow should not be significantly different compared to the intact skull (present study). On the other hand, the used electrodes montages (silver balls vs. silver chloride disc) presented a different electrode surface area (1.6 mm^2/ball vs. 1 cm^2) in contact with the bone, and thus the applied current density (15.6 mA/cm^2 per ball vs. 2 mA/cm^2) and consequently the strength of the induced electric field was of a different magnitude in each study. Another point which must be taken into account is that both studies investigated a slightly different type of associative learning (trace vs. delay paradigm). Together, the differences between both studies have to be considered when making conclusions about the discrepant results observed for cathodal tDCS.

Based on previous tDCS studies, inconsistent results are not uncommon to observe. For example, several studies have reported enhanced performance and retention of a reaction time task with simultaneous anodal tDCS over MC (Nitsche et al., 2003b; Kang and Paik, 2011; Kantak et al., 2012; Ehsani et al., 2016), whereas a few studies have presented null effects of tDCS on the same type of learning (Stagg et al., 2011; Ambrus et al., 2016). On the other hand, Herzfeld and colleagues (2014) tested tDCS over cerebellum and MC during force field motor adaptation – a type of error-based learning where quickly accounting for perturbations leads to large behavioral changes (Krakauer and Mazzoni, 2011) – and found that cerebellar anodal tDCS enhanced the rate of acquisition. In contrast, Taubert and colleagues (2016) observed impaired adaptation and re-acquisition of a force field perturbation with cerebellar anodal tDCS. In brief, variability and contradictions between studies need to be considered. However, this is frequently caused by minor modifications of the experimental procedures between studies (Paulus, 2011; Horvath et al., 2014, 2015).

Nevertheless, the following section will discuss possible physiological origins for the different effects observed on associative learning induced by cathodal tDCS on MC (present results) and S1 (Márquez-Ruiz et al., 2012), assuming that the previously

mentioned methodological differences between the two studies might have contributed to but not ultimately caused these divergent results.

5.3.3. Modulation of response quality during the acquisition of classical eyeblink conditioning induced by MC-tDCS

As explained in the previous section, the rate of conditioning learning (CR quantity) was not different to the control group when cathodal tDCS was applied over the MC. However, additional analysis revealed that CR quality (response latency and magnitude) was modified regardless of the well-trained state of the animal. In this context, animals showed weaker and a tendency of slower CRs on C8 when cathodal tDCS was applied compared to the conditioning sessions performed the day before and after. Therefore, it can be assumed that modulation of MC excitability via cathodal tDCS took place, causing a change in response quality rather than in response quantity of well-acquired CRs. In agreement, the possibility of altering learning performance through interference with memory consolidation even in a well-trained phase has been repeatedly demonstrated (Misanin et al., 1968; Nadel and Land, 2000; Nader et al., 2000).

Previous research performed in animals supports the hypothesis that this change in quality of the learned response was caused by a direct modulation of MC excitability and not by indirect processes induced in other neuronal structures. In this sense, Cambiaghi and colleagues (2010) reported significant modulation of evoked motor potentials (being a physiological marker for MC excitability) from the forelimbs when tDCS was applied over the MC in anaesthetized mice. Specifically, the authors found that MEP amplitude was significantly reduced with cathodal tDCS (and increased by anodal tDCS) compared to sham. It must be considered that these effects are measured *after* the application of tDCS (after-effects), whereas in the present study the recording of CRs and tDCS is performed *during* the conditioning session (series 1, 3, and 5: tDCS-OFF; series 2, 4, and 6 tDCS-ON). Consequently, the occurring physiological mechanisms might be different, since immediate (tDCS-ON) and after-effects (tDCS-OFF) are involved.

In this context, the present results are in agreement with the findings reported by Márquez-Ruiz and colleagues (2012). Thus, the authors determined the immediate effect of cathodal (as well as anodal) tDCS on neuronal excitability through recording S1-LFPs during concurrent tDCS pulses. As a result, the first negative LFP component (N1) was significantly reduced in amplitude and area in response to simultaneous cathodal tDCS, and amplified by the simultaneous presence of anodal tDCS, whereas long-lasting changes were only observed for cathodal currents (LTD-like induced reduction of N1 amplitude). Thus, this study and the present work demonstrate the capability of anodal and cathodal tDCS to induce cortical-excitability and plastic changes during eyeblink conditioning. Although MC modulation induced by cathodal tDCS did not have an effect on the quantity of CRs in the present study, the results suggest that the observed decrease of response magnitude and the modest increase of response latency (slower CRs) with concurrent cathodal tDCS were caused by a shift towards decreased cortical excitability (immediate effect) and/or by LTD-like plasticity mechanisms occurring in MC. Anodal tDCS may have provoked a shift towards increased MC cortical excitability and/or LTP-like plasticity processes, explaining the significantly greater number of CRs observed during early conditioning. In addition, CR quality was also changed by anodal tDCS, manifested as an increase of response magnitude together with a tendency of slower CRs (decrease in response latency) compared to the sham group.

As proposed by Márquez-Ruiz and colleagues (2012), modulating the excitability of the sensory cortex most likely interferes with the CS presentation, i.e., CS perception could be enhanced (through anodal tDCS) or impaired (through cathodal tDCS), accompanied by a higher number of CRs (anodal) or by response failures leading to a significant reduction of CRs (cathodal). In the present work, modulating MC excitability via cathodal MC-tDCS modified response quality but did not result in a significant change in the number of CRs. Thus, one possible explanation is that the animal in this case received uninterrupted information about when to respond since tDCS was delivered at a different cortical level, supposedly without interfering with CS perception. This could ultimately justify the different findings of cathodal tDCS presented to MC or S1 during eyeblink conditioning.

In summary, the present findings complement the statement from section 5.2 suggesting that the MC plays a critical role in acquisition of classical eyeblink conditioning. The evidence for this crucial cortical contribution has been raised not only by recording MC neurons, which started firing well in advance (>50 ms) with respect to the initiation of CRs, but also by the enhancement or impairment of the learning acquisition and performance (response quantity and quality) through modulating the cortical excitability via the application of anodal or cathodal MC-tDCS.

5.4 Modulation of associative learning by changing visual cortex's excitability

5.4.1. VEP components and neuronal contributions

The third experiment series tested whether the modulation of neuronal excitability of the sensory cortex, specifically V1, would bring forth a comparable impact on classical eyeblink conditioning as observed with the previously performed MC (present results) or S1 (Márquez-Ruiz et al., 2012) modulation. Similarly, the procedure to modify V1's excitability was based on applying transcranially direct currents, with the difference that the assessment of physiological markers (VEPs) was established to determine the direct impact of tDCS on neuronal activity. VEPs, induced by light flashes and recorded epicranially, presented an early positive component with a peak at ≈ 21 ms after the flash onset and a late negative component (≈ 49 ms). This observation is in accordance with previous studies performed in rabbits that recorded epidural VEPs with an early positive wave induced 20 – 30 ms after monocular light stimulation of the contralateral eye (Thompson et al., 1950; Yonemura and Tsuchida, 1968; Gerritsen, 1971; Arezzo et al., 1988; Sakaguchi et al., 2004; Soto et al., 2004; Siu and Morley, 2007). Other investigations indicate that VEPs of the rabbit presented first a negative wave at ≈ 20 ms. However, the authors reveal that, when the recording electrode was not inserted deep enough in the epidural space, the polarity of the N1 peak was reversed (Okuno et al., 2002). In this context, Porciatti and colleagues (1999) recorded VEPs intracortically in mice at different cortical depths and showed that VEPs recorded closer to the cortical surface displayed a positive waveform, whereas polarity was reversed with increasing cortical depths.

In the present study, VEPs were obtained by surface EEG recordings. In this context, it has been shown that the polarity of the EEG depends on the location of the synaptic activity within the cortex. Positive or negative deflections arise from both excitatory and inhibitory afferents of the pyramidal dendrites in the cerebral cortex. Thus, excitatory inputs in superficial layers or inhibitory inputs in deeper layers cause a negative deflection in the EEG, whereas excitatory inputs in deeper layers or inhibitory inputs in superficial layers generate positive deflections (Kirschstein and Kohling, 2009; Westbrook, 2013).

Regarding the neural origins underlying the generation of VEPs, the findings based on animal studies remain incomplete. In awake macaques, the VEP components induced by flash stimulation arise from different neural generators. For early positive components, a subcortical origin was proposed, while later negative and positive components originated from cortical V1 activity (Kraut et al., 1985). This is in discordance with the results from another study performed in awake macaques where V1 was suggested to contribute to early components, whereas later components may arise from V4 (Givre et al., 1994). One study performed in rats used visual pattern stimulation and the authors suggested that the early component (in this case negative) arises from the extrastriate cortex, whereas the later components (positive-negative) originate from V1 (Onofrj et al., 1985). However, they explain that the distinction of neural generators for flash VEPs is complicated, since their components arise from multiple origins [see for flash and pattern-reversal VEP comparison (Onofrj et al., 1982)].

The literature about the neural generators of VEPs in humans is more extensive, and proposes that the first VEP component named C1 (not labeled with P or N since its polarity can vary) with a peak at ≈ 100 ms originates from V1. The C1 wave is followed by the P1 wave possibly generated in the extrastriate cortex (early portion) and in the fusiform gyrus (later portion). The human VEP is constructed by more than the C1 and P1 wave, including the N1 wave (among others) probably arising from parietal and occipital cortex (Di Russo et al., 2002; Luck, 2005). Similar to the previously mentioned findings in rats, the neural origins of VEPs are induced by checkerboard pattern stimulation, while flash stimulation activates a large volume of

the visual areas (Farrell et al., 2007), which could explain the difficulty of defining the neural origins underlying this type of visual stimulation.

On the other hand, it is known that the magnocellular and parvocellular pathways, two anatomically and physiologically distinct pathways that lead from the retina to the striate cortex, are the two major streams contributing to the visual perception (Nealey and Maunsell, 1994; Purves et al., 2004). Several studies performed in humans established magnocellular and parvocellular contributions that underlie the generation of VEPs and can be successfully isolated by the contrast level of the stimulus pattern. The magnocellular pathway responds to low-contrast stimulation while the parvocellular pathway responds to high-contrast stimulation (Rudvin et al., 2000; Souza et al., 2007).

5.4.2. VEPs as physiological markers to measure cortical excitability

Although neural origins of the different VEP components recorded in the rabbit cannot be determined with certainty, the application of tDCS could give information about the existence of different underlying neural generators, besides the aim of using this technique as a medium to address the role of V1 during classical eyeblink conditioning.

Accordingly, the present findings show that significant tDCS effects were limited to specific components of VEPs, probably due to the fact that tDCS affects distinctively different cell groups in the visual cortex (Costa et al., 2015). Thus, no significant change in either amplitude or in latency of VEP components was observed after applying anodal currents for 20 min over V1. In contrast, cathodal currents induced a significant change in amplitude and latency for component P1 lasting up to 60 min after applying the stimulation, while for component N1 only a slight change in latency was induced and amplitude stayed unchanged. This finding could suggest a cortical origin for both components, specifically, P1 component from V1 (being the region stimulated directly under the tDCS electrodes) and N1 from extrastriate areas less affected by the induced electric field, since the cortex has been shown to be the most susceptible region to tDCS (Miranda et al. 2006, 2013; Ruffini et al., 2014). However, effects on VEPs are measured after 20 min of application of V1-tDCS, i.e., differences in VEP amplitude

could also arise from plastic changes in subcortical structures. Prior research has demonstrated that tDCS is capable of modulating the excitability of neural structures beyond the cortex, as has been shown in human (Polania et al., 2012; Nonnekes et al., 2014) and animal (Bolzoni et al., 2013a-b) investigations. Moreover, presynaptic actions of tDCS have been described for thalamocortical synapses during the application of S1-tDCS in the awake rabbit (Márquez-Ruiz et al., 2012) and for preterminal axonal branches of interpositorubral neurons when tDCS was applied over the sensorimotor cortex in anaesthetized rats (Baczyk and Jankowska, 2014). However, further investigations are needed to confirm these hypotheses about the possible origin of VEP components in the rabbit. Surprisingly, cathodal tDCS increased VEP amplitude, which is in contrast with the reported 'classical' decrease in amplitude of both human and animal MEPs (Nitsche and Paulus, 2000; Cambiaghi et al., 2011), or sensory LFPs in rabbits (Márquez-Ruiz et al., 2012) and human somatosensory evoked potentials (Dieckhöfer et al., 2006; Vaseghi et al., 2015).

Interestingly, the present finding is not the first indication of augmented amplitude of the positive VEP component observed after applying cathodal V1-tDCS. Antal and colleagues (2004b) recorded (besides the 'classical' increase/decrease of N70 amplitude induced by anodal/cathodal tDCS) enlarged amplitude of P100 immediately after applying cathodal stimulation on healthy participants, similar to the observations of Accornero and colleagues (2007) with the difference that they also observed significant effects for anodal polarization manifested by smaller P100 amplitude. Moreover, similar to the present results, Viganò and colleagues (2013) observed unmodified VEP amplitudes after applying anodal tDCS to V1 in healthy volunteers and episodic migraine patients.

Thus, even with methodological differences across studies (animal vs. human; flash vs. pattern stimulation), results are in partial agreement showing neuronal modulation induced by cathodal V1-tDCS does not always manifest as the 'classical' decrease in potential size, in addition to a lack of neuromodulatory effects with anodal V1-tDCS. Nevertheless, a recent study performed with anesthetized mice used flash stimulation (20 flash stimuli at 1 Hz) to induce VEPs recorded from two epidural screw electrodes implanted in V1. The authors observed VEPs with a first negative N1 (≈ 28 ms), followed by a positive P1 (≈ 38 ms) and a second negative N2 (≈ 57 ms) component.

The application of 10 min anodal or cathodal tDCS significantly increased or decreased, respectively, P1 amplitude by about 30% compared to the control condition (Cambiaghi et al., 2011). It must be taken into account that recorded VEPs from anesthetized animals do not present the same characteristics as the VEPs observed in awake animals (Gerritsen, 1971; Sisson and Siegel, 1989; Tomiyama et al., 2016), and thus comparison between the results obtained from Cambiaghi and colleagues (2011) with the present results is limited.

Since literature about tDCS effects on VEPs is lacking and shows quite inconsistent findings across studies, an interpretation of the underlying processes occurring after the application of tDCS is rather difficult. Results obtained from the previously mentioned tDCS studies show that VEPs can be used as physiological markers to reveal changes in cortical excitability of V1. However, the underlying mechanisms responsible for an increase of VEP amplitude have not been investigated in more detail. As mentioned previously in section 5.4.1, a positive deflection in the EEG can represent synaptic activity of inhibitory pyramidal afferents in superficial cortical layers. If this is the case, cathodal currents might act over these inhibitory afferents at pre- or postsynaptic sites and enhance their activity, i.e., decreasing the excitability of pyramidal cells which is expressed as an ultimate increase in amplitude of the P1 component. Thus, the present findings would be in line with the 'classical' excitability decrease induced by cathodal tDCS.

Finally, to examine the contribution of V1 – which represents a sensory input necessary for the acquisition of many learning paradigms – during a light stimulation protocol of classical eyeblink conditioning, learning acquisition with concurrent V1 modulation induced by tDCS was characterized and compared with the results obtained from MC modulation. At the same time, the conditioning results provided more information regarding the question whether the present findings of VEP-amplitude modulation after applying tDCS are rather caused by an increase or decrease of cortical excitability (see next section).

5.4.3. Impairment of acquisition of classical eyeblink conditioning induced by cathodal V1-tDCS

The results show that V1 modulation impaired the acquisition rate of trace eyeblink conditioning, confirming recent investigations based on visual cortex lesions in rats (Steinmetz et al., 2013). These findings are of great importance, highlighting that sensory cortex areas are part of the CS pathway and that changes in these areas can modify the acquisition of CRs. This is in accordance with the common belief that only after initial processing in V1 are other neural structures thought to contribute to the significance of the visual input (Shuler and Bear, 2006). Independently from the applied tDCS polarity, the extent to which tDCS-induced modulation of V1 excitability influenced associative learning expressed by the absolute change in CR percentage was lower ($\Delta CR \approx 30\%$) than that observed with concurrent MC-tDCS ($\Delta CR \approx 60\%$). Specifically, V1 modulation was characterized by an impairment of learning (↓ CRs) induced by cathodal tDCS, whereas MC-tDCS with anodal polarity enhanced the learning rate (↑CRs). Although different learning paradigms of classical eyeblink conditioning were applied between the experiments (trace vs. delay), the learning curves were similar to each other. However, flash stimulation conditioning resulted in larger between-animal variability across the entire learning curve compared to the tone conditioning. Asymptotic values in both cases were reached around day C5, but animals reached lower mean CR percentages with flash stimulation in the trace paradigm than with the tone used for the delay paradigm. A possible reason could be that the presentation of non-contiguous stimuli in the trace conditioning represents a more complex training procedure than the delay paradigm (Christian and Thompson 2003). Indeed, previous studies reported that rabbits reached a level of 80% CRs after ≈ 6 sessions with a delay paradigm (Lewis et al., 1987; Miller et al., 2008) and after ≈ 8 sessions with a trace paradigm (Miller et al. 2008) in both using light stimulation as CS. Nonetheless, an accurate comparison between delay and trace results in the present work is rather difficult due to the lacking control group in the trace paradigm experiment. For the same reason, the interpretation of anodal tDCS-induced V1 modulation during learning acquisition is limited, specifically regarding the impact of anodal tDCS during the 2nd conditioning day (C2) when animals start to acquire the learning. In this situation, it is not possible to separate whether an increase in CR percentage was simply caused by the natural learning improvement or influenced by

anodal modulation of V1. However, this is different for the cathodal situation since animals are already well-trained on day C8 and a significant decrease in CR percentage can be interpreted as a result of tDCS modulation. A significant within-group change on day C8 compared to the other advanced-learning days (C3-C7, C9-C10) showed that modulation of V1 through concurrent cathodal tDCS reduced the number of CRs as well as the response variability in all three animals. A supplementary experiment performed with the same animals on additional conditioning days, i.e., when motor memory was strongly stabilized, reproduced the effect of cathodal V1 modulation represented by a significantly reduced number of CRs and additionally showed that eyelid responses recorded during the presentation of cathodal tDCS had a similar strength and latency as observed for CRs from the session without concurrent tDCS. On the other hand, this experiment served to check whether learning could be enhanced via anodal V1-tDCS in a strongly-trained state (≈ 80% of CRs) of the animal. Even if analysis revealed no change of CR percentage with anodal tDCS over V1, response magnitude was larger when compared to the cathodal and control tDCS sessions (the latter without statistical significance), whereas latency remained unchanged. This result is in line with the noted boosting effect of anodal tDCS on learning performance (Márquez-Ruiz et al., 2012).

The impairment (reduced number of CRs) of learning by applying cathodal tDCS at first sight seemed to be inconsistent with the augmented amplitude of VEPs likewise elicited by cathodal stimulation. Nonetheless, similar to the findings from Márquez-Ruiz and colleagues (2012), a reduction of learning performance points toward an interference with CS perception processes. This reduction was supported by an immediate as well as long-term decrease of LFP amplitude and area during and after cathodal S1-tDCS, whilst anodal tDCS exclusively elicited immediate effects (Márquez-Ruiz et al., 2012). Thus, a cathodally-induced increase of VEP amplitude might not represent a direct excitatory effect based on the present conditioning results. The conditioning findings instead support the previously stated hypothesis (section 5.4.2) that cathodal currents boosted the activity of inhibitory inputs of pyramidal dendrites located in superficial cortical layers causing an excitability decrease of pyramidal cells in the primary visual areas. This suggested inhibition of pyramidal cells may have ultimately interfered with the perception of light stimuli resulting in an impairment of CR performance.

Complementary recordings of cortical activity within V1 could provide more information about the role of this brain structure and its excitability state during classical eyeblink conditioning, especially when light stimulation is used as CS. In this context, fMRI studies observed a significant learning-related activation within V1 with CS presentation in human fear conditioning (Knight et al., 2004) and during trace eyeblink conditioning in rabbits (Miller et al., 2008). Furthermore, a recent study examined associative plasticity in the sensory cortex for two neutral stimuli (tone and flash) using a sensory preconditioning task (Headley and Weinberger, 2015). This training consists of pairing the two stimuli to create an association between them, for example to later reinforce/associate one of the stimuli with food, causing a situation which induces the generation of CRs. If a prior association had occurred between the tone and flash, then the CR should also be evoked by the stimulus that was never paired with the food (Rizley and Rescorla, 1972). Headley and Weinberger (2015) found that the pairing of the two neutral stimuli evoked an enhancement in the responsiveness of V1 to auditory stimuli measured through extracellular potentials in the infragranular layer, concluding that this enhanced associative plasticity in V1 (not observed in auditory or S1 regions excluding the possibility of a generalized increase in cortical excitability) may constitute a memory trace between sensory cortices with V1 serving as an essential neural structure in associative learning.

With regard to modulating V1 excitability by applying external currents, initial animal experiments showed a decreased cortical excitability in visual areas induced by cathodal currents delivered to the surface of V1, causing a reduction of the neuronal firing rate, whilst anodal current resulted in the reverse effect (Creutzfeldt et al., 1962; Ward and Weiskrantz, 1969). A few other studies examined learning processes under the influence of DCS applied on visual cortex areas. Morrell and Naitoh (1962) trained rabbits to perform a conditioned-avoidance response using light flashes as CS with concurrent bilateral presentation of polarizing currents to the visual cortex. The authors observed a noticeable performance decrement that resulted from cathodal polarization for the entire cathodal session which persisted to the following training session when no cathodal current was applied. No significant change resulted from the application of anodal polarization. In accordance, Kupfermann (1965) reported a reduced learning rate induced by cathodal stimulation of the visual cortex in rats using a visual pattern or brightness discrimination task, whilst anodal DC stimulation was not effective.

Regarding other visual areas, Schweid and colleagues (2008) evaluated learning in a paradigm intended to assess the ability to detect, localize and orient motionless targets emerging at different spatial eccentricities within the visual field by applying unilateral cathodal tDCS on extrastriate visual areas of cats. The authors showed a significant reduction of the ability to detect and localize visual targets displayed in the contralateral visual hemifield (half of the field of vision) with respect to the stimulated side when the visual areas were exposed to cathodal currents.

Together, these previous results as well as the reported decrease of CRs in the present work support the potential of cathodal currents to impair learning performance when applied on cortical visual areas. Moreover, recent findings reported by Aguila and colleagues (2016) show certain parallels using a different non-invasive brain stimulation technique named transcranial static magnetic stimulation (SMS). Similar to cathodal tDCS, this neuromodulatory method, proved to be effective to decrease the excitability of cortical neurons (Oliviero et al., 2011). Aguila and colleagues (2016) applied SMS to V1 of behaving monkeys during a visual detection task and additionally over V1 of anesthetized cats while recording neural responses. As a result, both detection of visual stimuli in monkeys and neuronal activity in cats were significantly reduced by SMS.

In conclusion, each of these studies reinforces the evidence of a critical role of V1 during learning, with the hypothesis that the cathodally-induced impairment of CR performance during acquisition of classical eyeblink conditioning is a consequence of an excitability decrease of pyramidal cells generated by the augmented activity of inhibitory synapses located at pyramidal dendrites in superficial layers. It appears that, at least based on the mentioned results, the cathodal effect on V1 excitability (perturbing the CS perception) is stronger than the effect of anodal stimulation (improving the CS perception). This might be related to the observation that in the central nervous system, the underlying processes of neocortical LTP and LTD effects are dissimilar, i.e., the sensitivity to neuromodulation seems to be asymmetrical (Froc et al., 2000).

5.4.4. Modulation of the human visual cortex and its impact on learning

In the last few years, human tDCS studies brought up new findings about the involvement of visual areas in the acquisition of specific learning tasks. For instance, anodal tDCS applied either over MC or an extrastriate visual area (V5) during a visuo-motor coordination task improved early performance of correctly tracked movements (Antal et al., 2004b), whereas performance was enhanced for both tDCS polarities when stimulation was applied prior to training (Antal et al., 2008c). On the other hand, Peters and colleagues (2013) reported an overnight impairment of consolidation of a visual contrast detection task induced by anodal V1-tDCS, whilst with cathodal and sham tDCS subjects regularly improved their task performance from Day 1 to Day 2. No significant main effect of stimulation type was found for Day 1. In contrast, Sczesny-Kaiser and colleagues (2016) trained subjects to perform a visual orientation-discrimination task while receiving tDCS during learning. The analysis revealed significant improvement of discrimination learning and increased cortical excitability with anodal V1-tDCS compared to sham condition. However, when cathodal tDCS was applied over V1 neither learning nor V1 excitability were modulated. Since the net effect of tDCS depends on multiple parameters (stimulated brain area, applied current intensity, polarity, brain state, etc.), a comparison of the observed effects across studies can be complicated. Task-specificity is another parameter influencing the ultimate tDCS outcome on learning (Leite et al., 2011; Saucedo Marquez et al., 2013; Bortoletto et al., 2015; Ehlis et al., 2016; Karok et al., 2017) which might be one more reason why findings across studies where tDCS was applied over visual areas are inconsistent.

In conclusion, several studies have shown that the role of visual cortex areas during learning can be investigated via the application of direct current stimulation. In particular, animal studies have shown that visual areas seem to be more susceptible to cathodal currents resulting in impairment of learning, probably due to a disturbed sensory perception. The findings across human studies remain by some means inconsistent.

5.5. Considerations of studying the role of the cerebral cortex during learning through the application of tDCS and new perspectives

The modulatory effect and simplicity of tDCS have caught the attention of both basic and clinical neuroresearchers for studying its potential of learning modulation with a major focus on motor learning (Lang et al., 2003; Orban de Xivry and Shadmehr, 2014; Ammann et al., 2016). The findings presented in this Doctoral Thesis acquired from different brain areas (MC and V1) support the neuromodulatory effect of tDCS and its impact on learning, specifically on associative learning. However, the studies stated throughout the Discussion section, including the present findings, highlight the need for more unified and comparable stimulation paradigms, aiming to optimize the desired stimulation effects. In this context, the low focality inherent to this technique, currently under debate by numerous researchers, is constantly bringing up new approaches aiming to improve experimental outcomes by establishing greater specificity of the applied electrical currents (Edwards et al., 2013; Ruffini et al., 2014; Guler et al., 2016).

On the other hand, the existence of hundreds of tDCS-protocol variations causes the complication of formulating universal conclusions regarding the tDCS effects on learning. When considering that different brain regions are likely involved in distinct motor learning processes (Shmuelof and Krakauer, 2011; Penhune and Steele, 2012), the simultaneous (or sequential) electrical stimulation of these areas using the proper polarity and intensity could be one possible solution for the mentioned problem and potentially optimize tDCS effects. However, the characterization of the effects associated to concomitant stimulation of different brain regions is nearly absent in the literature (Kaminski et al., 2013; Minichino et al., 2015). Indeed, there has been some progression in recent years. Thus, multifocal tDCS devices using several small-size electrodes (Ruffini et al., 2014), High-Definition tDCS (HD-tDCS) scalp montage (4 × cathode, surrounding a single central anode; Edwards et al., 2013), or concentric electrodes (Bortoletto et al., 2016) are being tested currently, with the aim to generate more personalized, reproducible and predictable results in human studies.

In summary, more investigations are needed to provide a better understanding of the effects induced by tDCS. However, its potential to study the cerebral cortex among other brain structures during learning and its use for exploring neural substrates

underlying learning have been demonstrated successfully. The capability of modulating motor learning through the application of transcranial electrical currents represents an attractive opportunity for current and future investigations, especially for clinical research focused on implementing new therapies and treatments for motor learning disabilities.

5.6 Potential interferences of thermal effects induced by tDCS over the cerebral cortex and safety limits implications

The last series of experiments of the present Doctoral Thesis were performed to discard the possibility that the observed tDCS effects on cortical excitability and associative learning were affected by simple tissue heating under the stimulation electrodes. Thus, for an accurate interpretation of study results on cortical excitability and learning, thermal effects generated by tDCS should be absent or at least controlled. The results show that even long stimulation periods (up to 2 hours) and high density currents (up to two orders of magnitude higher than usually applied in humans) did not produce significant variations of the epidural temperature in the awake rabbit. In all likelihood, minor and slow appearing temperature variations were probably due to natural physiological fluctuations (Kawamura et al., 1966), rather than to the prolonged tDCS presentation. This is the first direct physiological evidence of the absence of thermal variations in the brain tissue during and after the application of anodal or cathodal tDCS, therefore no tissue heating with subsequent neural damage is caused (Agnew and McCreery, 1987; Kiyatkin, 2007).

One related study has been performed by Liebetanz and colleagues (2009) in behaving rats. Animals received cathodal tDCS transcranially applied to the frontal cortex with current densities up to 28.6 mA/cm^2 (more than two orders of magnitude higher than usually applied in humans) and stimulation durations up to 270 min. The authors demonstrated that first brain lesions took place at a current density of 14.3 mA/cm^2 for durations greater than 10 min, thus establishing as a safety threshold for tDCS. Their final conclusion is that brain lesions were caused by increased tissue temperature due to Joule heating, a type of heat which is generated in any electrical field with circulating electrical currents (Steffens, 1979), suggesting that brain temperature raised above

43°C inducing a thermal protein denaturation (Liebetanz et al., 2009). Specifically, a mathematical model regarding the results from Liebetanz and colleagues (2009) calculated a brain temperature increase up to 47.75°C when 10 min of 14.3 mA/cm^2 of cathodal tDCS was applied (Bikson et al., 2009). The obtained results in rabbits (present results) and rats should not be translated directly for human safety standards, but promote the development of enhanced tDCS protocols. However, as already mentioned by Liebetanz and colleagues (2009), the epicranial montage applied in animals offers an extra margin of safety, since the skull bone of the rabbit (≈ 2 mm), as well as from the rat (≈ 1.5 mm) is much thinner than the human skull (6-7 mm). In addition, the brain tissue in the rabbit and rat tDCS model is more exposed to the electric currents, given that the skin layer from human tDCS is absent. Together, the findings obtained from the animal studies provide essential information about tDCS safety. Nonetheless, in the present study, the key finding is that none of the reported effects on learning or brain excitability have been affected by tDCS-induced thermal variations. As addressed previously, this conclusion can be made for the results obtained from Experiment 2 (disc electrode for tDCS). Regarding Experiment 3 (4 silver-ball electrodes), possible thermal variations induced by tDCS cannot completely be discarded because applied current densities were higher (up to 7.82 mA/cm^2 per ball when 2 mA tDCS was used).

Since a direct measurement of brain temperature in humans is not realizable (Kiyatkin, 2007), recent studies addressing possible thermal effects of tDCS based their conclusions on mathematical models. Datta and colleagues (2009) reported no increase of scalp or brain temperature for the conventional 7 × 5 cm^2 rectangular-pad tDCS montage (1 mA) generally used in humans, based on a MRI-derived finite element human head model. The authors also applied their model to a 4 × 1 ring electrode configuration (< 11 mm electrode diameter) at two different intensities (2 mA and 13.6 mA), only for the higher intensity a scalp temperature rise of 14.7 °C and a brain temperature increase of 0.55°C were expected. Another interesting study examined the effect of temperature to the scalp and brain during tDCS from a different perspective. Gholami-Boroujeny and colleagues (2015) performed computer simulations based on a mathematical model to test how temperature variations can enhance/reduce current delivery to the human brain and influence the efficacy of tDCS. The authors found that by increasing the scalp temperature, less current is delivered to the brain, whereas

cooling the scalp during tDCS enhanced the current delivery and could possibly increase the efficiency of tDCS.

Only isolated studies performed in healthy individuals reported skin irritations or inclusive lesions on the scalp after applying tDCS (Dundas et al., 2007; Poreisz et al., 2007; Bikson et al., 2008; Lagopoulos and Degabriele, 2008; Palm et al., 2008; Minhas et al., 2010; Paneri et al., 2016). However, it must be taken into consideration that an increase of skin temperature is not automatically associated to a rising brain tissue temperature (Bikson et al., 2009). Nevertheless, a recent study performed in healthy subjects reported a gradual non-hazardous increase of skin temperature of ≈ 1°C (which is within normal temperature variation) during 20 min of 2 mA tDCS using conventional sponge electrodes with 35 cm^2 skin contact area. This increase was polarity-independent and caused by induced blood flow heat rather than joule heating, as the authors concluded (Khadka et al., 2017).

With regard to other brain stimulation techniques, it has been estimated for single-pulse TMS that an insignificant increase in brain temperature of less than 0.1 °C would be induced (Ruohonen and Ilmoniemi, 2002). Similar results have been observed for transcranial infrared laser therapy (TLT), a method which has been shown to enhance neurological conditions in animal stroke models (Lapchak et al., 2004; Oron et al., 2006; Lapchak et al., 2007). The authors found that TLT applied to the rabbit cortex does not produce tissue heating when power density normally applied in animal studies is used, whereas over a certain power density brain temperature increased gradually by 0.5 °C (Chen et al., 2013). On the other side, chronic deep brain stimulation (DBS), a more invasive technique, induces an estimated increase of the surrounding brain temperature up to 1 °C as predicted by a bio-heat transfer model for DBS (Elwassif et al., 2006).

In summary, further investigations are needed regarding the impact of non-invasive brain stimulation techniques on brain tissue temperature, especially for different tDCS configurations in animal and human studies. The importance of understanding the relationship between brain temperature and brain stimulation arises not only from the urgency to avoid brain tissue damage specially for prolonged and repeated stimulation protocols, but also from the fact that prior research has shown that changes in brain

temperature modify synaptic transmission processes (Pierau et al., 1976; Moser et al., 1993; Masino and Dunwiddie, 1999; Fujii et al., 2002).

6. CONCLUSIONS

The present Doctoral Thesis primarily focused on studying the role of the primary motor cortex – specifically the area corresponding to the *orbicularis oculi* muscle – in the acquisition and generation of classical conditioned eyeblink responses. Additionally, the primary visual cortex activity was examined and modulated during the learning process. To accomplish this, electrophysiological, neuromodulatory, and immunohistological techniques have been used in behaving rabbits. The main conclusions of this study are the following:

1. Motor cortex neurons located in the area corresponding to the *orbicularis oculi* muscle are clearly involved in the generation of conditioned eyelid responses in a delay paradigm as demonstrated by the increased firing activity well in advance of the conditioned response.

2. The identified monosynaptic projections from the primary motor cortex to the *orbicularis oculi* motoneurons in the facial nucleus together with the disynaptic projections from the motor cortex to the facial nucleus via the red nucleus seem to be the underlying neural pathways corresponding to the identified learning-related neurons in the motor cortex.

3. The modulation of motor cortex excitability induced by tDCS and the subsequent impact on learning confirmed the participation of the motor cortex in the acquisition process of classical eyeblink conditioning.

4. The modulation of visual cortex's excitability induced by tDCS and the related impact on learning performance confirm that the visual cortex forms part of the neural pathway which is activated through perception of the conditioned stimulus in a trace conditioning.

5. The cerebral cortex of the rabbit has been demonstrated to be a brain structure crucial for the correct acquisition and performance of classical eyeblink conditioning paradigms, supporting the hypothesis of a distributed neuronal network operating during this associative learning process rather than an exclusive participation of the cerebellum and hippocampus.

6. The results confirm that non-invasive transcranial current stimulation can be used for modulating neuronal excitability of different brain structures, as well as for studying their role during the acquisition of learning.

7. Significant thermal effects induced by the transcranial stimulation have not been detected. In all likelihood, brain temperature variations negligibly affected the observed learning results.

7. REFERENCES

Accornero, N., Li Voti, P., La Riccia, M. and Gregori, B. (2007). Visual evoked potentials modulation during direct current cortical polarization. Exp Brain Res 178(2): 261-266.

Agnew, W. F. and McCreery, D. B. (1987). Considerations for safety in the use of extracranial stimulation for motor evoked potentials. Neurosurgery 20(1): 143-147.

Aguila, J., Cudeiro, J. and Rivadulla, C. (2016). Effects of Static Magnetic Fields on the Visual Cortex: reversible Visual Deficits and Reduction of Neuronal Activity. Cereb Cortex 26(2): 628-638.

Aiba, A., Kano, M., Chen, C., Stanton, M. E., Fox, G. D., Herrup, K., Zwingman, T. A. and Tonegawa, S. (1994). Deficient cerebellar long-term depression and impaired motor learning in mGluR1 mutant mice. Cell 79(2): 377-388.

Akaneya, Y., Tsumoto, T., Kinoshita, S. and Hatanaka, H. (1997). Brain-derived neurotrophic factor enhances long-term potentiation in rat visual cortex. J Neurosci 17(17): 6707-6716.

Albus, J. (1971). Theory of Cerebellar Function. Math. Biosci. 10(1/2): 25-61.

Ambrus, G. G., Chaieb, L., Stilling, R., Rothkegel, H., Antal, A. and Paulus, W. (2016). Monitoring transcranial direct current stimulation induced changes in cortical excitability during the serial reaction time task. Neurosci Lett 616: 98-104.

Ammann, C., Spampinato, D. and Márquez-Ruiz, J. (2016). Modulating Motor Learning through Transcranial Direct-Current Stimulation: An Integrative View. Front Psychol 7: 1981.

Ammann, C., Lindquist, M. A. and Celnik, P. A. (2017). Response variability of different anodal transcranial direct current stimulation intensities across multiple sessions. Brain Stimul *in Press*.

Andrews, S. C., Hoy, K. E., Enticott, P. G., Daskalakis, Z. J. and Fitzgerald, P. B. (2011). Improving working memory: the effect of combining cognitive activity and anodal transcranial direct current stimulation to the left dorsolateral prefrontal cortex. Brain Stimul 4(2): 84-89.

Antal, A., Kincses, T. Z., Nitsche, M. A. and Paulus, W. (2003). Modulation of moving phosphene thresholds by transcranial direct current stimulation of V1 in human. Neuropsychologia 41(13): 1802-1807.

Antal, A., Nitsche, M. A., Kruse, W., Kincses, T. Z., Hoffmann, K. P. and Paulus, W. (2004a). Direct current stimulation over V5 enhances visuomotor coordination by improving motion perception in humans. J Cogn Neurosci 16(4): 521-527.

Antal, A., Kincses, T. Z., Nitsche, M. A., Bartfai, O. and Paulus, W. (2004b). Excitability changes induced in the human primary visual cortex by transcranial direct current stimulation: direct electrophysiological evidence. Invest Ophthalmol Vis Sci 45(2): 702-707.

Antal, A., Boros, K., Poreisz, C., Chaieb, L., Terney, D. and Paulus, W. (2008a). Comparatively weak after-effects of transcranial alternating current stimulation (tACS) on cortical excitability in humans. Brain Stimul 1(2): 97-105.

Antal, A., Brepohl, N., Poreisz, C., Boros, K., Csifcsak, G. and Paulus, W. (2008b). Transcranial direct current stimulation over somatosensory cortex decreases experimentally induced acute pain perception. Clin J Pain 24(1): 56-63.

Antal, A., Begemeier, S., Nitsche, M. A. and Paulus, W. (2008c). Prior state of cortical activity influences subsequent practicing of a visuomotor coordination task. Neuropsychologia 46(13): 3157-3161.

Antal, A. and Herrmann, C. S. (2016). Transcranial Alternating Current and Random Noise Stimulation: Possible Mechanisms. Neural Plast 2016: 3616807.

Aou, S., Woody, C. D. and Birt, D. (1992). Changes in the activity of units of the cat motor cortex with rapid conditioning and extinction of a compound eye blink movement. J Neurosci 12(2): 549-559.

Arezzo, J. C., Brosnan, C. F., Schroeder, C. E., Litwak, M. S. and Bornstein, M. B. (1988). Electrophysiological analysis of factors involved in the primary demyelinating diseases: the rabbit eye model system. Brain Res 462(2): 286-300.

Baczyk, M. and Jankowska, E. (2014). Presynaptic actions of transcranial and local direct current stimulation in the red nucleus. J Physiol 592(19): 4313-4328.

Bahro, M., Molchan, S. E., Sunderland, T., Herscovitch, P. and Schreurs, B. G. (1999). The effects of scopolamine on changes in regional cerebral blood flow during classical conditioning of the human eyeblink response. Neuropsychobiology 39(4): 187-195.

Baker, R., McCrea, R. A. and Spencer, R. F. (1980). Synaptic organization of cat accessory abducens nucleus. J Neurophysiol 43(3): 771-791.

Barbieri, M., Negrini, M., Nitsche, M. A. and Rivolta, D. (2016). Anodal-tDCS over the human right occipital cortex enhances the perception and memory of both faces and objects. Neuropsychologia 81: 238-244.

Barker, A. T., Jalinous, R. and Freeston, I. L. (1985). Non-invasive magnetic stimulation of human motor cortex. Lancet 1(8437): 1106-1107.

Batsikadze, G., Moliadze, V., Paulus, W., Kuo, M. F. and Nitsche, M. A. (2013). Partially non-linear stimulation intensity-dependent effects of direct current stimulation on motor cortex excitability in humans. J Physiol 591(Pt 7): 1987-2000.

Bennabi, D., Pedron, S., Haffen, E., Monnin, J., Peterschmitt, Y. and Van Waes, V. (2014). Transcranial direct current stimulation for memory enhancement: from clinical research to animal models. Front Syst Neurosci 8: 159.

Berger, T. W., Rinaldi, P. C., Weisz, D. J. and Thompson, R. F. (1983). Single-unit analysis of different hippocampal cell types during classical conditioning of rabbit nictitating membrane response. J Neurophysiol 50(5): 1197-1219.

Berthier, N. E. and Moore, J. W. (1986). Cerebellar Purkinje cell activity related to the classically conditioned nictitating membrane response. Exp Brain Res 63(2): 341-350.

Beyer, L., Batsikadze, G., Timmann, D. and Gerwig, M. (2017). Cerebellar tDCS Effects on Conditioned Eyeblinks using Different Electrode Placements and Stimulation Protocols. Front Hum Neurosci 11: 23.

Bikson, M., Inoue, M., Akiyama, H., Deans, J. K., Fox, J. E., Miyakawa, H. and Jefferys, J. G. (2004). Effects of uniform extracellular DC electric fields on excitability in rat hippocampal slices in vitro. J Physiol 557(Pt 1): 175-190.

Bikson, M., Bulow, P., Stiller, J. W., Datta, A., Battaglia, F., Karnup, S. V. and Postolache, T. T. (2008). Transcranial direct current stimulation for major depression: a

general system for quantifying transcranial electrotherapy dosage. Curr Treat Options Neurol 10(5): 377-385.

Bikson, M., Datta, A. and Elwassif, M. (2009). Establishing safety limits for transcranial direct current stimulation. Clin Neurophysiol 120(6): 1033-1034.

Bikson, M. and Rahman, A. (2013). Origins of specificity during tDCS: anatomical, activity-selective, and input-bias mechanisms. Front Hum Neurosci 7: 688.

Bikson, M., Grossman, P., Thomas, C., Zannou, A. L., Jiang, J., Adnan, T., Mourdoukoutas, A. P., Kronberg, G., Truong, D., Boggio, P., Brunoni, A. R., Charvet, L., Fregni, F., Fritsch, B., Gillick, B., Hamilton, R. H., Hampstead, B. M., Jankord, R., Kirton, A., Knotkova, H., Liebetanz, D., Liu, A., Loo, C., Nitsche, M. A., Reis, J., Richardson, J. D., Rotenberg, A., Turkeltaub, P. E. and Woods, A. J. (2016). Safety of Transcranial Direct Current Stimulation: Evidence Based Update 2016. Brain Stimul 9(5): 641-661.

Bindman, L. J., Lippold, O. C. and Redfearn, J. W. (1964). The action of brief polarizing currents on the cerebral cortex of the rat (1) during current flow and (2) in the production of long-lasting after-effects. J Physiol 172: 369-382.

Birt, D., Aou, S. and Woody, C. D. (2003). Intracellularly recorded responses of neurons of the motor cortex of awake cats to presentations of Pavlovian conditioned and unconditioned stimuli. Brain Res 969(1-2): 205-216.

Blázquez, P. M., Fujii, N., Kojima, J. and Graybiel, A. M. (2002). A network representation of response probability in the striatum. Neuron 33(6): 973-982.

Bliss, T. V. and Gardner-Medwin, A. R. (1973). Long-lasting potentiation of synaptic transmission in the dentate area of the unanaestetized rabbit following stimulation of the perforant path. J Physiol 232(2): 357-374.

Bliss, T. V. and Lømo, T. (1973). Long-lasting potentiation of synaptic transmission in the dentate area of the anaesthetized rabbit following stimulation of the perforant path. J Physiol 232(2): 331-356.

Block, H. and Celnik, P. (2013). Stimulating the cerebellum affects visuomotor adaptation but not intermanual transfer of learning. Cerebellum 12(6): 781-793.

Bloedel, J. R., Bracha, V., Kelly, T. M. and Wu, J. Z. (1991). Substrates for motor learning. Does the cerebellum do it all? Ann N Y Acad Sci 627: 305-318.

Boele, H. J., Koekkoek, S. K. and De Zeeuw, C. I. (2010). Cerebellar and extracerebellar involvement in mouse eyeblink conditioning: the ACDC model. Front Cell Neurosci 3: 19.

Boggio, P. S., Castro, L. O., Savagim, E. A., Braite, R., Cruz, V. C., Rocha, R. R., Rigonatti, S. P., Silva, M. T. and Fregni, F. (2006a). Enhancement of non-dominant hand motor function by anodal transcranial direct current stimulation. Neurosci Lett 404(1-2): 232-236.

Boggio, P. S., Ferrucci, R., Rigonatti, S. P., Covre, P., Nitsche, M. A., Pascual-Leone, A. and Fregni, F. (2006b). Effects of transcranial direct current stimulation on working memory in patients with Parkinson's disease. J Neurol Sci 249(1): 31-38.

Boggio, P. S., Zaghi, S., Lopes, M. and Fregni, F. (2008). Modulatory effects of anodal transcranial direct current stimulation on perception and pain thresholds in healthy volunteers. Eur J Neurol 15(10): 1124-1130.

Boller, F., Keefe, N. C. and Zoccolotti, P. (1989). Luigi Galvani, body electricity, and the 'galvanic skin response'. Neurology 39(6): 868-870.

Bolognini, N., Pascual-Leone, A. and Fregni, F. (2009). Using non-invasive brain stimulation to augment motor training-induced plasticity. J Neuroeng Rehabil 6: 8.

Bolzoni, F., Baczyk, M. and Jankowska, E. (2013a). Subcortical effects of transcranial direct current stimulation in the rat. J Physiol 591(Pt 16): 4027-4042.

Bolzoni, F., Pettersson, L. G. and Jankowska, E. (2013b). Evidence for long-lasting subcortical facilitation by transcranial direct current stimulation in the cat. J Physiol 591(13): 3381-3399.

Bortoletto, M., Pellicciari, M. C., Rodella, C. and Miniussi, C. (2015). The interaction with task-induced activity is more important than polarization: a tDCS study. Brain Stimul 8(2): 269-276.

Bortoletto, M., Rodella, C., Salvador, R., Miranda, P. C. and Miniussi, C. (2016). Reduced Current Spread by Concentric Electrodes in Transcranial Electrical Stimulation (tES). Brain Stimul 9(4): 525-528.

Brecht, M., Hatsopoulos, N. G., Kaneko, T. and Shepherd, G. M. (2013). Motor cortex microcircuits. Front Neural Circuits 7: 196.

Brodal, P. (1987). Oraganization of the cerebropontocerebellar connections as studied with anterograde and retrograde transport of HRP-WGA in the cat. New concepts in cerebellar neurobiology. A. Liss and J. King. New York. 22**:** 151-182.

Broeder, S., Nackaerts, E., Heremans, E., Vervoort, G., Meesen, R., Verheyden, G. and Nieuwboer, A. (2015). Transcranial direct current stimulation in Parkinson's disease: Neurophysiological mechanisms and behavioral effects. Neurosci Biobehav Rev 57: 105-117.

Brunoni, A. R., Nitsche, M. A., Bolognini, N., Bikson, M., Wagner, T., Merabet, L., Edwards, D. J., Valero-Cabre, A., Rotenberg, A., Pascual-Leone, A., Ferrucci, R., Priori, A., Boggio, P. S. and Fregni, F. (2012). Clinical research with transcranial direct current stimulation (tDCS): challenges and future directions. Brain Stimul 5(3): 175-195.

Buch, E. R., Santarnecchi, E., Antal, A., Born, J., Celnik, P. A., Classen, J., Gerloff, C., Hallett, M., Hummel, F. C., Nitsche, M. A., Pascual-Leone, A., Paulus, W. J., Reis, J., Robertson, E. M., Rothwell, J. C., Sandrini, M., Schambra, H. M., Wassermann, E. M., Ziemann, U. and Cohen, L. G. (2017). Effects of tDCS on motor learning and memory formation: A consensus and critical position paper. Clin Neurophysiol 128(4): 589-603.

Bures, J. and Buresova, W. (1963). Cortical spreading depression as a memory disturbing factor. J Comp Physiol Psychol 56: 268-272.

Button, K. S., Ioannidis, J. P. A., Mokrysz, C., Nosek, B. A., Flint, J., Robinson, E. S. J. and Munafo, M. R. (2013). Power failure: why small sample size undermines the reliability of neuroscience. Nat Rev Neurosci 14(5): 365-376.

Calabresi, P., Maj, R., Pisani, A., Mercuri, N. B. and Bernardi, G. (1992). Long-term synaptic depression in the striatum: physiological and pharmacological characterization. J Neurosci 12(11): 4224-4233.

Cambiaghi, M., Velikova, S., González-Rosa, J. J., Cursi, M., Comi, G. and Leocani, L. (2010). Brain transcranial direct current stimulation modulates motor excitability in mice. Eur J Neurosci 31(4): 704-709.

Cambiaghi, M., Teneud, L., Velikova, S., González-Rosa, J. J., Cursi, M., Comi, G. and Leocani, L. (2011). Flash visual evoked potentials in mice can be modulated by transcranial direct current stimulation. Neuroscience 185: 161-165.

Campolattaro, M. M., Halverson, H. E. and Freeman, J. H. (2007). Medial auditory thalamic stimulation as a conditioned stimulus for eyeblink conditioning in rats. Learn Mem 14(3): 152-159.

Cantarero, G., Spampinato, D., Reis, J., Ajagbe, L., Thompson, T., Kulkarni, K. and Celnik, P. (2015). Cerebellar direct current stimulation enhances on-line motor skill acquisition through an effect on accuracy. J Neurosci 35(7): 3285-3290.

Caro-Martín, C. R., Leal-Campanario, R., Sánchez-Campusano, R., Delgado-García, J. M. and Gruart, A. (2015). A Variable Oscillator Underlies the Measurement of Time Intervals in the Rostral Medial Prefrontal Cortex during Classical Eyeblink Conditioning in Rabbits. J Neurosci 35(44): 14809-14821.

Carretero-Guillén, A., Pacheco-Calderón, R., Delgado-García, J. M. and Gruart, A. (2015). Involvement of hippocampal inputs and intrinsic circuit in the acquisition of context and cues during classical conditioning in behaving rabbits. Cereb Cortex 25(5): 1278-1289.

Cason, H. (1922). The conditionined eyelid reaction. J Exp Psychol 5: 153-196.

Chapman, P. F., Steinmetz, J. E., Sears, L. L. and Thompson, R. F. (1990). Effects of lidocaine injection in the interpositus nucleus and red nucleus on conditioned behavioral and neuronal responses. Brain Res 537(1-2): 149-156.

Chau, L. S., Prakapenka, A. V., Zendeli, L., Davis, A. S. and Gálvez, R. (2014). Training-dependent associative learning induced neocortical structural plasticity: a trace eyeblink conditioning analysis. PLoS One 9(4): e95317.

Chen, J. L., Margolis, D. J., Stankov, A., Sumanovski, L. T., Schneider, B. L. and Helmchen, F. (2015). Pathway-specific reorganization of projection neurons in somatosensory cortex during learning. Nat Neurosci 18(8): 1101-1108.

Chen, L., Bao, S., Lockard, J. M., Kim, J. K. and Thompson, R. F. (1996). Impaired classical eyeblink conditioning in cerebellar-lesioned and Purkinje cell degeneration (pcd) mutant mice. J Neurosci 16(8): 2829-2838.

Chen, Y., De Taboada, L., O'Connor, M., Delapp, S. and Zivin, J. A. (2013). Thermal effects of transcranial near-infrared laser irradiation on rabbit cortex. Neurosci Lett 553: 99-103.

Cheron, G., Marquez-Ruiz, J. and Dan, B. (2015). Oscillations, Timing, Plasticity, and Learning in the Cerebellum. Cerebellum 15(2): 122-138.

Christian, K. M. and Thompson, R. F. (2003). Neural substrates of eyeblink conditioning: acquisition and retention. Learn Mem 10(6): 427-455.

Christian, K. M. and Thompson, R. F. (2005). Long-term storage of an associative memory trace in the cerebellum. Behav Neurosci 119(2): 526-537.

Cirillo, G., Di Pino, G., Capone, F., Ranieri, F., Florio, L., Todisco, V., Tedeschi, G., Funke, K. and Di Lazzaro, V. (2017). Neurobiological after-effects of non-invasive brain stimulation. Brain Stimul 10(1): 1-18.

Clark, R. E., Zhang, A. A. and Lavond, D. G. (1992). Reversible lesions of the cerebellar interpositus nucleus during acquisition and retention of a classically conditioned behavior. Behav Neurosci 106(6): 879-888.

Collingridge, G. L., Kehl, S. J. and McLennan, H. (1983). Excitatory amino acids in synaptic transmission in the Schaffer collateral-commissural pathway of the rat hippocampus. J Physiol 334: 33-46.

Costa, T. L., Hamer, R. D., Nagy, B. V., Barboni, M. T., Gualtieri, M., Boggio, P. S. and Ventura, D. F. (2015). Transcranial direct current stimulation can selectively affect different processing channels in human visual cortex. Exp Brain Res 233(4): 1213-1223.

Courville, J. (1966). The nucleus of the facial nerve; the relation between cellular groups and peripheral branches of the nerve. Brain Res 1(4): 338-354.

Creutzfeldt, O. D., Fromm, G. H. and Kapp, H. (1962). Influence of transcortical d-c currents on cortical neuronal activity. Exp Neurol 5(6): 436-452.

Das, S., Weiss, C. and Disterhoft, J. F. (2001). Eyeblink conditioning in the rabbit (Oryctolagus cuniculus) with stimulation of the mystacial vibrissae as a conditioned stimulus. Behav Neurosci 115(3): 731-736.

Datta, A., Elwassif, M. and Bikson, M. (2009). Bio-heat transfer model of transcranial DC stimulation: comparison of conventional pad versus ring electrode. Conf Proc IEEE Eng Med Biol Soc 2009: 670-673.

Davies, J., Qume, M. and Harris, N. C. (1994). Pharmacological characterisation of excitatory synaptic transmission in the cat red nucleus in vivo. Brain Res 649(1-2): 43-52.

Delgado-García, J. M. and Gruart, A. (2002). The role of interpositus nucleus in eyelid conditioned responses. Cerebellum 1(4): 289-308.

Delgado-García, J. M., Gruart, A. and Múnera, A. (2002). Neural organization of eyelid responses. Mov Disord 17 Suppl 2: S33-36.

Delgado-García, J. M. and Gruart, A. (2005). Firing activities of identified posterior interpositus nucleus neurons during associative learning in behaving cats. Brain Res Rev 49(2): 367-376.

Delgado-García, J. M. and Gruart, A. (2006). Building new motor responses: eyelid conditioning revisited. Trends Neurosci 29(6): 330-338.

Desmond, N. L., Colbert, C. M., Zhang, D. X. and Levy, W. B. (1991). NMDA receptor antagonists block the induction of long-term depression in the hippocampal dentate gyrus of the anesthetized rat. Brain Res 552(1): 93-98.

Di Lazzaro, V., Manganelli, F., Dileone, M., Notturno, F., Esposito, M., Capasso, M., Dubbioso, R., Pace, M., Ranieri, F., Minicuci, G., Santoro, L. and Uncini, A. (2012). The effects of prolonged cathodal direct current stimulation on the excitatory and inhibitory circuits of the ipsilateral and contralateral motor cortex. J Neural Transm (Vienna) 119(12): 1499-1506.

Di Russo, F., Martinez, A., Sereno, M. I., Pitzalis, S. and Hillyard, S. A. (2002). Cortical sources of the early components of the visual evoked potential. Hum Brain Mapp 15(2): 95-111.

Dieckhöfer, A., Waberski, T. D., Nitsche, M. A., Paulus, W., Buchner, H. and Gobbele, R. (2006). Transcranial direct current stimulation applied over the somatosensory cortex - differential effect on low and high frequency SEPs. Clin Neurophysiol 117(10): 2221-2227.

Dockery, C. A., Liebetanz, D., Birbaumer, N., Malinowska, M. and Wesierska, M. J. (2011). Cumulative benefits of frontal transcranial direct current stimulation on visuospatial working memory training and skill learning in rats. Neurobiol Learn Mem 96(3): 452-460.

Doyon, J., Penhune, V. and Ungerleider, L. G. (2003). Distinct contribution of the cortico-striatal and cortico-cerebellar systems to motor skill learning. Neuropsychologia 41(3): 252-262.

Doyon, J. and Benali, H. (2005). Reorganization and plasticity in the adult brain during learning of motor skills. Curr Opin Neurobiol 15(2): 161-167.

Dundas, J. E., Thickbroom, G. W. and Mastaglia, F. L. (2007). Perception of comfort during transcranial DC stimulation: effect of NaCl solution concentration applied to sponge electrodes. Clin Neurophysiol 118(5): 1166-1170.

Dyke, K., Kim, S., Jackson, G. M. and Jackson, S. R. (2016). Intra-Subject Consistency and Reliability of Response Following 2 mA Transcranial Direct Current Stimulation. Brain Stimul 9(6): 819-825.

Edwards, D., Cortes, M., Datta, A., Minhas, P., Wassermann, E. M. and Bikson, M. (2013). Physiological and modeling evidence for focal transcranial electrical brain stimulation in humans: a basis for high-definition tDCS. Neuroimage 74: 266-275.

Ehlis, A. C., Haeussinger, F. B., Gastel, A., Fallgatter, A. J. and Plewnia, C. (2016). Task-dependent and polarity-specific effects of prefrontal transcranial direct current stimulation on cortical activation during word fluency. Neuroimage 140: 134-140.

Ehsani, F., Bakhtiary, A. H., Jaberzadeh, S., Talimkhani, A. and Hajihasani, A. (2016). Differential effects of primary motor cortex and cerebellar transcranial direct current stimulation on motor learning in healthy individuals: A randomized double-blind sham-controlled study. Neurosci Res 112: 10-19.

Elwassif, M. M., Kong, Q., Vazquez, M. and Bikson, M. (2006). Bio-heat transfer model of deep brain stimulation-induced temperature changes. J Neural Eng 3(4): 306-315.

Evarts, E. V., Fromm, C., Kroller, J. and Jennings, V. A. (1983). Motor Cortex control of finely graded forces. J Neurophysiol 49(5): 1199-1215.

Fanardjian, V. V., Kasabyan, S. A. and Manvelyan, L. R. (1983). Mechanisms regulating the activity of facial nucleus motoneurones 2. Synaptic activation from the caudal trigeminal nucleus. Neuroscience 9(4): 823-835.

Fanardjian, V. V. and Manvelyan, L. R. (1987). Mechanisms regulating the activity of facial nucleus motoneurons 3. Synaptic influences from the cerebral cortex and subcortical structures. Neuroscience 20(3): 835-843.

Faraji, J., Gomez-Palacio-Schjetnan, A., Luczak, A. and Metz, G. A. (2013). Beyond the silence: bilateral somatosensory stimulation enhances skilled movement quality and neural density in intact behaving rats. Behav Brain Res 253: 78-89.

Farrell, D. F., Leeman, S. and Ojemann, G. A. (2007). Study of the human visual cortex: direct cortical evoked potentials and stimulation. J Clin Neurophysiol 24(1): 1-10.

Feurra, M., Paulus, W., Walsh, V. and Kanai, R. (2011). Frequency specific modulation of human somatosensory cortex. Front Psychol 2: 13.

Fiori, V., Coccia, M., Marinelli, C. V., Vecchi, V., Bonifazi, S., Ceravolo, M. G., Provinciali, L., Tomaiuolo, F. and Marangolo, P. (2011). Transcranial direct current stimulation improves word retrieval in healthy and nonfluent aphasic subjects. J Cogn Neurosci 23(9): 2309-2323.

Firmin, L., Field, P., Maier, M. A., Kraskov, A., Kirkwood, P. A., Nakajima, K., Lemon, R. N. and Glickstein, M. (2014). Axon diameters and conduction velocities in the macaque pyramidal tract. J Neurophysiol 112(6): 1229-1240.

Flöel, A., Rosser, N., Michka, O., Knecht, S. and Breitenstein, C. (2008). Noninvasive brain stimulation improves language learning. J Cogn Neurosci 20(8): 1415-1422.

Freeman, J. H., Halverson, H. E. and Hubbard, E. M. (2007). Inferior colliculus lesions impair eyeblink conditioning in rats. Learn Mem 14(12): 842-846.

Freeman, J. H. and Steinmetz, A. B. (2011). Neural circuitry and plasticity mechanisms underlying delay eyeblink conditioning. Learn Mem 18(10): 666-677.

Fregni, F., Boggio, P. S., Nitsche, M. A., Bermpohl, F., Antal, A., Feredoes, E., Marcolin, M. A., Rigonatti, S. P., Silva, M. T., Paulus, W. and Pascual-Leone, A. (2005). Anodal transcranial direct current stimulation of prefrontal cortex enhances working memory. Exp Brain Res 166(1): 23-30.

Fritsch, B., Reis, J., Martinowich, K., Schambra, H. M., Ji, Y., Cohen, L. G. and Lu, B. (2010). Direct current stimulation promotes BDNF-dependent synaptic plasticity: potential implications for motor learning. Neuron 66(2): 198-204.

Froc, D. J., Chapman, C. A., Trepel, C. and Racine, R. J. (2000). Long-term depression and depotentiation in the sensorimotor cortex of the freely moving rat. J Neurosci 20(1): 438-445.

Fröhlich, F. and McCormick, D. A. (2010). Endogenous electric fields may guide neocortical network activity. Neuron 67(1): 129-143.

Fujii, S., Sasaki, H., Ito, K., Kaneko, K. and Kato, H. (2002). Temperature dependence of synaptic responses in guinea pig hippocampal CA1 neurons in vitro. Cell Mol Neurobiol 22(4): 379-391.

Galea, J. M. and Celnik, P. (2009). Brain polarization enhances the formation and retention of motor memories. J Neurophysiol 102(1): 294-301.

Galea, J. M., Vazquez, A., Pasricha, N., de Xivry, J. J. and Celnik, P. (2011). Dissociating the roles of the cerebellum and motor cortex during adaptive learning: the motor cortex retains what the cerebellum learns. Cereb Cortex 21(8): 1761-1770.

Galvani, L. (1791). De viribus electricitatis in motu muscolari animalium. Bon. Sci. Art. Inst. Acad. Comm. 7: 363-418.

Gálvez, R., Weiss, C., Weible, A. P. and Disterhoft, J. F. (2006). Vibrissa-signaled eyeblink conditioning induces somatosensory cortical plasticity. J Neurosci 26(22): 6062-6068.

Gálvez, R., Weible, A. P. and Disterhoft, J. F. (2007). Cortical barrel lesions impair whisker-CS trace eyeblink conditioning. Learn Mem 14(1): 94-100.

Garcia, K. S. and Mauk, M. D. (1998). Pharmacological analysis of cerebellar contributions to the timing and expression of conditioned eyelid responses. Neuropharmacology 37(4-5): 471-480.

Gerritsen, B. G. (1971). The effect of anaesthetics on the electroretinogram and the visually evoked response in the rabbit. Doc Ophthalmol 29(2): 289-330.

Gershon, A. A., Dannon, P. N. and Grunhaus, L. (2003). Transcranial magnetic stimulation in the treatment of depression. Am J Psychiatry 160(5): 835-845.

Gerwig, M., Kolb, F. P. and Timmann, D. (2007). The involvement of the human cerebellum in eyeblink conditioning. Cerebellum 6(1): 38-57.

Gholami-Boroujeny, S., Mekonnen, A., Batkin, I. and Bolic, M. (2015). Theoretical Analysis of the Effect of Temperature on Current Delivery to the Brain During tDCS. Brain Stimul 8(3): 509-514.

Girgis, M. and Shih-Chang, W. (1981). A new stereotaxic atlas of the rabbit brain, W.H. Green.

Givre, S. J., Schroeder, C. E. and Arezzo, J. C. (1994). Contribution of extrastriate area V4 to the surface-recorded flash VEP in the awake macaque. Vision Res 34(4): 415-428.

Gloor, C., Luft, A. R. and Hosp, J. A. (2015). Biphasic plasticity of dendritic fields in layer V motor neurons in response to motor learning. Neurobiol Learn Mem 125: 189-194.

Goedert, K. M. and Willingham, D. B. (2002). Patterns of interference in sequence learning and prism adaptation inconsistent with the consolidation hypothesis. Learn Mem 9(5): 279-292.

Gonzalez-Joekes, J. and Schreurs, B. G. (2012). Anatomical characterization of a rabbit cerebellar eyeblink premotor pathway using pseudorabies and identification of a local modulatory network in anterior interpositus. J Neurosci 32(36): 12472-12487.

Gormezano, I., Schneiderman, N., Deaux, E. and Fuentes, I. (1962). Nictitating membrane: classical conditioning and extinction in the albino rabbit. Science 138(3536): 33-34.

Gormezano, I. (1966). Classical conditioning. In J.B. Sidowski (Ed.),. Experimental methods and instrumentation in psychology 1: 385-420. McGraw-Hill, New York.

Gormezano, I., Kehoe, E. J. and Marshall, B. S. (1983). Twenty years of classical conditioning research with the rabbit. Prog Psychobiol Physiol Psychol 10: 197-275.

Grant, D. and Adams, J. (1944). 'Alpha' conditioning in the eyelid. J Exp Psychol 34 (2): 136-142.

Green, J. T. and Arenos, J. D. (2007). Hippocampal and cerebellar single-unit activity during delay and trace eyeblink conditioning in the rat. Neurobiol Learn Mem 87(2): 269-284.

Grinevich, V., Brecht, M. and Osten, P. (2005). Monosynaptic pathway from rat vibrissa motor cortex to facial motor neurons revealed by lentivirus-based axonal tracing. J Neurosci 25(36): 8250-8258.

Gruart, A., Blázquez, P. and Delgado-García, J. M. (1994). Kinematic analyses of classically-conditioned eyelid movements in the cat suggest a brain stem site for motor learning. Neurosci Lett 175(1-2): 81-84.

Gruart, A. and Delgado-García, J. M. (1994). Discharge of identified deep cerebellar nuclei neurons related to eye blinks in the alert cat. Neuroscience 61(3): 665-681.

Gruart, A., Schreurs, B. G., del Toro, E. D. and Delgado-García, J. M. (2000a). Kinetic and frequency-domain properties of reflex and conditioned eyelid responses in the rabbit. J Neurophysiol 83(2): 836-852.

Gruart, A., Morcuende, S., Martínez, S. and Delgado-García, J. M. (2000b). Involvement of cerebral cortical structures in the classical conditioning of eyelid responses in rabbits. Neuroscience 100(4): 719-730.

Gruart, A., Guillazo-Blanch, G., Fernández-Mas, R., Jiménez-Díaz, L. and Delgado-García, J. M. (2000c). Cerebellar posterior interpositus nucleus as an enhancer of classically conditioned eyelid responses in alert cats. J Neurophysiol 84(5): 2680-2690.

Gruart, A., Muñoz, M. D. and Delgado-García, J. M. (2006). Involvement of the CA3-CA1 synapse in the acquisition of associative learning in behaving mice. J Neurosci 26(4): 1077-1087.

Gruart, A., Leal-Campanario, R., López-Ramos, J. C. and Delgado-García, J. M. (2015). Functional basis of associative learning and their relationships with long-term potentiation evoked in the involved neural circuits: Lessons from studies in behaving mammals. Neurobiol Learn Mem 124: 3-18.

Gruber, P. and Gould, D. (2010). The red nucleus: past, present, and future. Neuroanatomy 9: 1-3.

Guler, S., Dannhauer, M., Erem, B., Macleod, R., Tucker, D., Turovets, S., Luu, P., Erdogmus, D. and Brooks, D. H. (2016). Optimization of focality and direction in dense electrode array transcranial direct current stimulation (tDCS). J Neural Eng 13(3): 036020.

Haley, D. A., Thompson, R. F. and Madden, J. t. (1988). Pharmacological analysis of the magnocellular red nucleus during classical conditioning of the rabbit nictitating membrane response. Brain Res 454(1-2): 131-139.

Hallett, M. (2000). Transcranial magnetic stimulation and the human brain. Nature 406(6792): 147-150.

Halverson, H. E. and Freeman, J. H. (2006). Medial auditory thalamic nuclei are necessary for eyeblink conditioning. Behav Neurosci 120(4): 880-887.

Halverson, H. E., Hubbard, E. M. and Freeman, J. H. (2009). Stimulation of the lateral geniculate, superior colliculus, or visual cortex is sufficient for eyeblink conditioning in rats. Learn Mem 16(5): 300-307.

Halverson, H. E., Lee, I. and Freeman, J. H. (2010). Associative plasticity in the medial auditory thalamus and cerebellar interpositus nucleus during eyeblink conditioning. J Neurosci 30(26): 8787-8796.

Halverson, H. E. and Freeman, J. H. (2010a). Ventral lateral geniculate input to the medial pons is necessary for visual eyeblink conditioning in rats. Learn Mem 17(2): 80-85.

Halverson, H. E. and Freeman, J. H. (2010b). Medial auditory thalamic input to the lateral pontine nuclei is necessary for auditory eyeblink conditioning. Neurobiol Learn Mem 93(1): 92-98.

Hardwick, R. M. and Celnik, P. A. (2014). Cerebellar direct current stimulation enhances motor learning in older adults. Neurobiol Aging 35(10): 2217-2221.

Harris, E. W., Ganong, A. H. and Cotman, C. W. (1984). Long-term potentiation in the hippocampus involves activation of N-methyl-D-aspartate receptors. Brain Res 323(1): 132-137.

Hasan, M. T., Hernández-González, S., Dogbevia, G., Trevino, M., Bertocchi, I., Gruart, A. and Delgado-García, J. M. (2013). Role of motor cortex NMDA receptors in learning-dependent synaptic plasticity of behaving mice. Nat Commun 4: 2258.

Hashimoto, T., Ueno, K., Ogawa, A., Asamizuya, T., Suzuki, C., Cheng, K., Tanaka, M., Taoka, M., Iwamura, Y., Suwa, G. and Iriki, A. (2013). Hand before foot? Cortical somatotopy suggests manual dexterity is primitive and evolved independently of bipedalism. Philos Trans R Soc Lond B Biol Sci 368(1630).

Hayashi-Takagi, A., Yagishita, S., Nakamura, M., Shirai, F., Wu, Y. I., Loshbaugh, A. L., Kuhlman, B., Hahn, K. M. and Kasai, H. (2015). Labelling and optical erasure of synaptic memory traces in the motor cortex. Nature 525(7569): 333-338.

Headley, D. B. and Weinberger, N. M. (2015). Relational associative learning induces cross-modal plasticity in early visual cortex. Cereb Cortex 25(5): 1306-1318.

Hebb, D. (1949). The organization of behavior: A Neuropsychological Theory. New York: Wiley.

Heiney, S. A., Wohl, M. P. and Chettih, S. N. (2014). Cerebellar-dependent expression of motor learning during eyeblink conditioning in head-fixed mice. J Neurosci 34(45): 14845-14853.

Herzfeld, D. J., Pastor, D., Haith, A. M., Rossetti, Y., Shadmehr, R. and O'Shea, J. (2014). Contributions of the cerebellum and the motor cortex to acquisition and retention of motor memories. Neuroimage 98: 147-158.

Hesslow, G. (1994). Inhibition of classically conditioned eyeblink responses by stimulation of the cerebellar cortex in the decerebrate cat. J Physiol 476(2): 245-256.

Hesslow, G., Svensson, P. and Ivarsson, M. (1999). Learned movements elicited by direct stimulation of cerebellar mossy fiber afferents. Neuron 24(1): 179-185.

Hikosaka, O., Nakamura, K., Sakai, K. and Nakahara, H. (2002). Central mechanisms of motor skill learning. Curr Opin Neurobiol 12(2): 217-222.

Hilgard, E. and Marquis, D. (1935). Acquisition, extinction, and retention of conditioned lid responses to light in dogs. J Comp Psychol 19: 29-58.

Hirano, T. (2014). Around LTD hypothesis in motor learning. Cerebellum 13(5): 645-650.

Holst, E. and Mittelstaedt, H. (1950). Das Reafferenzprinzip, Naturwissenschaften. 37**:** 464-476.

Holstege, G. and Collewijn, H. (1982). The efferent connections of the nucleus of the optic tract and the superior colliculus in the rabbit. J Comp Neurol 209(2): 139-175.

Holstege, G., van Ham, J. J. and Tan, J. (1986). Afferent projections to the orbicularis oculi motoneuronal cell group. An autoradiographical tracing study in the cat. Brain Res 374(2): 306-320.

Horn, K. M., Pong, M., Batni, S. R., Levy, S. M. and Gibson, A. R. (2002). Functional specialization within the cat red nucleus. J Neurophysiol 87(1): 469-477.

Horvath, J. C., Carter, O. and Forte, J. D. (2014). Transcranial direct current stimulation: five important issues we aren't discussing (but probably should be). Front Syst Neurosci 8: 2.

Horvath, J. C., Forte, J. D. and Carter, O. (2015). Evidence that transcranial direct current stimulation (tDCS) generates little-to-no reliable neurophysiologic effect beyond MEP amplitude modulation in healthy human subjects: A systematic review. Neuropsychologia 66: 213-236.

Houk, J., Buckingham, J. and Barto, A. (1996). Models of the cerebellum and motor learning. Behav Brain Sci 119(3): 368-383.

Huang, C. S., Sirisko, M. A., Hiraba, H., Murray, G. M. and Sessle, B. J. (1988). Organization of the primate face motor cortex as revealed by intracortical microstimulation and electrophysiological identification of afferent inputs and corticobulbar projections. J Neurophysiol 59(3): 796-818.

Hummel, F. C., Heise, K., Celnik, P., Flöel, A., Gerloff, C. and Cohen, L. G. (2010). Facilitating skilled right hand motor function in older subjects by anodal polarization over the left primary motor cortex. Neurobiol Aging 31(12): 2160-2168.

Humphrey, D. R., Corrie, W. S. and Rietz, R. (1978). Properties of the pyramidal tract neuron system within the precentral wrist and hand area of primate motor cortex. J Physiol (Paris) 74(3): 215-226.

Inda, M. C., Delgado-García, J. M. and Carrión, A. M. (2005). Acquisition, consolidation, reconsolidation, and extinction of eyelid conditioning responses require de novo protein synthesis. J Neurosci 25(8): 2070-2080.

Ito, M. and Kano, M. (1982). Long-lasting depression of parallel fiber-Purkinje cell transmission induced by conjunctive stimulation of parallel fibers and climbing fibers in the cerebellar cortex. Neurosci Lett 33(3): 253-258.

Ito, M., Sakurai, M. and Tongroach, P. (1982). Climbing fibre induced depression of both mossy fibre responsiveness and glutamate sensitivity of cerebellar Purkinje cells. J Physiol 324: 113-134.

Ito, M. (2000). Mechanisms of motor learning in the cerebellum. Brain Res 886(1-2): 237-245.

Ivkovich, D. and Thompson, R. F. (1997). Motor cortex lesions do not affect learning or performance of the eyeblink response in rabbits. Behav Neurosci 111(4): 727-738.

Iwata, N., Kitai, S. T. and Olson, S. (1972). Afferent component of the facial nerve: its relation to the spinal trigeminal and facial nucleus. Brain Res 43(2): 662-667.

Iyer, M. B., Schleper, N. and Wassermann, E. M. (2003). Priming stimulation enhances the depressant effect of low-frequency repetitive transcranial magnetic stimulation. J Neurosci 23(34): 10867-10872.

Jackson, M. P., Rahman, A., Lafon, B., Kronberg, G., Ling, D., Parra, L. C. and Bikson, M. (2016). Animal models of transcranial direct current stimulation: Methods and mechanisms. Clin Neurophysiol 127(11): 3425-3454.

Jayaram, G., Tang, B., Pallegadda, R., Vasudevan, E. V., Celnik, P. and Bastian, A. (2012). Modulating locomotor adaptation with cerebellar stimulation. J Neurophysiol 107(11): 2950-2957.

Jiménez-Díaz, L., Sancho-Bielsa, F., Gruart, A., López-García, C. and Delgado-García, J. M. (2006). Evolution of cerebral cortex involvement in the acquisition of associative learning. Behav Neurosci 120(5): 1043-1056.

Jo, J. M., Kim, Y. H., Ko, M. H., Ohn, S. H., Joen, B. and Lee, K. H. (2009). Enhancing the working memory of stroke patients using tDCS. Am J Phys Med Rehabil 88(5): 404-409.

Kabakov, A. Y., Muller, P. A., Pascual-Leone, A., Jensen, F. E. and Rotenberg, A. (2012). Contribution of axonal orientation to pathway-dependent modulation of excitatory transmission by direct current stimulation in isolated rat hippocampus. J Neurophysiol 107(7): 1881-1889.

Kaminski, E., Hoff, M., Sehm, B., Taubert, M., Conde, V., Steele, C. J., Villringer, A. and Ragert, P. (2013). Effect of transcranial direct current stimulation (tDCS) during complex whole body motor skill learning. Neurosci Lett 552: 76-80.

Kanai, R., Paulus, W. and Walsh, V. (2010). Transcranial alternating current stimulation (tACS) modulates cortical excitability as assessed by TMS-induced phosphene thresholds. Clin Neurophysiol 121(9): 1551-1554.

Kang, E. K. and Paik, N. J. (2011). Effect of a tDCS electrode montage on implicit motor sequence learning in healthy subjects. Exp Transl Stroke Med 3(1): 4.

Kantak, S. S., Mummidisetty, C. K. and Stinear, J. W. (2012). Primary motor and premotor cortex in implicit sequence learning--evidence for competition between implicit and explicit human motor memory systems. Eur J Neurosci 36(5): 2710-2715.

Karok, S., Fletcher, D. and Witney, A. G. (2017). Task-specificity of unilateral anodal and dual-M1 tDCS effects on motor learning. Neuropsychologia 94: 84-95.

Kaski, D., Quadir, S., Patel, M., Yousif, N. and Bronstein, A. M. (2012). Enhanced locomotor adaptation aftereffect in the "broken escalator" phenomenon using anodal tDCS. J Neurophysiol 107(9): 2493-2505.

Kaufman, M. T., Churchland, M. M., Ryu, S. I. and Shenoy, K. V. (2015). Vacillation, indecision and hesitation in moment-by-moment decoding of monkey motor cortex. Elife 4: e04677.

Kawamura, H., Whitmoyer, D. I. and Sawyer, C. H. (1966). Temperature changes in the rabbit brain during paradoxical sleep. Electroencephalogr Clin Neurophysiol 21(5): 469-477.

Kelly, T. M., Zuo, C. C. and Bloedel, J. R. (1990). Classical conditioning of the eyeblink reflex in the decerebrate-decerebellate rabbit. Behav Brain Res 38(1): 7-18.

Khadka, N., Zannou, A. L., Zunara, F., Truong, D. Q., Dmochowski, J. and Bikson, M. (2017). Minimal Heating at the Skin Surface During Transcranial Direct Current Stimulation. Neuromodulation *in Press*.

Kirschstein, T. and Kohling, R. (2009). What is the source of the EEG? Clin EEG Neurosci 40(3): 146-149.

Kitago, T. and Krakauer, J. W. (2013). Motor learning principles for neurorehabilitation. Handb Clin Neurol 110: 93-103.

Kiyatkin, E. A. (2007). Physiological and pathological brain hyperthermia. Prog Brain Res 162: 219-243.

Knight, D. C., Cheng, D. T., Smith, C. N., Stein, E. A. and Helmstetter, F. J. (2004). Neural substrates mediating human delay and trace fear conditioning. J Neurosci 24(1): 218-228.

Koekkoek, S. K., Den Ouden, W. L., Perry, G., Highstein, S. M. and De Zeeuw, C. I. (2002). Monitoring kinetic and frequency-domain properties of eyelid responses in mice with magnetic distance measurement technique. J Neurophysiol 88(4): 2124-2133.

Koekkoek, S. K., Hulscher, H. C., Dortland, B. R., Hensbroek, R. A., Elgersma, Y., Ruigrok, T. J. and De Zeeuw, C. I. (2003). Cerebellar LTD and learning-dependent timing of conditioned eyelid responses. Science 301(5640): 1736-1739.

Komiyama, M., Shibata, H. and Suzuki, T. (1984). Somatotopic representation of facial muscles within the facial nucleus of the mouse. A study using the retrograde horseradish peroxidase and cell degeneration techniques. Brain Behav Evol 24(2-3): 144-151.

Koo, H., Kim, M. S., Han, S. W., Paulus, W., Nitche, M. A., Kim, Y. H., Kim, H. I., Ko, S. H. and Shin, Y. I. (2016). After-effects of anodal transcranial direct current stimulation on the excitability of the motor cortex in rats. Restor Neurol Neurosci 34(5): 859-868.

Kosinski, R. J., Azizi, S. A. and Mihailoff, G. A. (1988). Convergence of cortico- and cuneopontine projections onto components of the pontocerebellar system in the rat: an anatomical and electrophysiological study. Exp Brain Res 71(3): 541-556.

Kotani, S., Kawahara, S. and Kirino, Y. (2003). Trace eyeblink conditioning in decerebrate guinea pigs. Eur J Neurosci 17(7): 1445-1454.

Kotilainen, T., Lehto, S. M. and Wikgren, J. (2015). Effect of transcranial direct current stimulation on semantic discrimination eyeblink conditioning. Behav Brain Res 292: 142-146.

Koutalidis, O., Foster, A. and Weisz, D. J. (1988). Parallel pathways can conduct visual CS information during classical conditioning of the NM response. J Neurosci 8(2): 417-427.

Krakauer, J. W. and Mazzoni, P. (2011). Human sensorimotor learning: adaptation, skill, and beyond. Curr Opin Neurobiol 21(4): 636-644.

Kraus, N. and Disterhoft, J. F. (1982). Response plasticity of single neurons in rabbit auditory association cortex during tone-signalled learning. Brain Res 246(2): 205-215.

Krause, B. and Cohen Kadosh, R. (2014). Not all brains are created equal: the relevance of individual differences in responsiveness to transcranial electrical stimulation. Front Syst Neurosci 8: 25.

Kraut, M. A., Arezzo, J. C. and Vaughan, H. G., Jr. (1985). Intracortical generators of the flash VEP in monkeys. Electroencephalogr Clin Neurophysiol 62(4): 300-312.

Kronberg, G., Bridi, M., Abel, T., Bikson, M. and Parra, L. C. (2017). Direct Current Stimulation Modulates LTP and LTD: Activity Dependence and Dendritic Effects. Brain Stimul 10(1): 51-58.

Kronforst-Collins, M. A. and Disterhoft, J. F. (1998). Lesions of the caudal area of rabbit medial prefrontal cortex impair trace eyeblink conditioning. Neurobiol Learn Mem 69(2): 147-162.

Kuo, H. I., Bikson, M., Datta, A., Minhas, P., Paulus, W., Kuo, M. F. and Nitsche, M. A. (2013). Comparing cortical plasticity induced by conventional and high-definition 4 x 1 ring tDCS: a neurophysiological study. Brain Stimul 6(4): 644-648.

Kupfermann, I. (1965). Effects of cortical polarization on visual discriminations. Exp Neurol 12(2): 179-189.

Lagopoulos, J. and Degabriele, R. (2008). Feeling the heat: the electrode–skin interface during DCS. Acta Neuropsych 20(2): 98-100.

Lang, N., Nitsche, M. A., Sommer, M., Tergau, F. and Paulus, W. (2003). Modulation of motor consolidation by external DC stimulation. Suppl Clin Neurophysiol 56: 277-281.

Lapchak, P. A., Wei, J. and Zivin, J. A. (2004). Transcranial infrared laser therapy improves clinical rating scores after embolic strokes in rabbits. Stroke 35(8): 1985-1988.

Lapchak, P. A., Salgado, K. F., Chao, C. H. and Zivin, J. A. (2007). Transcranial near-infrared light therapy improves motor function following embolic strokes in rabbits: an extended therapeutic window study using continuous and pulse frequency delivery modes. Neuroscience 148(4): 907-914.

Lavond, D. G., Hembree, T. L. and Thompson, R. F. (1985). Effect of kainic acid lesions of the cerebellar interpositus nucleus on eyelid conditioning in the rabbit. Brain Res 326(1): 179-182.

Leal-Campanario, R., Delgado-García, J. M. and Gruart, A. (2006). Microstimulation of the somatosensory cortex can substitute for vibrissa stimulation during Pavlovian conditioning. Proc Natl Acad Sci U S A 103(26): 10052-10057.

Lee, T. and Kim, J. J. (2004). Differential effects of cerebellar, amygdalar, and hippocampal lesions on classical eyeblink conditioning in rats. J Neurosci 24(13): 3242-3250.

Lefaucheur, J. P., Antal, A., Ahdab, R., Ciampi de Andrade, D., Fregni, F., Khedr, E. M., Nitsche, M. A. and Paulus, W. (2008). The use of repetitive transcranial magnetic stimulation (rTMS) and transcranial direct current stimulation (tDCS) to relieve pain. Brain Stimul 1(4): 337-344.

Leite, J., Carvalho, S., Fregni, F. and Goncalves, O. F. (2011). Task-specific effects of tDCS-induced cortical excitability changes on cognitive and motor sequence set shifting performance. PLoS One 6(9): e24140.

Lewis, J. L., Lo Turco, J. J. and Solomon, P. R. (1987). Lesions of the middle cerebellar peduncle disrupt acquisition and retention of the rabbit's classically conditioned nictitating membrane response. Behav Neurosci 101(2): 151-157.

Liebetanz, D., Nitsche, M. A., Tergau, F. and Paulus, W. (2002). Pharmacological approach to the mechanisms of transcranial DC-stimulation-induced after-effects of human motor cortex excitability. Brain 125: 2238-2247.

Liebetanz, D., Koch, R., Mayenfels, S., König, F., Paulus, W. and Nitsche, M. A. (2009). Safety limits of cathodal transcranial direct current stimulation in rats. Clin Neurophysiol 120(6): 1161-1167.

Lindquist, C. and Martensson, A. (1970). Mechanisms involved in the cat's blink reflex. Acta Physiol Scand 80(2): 149-159.

Lipski, J. (1981). Antidromic activation of neurons as an analytic tool in the study of the central nervous system. J Neurosci Methods 4(1): 1-32.

Lu, B. (2003). BDNF and activity-dependent synaptic modulation. Learn Mem 10(2): 86-98.

Luck, S. J. (2005). An Introduction to the Event-related Potential Technique, MIT Press.

Ma, L., Qiao, Q., Tsai, J. W., Yang, G., Li, W. and Gan, W. B. (2016). Experience-dependent plasticity of dendritic spines of layer 2/3 pyramidal neurons in the mouse cortex. Dev Neurobiol 76(3): 277-286.

Manto, M., Bower, J. M., Conforto, A. B., Delgado-García, J. M., da Guarda, S. N., Gerwig, M., Habas, C., Hagura, N., Ivry, R. B., Marien, P., Molinari, M., Naito, E., Nowak, D. A., Oulad Ben Taib, N., Pelisson, D., Tesche, C. D., Tilikete, C. and Timmann, D. (2012). Consensus paper: roles of the cerebellum in motor control--the diversity of ideas on cerebellar involvement in movement. Cerebellum 11(2): 457-487.

Márquez-Ruiz, J., Leal-Campanario, R., Sánchez-Campusano, R., Molaee-Ardekani, B., Wendling, F., Miranda, P. C., Ruffini, G., Gruart, A. and Delgado-García, J. M. (2012). Transcranial direct-current stimulation modulates synaptic mechanisms involved in associative learning in behaving rabbits. Proc Natl Acad Sci U S A 109(17): 6710-6715.

Márquez-Ruiz, J., Leal-Campanario, R., Wendling, F., Ruffini, G., Gruart, A. and Delgado-García, J. M. (2014). Transcranial electrical-current stimulation in animals. The Stimulated Brain: Cognitive Enhancement Using Non-Invasive Brain Stimulation. R. Cohen Kadosh. Amsterdam, Elsevier**:** 117-143.

Márquez-Ruiz, J., Ammann, C., Leal-Campanario, R., Ruffini, G., Gruart, A. and Delgado-García, J. M. (2016). Synthetic tactile perception induced by transcranial alternating-current stimulation can substitute for natural sensory stimulus in behaving rabbits. Sci Rep 6: 19753.

Marr, D. (1969). A theory of cerebellar cortex. J Physiol 202(2): 437-470.

Marshall, L., Molle, M., Siebner, H. R. and Born, J. (2005). Bifrontal transcranial direct current stimulation slows reaction time in a working memory task. BMC Neurosci 6: 23.

Marshall, L. and Binder, S. (2013). Contribution of transcranial oscillatory stimulation to research on neural networks: an emphasis on hippocampo-neocortical rhythms. Front Hum Neurosci 7: 614.

Martin, M. R. and Lodge, D. (1977). Morphology of the facial nucleus of the rat. Brain Res 123(1): 1-12.

Masino, S. A. and Dunwiddie, T. V. (1999). Temperature-dependent modulation of excitatory transmission in hippocampal slices is mediated by extracellular adenosine. J Neurosci 19(6): 1932-1939.

Mauk, M. D. and Thompson, R. F. (1987). Retention of classically conditioned eyelid responses following acute decerebration. Brain Res 403(1): 89-95.

Mauk, M. D., Garcia, K. S., Medina, J. F. and Steele, P. M. (1998). Does cerebellar LTD mediate motor learning? Toward a resolution without a smoking gun. Neuron 20(3): 359-362.

Mauro, A. (1969). The role of the Voltaic pile in the Galvani-Volta controversy concerning animal vs. metallic electricity. J Hist Med Allied Sci 24(2): 140-150.

McCormick, D. A., Lavond, D. G., Clark, G. A., Kettner, R. E., Rising, C. E. and Thompson, R. F. (1981). The engram found? Role of the cerebellum in classical conditioning of nictitating membrane and eyelid responses. Bull Psychon Soc 18(3): 103-105.

McCormick, D. A., Clark, G. A., Lavond, D. G. and Thompson, R. F. (1982). Initial localization of the memory trace for a basic form of learning. Proc Natl Acad Sci U S A 79(8): 2731-2735.

Medina, J. F., Nores, W. L., Ohyama, T. and Mauk, M. D. (2000). Mechanisms of cerebellar learning suggested by eyelid conditioning. Curr Opin Neurobiol 10(6): 717-724.

Medina, J. F., Nores, W. L. and Mauk, M. D. (2002). Inhibition of climbing fibres is a signal for the extinction of conditioned eyelid responses. Nature 416(6878): 330-333.

Megirian, D. (1973). Unilateral cortical spreading depression and conditioned eye blink responses in rabbits. Acta Neurobiol Exp (Wars) 33(4): 699-710.

Meinzer, M., Jahnigen, S., Copland, D. A., Darkow, R., Grittner, U., Avirame, K., Rodriguez, A. D., Lindenberg, R. and Flöel, A. (2014). Transcranial direct current

stimulation over multiple days improves learning and maintenance of a novel vocabulary. Cortex 50: 137-147.

Miller, L. and Gibson, A. (2009). Red Nucleus. Encyclopedia of Neuroscience. L. Squire. Oxford: Academic Press. 8**:** 55-62.

Miller, M. J., Weiss, C., Song, X., Iordanescu, G., Disterhoft, J. F. and Wyrwicz, A. M. (2008). Functional magnetic resonance imaging of delay and trace eyeblink conditioning in the primary visual cortex of the rabbit. J Neurosci 28(19): 4974-4981.

Minhas, P., Bansal, V., Patel, J., Ho, J. S., Diaz, J., Datta, A. and Bikson, M. (2010). Electrodes for high-definition transcutaneous DC stimulation for applications in drug delivery and electrotherapy, including tDCS. J Neurosci Methods 190(2): 188-197.

Minichino, A., Bersani, F. S., Bernabei, L., Spagnoli, F., Vergnani, L., Corrado, A., Taddei, I., Biondi, M. and Delle Chiaie, R. (2015). Prefronto-cerebellar transcranial direct current stimulation improves visuospatial memory, executive functions, and neurological soft signs in patients with euthymic bipolar disorder. Neuropsychiatr Dis Treat 11: 2265-2270.

Miranda, P. C., Lomarev, M. and Hallett, M. (2006). Modeling the current distribution during transcranial direct current stimulation. Clin Neurophysiol 117(7): 1623-1629.

Miranda, P. C. (2013). Physics of effects of transcranial brain stimulation. Handb Clin Neurol 116: 353-366.

Miranda, P. C., Mekonnen, A., Salvador, R. and Ruffini, G. (2013). The electric field in the cortex during transcranial current stimulation. Neuroimage 70: 48-58.

Misanin, J. R., Miller, R. R. and Lewis, D. J. (1968). Retrograde amnesia produced by electroconvulsive shock after reactivation of a consolidated memory trace. Science 160(3827): 554-555.

Mizuno, N. and Nakamura, Y. (1971). Rubral fibers to the facial nucleus in the rabbit. Brain Res 28(3): 545-549.

Molchan, S. E., Sunderland, T., McIntosh, A. R., Herscovitch, P. and Schreurs, B. G. (1994). A functional anatomical study of associative learning in humans. Proc Natl Acad Sci U S A 91(17): 8122-8126.

Monai, H., Ohkura, M., Tanaka, M., Oe, Y., Konno, A., Hirai, H., Mikoshiba, K., Itohara, S., Nakai, J., Iwai, Y. and Hirase, H. (2016). Calcium imaging reveals glial involvement in transcranial direct current stimulation-induced plasticity in mouse brain. Nat Commun 7: 11100.

Monfils, M. H. and Teskey, G. C. (2004). Skilled-learning-induced potentiation in rat sensorimotor cortex: a transient form of behavioural long-term potentiation. Neuroscience 125(2): 329-336.

Monte-Silva, K., Kuo, M. F., Hessenthaler, S., Fresnoza, S., Liebetanz, D., Paulus, W. and Nitsche, M. A. (2013). Induction of late LTP-like plasticity in the human motor cortex by repeated non-invasive brain stimulation. Brain Stimul 6(3): 424-432.

Morcuende, S., Delgado-García, J. M. and Ugolini, G. (2002). Neuronal premotor networks involved in eyelid responses: retrograde transneuronal tracing with rabies virus from the orbicularis oculi muscle in the rat. J Neurosci 22(20): 8808-8818.

Morecraft, R. J., Louie, J. L., Herrick, J. L. and Stilwell-Morecraft, K. S. (2001). Cortical innervation of the facial nucleus in the non-human primate: a new interpretation of the effects of stroke and related subtotal brain trauma on the muscles of facial expression. Brain 124(Pt 1): 176-208.

Morecraft, R. J., Stilwell-Morecraft, K. S. and Rossing, W. R. (2004). The motor cortex and facial expression: new insights from neuroscience. Neurologist 10(5): 235-249.

Morgado Bernal, I. (2005). Psicobiología del aprendizaje y la memoria. Rev Neurol 40(5): 289-297.

Morrell, F. and Naitoh, P. (1962). Effect of cortical polarization on a conditioned avoidance response. Exp Neurol 6(6): 507-523.

Moser, E., Mathiesen, I. and Andersen, P. (1993). Association between brain temperature and dentate field potentials in exploring and swimming rats. Science 259(5099): 1324-1326.

Moyer, J. R., Jr., Deyo, R. A. and Disterhoft, J. F. (1990). Hippocampectomy disrupts trace eye-blink conditioning in rabbits. Behav Neurosci 104(2): 243-252.

Muellbacher, W., Ziemann, U., Wissel, J., Dang, N., Kofler, M., Facchini, S., Boroojerdi, B., Poewe, W. and Hallett, M. (2002). Early consolidation in human primary motor cortex. Nature 415(6872): 640-644.

Mulkey, R. M. and Malenka, R. C. (1992). Mechanisms underlying induction of homosynaptic long-term depression in area CA1 of the hippocampus. Neuron 9(5): 967-975.

Múnera, A., Gruart, A., Muñoz, M. D., Fernández-Mas, R. and Delgado-García, J. M. (2001). Hippocampal pyramidal cell activity encodes conditioned stimulus predictive value during classical conditioning in alert cats. J Neurophysiol 86(5): 2571-2582.

Müri, R. M. (2016). Cortical control of facial expression. J Comp Neurol 524(8): 1578-1585.

Nadel, L. and Land, C. (2000). Memory traces revisited. Nat Rev Neurosci 1(3): 209-212.

Nader, K., Schafe, G. E. and Le Doux, J. E. (2000). Fear memories require protein synthesis in the amygdala for reconsolidation after retrieval. Nature 406(6797): 722-726.

Nealey, T. A. and Maunsell, J. H. (1994). Magnocellular and parvocellular contributions to the responses of neurons in macaque striate cortex. J Neurosci 14(4): 2069-2079.

Nekhendzy, V., Fender, C. P., Davies, M. F., Lemmens, H. J. M., Kim, M. S., Bouley, D. M. and Maze, M. (2004). The Antinociceptive Effect of Transcranial Electrostimulation with Combined Direct and Alternating Current in Freely Moving Rats. Anesth Analg: 730-737.

Nicholson, D. A. and Freeman, J. H., Jr. (2002). Neuronal correlates of conditioned inhibition of the eyeblink response in the anterior interpositus nucleus. Behav Neurosci 116(1): 22-36.

Nieoullon, A. and Rispal-Padel, L. (1976). Somatotopic localization in cat motor cortex. Brain Res 105(3): 405-422.

Nitsche, M. A. and Paulus, W. (2000). Excitability changes induced in the human motor cortex by weak transcranial direct current stimulation. J Physiol 527.3: 633-639.

Nitsche, M. A., Fricke, K., Henschke, U., Schlitterlau, A., Liebetanz, D., Lang, N., Henning, S., Tergau, F. and Paulus, W. (2003a). Pharmacological modulation of cortical excitability shifts induced by transcranial direct current stimulation in humans. J Physiol 553(Pt 1): 293-301.

Nitsche, M. A., Schauenburg, A., Lang, N., Liebetanz, D., Exner, C., Paulus, W. and Tergau, F. (2003b). Facilitation of implicit motor learning by weak transcranial direct current stimulation of the primary motor cortex in the human. J Cogn Neurosci 15(4): 619-626.

Nitsche, M. A., Seeber, A., Frommann, K., Klein, C. C., Rochford, C., Nitsche, M. S., Fricke, K., Liebetanz, D., Lang, N., Antal, A., Paulus, W. and Tergau, F. (2005). Modulating parameters of excitability during and after transcranial direct current stimulation of the human motor cortex. J Physiol 568(Pt 1): 291-303.

Nitsche, M. A., Doemkes, S., Karakose, T., Antal, A., Liebetanz, D., Lang, N., Tergau, F. and Paulus, W. (2007). Shaping the effects of transcranial direct current stimulation of the human motor cortex. J Neurophysiol 97(4): 3109-3117.

Nitsche, M. A., Cohen, L. G., Wassermann, E. M., Priori, A., Lang, N., Antal, A., Paulus, W., Hummel, F., Boggio, P. S., Fregni, F. and Pascual-Leone, A. (2008). Transcranial direct current stimulation: State of the art 2008. Brain Stimul 1(3): 206-223.

Nonnekes, J., Arrogi, A., Munneke, M. A., van Asseldonk, E. H., Oude Nijhuis, L. B., Geurts, A. C. and Weerdesteyn, V. (2014). Subcortical structures in humans can be facilitated by transcranial direct current stimulation. PLoS One 9(9): e107731.

Norman, R. J., Villablanca, J. R., Brown, K. A., Schwafel, J. A. and Buchwald, J. S. (1974). Classical eyeblink conditioning in the bilaterally hemispherectomized cat. Exp Neurol 44(3): 363-380.

Nudo, R. J., Plautz, E. J. and Frost, S. B. (2001). Role of adaptive plasticity in recovery of function after damage to motor cortex. Muscle Nerve 24(8): 1000-1019.

Nuzum, N. D., Hendy, A. M., Russell, A. P. and Teo, W. P. (2016). Measures to Predict The Individual Variability of Corticospinal Responses Following Transcranial Direct Current Stimulation. Front Hum Neurosci 10: 487.

Oakley, D. A. and Russell, I. S. (1972). Neocortical lesions and Pavlovian conditioning. Physiol Behav 8(5): 915-926.

Oakley, D. A. and Russell, I. S. (1977). Subcortical storage of Pavlovian conditioning in the rabbit. Physiol Behav 18(5): 931-937.

Ohn, S. H., Park, C. I., Yoo, W. K., Ko, M. H., Choi, K. P., Kim, G. M., Lee, Y. T. and Kim, Y. H. (2008). Time-dependent effect of transcranial direct current stimulation on the enhancement of working memory. Neuroreport 19(1): 43-47.

Okuno, T., Oku, H., Sugiyama, T., Yang, Y. and Ikeda, T. (2002). Evidence that nitric oxide is involved in autoregulation in optic nerve head of rabbits. Invest Ophthalmol Vis Sci 43(3): 784-789.

Oliviero, A., Mordillo-Mateos, L., Arias, P., Panyavin, I., Foffani, G. and Aguilar, J. (2011). Transcranial static magnetic field stimulation of the human motor cortex. J Physiol 589(Pt 20): 4949-4958.

Onofrj, M., Bodis-Wollner, I. and Bobak, P. (1982). Pattern visual evoked potentials in the rat. Physiol Behav 28(2): 227-230.

Onofrj, M., Harnois, C. and Bodis-Wollner, I. (1985). The hemispheric distribution of the transient rat VEP: a comparison of flash and pattern stimulation. Exp Brain Res 59(3): 427-433.

Orban de Xivry, J. J. and Shadmehr, R. (2014). Electrifying the motor engram: effects of tDCS on motor learning and control. Exp Brain Res 232(11): 3379-3395.

Orlov, N. D., Tracy, D. K., Joyce, D., Patel, S., Rodzinka-Pasko, J., Dolan, H., Hodsoll, J., Collier, T., Rothwell, J. and Shergill, S. S. (2016). Stimulating cognition in schizophrenia: A controlled pilot study of the effects of prefrontal transcranial direct current stimulation upon memory and learning. Brain Stimul 10(3): 560-566.

Oron, A., Oron, U., Chen, J., Eilam, A., Zhang, C., Sadeh, M., Lampl, Y., Streeter, J., DeTaboada, L. and Chopp, M. (2006). Low-level laser therapy applied transcranially to

rats after induction of stroke significantly reduces long-term neurological deficits. Stroke 37(10): 2620-2624.

Pacheco-Calderón, R., Carretero-Guillén, A., Delgado-García, J. M. and Gruart, A. (2012). Red nucleus neurons actively contribute to the acquisition of classically conditioned eyelid responses in rabbits. J Neurosci 32(35): 12129-12143.

Padel, Y., Sybirska, E., Bourbonnais, D. and Vinay, L. (1988). Electrophysiological identification of a somaesthetic pathway to the red nucleus. Behav Brain Res 28(1-2): 139-151.

Palm, U., Keeser, D., Schiller, C., Fintescu, Z., Nitsche, M. A., Reisinger, E. and Padberg, F. (2008). Skin lesions after treatment with transcranial direct current stimulation (tDCS). Brain Stimul 1(4): 386-387.

Paneri, B., Adair, D., Thomas, C., Khadka, N., Patel, V., Tyler, W. J., Parra, L. and Bikson, M. (2016). Tolerability of Repeated Application of Transcranial Electrical Stimulation with Limited Outputs to Healthy Subjects. Brain Stimul 9(5): 740-754.

Paulus, W. (2011). Transcranial electrical stimulation (tES - tDCS; tRNS, tACS) methods. Neuropsychol Rehabil 21(5): 602-617.

Pavlov, I. (1927). Conditioned reflexes: An investigation of the physiological activity of the cerebral cortex. Oxford University Press, London.

Peinemann, A., Reimer, B., Loer, C., Quartarone, A., Munchau, A., Conrad, B. and Siebner, H. R. (2004). Long-lasting increase in corticospinal excitability after 1800 pulses of subthreshold 5 Hz repetitive TMS to the primary motor cortex. Clin Neurophysiol 115(7): 1519-1526.

Penhune, V. B. and Steele, C. J. (2012). Parallel contributions of cerebellar, striatal and M1 mechanisms to motor sequence learning. Behav Brain Res 226(2): 579-591.

Peters, M. A., Thompson, B., Merabet, L. B., Wu, A. D. and Shams, L. (2013). Anodal tDCS to V1 blocks visual perceptual learning consolidation. Neuropsychologia 51(7): 1234-1239.

Pierau, F. K., Klee, M. R. and Klussmann, F. W. (1976). Effect of temperature on postsynaptic potentials of cat spinal motoneurones. Brain Res 114(1): 21-34.

Podda, M. V., Cocco, S., Mastrodonato, A., Fusco, S., Leone, L., Barbati, S. A., Colussi, C., Ripoli, C. and Grassi, C. (2016). Anodal transcranial direct current stimulation boosts synaptic plasticity and memory in mice via epigenetic regulation of Bdnf expression. Sci Rep 6: 22180.

Polania, R., Paulus, W. and Nitsche, M. A. (2012). Modulating cortico-striatal and thalamo-cortical functional connectivity with transcranial direct current stimulation. Hum Brain Mapp 33(10): 2499-2508.

Polyanskii, V. B., Alymkulov, D. E., Sokolov, E. N., Radzievskaya, M. G. and Ruderman, G. L. (2010). Evoked potentials in the rabbit visual cortex reflect changes in line orientation and intensity. Neurosci Behav Physiol 40(2): 205-213.

Porciatti, V., Pizzorusso, T. and Maffei, L. (1999). The visual physiology of the wild type mouse determined with pattern VEPs. Vision Res 39(18): 3071-3081.

Poreisz, C., Boros, K., Antal, A. and Paulus, W. (2007). Safety aspects of transcranial direct current stimulation concerning healthy subjects and patients. Brain Res Bull 72(4-6): 208-214.

Porter, J. D., Burns, L. A. and May, P. J. (1989). Morphological substrate for eyelid movements: innervation and structure of primate levator palpebrae superioris and orbicularis oculi muscles. J Comp Neurol 287(1): 64-81.

Prichard, G., Weiller, C., Fritsch, B. and Reis, J. (2014). Effects of different electrical brain stimulation protocols on subcomponents of motor skill learning. Brain Stimul 7(4): 532-540.

Priori, A., Berardelli, A., Rona, S., Accornero, N. and Manfredi, M. (1998). Polarization of the human motor cortex through the scalp. NeuroReport 9: 2257-2260.

Priori, A. (2003). Brain polarization in humans: a reappraisal of an old tool for prolonged non-invasive modulation of brain excitability. Clin Neurophysiol 114(4): 589-595.

Purves, D., Augustine, G. J., Fitzpatrick, D., Hall, W. C., LaMantia, A. S., McNamara, J. O. and Williams, S. M. (2004). Central Visual Pathways. Neuroscience. Sunderland (MA), Sinauer Associates.

Radman, T., Ramos, R. L., Brumberg, J. C. and Bikson, M. (2009). Role of cortical cell type and morphology in subthreshold and suprathreshold uniform electric field stimulation in vitro. Brain Stimul 2(4): 215-228, 228.e211-213.

Radpour, S. (1977). Organization of the facial nerve nucleus in the cat. Laryngoscope 87(4 Pt 1): 557-574.

Ragert, P., Vandermeeren, Y., Camus, M. and Cohen, L. G. (2008). Improvement of spatial tactile acuity by transcranial direct current stimulation. Clin Neurophysiol 119(4): 805-811.

Rahman, A., Reato, D., Arlotti, M., Gasca, F., Datta, A., Parra, L. C. and Bikson, M. (2013). Cellular effects of acute direct current stimulation: somatic and synaptic terminal effects. J Physiol 591(Pt 10): 2563-2578.

Rahman, A., Toshev, P. K. and Bikson, M. (2014). Polarizing cerebellar neurons with transcranial Direct Current Stimulation. Clin Neurophysiol 125(3): 435-438.

Reis, J., Robertson, E. M., Krakauer, J. W., Rothwell, J., Marshall, L., Gerloff, C., Wassermann, E. M., Pascual-Leone, A., Hummel, F., Celnik, P. A., Classen, J., Flöel, A., Ziemann, U., Paulus, W., Siebner, H. R., Born, J. and Cohen, L. G. (2008). Consensus: Can transcranial direct current stimulation and transcranial magnetic stimulation enhance motor learning and memory formation? Brain Stimul 1(4): 363-369.

Reis, J., Schambra, H. M., Cohen, L. G., Buch, E. R., Fritsch, B., Zarahn, E., Celnik, P. A. and Krakauer, J. W. (2009). Noninvasive cortical stimulation enhances motor skill acquisition over multiple days through an effect on consolidation. Proc Natl Acad Sci U S A 106(5): 1590-1595.

Reis, J. and Fritsch, B. (2011). Modulation of motor performance and motor learning by transcranial direct current stimulation. Curr Opin Neurol 24(6): 590-596.

Rescorla, R. A. (1988). Pavlovian conditioning. It's not what you think it is. Am Psychol 43(3): 151-160.

Rieke, F., Warlan, D., de Ruyter van Steveninck, R. and Bialck, W. (1997). Spike: exploring the neural code, Bradford Books, Cambridge, MA: MIT Press.

Rioult-Pedotti, M. S., Friedman, D., Hess, G. and Donoghue, J. P. (1998). Strengthening of horizontal cortical connections following skill learning. Nat Neurosci 1(3): 230-234.

Rioult-Pedotti, M. S., Friedman, D. and Donoghue, J. P. (2000). Learning-induced LTP in neocortex. Science 290(5491): 533-536.

Rizley, R. C. and Rescorla, R. A. (1972). Associations in second-order conditioning and sensory preconditioning. J Comp Physiol Psychol 81(1): 1-11.

Robertson, E. M., Pascual-Leone, A. and Miall, R. C. (2004). Current concepts in procedural consolidation. Nat Rev Neurosci 5(7): 576-582.

Rogalewski, A., Breitenstein, C., Nitsche, M. A., Paulus, W. and Knecht, S. (2004). Transcranial direct current stimulation disrupts tactile perception. Eur J Neurosci 20(1): 313-316.

Rohan, J. G., Carhuatanta, K. A., McInturf, S. M., Miklasevich, M. K. and Jankord, R. (2015). Modulating Hippocampal Plasticity with In Vivo Brain Stimulation. J Neurosci 35(37): 12824-12832.

Rossi, S. and Rossini, P. M. (2004). TMS in cognitive plasticity and the potential for rehabilitation. Trends Cogn Sci 8(6): 273-279.

Rossi, S., Hallett, M., Rossini, P. M., Pascual-Leone, A. and Safety of, T. M. S. C. G. (2009). Safety, ethical considerations, and application guidelines for the use of transcranial magnetic stimulation in clinical practice and research. Clin Neurophysiol 120(12): 2008-2039.

Rudvin, I., Valberg, A. and Kilavik, B. E. (2000). Visual evoked potentials and magnocellular and parvocellular segregation. Vis Neurosci 17(4): 579-590.

Ruffini, G., Wendling, F., Merlet, I., Molaee-Ardekani, B., Mekonnen, A., Salvador, R., Soria-Frisch, A., Grau, C., Dunne, S. and Miranda, P. C. (2013). Transcranial current brain stimulation (tCS): models and technologies. IEEE Trans Neural Syst Rehabil Eng 21(3): 333-345.

Ruffini, G., Fox, M. D., Ripolles, O., Miranda, P. C. and Pascual-Leone, A. (2014). Optimization of multifocal transcranial current stimulation for weighted cortical pattern targeting from realistic modeling of electric fields. Neuroimage 89: 216-225.

Ruohonen, J. and Ilmoniemi, R. (2002). Physical principles for transcranial magnetic stimulation. Handbook of transcranial magnetic stimulation. A. Pascual-Leone, N. Davey, J. Rothwell, E. M. Wassermann and B. Puri. New York, Oxford University Press.

Russell, I. S., Kleinman, D., Plotkin, H. C. and Ross, R. B. (1969). The role of the cortex in acquisition and retention of a classically conditioned passive avoidance response. Physiol Behav 4(4): 575-581.

Sakaguchi, H., Fujikado, T., Fang, X., Kanda, H., Osanai, M., Nakauchi, K., Ikuno, Y., Kamei, M., Yagi, T., Nishimura, S., Ohji, M., Yagi, T. and Tano, Y. (2004). Transretinal electrical stimulation with a suprachoroidal multichannel electrode in rabbit eyes. Jpn J Ophthalmol 48(3): 256-261.

Sakamoto, T. and Endo, S. (2010). Amygdala, deep cerebellar nuclei and red nucleus contribute to delay eyeblink conditioning in C57BL /6 mice. Eur J Neurosci 32(9): 1537-1551.

Salvador, R., Wenger, C. and Miranda, P. C. (2015). Investigating the cortical regions involved in MEP modulation in tDCS. Front Cell Neurosci 9(405).

Sánchez-Campusano, R., Gruart, A. and Delgado-García, J. M. (2007). The cerebellar interpositus nucleus and the dynamic control of learned motor responses. J Neurosci 27(25): 6620-6632.

Sánchez-Campusano, R., Gruart, A. and Delgado-García, J. M. (2011). Dynamic changes in the cerebellar-interpositus/red-nucleus-motoneuron pathway during motor learning. Cerebellum 10(4): 702-710.

Santos, F. J., Oliveira, R. F., Jin, X. and Costa, R. M. (2015). Corticostriatal dynamics encode the refinement of specific behavioral variability during skill learning. eLife 4: e09423.

Saucedo Marquez, C. M., Zhang, X., Swinnen, S. P., Meesen, R. and Wenderoth, N. (2013). Task-specific effect of transcranial direct current stimulation on motor learning. Front Hum Neurosci 7: 333.

Savic, B. and Meier, B. (2016). How Transcranial Direct Current Stimulation Can Modulate Implicit Motor Sequence Learning and Consolidation: A Brief Review. Front Hum Neurosci 10: 26.

Schacter, D. and Wagner, A. (2013). Learning and Memory. Principles of Neural Science. E. Kandel, J. Schwartz, T. Jessell, S. Siegelbaum and A. Hudspeth, McGraw-Hill. 5th Edition**:** 1441-1461.

Schambra, H. M., Abe, M., Luckenbaugh, D. A., Reis, J., Krakauer, J. W. and Cohen, L. G. (2011). Probing for hemispheric specialization for motor skill learning: a transcranial direct current stimulation study. J Neurophysiol 106(2): 652-661.

Schmajuk, N. A. and Christiansen, B. A. (1990). Eyeblink conditioning in rats. Physiol Behav 48(5): 755-758.

Schmidt, S. L., Iyengar, A. K., Foulser, A. A., Boyle, M. R. and Fröhlich, F. (2014). Endogenous cortical oscillations constrain neuromodulation by weak electric fields. Brain Stimul 7(6): 878-889.

Schweid, L., Rushmore, R. J. and Valero-Cabre, A. (2008). Cathodal transcranial direct current stimulation on posterior parietal cortex disrupts visuo-spatial processing in the contralateral visual field. Exp Brain Res 186(3): 409-417.

Sczesny-Kaiser, M., Beckhaus, K., Dinse, H. R., Schwenkreis, P., Tegenthoff, M. and Hoffken, O. (2016). Repetitive Transcranial Direct Current Stimulation Induced Excitability Changes of Primary Visual Cortex and Visual Learning Effects-A Pilot Study. Front Behav Neurosci 10: 116.

Sears, L. L., Logue, S. F. and Steinmetz, J. E. (1996). Involvement of the ventrolateral thalamic nucleus in rabbit classical eyeblink conditioning. Behav Brain Res 74(1-2): 105-117.

Seidler, R. D., Purushotham, A., Kim, S. G., Ugurbil, K., Willingham, D. and Ashe, J. (2002). Cerebellum activation associated with performance change but not motor learning. Science 296(5575): 2043-2046.

Shaw, M. D. and Baker, R. (1985). Morphology of motoneurons in a mixed motor pool of the cat facial nucleus that innervate orbicularis oculis and quadratus labii superioris, stained intracellularly with horseradish peroxidase. Neuroscience 14(2): 627-643.

Sherwood, C. C. (2005). Comparative anatomy of the facial motor nucleus in mammals, with an analysis of neuron numbers in primates. Anat Rec A Discov Mol Cell Evol Biol 287(1): 1067-1079.

Shibuki, K., Gomi, H., Chen, L., Bao, S., Kim, J. J., Wakatsuki, H., Fujisaki, T., Fujimoto, K., Katoh, A., Ikeda, T., Chen, C., Thompson, R. F. and Itohara, S. (1996). Deficient cerebellar long-term depression, impaired eyeblink conditioning, and normal motor coordination in GFAP mutant mice. Neuron 16(3): 587-599.

Shmuelof, L. and Krakauer, J. W. (2011). Are we ready for a natural history of motor learning? Neuron 72(3): 469-476.

Shuler, M. G. and Bear, M. F. (2006). Reward timing in the primary visual cortex. Science 311(5767): 1606-1609.

Siegel, J. J. and Mauk, M. D. (2013). Persistent activity in prefrontal cortex during trace eyelid conditioning: dissociating responses that reflect cerebellar output from those that do not. J Neurosci 33(38): 15272-15284.

Siegel, J. J., Taylor, W., Gray, R., Kalmbach, B., Zemelman, B. V., Desai, N. S., Johnston, D. and Chitwood, R. A. (2015). Trace Eyeblink Conditioning in Mice Is Dependent upon the Dorsal Medial Prefrontal Cortex, Cerebellum, and Amygdala: Behavioral Characterization and Functional Circuitry(1,2,3). eNeuro 2(4).

Silvanto, J. and Pascual-Leone, A. (2008). State-dependency of transcranial magnetic stimulation. Brain Topogr 21(1): 1-10.

Sisson, D. F. and Siegel, J. (1989). Chloral hydrate anesthesia: EEG power spectrum analysis and effects on VEPs in the rat. Neurotoxicol Teratol 11(1): 51-56.

Siu, T. L. and Morley, J. W. (2007). Influence of callosal transfer on visual cortical evoked response and the implication in the development of a visual prosthesis. Graefes Arch Clin Exp Ophthalmol 245(12): 1797-1803.

Solomon, P. R., Lewis, J. L., LoTurco, J. J., Steinmetz, J. E. and Thompson, R. F. (1986). The role of the middle cerebellar peduncle in acquisition and retention of the rabbit's classically conditioned nictitating membrane response. Bull Psychon Soc 24(1): 75-78.

Sotelo, C. (2003). Viewing the brain through the master hand of Ramon y Cajal. Nat Rev Neurosci 4(1): 71-77.

Soto, A., Perez-Samartin, A. L., Etxebarria, E. and Matute, C. (2004). Excitotoxic insults to the optic nerve alter visual evoked potentials. Neuroscience 123(2): 441-449.

Souza, G. S., Gomes, B. D., Saito, C. A., da Silva Filho, M. and Silveira, L. C. (2007). Spatial luminance contrast sensitivity measured with transient VEP: comparison with psychophysics and evidence of multiple mechanisms. Invest Ophthalmol Vis Sci 48(7): 3396-3404.

Sperry, R. W. (1950). Neural basis of the spontaneous optokinetic response produced by visual inversion. J Comp Physiol Psychol 43(6): 482-489.

Stagg, C. J., Jayaram, G., Pastor, D., Kincses, Z. T., Matthews, P. M. and Johansen-Berg, H. (2011). Polarity and timing-dependent effects of transcranial direct current stimulation in explicit motor learning. Neuropsychologia 49(5): 800-804.

Stagg, C. J. and Nitsche, M. A. (2011). Physiological basis of transcranial direct current stimulation. Neuroscientist 17(1): 37-53.

Stanton, M. E., Freeman, J. H., Jr. and Skelton, R. W. (1992). Eyeblink conditioning in the developing rat. Behav Neurosci 106(4): 657-665.

Steffens, H. J. (1979). James Prescott Joule and the concept of energy, Dawson.

Steinmetz, A. B., Harmon, T. C. and Freeman, J. H. (2013). Visual cortical contributions to associative cerebellar learning. Neurobiol Learn Mem 104: 103-109.

Steinmetz, J. E., Logan, C. G., Rosen, D. J., Thompson, J. K., Lavond, D. G. and Thompson, R. F. (1987). Initial localization of the acoustic conditioned stimulus projection system to the cerebellum essential for classical eyelid conditioning. Proc Natl Acad Sci U S A 84(10): 3531-3535.

Steinmetz, J. E., Logue, S. F. and Steinmetz, S. S. (1992a). Rabbit classically conditioned eyelid responses do not reappear after interpositus nucleus lesion and extensive post-lesion training. Behav Brain Res 51(1): 103-114.

Steinmetz, J. E., Lavond, D. G., Ivkovich, D., Logan, C. G. and Thompson, R. F. (1992b). Disruption of classical eyelid conditioning after cerebellar lesions: damage to a memory trace system or a simple performance deficit? J Neurosci 12(11): 4403-4426.

Swadlow, H. A. (1998). Neocortical efferent neurons with very slowly conducting axons: strategies for reliable antidromic identification. J Neurosci Methods 79(2): 131-141.

Takatsuki, K., Kawahara, S., Kotani, S., Fukunaga, S., Mori, H., Mishina, M. and Kirino, Y. (2003). The hippocampus plays an important role in eyeblink conditioning with a short trace interval in glutamate receptor subunit delta 2 mutant mice. J Neurosci 23(1): 17-22.

Tanaka, T., Yu, H. and Kitai, S. T. (1971). Trigeminal and spinal inputs to the facial nucleus. Brain Res 33(2): 504-508.

Taubert, M., Stein, T., Kreutzberg, T., Stockinger, C., Hecker, L., Focke, A., Ragert, P., Villringer, A. and Pleger, B. (2016). Remote Effects of Non-Invasive Cerebellar Stimulation on Error Processing in Motor Re-Learning. Brain Stimul 9(5): 692-699.

Terney, D., Chaieb, L., Moliadze, V., Antal, A. and Paulus, W. (2008). Increasing human brain excitability by transcranial high-frequency random noise stimulation. J Neurosci 28(52): 14147-14155.

Thompson, J. M., Woolsey, C. N. and Talbot, S. A. (1950). Visual areas I and II of cerebral cortex of rabbit. J Neurophysiol 13(4): 277-288.

Thompson, R. F., Swain, R., Clark, R. and Shinkman, P. (2000). Intracerebellar conditioning--Brogden and Gantt revisited. Behav Brain Res 110(1-2): 3-11.

Thompson, R. F. and Steinmetz, J. E. (2009). The role of the cerebellum in classical conditioning of discrete behavioral responses. Neuroscience 162(3): 732-755.

Tomiyama, Y., Fujita, K., Nishiguchi, K. M., Tokashiki, N., Daigaku, R., Tabata, K., Sugano, E., Tomita, H. and Nakazawa, T. (2016). Measurement of Electroretinograms and Visually Evoked Potentials in Awake Moving Mice. PLoS One 11(6): e0156927.

Trigo, J. A., Gruart, A. and Delgado-García, J. M. (1999a). Discharge profiles of abducens, accessory abducens, and orbicularis oculi motoneurons during reflex and conditioned blinks in alert cats. J Neurophysiol 81(4): 1666-1684.

Trigo, J. A., Gruart, A. and Delgado-García, J. M. (1999b). Role of proprioception in the control of lid position during reflex and conditioned blink responses in the alert behaving cat. Neuroscience 90(4): 1515-1528.

Tseng, W., Guan, R., Disterhoft, J. F. and Weiss, C. (2004). Trace eyeblink conditioning is hippocampally dependent in mice. Hippocampus 14(1): 58-65.

Vaseghi, B., Zoghi, M. and Jaberzadeh, S. (2015). Differential effects of cathodal transcranial direct current stimulation of prefrontal, motor and somatosensory cortices on cortical excitability and pain perception - a double-blind randomised sham-controlled study. Eur J Neurosci 42(7): 2426-2437.

Vigano, A., D'Elia, T. S., Sava, S. L., Auve, M., De Pasqua, V., Colosimo, A., Di Piero, V., Schoenen, J. and Magis, D. (2013). Transcranial Direct Current Stimulation (tDCS) of the visual cortex: a proof-of-concept study based on interictal electrophysiological abnormalities in migraine. J Headache Pain 14: 23.

Ward, R. and Weiskrantz, L. (1969). Impaired discrimination following polarisation of the striate cortex. Exp Brain Res 9(4): 346-356.

Ward, R. L., Flores, L. C. and Disterhoft, J. F. (2012). Infragranular barrel cortex activity is enhanced with learning. J Neurophysiol 108(5): 1278-1287.

Wassermann, E. M. and Lisanby, S. H. (2001). Therapeutic application of repetitive transcranial magnetic stimulation: a review. Clin Neurophysiol 112(8): 1367-1377.

Weible, A. P., Weiss, C. and Disterhoft, J. F. (2003). Activity profiles of single neurons in caudal anterior cingulate cortex during trace eyeblink conditioning in the rabbit. J Neurophysiol 90(2): 599-612.

Weiss, C., Bouwmeester, H., Power, J. M. and Disterhoft, J. F. (1999). Hippocampal lesions prevent trace eyeblink conditioning in the freely moving rat. Behav Brain Res 99(2): 123-132.

Welsh, J. P. and Harvey, J. A. (1989). Cerebellar lesions and the nictitating membrane reflex: performance deficits of the conditioned and unconditioned response. J Neurosci 9(1): 299-311.

Welsh, J. P. and Harvey, J. A. (1991). Pavlovian conditioning in the rabbit during inactivation of the interpositus nucleus. J Physiol 444: 459-480.

Wessel, M. J., Zimerman, M. and Hummel, F. C. (2015). Non-invasive brain stimulation: an interventional tool for enhancing behavioral training after stroke. Front Hum Neurosci 9: 265.

Westbrook, G. (2013). Seizures and Epilepsy. Principles of neural science. E. Kandel, J. Schwartz, T. Jessell, S. Siegelbaum and A. Hudspeth, McGraw-Hill Education.

Wiethoff, S., Hamada, M. and Rothwell, J. C. (2014). Variability in response to transcranial direct current stimulation of the motor cortex. Brain Stimul 7(3): 468-475.

Woodruff-Pak, D. S., Lavond, D. G. and Thompson, R. F. (1985). Trace conditioning: abolished by cerebellar nuclear lesions but not lateral cerebellar cortex aspirations. Brain Res 348(2): 249-260.

Woody, C., Yarowsky, P., Owens, J., Black-Cleworth, P. and Crow, T. (1974). Effect of lesions of cortical motor areas on acquisition of conditioned eye blink in the cat. J Neurophysiol 37(3): 385-394.

Woody, C. D., Vassilevsky, N. N. and Engel, J., Jr. (1970). Conditioned eye blink: unit activity at coronal-precruciate cortex of the cat. J Neurophysiol 33(6): 851-864.

Woody, C. D. and Yarowsky, P. J. (1972). Conditioned eye blink using electrical stimulation of coronal-precruciate cortex as conditional stimulus. J Neurophysiol 35(2): 242-252.

Woody, C. D., Gruen, E. and Birt, D. (1991). Changes in membrane currents during Pavlovian conditioning of single cortical neurons. Brain Res 539(1): 76-84.

Yang, Y., Lei, C., Feng, H. and Sui, J. F. (2015). The neural circuitry and molecular mechanisms underlying delay and trace eyeblink conditioning in mice. Behav Brain Res 278: 307-314.

Yonemura, D. and Tsuchida, Y. (1968). The short latency discharge of high light-threshold in the rabbit optic nerve. Jpn J Physiol 18(6): 703-722.

Zuchowski, M. L., Timmann, D. and Gerwig, M. (2014). Acquisition of conditioned eyeblink responses is modulated by cerebellar tDCS. Brain Stimul 7(4): 525-531.

8. ANNEX

Behavioral/Cognitive

The Motor Cortex Is Involved in the Generation of Classically Conditioned Eyelid Responses in Behaving Rabbits

Claudia Ammann, Javier Márquez-Ruiz, María Á. Gómez-Climent, José M. Delgado-García, and Agnès Gruart
Division of Neurosciences, Pablo de Olavide University, Seville 41013, Spain

Classical blink conditioning is a well known model for studying neural generation of acquired motor responses. The acquisition of this type of associative learning has been related to many cortical, subcortical, and cerebellar structures. However, until now, no one has studied the motor cortex (MC) and its possible role in classical eyeblink conditioning. We recorded in rabbits the activity of MC neurons during blink conditioning using a delay paradigm. Neurons were identified by their antidromic activation from facial nucleus (FN) or red nucleus (RN). For conditioning, we used a tone as a conditioned stimulus (CS) followed by an air puff as an unconditioned stimulus (US) that coterminated with it. Conditioned responses (CRs) were determined from the electromyographic activity of the orbicularis oculi muscle and/or from eyelid position recorded with the search coil technique. Type A neurons increased their discharge rates across conditioning sessions and reached peak firing during the CS–US interval, while type B cells presented a second peak during US presentation. Both of them project to the FN. Type C cells increased their firing across the CS–US interval, reaching peak values at the time of US presentation, and were activated from the RN. These three types of neurons fired well in advance of the beginning of CRs and changed with them. Reversible inactivation of the MC during conditioning evoked a decrease in learning curves and in the amplitude of CRs, while train stimulation of the MC simulated the profile and kinematics of conditioned blinks. In conclusion, MC neurons are involved in the acquisition and expression of CRs.

Key words: associative learning; delay conditioning; motor cortex; rabbits; unitary recordings

Significance Statement

Classical blink conditioning is a popular experimental model for studying neural mechanisms underlying the acquisition of motor skills. The acquisition of this type of associative learning has been related to many cortical, subcortical, and cerebellar structures. However, until now, no one has studied the motor cortex (MC) and its possible role in classical eyeblink conditioning. Here, we report that the firing activities of MC neurons, recorded in behaving rabbits, are related to and preceded the initiation of conditioned blinks. MC neurons were identified as projecting to the red or facial nuclei and encoded the kinematics of conditioned eyelid responses. The timed stimulation of recording sites simulated the profile of conditioned blinks. MC neurons play a role in the acquisition and expression of these acquired motor responses.

Introduction

The classical conditioning of the nictitating membrane/eyelid responses is a well known experimental procedure for the study of brain sites involved in the acquisition and storage of new motor abilities, as well as of the neural mechanisms underlying these processes. Although cerebellar cortical and/or nuclear centers have traditionally been assumed to be related to the acquisition and/or performance of conditioned blinks (Welsh and Harvey, 1991; Krupa et al., 1993; Gruart et al., 2000b; Christian and Thompson, 2003; Koekkoek et al., 2003; Perciavalle et al., 2013), many other cerebral cortical and subcortical structures have been reported as involved as well in different aspects of acquisition, storage, retrieval, and extinction processes. Thus, the hippocampal circuit (Weiss et al., 1999; Múnera et al., 2001; Gruart et al., 2006), the medial prefrontal (Weible et al., 2003; Siegel and Mauk, 2013; Caro-Martín et al., 2015) and the somatosensory (Leal-Campanario et al., 2006; Ward et al., 2012) cortices, as well as subcortical structures, such as the striatum (Blazquez et al., 2002), the amygdalar complex (Boele et al., 2010; Sakamoto and Endo, 2010), some thalamic nuclei (Sears et al., 1996; Bahro et al., 1999; Campolattaro et al., 2007), and the red nucleus (RN; Haley et al., 1988; Sakamoto and Endo, 2010; Pacheco-Calderón et al.,

Received Nov. 22, 2015; revised May 16, 2016; accepted May 20, 2016.

Author contributions: J.M.D.-G. and A.G. designed research; C.A., J.M.-R., M.Á.G.-C., J.M.D.-G., and A.G. performed research; C.A., J.M.-R., M.Á.G.-C., and A.G. analyzed data; J.M.D.-G. and A.G. wrote the paper.

This work was supported by grants from the Spanish Ministry of Economy and Competitiveness (BFU2014-56692-R) and Junta de Andalucía (BIO122, CVI 2487, and P07-CVI-02686) to A.G. and J.M.D.-G. M.Á.G.-C. had a postdoctoral contract (JCI-2011-09013) from the Spanish Ministry of Science and Innovation. We thank Roger Churchill for his help in manuscript editing.

The authors declare no competing financial interests.

Correspondence should be addressed to Prof. Agnès Gruart, Division of Neurosciences, Pablo de Olavide University, Ctra. de Utrera, Km. 1, Seville 41013, Spain. E-mail: agrumas@upo.es.

DOI:10.1523/JNEUROSCI.4190-15.2016

Copyright © 2016 the authors 0270-6474/16/366988-14$15.00/0

2012), have been shown to participate in the generation of conditioned blinks. Recent proposals suggest the joint involvement of cerebellar (cortex, nuclei), cortical (hippocampal, prefrontal), and subcortical (amygdala, striatum) structures in the different aspects (cognitive, motor, associative strength, etc.) of classical blink conditioning (Siegel et al., 2015; Yang et al., 2015).

It is surprising that the above list of neural sites related to classical blink conditioning does not include the motor cortex (MC). In fact, few past (Aou et al., 1992; Birt et al., 2003) or recent (Hasan et al., 2013) studies have addressed the involvement of this key cortical structure in the acquisition of this particular type of associative learning. However, the MC has a well defined and repeated representation of facial muscles (Huang et al., 1988; Morecraft et al., 2001; Müri, 2016), and traditionally has been assumed to be one of the main neural sites involved in the acquisition and proper performance of new motor abilities (Evarts et al., 1983; Doyon and Benali, 2005; Monfils et al., 2005; Brecht et al., 2013; Gloor et al., 2015; Hayashi-Takagi et al., 2015; Kaufman et al., 2015). In fact, MC dynamic activities have been described as interacting with cerebellar and striatal contributions to different types of motor sequence learning (Houk et al., 1996; Hikosaka et al., 2002; Penhune and Steele, 2012; Santos et al., 2015).

In accordance with the above contentions, we assumed that the facial area of the MC should play a role in this type of associative learning. Using a delay paradigm to check this hypothesis, rabbits were prepared for the chronic recording of the electromyographic (EMG) activity of the left orbicularis oculi muscle (or the position of the ipsilateral upper eyelid) and of the unitary activity of antidromically identified contralateral MC pyramidal neurons during the classical conditioning of eyelid responses (Gruart et al., 2000a; Pacheco-Calderón et al., 2012). Collected results, including the firing properties of recorded MC neurons, the transient inactivation of the recorded MC area, the comparison between neuronal oscillatory properties and eyelid acceleration profiles, and the simulation of conditioned response (CR) kinematics by train stimulation, lead to the conclusion that the eyelid area of the MC is directly involved in the generation of classically conditioned eyelid responses.

Materials and Methods

Animals. Experimental procedures were performed in adult male rabbits (New Zealand white albino) weighing 2.4–2.9 kg on arrival at the Animal House facilities of Pablo de Olavide University. Animals were obtained from an authorized supplier (Isoquimen). Rabbits were housed in individual cages for the whole experiment and kept on a 12/12 h light/dark cycle with constant ambient temperature (21 ± 1°C) and humidity (55 ± 7%). Food and water were available *ad libitum*. All experiments were performed in accordance with Spanish (BOE 34/11370-421, 2013) and European Union (2010/63/EU) guidelines for the use of laboratory animals in chronic experiments. In addition, these experiments were submitted to and approved by the local ethics committee of Pablo de Olavide University.

Surgery. Animals were anesthetized with an intramuscular injection of a ketamine–xylazine mixture (Ketaminol, 100 mg/ml; Rompun, 20 mg/ml; and atropine sulfate, 0.5 mg/kg) at an initial dosage of 0.85 ml/kg. Anesthesia was maintained by intravenous perfusion at a flow rate of 10 ml/kg/h.

As illustrated in Figure 1, animals ($n = 15$) were prepared for the chronic recording of unitary activity in the MC during classical blink conditioning. A window (4 × 6 mm) was drilled through the parietal bone centered on the right MC (anteroposterior, 2 mm; lateral, 2 mm; Girgis and Shih-Chang, 1981) corresponding to the eyelid motor area (Pacheco-Calderón et al., 2012). A recording chamber was built with acrylic cement around the window. A sterile stainless steel needle (21 gauge) with a curved tip was fixed with dental cement to one corner of the recording chamber to serve as a stereotaxic reference. The dura mater was removed and the cortical surface was protected with sterile gauze and an inert plastic cover between recording sessions. A silver electrode (1 mm in diameter) in contact with the dura mater was attached to the left parietal bone as a ground for unitary recordings. These animals were also implanted with stimulating electrodes aimed at the ipsilateral RN (anteroposterior, 8.5 mm, lateral, 1.5 mm; depth, 13 mm from the cortex surface) and the contralateral facial nuclei (FN; anteroposterior, −18 mm; lateral, 3.5 mm; depth, 15–17 mm from the cerebellum surface). When necessary, the targeted areas were approached from anteroposterior or lateral angles. Stimulating electrodes were made with 200 μm varnished silver wire (California Fine Wire). The final position of these stimulating electrodes was determined by eyelid-closing movements evoked by a pair of pulses (1 ms interpulse interval) applied to the corresponding electrode. Finally, animals were implanted with bipolar hook electrodes in the left orbicularis oculi muscle to record their EMG activities. These electrodes were made from multistranded Teflon-coated stainless steel wire (A-M Systems) with a total external diameter of 230 μm and bared ≈1 mm at the tip. A head-holding system, consisting of three bolts cemented to the skull perpendicular to the stereotaxic plane, was also implanted. All stimulating and recording electrodes were connected to two sockets attached to the holding system.

A second group of animals ($n = 6$) was implanted (under the same anesthetic and sterile conditions) with guide cannulas in the MC (anteroposterior, 2 mm; lateral, 2 mm; depth, 0.5 mm from cortex surface). Guide cannulas were made from 21 gauge stainless steel needles. Each of these was protected by a removable 25 gauge stainless steel rod during noninjecting periods (Pacheco-Calderón et al., 2012). These animals were also implanted with the above-described EMG recording electrodes.

A third group of animals ($n = 3$) was implanted with stimulating electrodes in the MC (anteroposterior, 2 mm; lateral, 2 mm; depth, 1 mm from cortex surface). Stimulating electrodes were made with 200 μm varnished silver wire (California Fine Wire). Animals were also implanted with the above-described EMG recording electrodes and with a five-turn coil (2.5–3 mm diameter) into the center of the left upper eyelid close to the lid margin. Coils were made of Teflon-coated stainless steel wire (A-M Systems) with an external diameter of 50 μm and a weight of 10–15 mg (Gruart et al., 2000a).

A fourth group of animals ($n = 3$) was injected with the anterograde biotinylated dextran amine (BDA) tracer to label MC axonal projections terminating in the FN (Fig. 2). For this, and under the above anesthetic conditions, a hole (2 mm diameter) was drilled in the skull according to the MC coordinates (anteroposterior, 2 mm; lateral, 2 mm). The BDA tracer was injected with a 10 μl microsyringe (Hamilton). The tracer was injected at different depths (1–3 mm) from the cortex surface to a final amount of 3 μl, at a rate of 0.3 μl/min.

Recording and stimulating procedures. Recording sessions began 2 weeks after surgery. Each rabbit was placed in a Perspex restrainer specially designed for limiting the animal's movements (Gruart et al., 2000a; Leal-Campanario et al., 2007). The box was placed on the recording table and was surrounded by a black cloth. The recording room was kept softly illuminated, and a 60 dB background white noise was switched on during the experiments. For all the subjects, the first two recording sessions consisted of adapting the rabbit to the restrainer and to the experimental conditions; no stimulus was presented during these two sessions.

The EMG activity of the orbicularis oculi muscle was recorded using Grass P511 differential amplifiers with a bandwidth of 0.1 Hz to 10 kHz (Grass-Telefactor). Neuronal unitary activity was recorded in the contralateral MC with the help of a NEX-1 preamplifier (Biomedical Engineering) and from there to a differential amplifier (AM 502, Tektronix). Unitary recordings were performed with glass micropipettes filled with 2 M NaCl (3–6 MΩ resistance) and filtered in a bandwidth of 1 Hz to 10 kHz. When necessary, field potentials were recorded with low-resistance electrodes (1–3 MΩ). The recording area was approached with the help of stereotaxic coordinates (Girgis and Shih-Chang, 1981), and antidromic or orthodromic (i.e., synaptic) field potentials were evoked by electrical stimulation of the FN or the RN. Criteria to determine whether the recorded and the activated neurons were the same, and to discrimi-

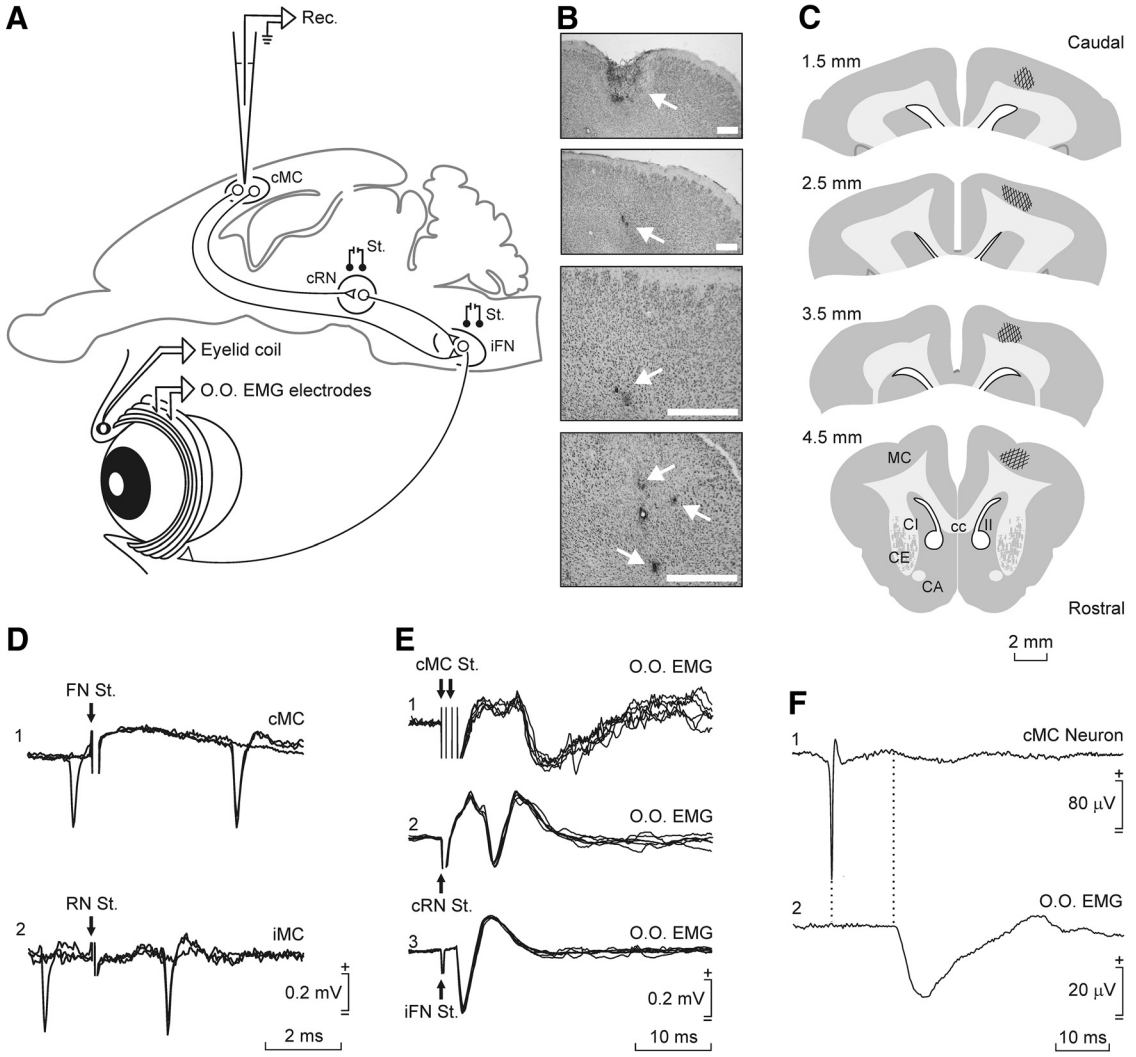

Figure 1. Experimental design and identification of recorded MC neurons. ***A***, Diagram representing the experimental design. Rabbits were chronically implanted with EMG recording electrodes in the left orbicularis oculi muscle (O.O. EMG). In some animals, eyelid movements were recorded with the magnetic search coil technique. MC neurons contralateral (cMC) to the left eye were recorded (Rec.) with glass micropipettes inserted into the MC area. For proper identification, MC neurons were activated antidromically from the RN or the FN. ***B***, Photomicrographs of MC coronal sections illustrating cannula implantation (top picture and arrow) and electrolytic marks (3 bottom pictures and arrows) made with stimulating metal microelectrodes implanted in selected recording sites. Calibration bars, 1 mm. ***C***, Diagrams illustrating the recording sites following the atlas of Girgis and Shih-Chang (1981). ***D***, Representative examples of the antidromic activation and collision tests of MC neurons from the FN (1) or the RN (2) at threshold-straddling intensities. Arrows indicate stimulus artifacts. ***E***, From top to bottom are illustrated the EMG activity evoked in the O.O. muscle by double (2 ms interval) pulses applied to the cMC (1) and single pulses presented to the contralateral RN (cRN; 2) and the ipsilateral FN (iFN; 3). ***F***, Spike-triggered extracellular activity recorded in the O.O. muscle (2). The triggering action potential corresponded to an identified cMC neuron (1). Average was repeated 1500 times.

nate somatic versus axonic recordings, were systematically followed (Fig. 1*D–F*; Delgado-García et al., 1988; Gruart and Delgado-García, 1994). At the end of each recording session, the recording micropipette was removed and the recording chamber sterilized and closed with sterile gauze, bone wax, and an inert plastic cover.

In the third group of animals, eyelid movements were recorded with the magnetic search coil technique (C-N-C Engineering). Upper eyelid maximum angular displacements ranged from 30 to 40° for the three animals. For the sake of homogeneity, the gain of the recording system was adjusted to yield 1 V per 10°.

Electrical stimulation of the MCs, RN, and FN consisted of single or paired (cathodal, square, 50 μs, $<$500 μA pulses, 1–2 ms interval) pulses programmed with a CS-220 stimulator across an ISU-220 isolation unit (Cibertec). The MCs were also stimulated with 10 Hz ($\leq$1 s) trains.

Drug microinjection. Following a previous description (Pacheco-Calderón et al., 2012), a 5% solution of lidocaine (Sigma-Aldrich) was injected in the selected animals with the help of a calibrated injection tube (30 gauge). The injection tube was coupled to a 10 μl Hamilton syringe and was advanced through the guide tube. Control animals were injected with the vehicle (9% saline). Drug solutions were injected from 5 min before until the end of the conditioning session at a rate of 0.1 μl/min with the help of a microinfusion pump (310, KD Scientific).

Classical conditioning. As described in detail previously (Leal-Campanario et al., 2007), classical conditioning of eyelid responses was achieved using a delay conditioning paradigm. A tone (600 Hz, 85 dB, 350 ms) was presented as conditioned stimulus (CS) and an air puff (3 kg/cm^2, 100 ms) directed at the cornea was used as the unconditioned stimulus (US). The tone coterminated with the air puff. A function generator (AFG 3022B, Tektronix), triggered by a digital output (1401-plus, Cambridge Electric Design), was used to produce the pulse with the specific tone characteristics (600 Hz, sine wave, 1 V). An amplifier (PA Amplifier FS-2035, Fonestar Systems) converted the pulse to a tone (85 dB) by means of a loudspeaker located 80 cm in front of the animal's head. Air puffs were delivered from an air compressor (Biomedical Engineering) and applied through the opening of a plastic pipette (3 mm diameter) attached to a holder fixed to the recording table. Conditioning sessions consisted of 66 trials (6 series of 11 trials each). Successive trials were separated at random by intervals of 50–70 s. Of the 66 trials, six were test trials in which the CS was presented alone. Conditioning sessions lasted for

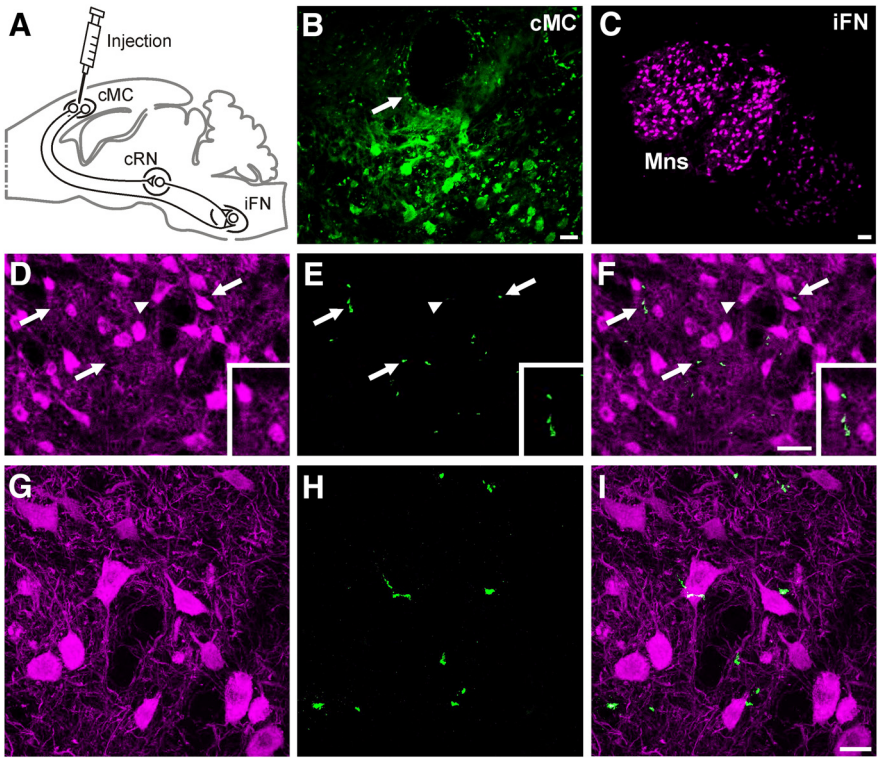

Figure 2. Confocal photomicrographs of BDA-labeled and ChAT-expressing cells. ***A***, Diagram of BDA tracer injection in the MC. ***B***, BDA-labeled cells located in the MC near the injection site (arrow). Scale bar, 30 μm. The photomicrograph is a 2D projection of 24 consecutive focal planes located 1 μm apart. ***C***, FN Mns expressing ChAT. Scale bar, 100 μm. ***D–F***, ChAT-expressing FN Mns (magenta) and fibers labeled with BDA (green). Arrows indicate axons anterogradely labeled with BDA. Scale bar: (in ***F***) ***D–F***, 50 μm. Insets in ***D–F*** are enlarged (30%) views of labeled FN Mns and MC projecting axons. Photomicrographs are 2D projections of 29 consecutive focal planes located 1 μm apart. ***G–I***, Same ChAT-expressing cells indicated in ***D–F*** with arrowheads. Note the axons anterogradely labeled with BDA near or closely apposed to ChAT-expressing FN Mns. Scale bar: (in ***I***) ***G–I***, 25 μm. Photomicrographs are 2D projections of 22 consecutive focal planes located 0.5 μm apart.

~80 min. Animals in the first group were conditioned for 20 sessions, while animals in Groups 2 and 3 where conditioned for 10 sessions. Animals had to generate ≥80% of CRs for two successive conditioning sessions.

Histology. For a proper identification of the recording sites, at the end of the recording sessions we performed small electrolytic lesions in selected places. Lesions were performed with the help of tungsten electrodes (1 MΩ resistance) using a direct current at 0.5–1 mA for 10–20 s. After all experimental sessions, animals were deeply anesthetized with sodium pentobarbital (50 mg/kg, i.p.) and perfused through the left ventricle with 9% saline followed by 4% paraformaldehyde in PBS (0.2 M), pH 7.4. The proper location of EMG recording and eyelid coil electrodes was then checked. Subsequently, brains were removed and preserved 24 h in 4% paraformaldehyde solution. Those brains aimed for immunohistochemistry were preserved only 2 h in the paraformaldehyde solution. Before tissue processing, brains were cryoprotected with 30% sucrose in 0.2 M PBS. Before the fixed tissue was cut, the brains had to descend completely to the bottom of the sucrose container. Brains destined for microscopic observation were cut into coronal sections (50 μm) with the aid of a sliding freezing microtome (SM2000R, Leica Biosystems). Collected slices were stored in 0.2 M PBS in successive series until used. Selected sections, including recording, stimulated, and cannula-implanted sites, were mounted on gelatinized glass slides and stained using the Nissl technique with 0.1% toluidine blue for proper identification of the recording and implanted sites (Fig. 1*B*,*C*).

Immunohistochemistry. Brains for fluorescence immunohistochemistry were cryoprotected after perfusion with 30% sucrose in PBS. After descending to the bottom of the sucrose container, brains were cut in coronal sections (50 μm) with the help of a freezing microtome (SM2000R, Leica) and stored at −20°C in a solution of glycerol (30%) and ethylene glycol (30%) in PBS until used. Tissue was processed "free-floating" for immunohistochemistry. Collected sections passed through all procedures simultaneously to minimize differences in immunohistochemical staining. To better analyze MC projections to the FN, a double-labeling was performed using primary antibody against the enzyme choline acetyltransferase (ChAT; Millipore Iberica), which synthesizes acetylcholine and avidin against BDA (molecular weight, 10,000; Invitrogen), injected as described above.

In short, sections were incubated for 1 h with 10% normal donkey serum (NDS; Bio-Rad) in PBS with 0.2% Triton X-100 (Sigma-Aldrich) and then incubated overnight at room temperature with goat polyclonal IgG anti-ChAT (1:100) with PBS containing 0.2% Triton X-100 and 3% NDS. The second day, sections were washed and incubated for 1 h with anti-goat IgG secondary antibody generated in donkey and conjugated with Alexa 555 (1:200; Millipore Iberica) in PBS containing 0.2% Triton X-100 and 3% NDS, and subsequently incubated with avidin conjugated with Alexa 488 (1:200; Millipore Iberica). Finally, sections were mounted on slides and coverslipped using Prolong Gold antifade reagent fluorescent mounting medium (Millipore Iberica). Selected sections were observed under a confocal microscope (TCS SPE, Leica). *Z*-series of optical sections (1 μm apart) were obtained using the sequential scanning mode. These stacks were processed with ImageJ software (http://rsb.info.nih.gov/ij/).

Data collection and analysis. Unitary activity and unrectified EMG activity of the orbicularis oculi muscle, and 1 V rectangular pulses corresponding to CS, US, air-puff, and electrical stimulations presented during the different experiments were stored digitally in a computer through an analog–digital converter (1401-plus, Cambridge Electric Design) for quantitative off-line analysis. Collected data were sampled at 25 kHz for unitary recordings or at 10 kHz for EMG and eyelid-position recordings, with an amplitude resolution of 12 bits. A computer program (Spike2, Cambridge Electric Design) was used to display single, overlapping, averaged, and raster representations of unitary activity; EMG activity of the orbicularis oculi muscle; and eyelid position, velocity, and acceleration.

As explained in detail previously (Domingo et al., 1997; Gruart et al., 2000a), velocity and acceleration traces were computed digitally as the first and second derivative of eyelid-position records, following low-pass filtering of the data (23 dB cutoff at 50 Hz and a zero gain at ≈100 Hz). The power of the spectral density function (i.e., the power spectrum) of selected data was calculated using a fast Fourier transform to determine the relative strength of the different frequencies present in eyelid movements. The power spectra of eyelid movements were calculated from the corresponding acceleration (Domingo et al., 1997; Gruart et al., 2000a). The spectral power of overlapped firing rate profiles collected from the three (A–C) types of neurons was calculated by fitting a waveform with the help of the equation $f(t) = a_0 \cos(wt)$, where a_0 is the mean value of the three dominant peaks in the averaged firing rates. Each waveform was calculated for the angular frequency $w = 2\pi/T$, where T is the average of the latency between the firing rate peaks with respect to the CS presentation. The value of T was determined following the analysis of recorded firing rate profiles (Caro-Martín et al., 2015).

In most cases, it was easy to identify the recorded MC neuron by isolating it from other neurons during experimental recording sessions. In cases where it was not possible to isolate and record a single cell, a spike sorting (Spike2, Cambridge Electric Design) was performed to classify the different recorded neurons. The spike-sorting analysis was per-

formed off-line by creating a new wave-mark based on the raw neuronal recording. Amplitude and duration thresholds were adjusted to include all types of spikes while excluding the noise of the recording. The spike duration threshold was set at >0.5 ms and the amplitude threshold was set at >0.1 mV, depending on the noise level from each recording. Templates created by the spike-sorting program were meticulously examined and those presenting nonphysiological signals were eliminated. Finally, an event channel for each identified neuron was created in which each event corresponded to a spike. The program enabled the representation of peristimulus time histograms (PSTHs) and/or the firing rates of recorded neurons. When necessary, PSTHs were converted to firing rates following this equation (Rieke et al., 1997): firing rate (spikes/s) = (spikes per bin/repetitions) × (1000/bin size, in milliseconds). With the aid of cursors, the latency, the PSTHs, and the instantaneous firing rate of unitary recordings could be quantified.

Statistical analyses were performed using the SPSS package (SPSS), for a statistical significance level of $P = 0.05$. Unless otherwise indicated, mean values are followed by their SEM. When necessary, the Student's t test was used for the comparison between two independent means and the paired t test when related to the same measurements. The Mann–Whitney U test was used when the normality test (Shapiro–Wilk) failed in the independent data test. Regression and correlation analyses were performed using ≥100 measurements collected from ≥3 animals. Peaks of power spectra were tested with the χ^2-distributed test for spectral density functions (Gruart et al., 2000a).

Results

Identification of recorded MC neurons

The MC eyelid recording area (Fig. 1*B*,*C*) was approached following a previous electrophysiological study (Pacheco-Calderón et al., 2012) and in accordance with available stereotaxic coordinates (Girgis and Shih-Chang, 1981). As illustrated in Figure 1, recorded neurons were identified by their antidromic activation from their projection sites (the contralateral FN or the ipsilateral RN) and with the help of the collision test (Fig. 1*D*). Mean activation latencies were 5.03 ± 0.18 ms (mean ± SEM; $n = 25$ neurons recorded from 5 animals; range: 2.02–6.63 ms) from the FN and 3.36 ± 0.09 ($n = 189$ neurons from 7 animals; range: 1.47–7.73 ms) from the RN. Additional support for the antidromic nature of spike activation was that it followed stimulation frequencies of ≤500 Hz (Trigo et al., 1999; Múnera et al., 2001; Pacheco-Calderón et al., 2012).

As already reported (Pacheco-Calderón et al., 2012), the MC recording area selected in our study was clearly related to eyelid movements, because its stimulation evoked a short-latency (10.1 ± 0.3 ms; $n = 20$ measurements from 3 animals; range: 9.2–11.7 ms) activation of the EMG activity of the contralateral orbicularis oculi muscle. Taking into account the anatomical distance, the small variability in latency of muscle activation from the MC is suggestive of a disynaptic projection (Fig. 1*E1*). As expected, the stimulation of the RN evoked responses of a shorter latency (6.5 ± 0.6 ms; $n = 20$ measurements from 3 animals; range: 4.7–9.2 ms; Fig. 1*E2*) indicating the RN′s shorter distance to the recorded muscle. Finally, orbicularis oculi muscle activation from the FN took place in 2.3 ± 0.2 ms ($n = 20$ measurements from 3 animals; range: 1.7–2.5 ms; Fig. 1*E3*). The latency of spike-triggered averaged activities of orbicularis oculi muscle was 12.5 ± 0.4 ms ($n = 15$ measurements from 3 animals; range: 11.3–13.6 ms). These results further confirmed that MC neurons recorded and analyzed here project directly to the FN and have a disynaptic activation effect on the orbicularis oculi muscle (Fig. 1*F*).

Small electrolytic-lesion marks made at the end of the recording sessions indicated that MC neurons related to reflex, spontaneous, and conditioned eyelid responses occupied a dorsal position in the rostral part of the rabbit cortical motor area (Fig. 1*B*,*C*). With the help of these electrolytic marks and collected information regarding stereotaxic coordinates, we reconstructed the location of recorded MC neurons ($n = 257$) included in this study. Figure 1*C* illustrates that these neurons (types A–C; see below) formed a cell column (anteroposterior, 1.5–4.5 mm; lateral, 2–4 mm) over the dorsal MC (Girgis and Shih-Chang, 1981), i.e., the facial area of the MC is not located laterally like in cats or primates.

To further confirm that these MC neurons were involved in eyelid responses, we injected the anterograde BDA tracer in the MC recording area of three animals (Fig. 2*A*,*B*) and checked axon terminals located within the FN. For identification purposes, FN motoneurons (Mns) were labeled with ChAT (Fig. 2*C*,*D*,*G*). Confocal photomicrographs of BDA labeling showed the presence of relatively few anterogradely labeled axons near or closely apposed to ChAT-expressing FN Mns (Fig. 2*E*,*F*,*H*,*I*). Apart from the longer distance, the low density of MC axon terminals present in the FN could explain the low number of antidromic MC neurons activated from this nucleus ($n = 25$) compared with those activated from the RN ($n = 189$), corresponding to a much larger and denser projection (Davies et al., 1994; Horn et al., 2002; Miller and Gibson, 2009).

Firing properties of MC neurons during classical conditioning of eyelid responses

In addition to two preliminary recording sessions in the absence of conditioning stimuli, performed to adapt animals to the recording setup, MC neurons were recorded during the two habituation and the successive (≤20) conditioning sessions. The experimental design for unitary recording during classical blink conditioning is shown in Figure 3*A*, while the learning curve corresponding to 10 animals recorded for two habituation and 20 conditioning sessions is represented in Figure 3*B*. Although animals reached the selected criterion by the seventh or eighth conditioning session, training was maintained for 12 additional days. In this way, we recorded the activity of MC neurons both during the acquisition process and when the learning curve reached asymptotic values.

The firing rates of MC neurons during air-puff-evoked reflex blinks were quite different from those during spontaneous blinks (Fig. 3*C*). The main difference was that MC neurons classified as types B and C (see below) increased their firing frequency after (25.3 ± 8 ms; $n = 32$ neurons collected from 7 animals; range: 5–55 ms) the beginning of the evoked reflex blink, but before (150.5 ± 40 ms; $n = 32$ neurons from 7 animals; range: 70–210 ms) the beginning of spontaneous blinks presented by unconditioned animals. Neurons classified as type A ($n = 11$ neurons from 6 animals) did not fire during air-puff-evoked reflex blinks, but they fired before (95.7 ± 32 ms; range: 57–112 ms) the beginning of spontaneous blinks.

Figure 3*D* shows a typical MC neuron recorded from a well trained animal (15th recording session). This neuron was recorded during a complete conditioning session. Interestingly, the cell was activated ≈60 ms following CS presentation, and its activation preceded the beginning of the CR (as determined from rectified EMG recordings) by ≈70 ms. The averaged firing rate of the neuron increased steadily from its early activation until reaching a peak firing of ≈95 spikes/s at the time of US presentation. Although this neuron was not identified by antidromic activation, its spike amplitude (1.7 mV) and duration (>0.5 ms), and its spontaneous firing (≈25 spikes/s)

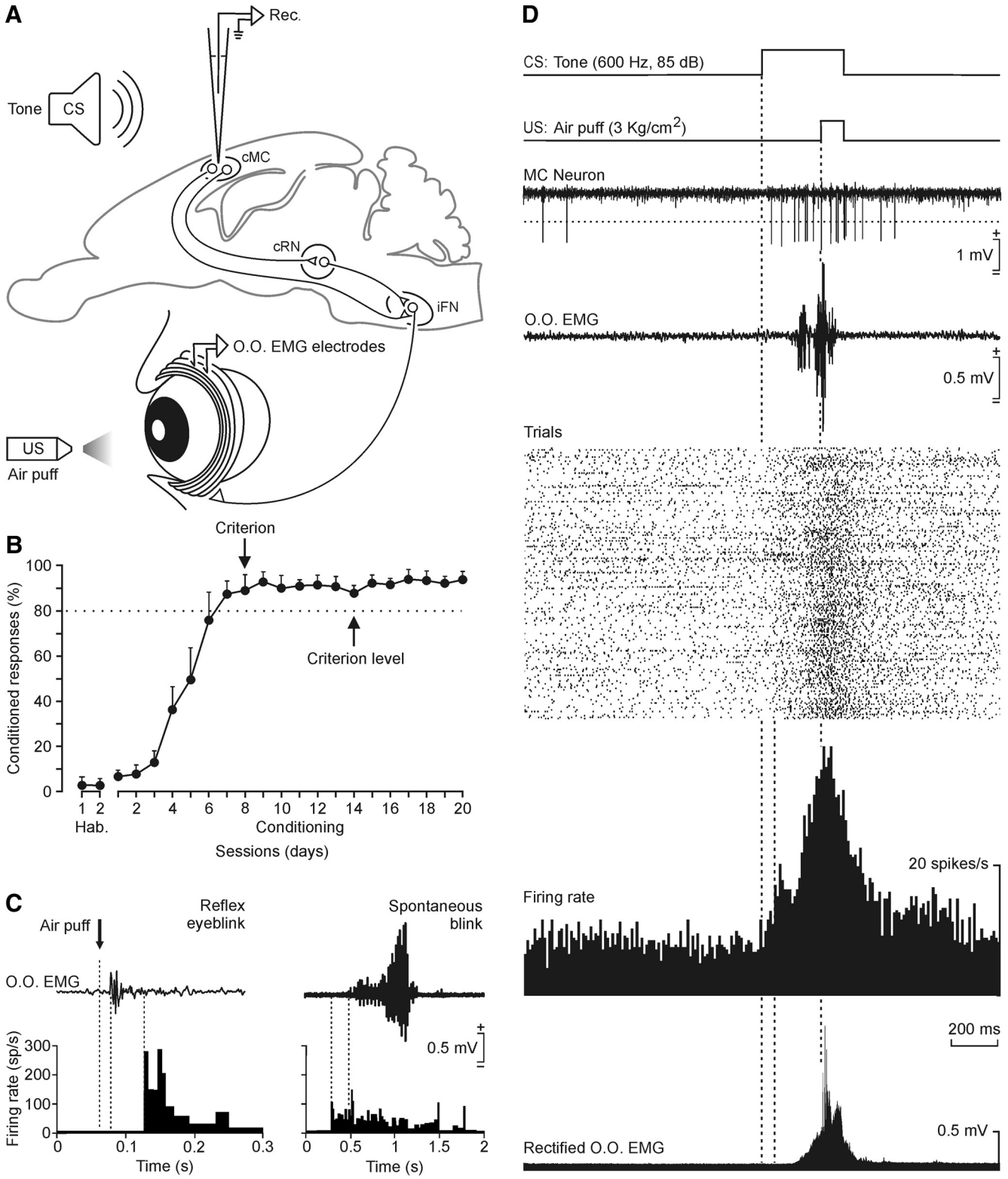

Figure 3. Firing activities of MC neurons during classical blink conditioning using a delay conditioning paradigm. ***A***, For conditioning, animals were presented with a tone (600 Hz, 85 dB, 350 ms) as CS and with an air puff (3 kg/cm^2, 100 ms) presented to the left cornea as US. The CS coterminated with the US. CRs were recorded with the help of chronically implanted orbicularis oculi (O.O.) EMG electrodes. Contralateral MC neurons (cMC) were recorded (Rec.) across conditioning sessions with glass microelectrodes. ***B***, Evolution of the percentage of CRs across conditioning sessions. Note that animals ($n = 10$) reached the selected criterion by the seventh or eighth conditioning sessions. MC neurons were recorded during the acquisition process and for >10 sessions after the selected criterion was reached. ***C***, Typical responses of MC neurons (classified as types B and C) to air puff (20 ms, 3 kg/cm^2) presentations (left) and during performance of a spontaneous blink. Note the different latencies and time scales. ***D***, Representative example of the firing activity of an MC neuron recorded during a session from a well trained animal. From top to bottom are represented the conditioning paradigm (CS and US presentations), the firing activity of the MC neuron and the EMG activity of the O.O. muscle for a single trial, the raster plot of >60 successive trials, the averaged firing rate, and the rectified EMG activity of the contralateral O.O. muscle. Note that the activation of the MC neuron substantially (>70 ms) preceded the beginning of the eyelid CR.

meant that it could be classified as a pyramidal cell (Swadlow et al., 1998; Beloozerova et al., 2003). Because of its characteristic double-peak activation during the CS–US interval and following US presentation, this neuron was classified as a type B neuron (see below).

Types of MC neurons related to classical blink conditioning

Recorded neurons were classified in three different groups (A–C), depending on their antidromic activation from the FN or the RN, their spontaneous firing, and their firing during the CS–US interval (Fig. 4).

Type A neurons (Figs. 4*A*,*B*, 5*A*) presented action potentials lasting >0.5 ms, and an irregular spontaneous firing rate, with mean values ranging from 3 to 15 spikes/s. To determine whether type A neurons were activated by CS-alone presentations, we compared their integrated activity during the 250 ms preceding versus the 250 ms following CS presentations. Indeed, type A neurons were not significantly ($t_{(21,0.05)} = -1.423$; $p = 0.17$; $n = 11$ neurons from 8 animals) activated during CS-alone presentations—that is, during the two habituation sessions. As illustrated in Figure 4*A*, type A neurons fired a burst of action potentials preceding (50–90 ms) the EMG activation of the orbicularis oculi muscle during the CS–US interval—i.e., during the generation of the CR. Characteristically, the peak firing of type A neurons took place during the CS–US interval, reaching not very high (20–30 spikes/s) peak firing rates (Figs. 4*B*, 5*A*). Their firing rates decreased steadily during US presentation until reaching (irregular) tonic firing 0.2–0.3 s afterward. The averaged firing rates of 11 type A neurons recorded from well trained animals (i.e., from the 9th to the 20th conditioning session) are illustrated in Figure 5*A*. In this situation, the averaged population of type A neurons was activated at ≈70 ms following CS presentation and preceded the beginning of the CR by ≈95 ms. The averaged peak firing rate of type A neurons took place at ≈200 ms from CS presentation. A total of 23 neurons recorded from eight animals were included in this group, 52% of them (i.e., 12 neurons) being activated antidromically from the FN. No neuron included in this group was activated antidromically from the RN.

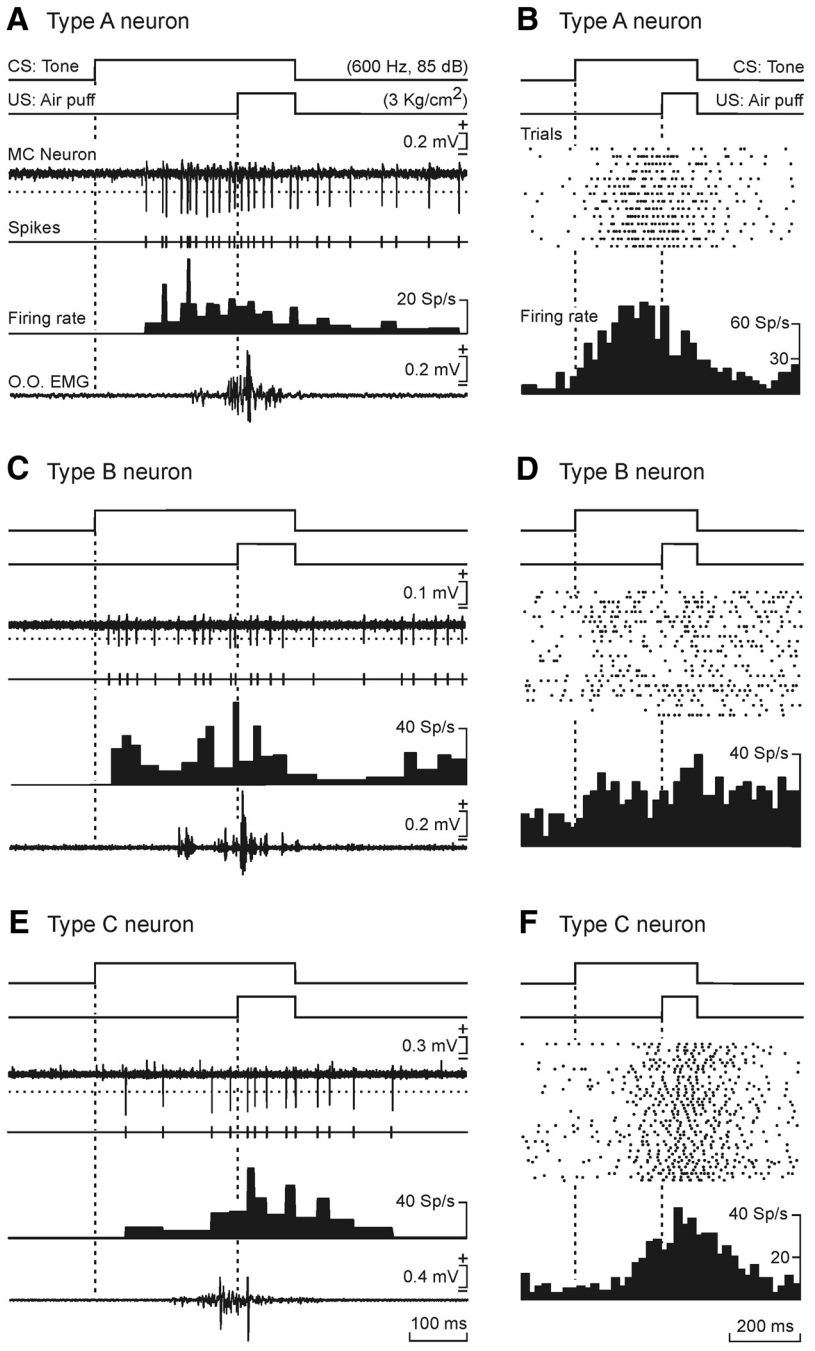

Figure 4. Different types of MC neurons activated during classical blink conditioning with a delay paradigm. ***A***, ***B***, Firing properties of type A neurons. ***A***, From top to bottom are illustrated the conditioning paradigm, the raw activity of a representative type A neuron, the event channel and firing rate of the selected neuron, and the raw EMG activity of the orbicularis oculi (O.O.) muscle during a single CS–US presentation. ***B***, Conditioning paradigm, raster plot of all spikes collected from the same MC neuron during 15 successive trials, and the averaged firing rate. Type A MC neurons were characterized by an increased firing rate before the CR and a noticeable decrease of their firing rates during US presentation. ***C***, ***D***, Same as in ***A*** and ***B*** for a representative type B MC neuron recorded for 26 trials. Type B neurons were characterized by an initial firing peak preceding the CR and by a second increase of firing rate during US presentation. ***E***, ***F***, Same as in ***A*** and ***B*** for a representative type C MC neuron recorded for 53 trials. Type C neurons were characterized by a continuous increase in their firing rates preceding the CR and by reaching the maximum peak during US presentation. Time calibration in ***E*** is also for ***A*** and ***C***. Time calibration in ***F*** is also for ***B*** and ***D***.

Type B neurons (Figs. 3*D*, 4*C*,*D*, 5*B*) presented action potentials lasting >0.5 ms, but with a more stable and higher (10–20 spikes/s) spontaneous firing rate than type A cells. Type B neurons were not activated ($t_{(29,0.05)} = -1.336$; $p = 0.19$; $n = 15$ neurons from 7 animals) during habituation sessions. As illustrated in Figures 3*D*, 4*C*,*D*, and 5*B*, this type of neuron presented two successive bursts of action potentials: one during the CS–US interval (20–40 spikes/s) and the other immediately following US presentation (25–75 spikes/s). Their firing decreased slowly after the

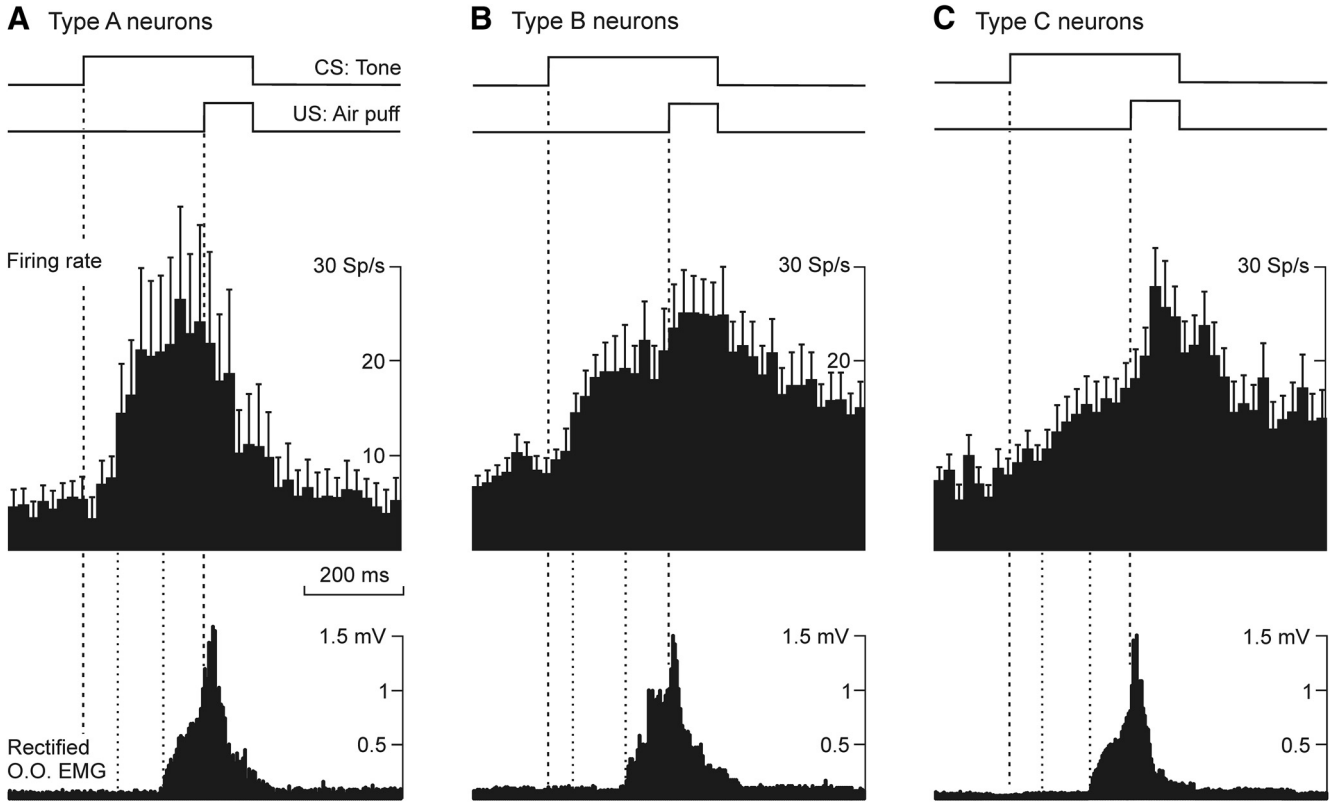

Figure 5. Averaged firing rates of representative type A–C MC neurons recorded from well conditioned animals. All recordings were performed after the eighth conditioning session. The averaged firing rates are represented as mean values ± SEM (bin size, 20 ms). ***A***, From top to bottom are illustrated the conditioning paradigm, the averaged firing rate of selected ($n = 11$) type A neurons, and the average of the rectified EMG responses of the orbicularis oculi (O.O.) muscle. Note that their peak firing rates occurred before US presentation and that they did not respond during the unconditioned response. ***B***, Averaged firing rates and rectified EMG responses collected from $n = 15$ type B neurons. These MC neurons were characterized by the presence of an initial peak in their firing rates before the CR and then by a second increase of their firing rates during the US. ***C***, Same than as in ***A*** for selected ($n = 17$) type C neurons. These MC neurons presented a continuous increase in their firing rates beginning well before (>90 ms) the start of CRs and reaching the maximum during US presentation—i.e., during the generation of the unconditioned eyelid response.

end of the US, reaching a spontaneous firing rate of >0.5 s thereafter. The averaged firing rates of 15 type B neurons recorded from seven well trained animals are illustrated in Figure 5*B*. In this case, the averaged population of type B neurons was activated at ≈50 ms following CS presentation and preceded the beginning of the CR by ≈110 ms. The averaged peak firing rate of type B neurons took place at ≈130 ms from the CS presentation. A total of 28 neurons recorded from nine animals were included in this group, 46.4% of them (i.e., 13 neurons) being activated antidromically from the FN. No neuron included in this group was activated antidromically from the RN.

Finally, type C neurons (Figs. 4*E*,*F*, 5*C*) also presented action potentials lasting >0.5 ms, and a spontaneous firing rate similar (10–20 spikes/s) to that presented by type B neurons. Like types A and B, type C neurons did not modify their firing ($t_{(29,0.05)} = -1.171$; $p = 0.23$; $n = 17$ neurons from 7 animals) following CS-alone presentations during the two habituation sessions. MC neurons included in this group presented a slow increase in their firing rates during the CS–US interval, reaching their peak firing (30–50 spikes/s) by the time of the US presentation (Figs. 4*E*,*F*, 5*C*). During CS-alone presentations in well trained animals, it was observed that the firing of type C neurons reached a peak rate for the time corresponding to the US presentation. Nevertheless, and as already indicated (Fig. 3*C*), type C neurons also fired following US-alone presentations. Like type B neurons, their firing decreased slowly after the end of the US presentation and remained above their mean spontaneous discharge rates for >0.5 s. The averaged firing rates of 17 type C neurons recorded from well trained animals are represented in Figure 5*C*. As shown, the averaged population of type C neurons was activated at ≈70 ms following CS presentation and preceded the beginning of the CR by ≈90 ms. The averaged peak firing rate of type B neurons took place at ≈310 ms from the CS presentation. A total of 37 neurons were included in group C, 20 (i.e., 54%) of them being activated antidromically from the RN. In this case, no neuron included in this group was activated antidromically from the FN. It is important to point out that although 189 neurons were activated antidromically from the RN, only 20 of them (i.e., 10.5%) presented a firing rate related to conditioned eyelid responses.

On the whole, these results indicate that the three types of MC neurons described here are activated during the CS–US interval well in advance of the initiation of the EMG activity of the orbicularis oculi muscle—i.e., of the CR. In addition, there is some specificity in the motor commands sent by MC neurons to the RN and to the FN.

Changes in the activity of MC neurons during the acquisition process of conditioned eyelid responses

Figure 3*B* illustrates the mean learning curve of classically conditioned animals ($n = 10$). As already described in preceding studies using similar conditioning protocols and training paradigms (Gruart et al., 2000a; Leal-Campanario et al., 2007; Pacheco-Calderón et al., 2012), conditioned animals started to generate CRs by the third to fourth conditioning session and reached the selected criterion by the seventh to eighth session. In our case, the mean rate of CRs was maintained at >80%

from the eighth to the 20th conditioning sessions. As shown above, the three types of MC neurons reported here presented stable values in their latency to CS presentation and in the start of CRs, as well as regarding their mean firing profiles.

However, we also wanted to know the putative relationships between the discharge rates of MC neurons during the acquisition process—i.e., during the first eight conditioning sessions. For this, and as illustrated in Figure 6*A–D*, we selected the firing profiles of type A–C neurons recorded during these early conditioning sessions (Fig. 6*A*), together with the rectified EMG activities of the orbicularis oculi muscle collected during the corresponding sessions and trials (Fig. 6*B*). As shown in Figure 6*A*,*B*, both firing profiles and rectified EMG profiles decreased in latency across the successive conditioning sessions. A linear analysis of the collected data ($n \geq 10$ neurons recorded from ≥100 trials and collected from 6 animals) indicates that there was a significant relationship between the decrease in the latency to CS presentation (in milliseconds) of recorded type A ($y = 94.8 + 1.2x$; $r_{(9,0.05)} = 0.67$; $p = 0.025$), B ($y = 137.3 + 0.4x$; $r_{(12,0.05)} = 0.57$; $p = 0.033$), and C ($y = 31.2 + 1.5x$; $r_{(9,0.05)} = 0.72$; $p = 0.012$) neurons and the corresponding latencies for rectified EMG responses (in milliseconds; Fig. 6*E*).

We also quantified the area below these profiles corresponding to the CS–US intervals (Fig. 6*C*,*D*). In this regard, an attempt was made to determine the linear relationships between the two variables included in Figure 6*C*,*D*—namely, the integrated firing profile area and the integrated EMG amplitude during the CS–US interval. As already reported, eyelid position can be precisely determined from the integral of the rectified activity of the orbicularis oculi muscle (Gruart et al., 1995). A representation (Fig. 6*F*) of integrated neural responses [in (spikes/s) × s] versus integrated EMG responses (in mV × s) from six animals demonstrated the presence of linear relationships between the firing rates of type A ($y = 0.74 + 0.13\times$; $r_{(10,0.05)} = 0.6$; $p = 0.04$), B ($y = -0.77 + 0.5\times$; $r_{(13,0.05)} = 0.8$; $p = 0.0003$), and C ($y = 4.04 + 1.3\times$; $r_{(9,0.05)} = 0.78$; $p = 0.005$) neurons and the corresponding CRs collected during the same trials and sessions. It is interesting to note that, contrary to values collected for type B and C neurons (0.5 and 1.3 slopes, respectively), type A neurons presented a low slope (0.13) for the linear

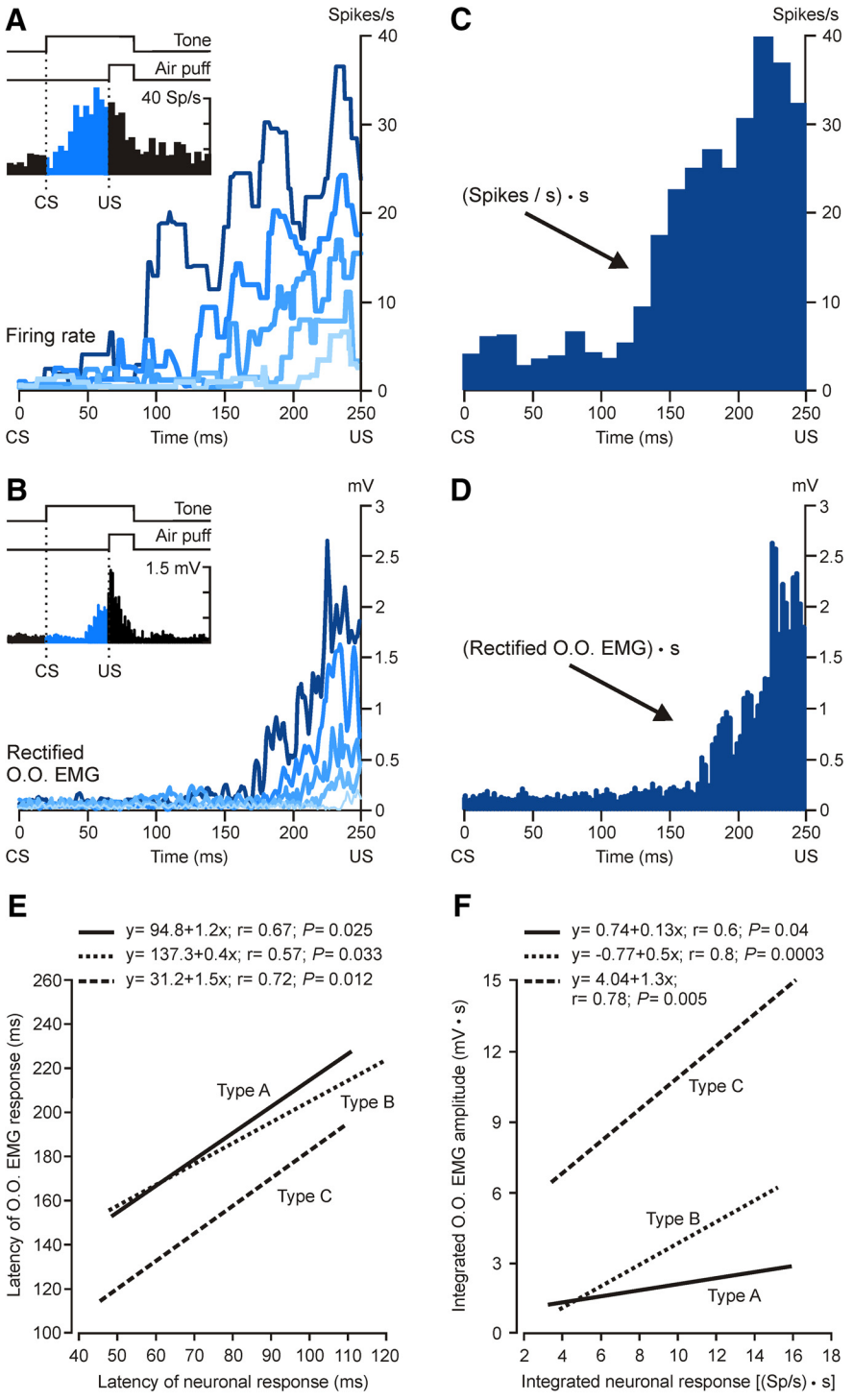

Figure 6. Relationships between changes in firing rates for type A–C neurons and the increase in CRs across conditioning sessions. Analyses were performed for data collected from the third to the seventh conditioning sessions. ***A***, Profiles of firing rates collected from representative type A neurons (inset) across the acquisition process corresponding to the CS–US interval, as indicated in blue. ***B***, Profiles of CRs collected during the conditioning sessions corresponding to data illustrated in ***A***. For ***A*** and ***B***, the increase in color intensity indicates the recording order across training. ***C***, Representation of the area of a firing response during the CS–US interval. ***D***, Representation of the area corresponding to the rectified activity of the orbicularis oculi (O.O.) muscle collected during the recording trials for the averaged firing rate illustrated in ***C***. ***E***, Linear relationships between the latency of neuronal responses to CS presentations versus the latency of the conditioned eyelid responses to CS presentations. Note that the three types of MC neurons presented similar relationships with the latency of CRs. ***F***, Linear relationships between integrated neuronal responses during the CS–US interval and the integrated EMG activity of the O.O. muscle corresponding to CRs. The length of the regression lines was restricted to the collected values.

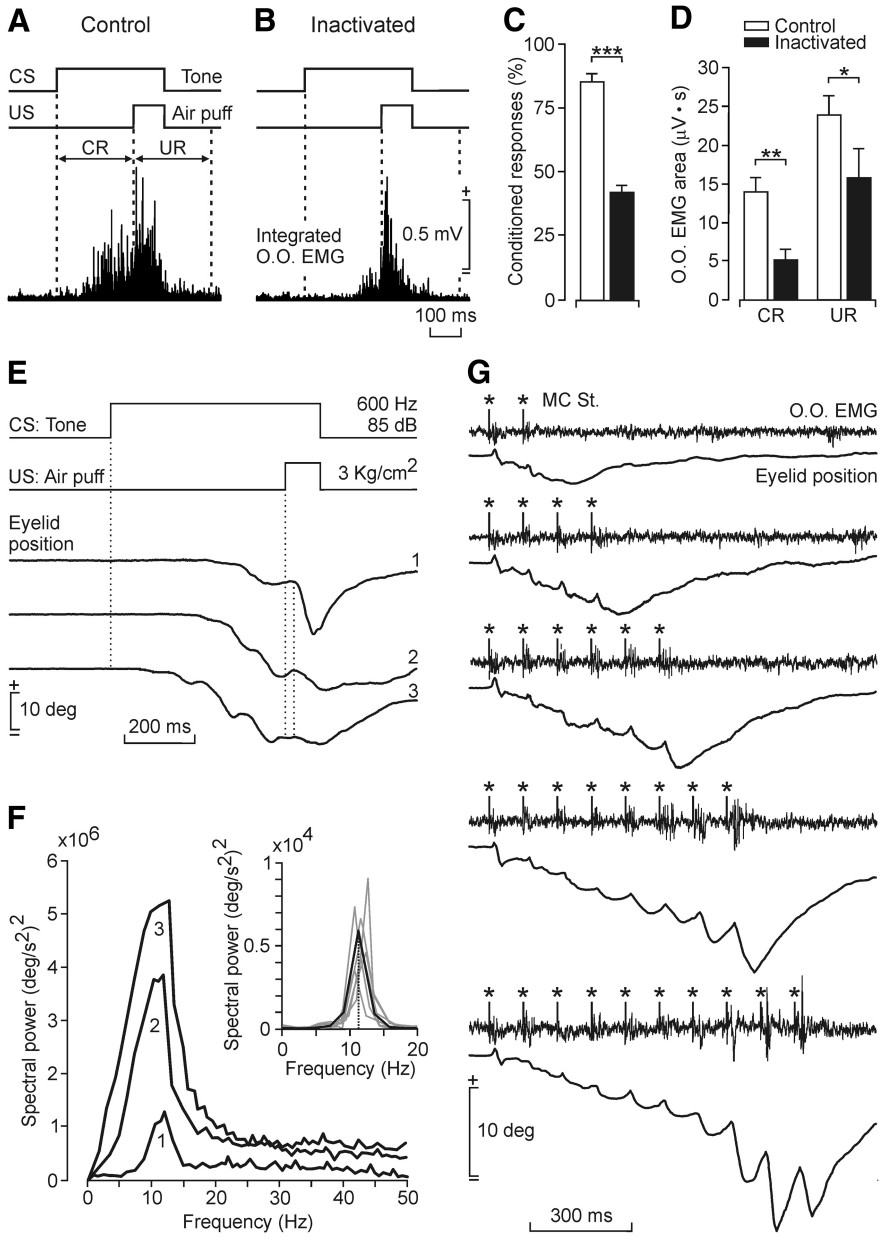

Figure 7. Effects of the chemical inactivation or the electrical stimulation of the MC on the generation and kinematics of CRs. ***A–D***, The contralateral MC was perfused with lidocaine (5% solution at a rate of 0.1 μl/min) or control (vehicle injection at the same rate). Three animals per group were injected. Note that lidocaine inactivation of the contralateral MC significantly decreased the percentage of CRs (***C***) and the integrated amplitude of both CRs and unconditioned responses (UR; ***D***). *$p = 0.046$; **$p = 0.002$; ***$p = 0.001$. ***E–G***, Representative examples of CRs recorded across successive conditioning sessions. Eyelid movements were recorded with the magnetic search coil technique. Note the wave nature of conditioned eyelid responses, and that the number of downward waves increased across conditioning (1, third session; 2, sixth session; 3, eighth session). Note also in ***F*** that the spectral power of CR profiles ($n = 60$) recorded during the same conditioning sessions increased with the number of waves, at ≈10 Hz. The inset in ***F*** illustrates spectral powers obtained from the averaged profiles of the firing rates of A–C neurons collected from six animals from the eighth to the 20th conditioning sessions. ***G***, Effects of the electrical stimulation of the contralateral MC on the EMG activity of the orbicularis oculi (O.O.) muscle and on eyelid position. The MC was stimulated with an increasing number of paired pulses (1 ms interpulse interval) at a frequency of 10 Hz. Note how similar the evoked eyelid responses were compared to those presented by actual CRs—i.e., both of them presented a similar ramp-like wavy profile.

relationships between integrated neural responses and integrated EMG amplitudes.

In contrast, the three types of neurons presented similar slopes (4.8–6.1; $r \leq 0.6$; $p \geq 0.13$) when their integrated neural responses were plotted against the acquisition curve for the initial eight conditioning sessions (not illustrated). These data suggest that while type A neurons were more related to the learning curve than to eyelid performance during CS–US presentations, the other two types of MC neurons were related to both (learning curve and integrated EMG activity). Together, these results indicate that MC neurons are significantly related to the acquisition of classically conditioned eyelid responses.

Effects of acute inactivation of the MC on already acquired CRs

In an additional series of experiments, we studied the effects of MC transient inactivation on the acquisition of CRs (Fig. 7*A–D*) in controls (vehicle-injected) and experimental (lidocaine-injected) animals ($n = 3$ per group). Lidocaine infusion in the MC of conditioned animals (fourth and fifth training sessions; $n = 6$ measurements collected from three animals/group) significantly ($t_{(10,0.05)} = 10.964$; $p = 0.001$) reduced the percentage of CRs (from 85 ± 3% to 42 ± 2.5%; Fig. 7*C*). The rectified and averaged ($n = 66$ trials/session) EMG activity of the orbicularis oculi muscle corresponding to vehicle-injected and lidocaine-injected animals during the fifth conditioning session is illustrated in Figure 7*A*, *B*. In accordance with the illustrated data (fourth and fifth training sessions; $n = 6$ measurements from 3 animals/group; Fig. 7*D*), lidocaine injection also significantly reduced the amplitude of CRs (by ~70%, $t_{(10,0.05)} = 4.321$; $p = 0.002$), with a lesser effect on the performance of the unconditioned responses (by ~35%, $t_{(10,0.05)} = 2.276$; $p = 0.046$). As already suggested in a previous study (Pacheco-Calderón et al., 2012) using similar lidocaine injections, these results further indicate that the MC plays a significant role in the immediate generation of classically conditioned eyelid responses, affecting both their acquisition and performance. In addition, it could be suggested that the MC could provide a general facilitatory tone to the system, affecting more directly conditioned versus unconditioned eyelid responses, because of the stronger nature of the reflex blinks.

Oscillatory properties of MC neurons compared with those of CRs

An attempt was made to determine whether the firing profiles of identified MC neurons presented oscillatory properties similar to those reported for eyelid CRs. As previously reported (Gruart et al., 2000a; Caro-Martín et al., 2015) and additionally illustrated

in Figure 7*E–G*, eyelid CRs in behaving rabbits consist of a ramp-downward displacement of the upper eyelid formed by successive waves or sags with a dominant frequency of ≈10 Hz. Although the number of waves composing CR profiles increased with the successive conditioning sessions—thereby increasing the duration of the CR (Fig. 7*E*)—the dominant frequency of these wavy components did not change with training (Fig. 7*F*). In addition, and following procedures described previously (Caro-Martín et al., 2015), we calculated the spectral power of overlapped firing-rate profiles collected from the three (A–C) types of neurons. Firing rate profiles were collected from six well trained animals, i.e., from the eighth to the 20th conditioning sessions. Indeed, and as indicated above, the three types of neurons described here presented peak firing rates of significantly different intervals with respect to CS presentation. As illustrated in the inset of Figure 7*F*, the averaged firing-rate profiles of the three types of neurons described in this study presented a dominant frequency of 11.3 ± 0.7 Hz, i.e., very close to that presented by eyelid CRs. Finally, we compared the usual profiles of eyelid CRs recorded using the magnetic search coil technique with those evoked by train stimulation of the MC eyelid area. As illustrated in Figure 7*G*, the electrical stimulation of the contralateral MC ($n = 3$ animals) at the same frequency (10 Hz) perfectly simulates the profile and kinematics of eyelid CRs. For example, the amplitude of downward eyelid sags evoked by each single stimulus presented to the MC (median, 2.5°; range, 1.75–9°) was similar ($U_{(60,60,0.05)} = 1545.5$; $p = 0.182$) to the amplitude recorded during actual CRs (median, 3.75°; range, 0.62–11.25°). In addition, peak amplitude (19.67 ± 0.803°; $n = 6$ measurements from 3 animals; range, 17–22°) of train-evoked eyelid responses and that presented by CRs (20.5 ± 0.764°; ± $n = 6$ measurements from 3 animals; range, 18–23°) were also similar ($t_{(10,0.05)} = -0.752$; $p = 0.469$). Thus, it can be concluded that the electrical train stimulation of the MC can generate CRs similar to those that are naturally evoked.

Discussion

Main findings of the present study

In accordance with the present results, the firing activities of identified MC neurons are related to the generation and profiles of eyelid CRs. Recorded neurons were classified as three different types (A–C) depending on the projection sites (FN, RN), activation profiles, and linear relationships with the latency and integrated amplitude of evoked CRs. Importantly, the firing of the three types of MC neurons started during the CS–US interval well in advance (≥90 ms) of the beginning of CRs. Type A neurons increased their discharge rates across conditioning sessions during the CS–US interval and reached peak firing during the CS–US interval, while type B cells presented a second peak during US presentations. Both of them were activated antidromically from the FN and modified their latency with the corresponding changes in latency of CRs across the successive conditioning sessions, but presented a low modulation of their firing rates (mainly type A) in relation to changes in the integrated amplitude of evoked CRs. In contrast, type C cells increased their firing rate across the CS–US interval, reaching peak values at the time of US presentation, and were activated from the RN. Type C cells modified their activation latency and their firing rates in relation to the changes in latency and integrated amplitude of CRs across training. The reversible inactivation of the facial MC area during conditioning evoked a significant reduction in the percentage and in the integrated amplitude of CRs, with a lesser effect on unconditioned responses. In contrast, train (10 Hz) stimulation of the MC simulated the profile and kinematics of CRs recorded with the magnetic search coil technique. In conclusion, results reported here clearly indicate the direct involvement of MC neurons in the acquisition and performance of eyelid CRs.

MC control of orbicularis oculi Mns

The intrinsic organization, within the FN, of the different groups of Mns innervating facial muscles is well preserved across mammals (Morecraft et al., 2001; Sherwood, 2005). In particular, orbicularis oculi Mns occupy preferentially the dorsolateral subdivision of the nucleus in primates (Morecraft et al., 2001), cats (Shaw and Baker, 1985), rabbits (Furutani et al., 2004), and rats (Martin and Lodge, 1977; Furutani et al., 2004). At the same time, facial muscles have distributed and repeated representations in different MC areas (Morecraft et al., 2001; Müri, 2016). Although it has been suggested that direct descending projections from the MC in the FN are present only in catarrhine primates, in relation to their enhanced facial expressions (Sherwood, 2005), the present results indicated the presence of a relatively low projection of MC neurons into the orbicularis oculi subdivision of the FN in the rabbit. In this regard, Grinevich et al. (2005) described in rats a more definite monosynaptic pathway from the vibrissa MC to facial Mns. Although MC projections to orbicularis oculi Mns in rabbits did not appear as dense as the one described for vibrissa Mns in the rat, the effects of MC stimulations on the EMG activity of the orbicularis muscle (Fig. 1*E1*) and the results collected from the MC spike-triggered activity (Fig. 1*F*) indicate the presence of effective postsynaptic effects of MC projecting neurons on orbicularis oculi Mns. Fanardjian and Manvelyan (1987) reported similar findings in acute electrophysiological experiments performed in anesthetized cats. As reported here, type A and B neurons started firing well in advance (≈95 and ≈110 ms, respectively) of the initiation of CRs. In contrast, identified orbicularis oculi Mns start their firing ≈2 ms before the initiation of the EMG activity of the innervated muscle (Trigo et al., 1999). These differences are suggestive of a slowly building depolarization of facial Mns preceding their firing during the generation of eyelid CRs. A comparison between the short latencies in the activation of facial Mns during the corneal reflex (Baker et al., 1980; Shaw and Baker, 1985; Trigo et al., 1999) and the long latencies for MC activation of orbicularis oculi Mns (present results) is suggestive of somatic projections of second-order trigeminal neurons versus distal dendritic projections of MC neurons on these Mns. This proposal is supported by acute electrophysiological experiments performed in anesthetized cats (Fanardjian et al., 1983; Fanardjian and Manvelyan, 1987). In addition, the different depolarization profiles and the strength of activation of facial Mns during the corneal reflex and during CRs (Trigo et al., 1999) explain at least in part the different profiles and kinematics of reflex versus conditioned eyelid responses (Trigo et al., 1999; Gruart et al., 2000a).

MC commands also reach the FN across cortical projections to the RN (Miller and Gibson, 2009). In fact, type C neurons described here seem to project to the RN and carry motor command signals preferentially related to the performance of CRs, along with other eyelid motor behaviors, a characteristic also present in RN neurons projecting to the FN (Pacheco-Calderón et al., 2012). Finally, it is well known that the MC also sends descending projections to the cerebellum via pontine nuclei (Brodal, 1987; Kosinski et al., 1988), a fact already taken into consideration in previous studies on classi-

cal blink conditioning (Ivkovich and Thompson, 1997). It should be noticed here that this important and massive projection reaches the cerebellum, providing an efference copy of cortical motor commands (Holst and Mittelstaedt, 1950; Sperry, 1950). Feedback projections from cerebellar nuclei to different cortical areas are then able to modulate those motor commands for a more proper performance of the aimed motor responses (Sánchez-Campusano et al., 2007; Bostan et al., 2013; Yang et al., 2015).

What are MC neurons encoding?

Different studies have recently confirmed the presence of activity-dependent mechanisms in the dendrites of MC pyramidal neurons and cortical reorganizations in relation to the acquisition of new motor abilities (Doyon and Benali, 2005). For example, an increase in dendritic length of layer V pyramidal neurons as a result of the acquisition of a motor reaching task has been described (Gloor et al., 2015). These cortical plasticity processes taking place in distal dendrites are dependent on proper NMDA-specific glutamate receptor functions (Hasan et al., 2013). Finally, in two seminal studies, Woody's group convincingly demonstrated the presence of depolarizing EPSPs in the pericruciate cortex of awake cats to CS and US presentations (Birt et al., 2003) and that the activation of recorded cortical units by CS presentations preceded the onset of the evoked CRs (Aou et al., 1992). The results collected by Woody et al. (Aou et al., 1992; Birt et al., 2003), further confirmed here, support the hypothesis that the MC is involved in the initiation of classically conditioned eyelid responses.

According to the present results, MC neurons are encoding both the profiles and kinematics of eyelid CRs. In fact, the firing rate of the three types of MC neurons described here was related not only to the learning curve, but also to the eyelid positions corresponding to CRs presented across the successive conditioning sessions, as determined by the integrated EMG activity of the orbicularis oculi muscle during the CS–US interval (Fig. 6*F*; Gruart et al., 1995). In addition, the electrical stimulation of the recorded MC area evoked eyelid profiles similar to those characterizing CRs in the rabbit (Fig. 7*D–F*). This is not a surprise, because the property of encoding different kinematic parameters of acquired motor abilities and the dynamics of the learned responses have been classically ascribed to diverse cortical areas involved in motor control (Evarts et al., 1983; Monfils et al., 2005; Orban et al., 2011; Hardwick et al., 2013).

As shown in a preceding study (Pacheco-Calderón et al., 2012) and further confirmed here (Fig. 7*A–C*), the reversible inactivation of the MC evoked a significant reduction in the integrated EMG amplitude of both conditioned and unconditioned responses, more noticeable in the former. These results are in contrast with those of classic studies indicating that even large MC lesions do not seem to affect the acquisition or performance of CRs in behaving rabbits (Ivkovich and Thompson, 1997). In contrast, Kelly et al. (1990) described the presence of noticeably modified CRs in the decerebrate-decerebellate rabbit. Moreover, it has been recently proposed that the RN and the surrounding pararubral area can substitute for the respective motor roles of cerebral cortical and cerebellar structures (Pacheco-Calderón et al., 2012), because they receive afferents from different sensory modalities (Padel et al., 1988) and present rich intrinsic circuits (Haley et al., 1988; Horn et al., 2002). Together, these studies suggest the presence of additional neural centers with a limited capacity to generate CRs.

References

Aou S, Woody CD, Birt D (1992) Changes in the activity of units of the cat motor cortex with rapid conditioning and extinction of a compound eye blink movement. J Neurosci 12:549–559. Medline

Bahro M, Molchan SE, Sunderland T, Herscovitch P, Schreurs BG (1999) The effects of scopolamine on changes in regional cerebral blood flow during classical conditioning of the human eyeblink response. Neuropsychobiology 39:187–195. CrossRef Medline

Baker R, McCrea RA, Spencer RF (1980) Synaptic organization of cat accessory abducens nucleus. J Neurophysiol 43:771–791. Medline

Beloozerova IN, Sirota MG, Swadlow HA (2003) Activity of different classes of neurons of the motor cortex during locomotion. J Neurosci 23:1087–1097. Medline

Birt D, Aou S, Woody CD (2003) Intracellularly recorded responses of neurons of the motor cortex of awake cats to presentations of Pavlovian conditioned and unconditioned stimuli. Brain Res 969:205–216. CrossRef Medline

Blazquez PM, Fujii N, Kojima J, Graybiel AM (2002) A network representation of response probability in the striatum. Neuron 33:973–982. CrossRef Medline

Boele HJ, Koekkoek SK, De Zeeuw CI (2010) Cerebellar and extracerebellar involvement in mouse eyeblink conditioning: the ACDC model. Front Cell Neurosci 3:19. CrossRef Medline

Bostan AC, Dum RP, Strick PL (2013) Cerebellar networks with the cerebral cortex and basal ganglia. Trends Cogn Sci 17:241–254. CrossRef Medline

Brecht M, Hatsopoulus NG, Kaneko T, Shepherd GM (2013) Motor cortex microcircuits. Front Neural Circuits 7:196. CrossRef Medline

Brodal P (1987) Organization of cerebropontocerebellar connections as studied with anterograde and retrograde transport of HRP-WGA in the cat. In: New concepts in cerebellar neurobiology (Liss AR, ed), pp 151–182. New York: Liss.

Campolattaro MM, Halverson HE, Freeman JH (2007) Medial auditory thalamic stimulation as a conditioned stimulus for eyeblink conditioning in rats. Learn Mem 14:152–159. CrossRef Medline

Caro-Martín CR, Leal-Campanario R, Sánchez-Campusano R, Delgado-García JM, Gruart A (2015) A variable oscillator underlies the measurement of time intervals in the rostral medial prefrontal cortex during classical eyeblink conditioning in rabbits. J Neurosci 35:14809–14821. CrossRef Medline

Christian KM, Thompson RF (2003) Neural substrates of eyeblink conditioning: acquisition and retention. Learn Mem 10:427–455. CrossRef Medline

Davies J, Qume M, Harris NC (1994) Pharmacological characterisation of excitatory synaptic transmission in the cat red nucleus in vivo. Brain Res 649:43–52. CrossRef Medline

Delgado-García JM, Vidal PP, Gómez C, Berthoz A (1988) Vertical eye movements related signals in antidromically identified medullary reticular formation neurons in the alert cat. Exp Brain Res 70:585–589. Medline

Domingo JA, Gruart A, Delgado-García JM (1997) Quantal organization of reflex and conditioned eyelid responses. J Neurophysiol 78:2518–2530. Medline

Doyon J, Benali H (2005) Reorganization and plasticity in the adult brain during learning of motor skills. Curr Opin Neurobiol 15:161–167. CrossRef Medline

Evarts EV, Fromm C, Kröller J, Jennings VA (1983) Motor cortex control of finely graded forces. J Neurophysiol 49:1199–1215. Medline

Fanardjian VV, Manvelyan LR (1987) Mechanisms regulating the activity of facial nucleus motoneurons. III. Synaptic influences from the cerebral cortex and subcortical structures. Neuroscience 20:835–843. CrossRef Medline

Fanardjian VV, Kasabyan SA, Manvelyan LR (1983) Mechanisms regulating the activity of facial nucleus motoneurones. II. Synaptic activation from the caudal trigeminal nucleus. Neuroscience 9:823–835. CrossRef Medline

Furutani R, Izawa T, Sugita S (2004) Distribution of facial motoneurons innervating the common facial muscles of the rabbit and rat. Okajimas Folia Anat Jpn 81:101–108. CrossRef Medline

Girgis M, Shih-Chang W (1981) A new stereotaxic atlas of the rabbit brain. St. Louis: Warren H. Green.

Gloor C, Luft AR, Hosp JA (2015) Biphasic plasticity of dendritic fields in layer V motor neurons in response to motor learning. Neurobiol Learn Mem 125:189–194. CrossRef Medline

Grinevich V, Brecht M, Osten P (2005) Monosynaptic pathway from rat vibrissa motor cortex to facial motor neurons revealed by lentivirus-based axonal tracing. J Neurosci 25:8250–8258. CrossRef Medline

Gruart A, Delgado-García JM (1994) Discharge of identified deep cerebellar nuclei neurons related to eye blinks in the alert cat. Neuroscience 61: 665–681. CrossRef Medline

Gruart A, Blázquez P, Delgado-García JM (1995) Kinematics of spontaneous, reflex, and conditioned eyelid movements in the alert cat. J Neurophysiol 74:226–248. Medline

Gruart A, Schreurs BG, del Toro ED, Delgado-García JM (2000a) Kinetic and frequency-domain properties of reflex and conditioned eyelid responses in the rabbit. J Neurophysiol 83:836–852. Medline

Gruart A, Guillazo-Blanch G, Fernández-Mas R, Jiménez-Díaz L, Delgado-García JM (2000b) Cerebellar posterior interpositus nucleus as an enhancer of classically conditioned eyelid responses in alert cats. J Neurophysiol 84:2680–2690. Medline

Gruart A, Muñoz MD, Delgado-García JM (2006) Involvement of the CA3–CA1 synapse in the acquisition of associative learning in behaving mice. J Neurosci 26:1077–1087. CrossRef Medline

Haley DA, Thompson RF, Madden J 4th (1988) Pharmacological analysis of the magnocellular red nucleus during classical conditioning of the rabbit nictitating membrane response. Brain Res 454:131–139. CrossRef Medline

Hardwick RM, Rottschy C, Miall RC, Eickhoff SB (2013) A quantitative meta-analysis and review of motor learning in the human brain. Neuroimage 67:283–297. CrossRef Medline

Hasan MT, Hernández-González S, Dogbevia G, Treviño M, Bertocchi I, Gruart A, Delgado-García JM (2013) Role of motor cortex NMDA receptors in learning-dependent synaptic plasticity of behaving mice. Nat Commun 4:2258. CrossRef Medline

Hayashi-Takagi A, Yagishita S, Nakamura M, Shirai F, Wu YI, Loshbaugh AL, Kuhlman B, Hahn KM, Kasai H (2015) Labelling and optical erasure of synaptic memory traces in the motor cortex. Nature 525:333–338. CrossRef Medline

Hikosaka O, Nakamura K, Sakai K, Nakahara H (2002) Central mechanisms of motor skill learning. Curr Opin Neurobiol 12:217–222. CrossRef Medline

Holst E, Mittelstaedt H (1950) Das Reafferenzprinzip (in German). Naturwissenschaften 37:464–476. CrossRef

Horn KM, Pong M, Batni SR, Levy SM, Gibson AR (2002) Functional specialization within the cat red nucleus. J Neurophysiol 87:469–477. Medline

Houk JC, Buckingham JT, Barto AG (1996) Models of the cerebellum and motor learning. Behav Brain Sci 19:368–383. CrossRef

Huang CS, Sirisko MA, Hiraba H, Murray GM, Sessle BJ (1988) Organization of the primate face motor cortex as revealed by intracortical microstimulation and electrophysiological identification of afferent inputs and corticobulbar projections. J Neurophysiol 59:796–818. Medline

Ivkovich D, Thompson RF (1997) Motor cortex lesions do not affect learning or performance of the eyeblink response in rabbits. Behav Neurosci 111:727–738. CrossRef Medline

Kaufman MT, Churchland MM, Ryu SI, Shenoy KV (2015) Vacillation, indecision and hesitation in moment-by-moment decoding of monkey motor cortex. Elife 4:04677. CrossRef Medline

Kelly TM, Zuo CC, Bloedel JR (1990) Classical conditioning of the eyeblink reflex in the decerebrate-decerebellate rabbit. Behav Brain Res 38:7–18. CrossRef Medline

Koekkoek SK, Hulscher HC, Dortland BR, Hensbroek RA, Elgersma Y, Ruigrok TJ, De Zeeuw CI (2003) Cerebellar LTD and learning-dependent timing of conditioned eyelid responses. Science 301: 1736–1739. CrossRef Medline

Kosinski RJ, Azizi SA, Mihailoff GA (1988) Convergence of cortico- and cuneopontine projections onto components of the pontocerebellar system in the rat: an anatomical and electrophysiological study. Exp Brain Res 71:541–556. CrossRef Medline

Krupa DJ, Thompson JK, Thompson RF (1993) Localization of a memory trace in the mammalian brain. Science 260:989–991. CrossRef Medline

Leal-Campanario R, Delgado-García JM, Gruart A (2006) Microstimulation of the somatosensory cortex can substitute for vibrissa stimulation during Pavlovian conditioning. Proc Natl Acad Sci U S A 103:10052–10057. CrossRef Medline

Leal-Campanario R, Fairén A, Delgado-García JM, Gruart A (2007) Electrical stimulation of the rostral medial prefrontal cortex in rabbits inhibits the expression of conditioned eyelid responses but not their acquisition. Proc Natl Acad Sci U S A 104:11459–11464. CrossRef Medline

Martin MR, Lodge D (1977) Morphology of the facial nucleus of the rat. Brain Res 123:1–12. CrossRef Medline

Miller LE, Gibson AR (2009) Red nucleus. In: Encyclopedia of neuroscience, volume 8 (Squire LR, ed), pp 55–62. Oxford: Academic.

Monfils MH, Plautz EJ, Kleim JA (2005) In search of the motor engram: motor map plasticity as a mechanism for encoding motor experience. Neuroscientist 11:471–483. CrossRef Medline

Morecraft RJ, Louie JL, Herrick JL, Stilwell-Morecraft KS (2001) Cortical innervation of the facial nucleus in the non-human primate: a new interpretation of the effects of stroke and related subtotal brain trauma on the muscles of facial expression. Brain 124:176–208. CrossRef Medline

Múnera A, Gruart A, Muñoz MD, Fernández-Mas R, Delgado-García JM (2001) Hippocampal pyramidal cell activity encodes conditioned stimulus predictive value during classical conditioning in alert cats. J Neurophysiol 86:2571–2582. Medline

Müri RM (2016) Cortical control of facial expression. J Comp Neurol 524: 1578–1585. CrossRef Medline

Orban P, Peigneux P, Lungu O, Debas K, Barakat M, Bellec P, Benali H, Maquet P, Doyon J (2011) Functional neuroanatomy associated with the expression of distinct movement kinematics in motor sequence learning. Neuroscience 179:94–103. CrossRef Medline

Pacheco-Calderón R, Carretero-Guillén A, Delgado-García JM, Gruart A (2012) Red nucleus neurons actively contribute to the acquisition of classically conditioned eyelid responses in rabbits. J Neurosci 32:12129–12143. CrossRef Medline

Padel Y, Sybirska E, Bourbonnais D, Vinay L (1988) Electrophysiological identification of a somaesthetic pathway to the red nucleus. Behav Brain Res 28:139–151. CrossRef Medline

Penhune VB, Steele CJ (2012) Parallel contributions of cerebellar, striatal and M1 mechanisms to motor sequence learning. Behav Brain Res 226: 579–591. CrossRef Medline

Perciavalle V, Apps R, Bracha V, Delgado-García JM, Gibson AR, Leggio M, Carrel AJ, Cerminara N, Coco M, Gruart A, Sánchez-Campusano R (2013) Consensus paper: current views on the role of cerebellar interpositus nucleus in movement control and emotion. Cerebellum 12: 738–757. CrossRef Medline

Rieke F, Warland D, de Ruyter van Steveninck R, Bialek W (1997) Spikes: exploring the neural code. Cambridge, MA: MIT.

Sakamoto T, Endo S (2010) Amygdala, deep cerebellar nuclei and red nucleus contribute to delay eyeblink conditioning in C57BL/6 mice. Eur J Neurosci 32:1537–1551. CrossRef Medline

Sánchez-Campusano R, Gruart A, Delgado-García JM (2007) The cerebellar interpositus nucleus and the dynamic control of learned motor responses. J Neurosci 27:6620–6632. CrossRef Medline

Santos FJ, Oliveira RF, Jin X, Costa RM (2015) Corticostriatal dynamics encode the refinement of specific behavioral variability during skill learning. Elife 4:e09423. CrossRef Medline

Sears LL, Logue SF, Steinmetz JE (1996) Involvement of the ventrolateral thalamic nucleus in rabbit classical eyeblink conditioning. Behav Brain Res 74:105–117. CrossRef Medline

Shaw MD, Baker R (1985) Morphology of motoneurons in a mixed motor pool of the cat facial nucleus that innervate orbicularis oculis and quadratus labii superioris, stained intracellularly with horseradish peroxidase. Neuroscience 14:627–643. CrossRef Medline

Sherwood CC (2005) Comparative anatomy of the facial motor nucleus in mammals, with an analysis of neuron numbers in primates. Anat Rec A Discov Mol Cell Evol Biol 287:1067–1079. Medline

Siegel JJ, Mauk MD (2013) Persistent activity in prefrontal cortex during trace eyelid conditioning: dissociating responses that reflect cerebellar output from those that do not. J Neurosci 33:15272–15284. CrossRef Medline

Siegel JJ, Taylor W, Gray R, Kalmbach B, Zemelman BV, Desai NS, Johnston D, Chitwood RA (2015) Trace eyeblink conditioning in mice is dependent upon the dorsal medial prefrontal cortex, cerebellum, and amygdala: behavioral characterization and functional circuitry. eNeuro 2:pii: ENEURO.0051-14.2015. CrossRef Medline

Sperry RW (1950) Neural basis of the spontaneous optokinetic response produced by visual inversion. J Comp Physiol Psychol 43:482–489. CrossRef Medline

Swadlow HA, Beloozerova IN, Sirota MG (1998) Sharp, local synchrony among putative feed-forward inhibitory interneurons of rabbit somatosensory cortex. J Neurophysiol 79:567–582. Medline

Trigo JA, Gruart A, Delgado-García JM (1999) Discharge profiles of abducens, accessory abducens, and orbicularis oculi motoneurons during reflex and conditioned blinks in alert cats. J Neurophysiol 81: 1666–1684. Medline

Ward RL, Flores LC, Disterhoft JF (2012) Infragranular barrel cortex activity is enhanced with learning. J Neurophysiol 108:1278–1287. CrossRef Medline

Weible AP, Weiss C, Disterhoft JF (2003) Activity profiles of single neurons in caudal anterior cingulate cortex during trace eyeblink conditioning in the rabbit. J Neurophysiol 90:599–612. CrossRef Medline

Weiss C, Bouwmeester H, Power JM, Disterhoft JF (1999) Hippocampal lesions prevent trace eyeblink conditioning in the freely moving rat. Behav Brain Res 99:123–132. CrossRef Medline

Welsh JP, Harvey JA (1991) Pavlovian conditioning in the rabbit during inactivation of the interpositus nucleus. J Physiol 444:459–480. CrossRef Medline

Yang Y, Lei C, Feng H, Sui JF (2015) The neural circuitry and molecular mechanisms underlying delay and trace eyeblink conditioning in mice. Behav Brain Res 278:307–314. CrossRef Medline